NTNU

Norwegian University of
Science and Technology

The Effects of Nanoparticle Drug Delivery Formulations on the Rheological Properties of Mucus

Nishan Katuwal

Biotechnology
Submission date: May 2017
Supervisor: Kurt Ingar Draget, IBT
Co-supervisor: Catherine Taylor Nordgård, IBT

Norwegian University of Science and Technology
Department of Biotechnology and Food Science

Preface

I have always been fascinated with applications of biotechnology in the field of medicine and drug delivery. This thesis has helped to fulfill my fascination and curiosity in every aspect. During the project, I was able to understand the concepts of nanoparticle formulations, drug delivery system, viscoelasticity, rheological properties and mucociliary clearance. This lead to an amazing learning experience during the lab works as well as while writing my thesis. In addition, I was exposed to the ethics of working in a multidisciplinary team and being a part of discussions that lead to conception such projects.

I would like to acknowledge my supervisors Professor Kurt I. Draget and Dr. Catherine Taylor Nordgård for this remarkable experience. They will always remain an ideal for me in the academic and personal life. Under their supervision, I was able to learn and understand the field of rheology, to which I was unaccustomed to. There were times during the project when the situations were confusing and frustrating. But with their help and guidance, I was able to tackle the problems with all new attitude. Therefore, I would like to thank Kurt and Catherine with all my heart, for believing in me and guiding me throughout. I am also grateful of Morten Johnsen Dille and Ann Sissel Ulset for their help in the laboratory techniques and equipment.

I had never thought that I would be doing my masters in Norway, let alone at NTNU. Therefore, I am indebted to all the people directly and indirectly involved in making this happen. My family has always been pillars of my confidence, believing in every aspect of my life. I am honored to be bestowed with their love, support and guidance.

21 May 2017, Trondheim

Nishan Katuwal

Abstract

The aerosol technology used in lungs drug delivery is not precise enough to target all the drugs to alveoli. Some off target deposition of nanoparticles occurs in airway mucus. In general, mucociliary clearance is capable of removing those off target deposition. However, the deposition of nanoparticles on the airway mucus layer could change mucus viscoelastic properties and may alter the dissipation of force through cilia. Thus, it is desirable to understand if the trapped nanoparticles (in off targets) change the normal mucus viscoelastic properties and rheology. Therefore, in this thesis, the viscoelastic properties of mucus are evaluated through oscillatory experiments on the basis of elastic modulus (G'), viscous modulus (G"), phase angle and shear stress developed in the mucus in presence of nanoparticle formulations.

It was found that after addition of nanoparticles, G' and G" of the pig gastric mucus (PGM) increased. However, phase angle of PGM with nanoparticles and PGM control were comparable. The change in moduli of the nanoparticles could be due to interactions between the nanoparticle and mucin. Interestingly, even the addition of just 200μl saline to a mucus, which was previously washed extensively in saline, did change the moduli of mucus. This supported the argument that mucus itself is variable material with aggregates. Nevertheless, it was postulated that the overall changes in moduli and phase angle were not substantial enough to change the rheology of the material, for a single dose of administration. This observation was based on the comparison of phase angles (at different steps of oscillatory experiments), stress developed in the material which remained substantially unchanged and the observation that even addition of 200μl 0.9% saline could slightly change the viscoelasticity.

From the observations, it was argued that the off target depositions of nanoparticle do not create substantial changes to viscoelasticity and rheology of the mucus. And, inside the body, even those small observed changes could be handled by homeostasis of the mucociliary clearance. However, these arguments are based on the deposition of single dose of nanoparticles, which may change considerably when multiple doses are administered to the lungs. Moreover, for conclusive arguments about effects on the mucociliary clearance, position of the nanoparticles in mucus layer and measurement of dissipation force would be required.

Abbreviations

δ	Phase Angle
COMPACT	Collaboration on the Optimization of Macromolecular Pharmaceutical Access to Cellular Targets
Chitosan-PLGA	Chitosan coated PLGA
Chitosan-PLGA siRNA	siRNA loaded Chitosan coated PLGA
CU	University of Copenhagen
F_D	Fraction of Deacetylation
G'	Elastic Modulus
G"	Viscous Modulus
HIPS	Helmholtz Institut für Pharmazeutische Forschung Saarland
L5	Lipidoid 5
L5-PLGA	L5 coated PLGA
L5-PLGA siRNA	siRNA loaded L5 coated PLGA
LPN	Lipid Polymer Hybrid Nanoparticles
LVR	Linear Viscoelastic Region
MPT	Multiple Particle Tracking
PEG	Poly lactic acid-poly ethylene glycol
PGM	Pig Gastric Mucus
PLA	Poly Lactic Acid
PLGA	Poly(lactic-co-glycolic acid)
siRNA	Small Interfering Ribonucleic Acid

Table of Contents

List of Tables

List of Figures

List of Graphs

1. INTRODUCTION

1.1. Scientific Introduction

1.1.1. Drug Delivery System

The potency of any drug is dependent upon their liberation at the right time and in the right environment. For this purpose, it is always desired to discover or develop a drug delivery route into the body through which the drug action is most effective. Some of the popular modes of delivery are oral, parenteral, transdermal and inhalation. Each of these routes have their own complications and advantages. For instance, inhalation route may give rapid absorption of drugs due to huge surface area of the lungs, however, bioavailability in lungs would depend upon the drugs, delivery technique and interference from mucus.[1] In addition, delivery modes would also depend upon several factors including the type of disease, effects preferred and type of drug itself.[2]

The inhalation route consists of the respiratory tract and the lungs. The respiratory tract is divided into upper and lower parts with upper part consisting of nose, nasal cavity and pharynx while lower part consists of larynx, trachea, bronchi and lungs, as shown in the figure.[3] The region from trachea to bronchi consists of ciliated cells and secretory cells, which are responsible for secretion of mucus. The alveoli on the other hand are covered just by monolayer of squamous epithelium over a thin basal lamina.

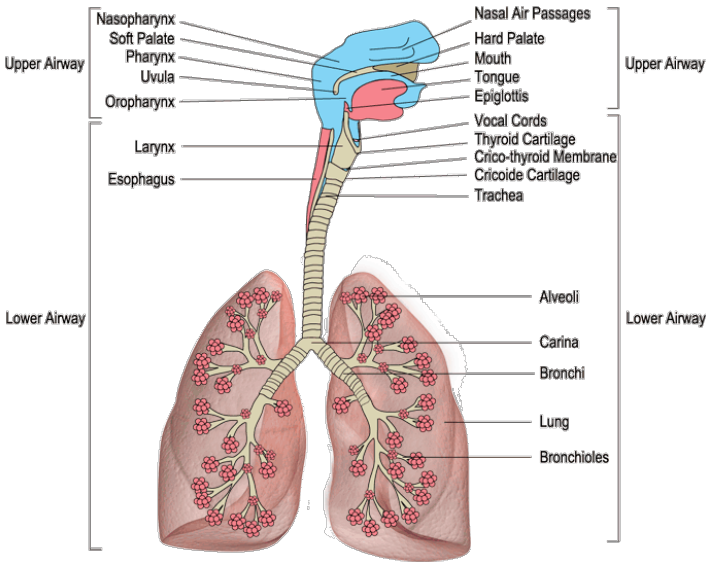

Figure 1-1 Depiction of different parts of the respiratory tract and the lungs[4]

The major target of the inhalation/lungs drug delivery would be the lungs, more specifically the alveolar region. This is because the smaller airway tracts and alveoli account for more than 95% of the lungs surface and are connected to the systemic circulation directly.[5] Thus, the particle landing on the alveoli epithelium cross the epithelial barrier reaching the lungs tissue for topical effect or into the circulation for systemic effects.[6]

The drug delivery to upper airways is limited because of small surface area, low blood flow, clearance by cilia and barrier by mucus.[5] However, different regions of the respiratory tract could be targeted based on the type of disease. For instance, airway cells could be targeted in case of airway diseases. Nevertheless, lungs are an exciting delivery target mainly because of its large surface area and high vascularization (alveolar region).[7] In addition, delivery in lungs would also avoid metabolism of the active ingredients, common in gastrointestinal tract.[7]

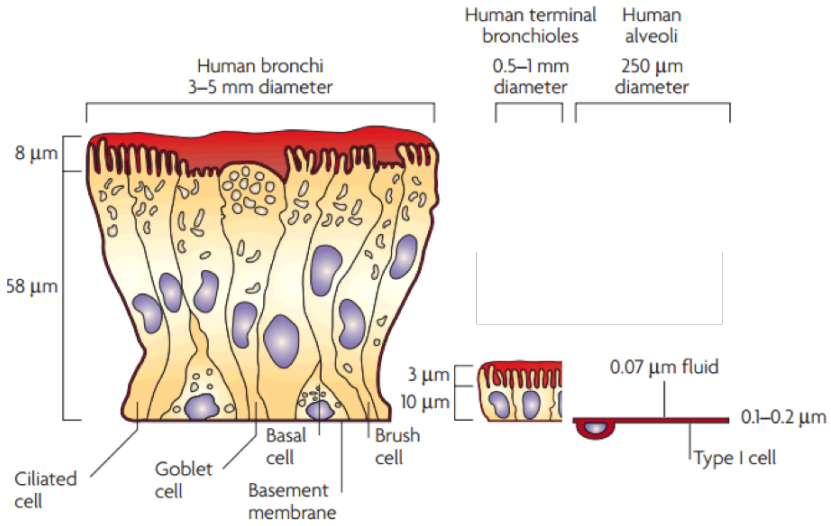

Figure 1-2 Comparison of the lung epithelium at different sites within the lungs. Lung epithelial cells found in different regions of the lung are drawn at their relative sizes [8]

Drug delivery to lungs is also not without its challenges. The challenge is mostly related to getting the drug to right target which depends upon the drug formulations and devices used. However, the delivery devices are less explored than the formulations.[9] There are dry power inhalers (DPI), which are used commonly for delivering proteins to lungs. There are also nebulizers which are driven by compressed air and then, there is aerosol technology which is based on mechanically generated vibration mesh.[10] The selection of delivery devices depends upon the drug formulation, site of action and pathophysiology of lungs. Nevertheless, there are still many challenges in this process.[5] For instance, when the drug formulation is delivered through aerosol technology, some amount of drugs land on the airway and get trapped in the mucus. In healthy conditions, the mucus and underlying cilia platform in the airway remove the

trapped drugs through mucociliary clearance. And in addition to mucociliary clearance, transporter proteins and macrophages are also important players in clearance of such particles from the lungs.[11] But, these drug formulations themselves sometimes alter the mucus rheology and mucociliary clearance, creating off target effects. Thus, it is important to understand every aspect of drug delivery from devices used to drug formulations to physiology of the system.

Nevertheless, during drug delivery, the main goal is the efficient and targeted delivery of drugs to the desired site.[12] Along with the normal physiology, the drug formulation also plays important role in influencing the delivery. The unique features of biologics drugs (peptides, proteins and nuclei acid) and need of sustained release add another challenge to drug delivery.[15] For delivery of such biologics, many types of drug formulations have been used for different routes of drug delivery. But, not all are suitable for delivery in lungs. Some of the suitable formulations are colloid dispersions, microparticles and nanoparticles. Nanoparticle are simply the particles in nano-sizes that is, generally, smaller than 500nm.[13] The shape, size and composition of these nanoparticles significantly influence their targeting properties and retention in the lungs.[14]

For delivery and extended release of biologics, nanoparticles are quite interesting approach. The use of nanoparticles ensures combination with large number of nucleic acids, peptides and proteins. This is because, during nanoparticle drug formulation, nanoparticles could be designed in such a way that modulates the physiochemical properties (such as size, surface characteristics) and drug release features (such as controlled or triggered by external stimuli).[15] Moreover, the small size of nanoparticles also contributes to large surface area leading to increased contact area with the epithelium and a greater chance of non-specific uptake or receptor mediated endocytosis.[16]

These nanoparticles could be polymers, dendrimers, lipid based nanoparticles, magnetic nanoparticles and nanospheres. The nanoparticles could be modified according to desired target and effects.

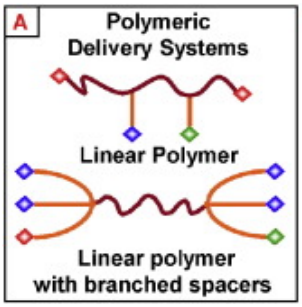

Figure 1-3 Architecture of polymer based nanoparticle formulations. [17]

In this study, polymer, lipid based systems and nucleic acid complexes are used. The polymer system consists of polymer conjugated with other component of the drug delivery system such as drugs, nucleic acid and targeting molecules. This conjugation could be done directly or through spacer molecules.[13] The lipid based systems allows for incorporation of different types of drugs. They provide prolonged retention in the lungs. Specifically, lipid polymer hybrids can easily be aerosolized and taken up by the lungs.[14] For instance, polymers such as Poly(lactic-co-glycolic acid) (PLGA) nanoparticles could be combined with lipidoids for more effective action and stability.

In addition, the nucleic acid complex may contain the complex between negatively charged nucleic acid and positively charged materials such as chitosan and lipidoids, protecting the nanoparticles from destruction during nebulization. It has been found that practically all types of cationic materials are suitable for complexation with nucleic acid and their inhalation delivery. [18] The specific nanoparticle formulations used in this thesis are discussed in section 1.1.6.

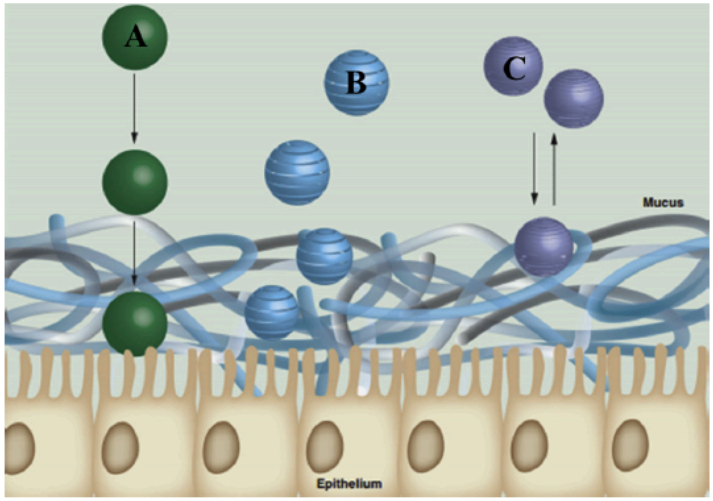

Figure 1-4 The fate of nano particles in mucus A) particles penetrating mucus B) mucoadhesive particles C) mucus excluding particles[19]

Despite all the knowledge on physiology and anatomy of inhalation route (lungs) and advances in drug formulation, lack of uptake information, transportation mode, information on clearance of particles and mechanism of delivery to systemic circulation makes the drug delivery process complicated. Nevertheless, the lungs/inhalation route is still desired because of its non-invasive mode of action. This is particularly important when the frequency of drug administration is high. The lungs are also permeable to more macromolecules than any other route of entry into the body.[20] This delivery route also avoid the first pass metabolism and

provides high speed of action.[21] For instance, small hydrophobic molecules are absorbed within seconds after inhalation, therefore are useful in treating conditions that require quick response such as pain, spasms and nausea [22] These advantages led to the innovation of inhalable insulin. US Food and Drug Administration (FDA) has already approved the use of such inhalable insulin Exubera in 2006.[23] While more recently, in 2014, Afrezza, another approved inhalable insulin, was being developed by Mannkind and Sanofi.[24]

1.1.2. Mucus and its interactions

Mucus is a heterogeneous mixture of mucin, secreted polypeptides, cells and cellular debris. The composition of mucus varies depending its physiological location such as gastro intestinal tract, reproductive tract, respiratory tract and its type: secreted or membrane bound.[25]

Nevertheless, mucus is synthesized by specialized cells in the underlying epithelium called the secretory cells.[26] Mucus present in all the organs that are exposed to external environment and not covered by skin.[25] There mucus performs various functions such as protection from pathogens (foreign particles) by trapping and clearing them; assisting in exchange and transport of nutrients and water; and lubricating the environment it is present in.[27] Mucus being a semi permeable membrane may also be a barrier to the drugs itself.[28]

The mucus is mainly composed of mucin (2-5%), water (95%), lipids (0.5-5%), mineral salts (0.5-1%) and free proteins (1%).[26] It has highly variable physical behavior with properties that are between of a viscous liquid and elastic solid, thus termed as a viscoelastic material. The secreted mucins generally contribute to the viscoelastic properties of the mucus layer.[29]

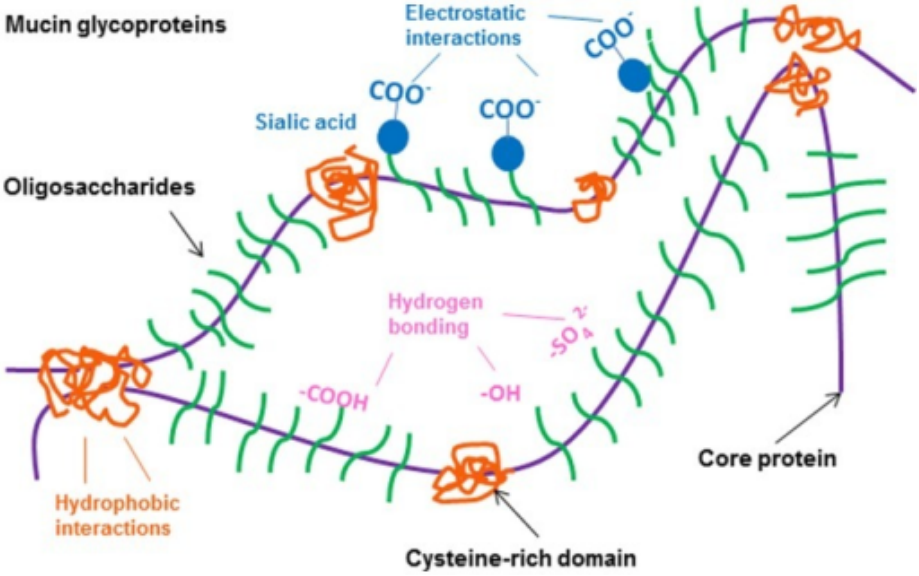

Figure 1-5 : Different regions and possible interactions of mucin[25]

The mucins are entangled fibers of glycoproteins with molecular weight of 0.5-20MDa.[25] The mucin mainly consists of protein and carbohydrate regions.

The protein core (accounting for 20% of mucin) is arranged into two regions. It has a central glycosylated region consisting of repeats rich in serine, threonine and proline.[25] Another protein region is located at amino and carboxy terminals. These second type of regions consist of few O-glycosylated and N-glycosylated sites and high cysteine content (>10%).[30]

The carbohydrate regions account to 80% of the total mucin and are too responsible for expansion of mucus gel. [31] They consist of N-acetylgalactosamine, N-acetylglucosamine, fucose, galactose and sialic acid. The oligosaccharide chains of mucin are attached to the protein cores by O-glycosidic bonds to the hydroxyl side chains of the amino acids serine and threonine. [25] They are arranged in bottle brush configuration around the protein core as shown in figure 1-5.

The glycosylated regions are highly hydrophilic while the protein moieties are hydrophobic in nature.[25] This makes the mucin accessible to both hydrophilic and hydrophobic interactions.[32] Mucin glycoproteins also have highly negatively charged surfaces due to high sialic acid and sulphate content.[33] The presence of high degree of glycosylation and negative charges causes the persistence length of mucin to increase making mucus more rigid.[28] Mucin can have other various interactions(as shown in figure 1-5) such as electrostatic interactions (carboxyl group), hydrogen bonding (sulphate, hydroxyl group) and Vander Waal interactions.

The mucins can be divided into membrane bound and secreted mucins. These mucins have different structural features. Membrane bound mucins have transmembrane and cytosolic domains that help in localization to surface of plasma membrane.[34] They can be proteolytically cleaved and spliced resulting in their subsequent release. On the other hand, secreted mucin is first stored in intracellular secretory granules after their synthesis. They are then released by regulated exocytosis process.[35] Secreted mucins are larger than the membrane bound mucins. As mentioned earlier, the mucin has cysteine rich domains. These cysteine rich domains link with each other through disulphide bonds, which are then glycosylated within clustered serine/threonine rich tandem repeat domains.[36] This leads to formation of mature mucin dimers. These dimers then further multimerise to form long linear oligomers that leads to crosslinked and adhesive mucous layer.[37]

Except mucin glycoproteins, mucus also consists of other different types of components such as water which makes up 95% of the mucus. It also consists of salts such as Na^+, K^+, Ca^{2+} and Cl^-. Lipids such as fatty acids, cholesterol, phospholipids are also present in mucus. The

proteins serving a defense function such as lysozyme, immunoglobulins and growth factors are also found in mucus.[25]

The genetic makeup of mucin is also equally important. Most of the mucin genes (19) denoted by MUC have been partially sequenced and identified.[25] Out of them, MUC5AC is the mucin gene most consistently reported to be upregulated during airway inflammation in humans and in animals.[38] This gene is also found expressed in conjunctiva, stomach, nasopharynx and lungs. MUC6 is expressed in stomach, duodenum, gall bladder, pancreas and kidney. Thus, different mucin genes are expressed in different types of tissues they are present in. This diverse expression also leads to difference in mucus between these tissues, making mucus more dynamic in nature.

Mucoadhesion and mucus turnover are of particular interest in the pharmaceutical sciences as for improving non-invasive drug delivery[39]. In mucoadhesion, prolonged contact and retention of the dosage form/drug delivery system at the mucosa improves uptake of the payload and thereby improves bioavailability and pharmacological effect [40]. The mucoadhesion is a result of various interactions of mucus through electrostatic interactions, hydrogen bonds, Vander Waal forces, hydrophilic and hydrophobic interactions.[39] There are various theories postulated about the mechanism of adhesion that exploits the mucus' capability of formation of these various interactions mentioned above.[41]

The mucus turnover is also another important process that affects the drug delivery. Mucus is constantly secreted, then shed, discarded and recycled. It is a part of dynamic nature of mucus. The mucus turnover rate is short and measured in minutes to hours.[42] Since the mucus is constantly secreted and shed, the drug formulations should be designed to penetrate the mucus at rate higher than mucus turnover cycle.[43]

Thus, the mucus networks are not permanent, as the many different interactions between and within mucus components are constantly shifting. The hydrophilic and negatively charged regions and hydrophobic cysteine-rich regions along the mucins gives rise to a heterogeneous charge profile, and many possible interaction sites with other mucins or mucus components and foreign particles.

1.1.3. Mucociliary Clearance

In lungs airway, there are other type epithelial cells that are covered by cilia. These ciliated cells have a layer of mucus above them. Each cilium is about 6μm long and 250nm wide.[44] However, the size of cilia depends upon its location in the respiratory tract. For instance,

in larger respiratory airways, cilia are longer and are more densely packed. The amount of cilia is also different at different regions of the respiratory tract, but general distribution is 10 cilia per cm.[45]

In addition to ciliated cells, the underlying epithelium also has secretory cells. These cells produces mucin, antimicrobial molecules and immunomodulatory molecules to protect the epithelium.[46] The secreted mucin along with water, lipids, salts and free proteins form the mucus, which by the help of periciliary liquid is elevated above the ciliary region. The underlying periciliary layer (sol layer) allows the cilia to beat and also prevent the mucus(gel layer) from fusing to the epithelium layer.[47]

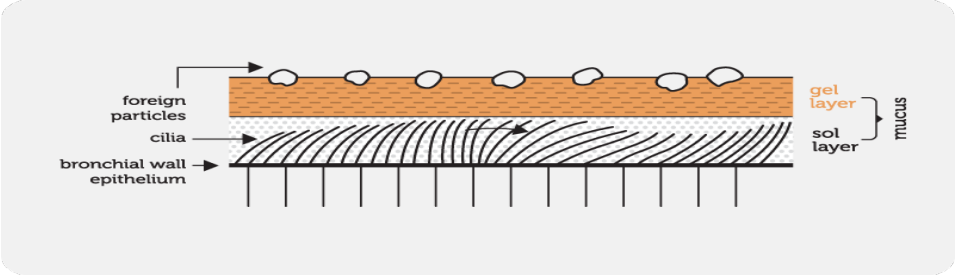

Figure 1-6 : depiction of mucociliary clearance in presence of foreign particles in the mucus layer.[48]

In lungs, the cilia beat in a synchronized manner and propel out the foreign materials that are trapped, out to the pharyngeal region.[49] For mucociliary clearance to function correctly and efficiently, the rheology of mucus should be in normal in the sense that the dissipation of force of tip of cilia to the epithelial region should result in bulk transport of entire mucus depth as cohesive mass, towards the pharynx.[50] In diseased condition, mucus rheology and the mucociliary clearance itself might get changed. Then, the incorrect or irregular dissipation of force would cause the failure in removal of entrapped particles in the lungs mucus. Thus, understanding the rheology of mucus and physiology of mucociliary clearance is very important.

As mentioned before, mucus can interact with non-mucus material through variety of interactions as hydrophilic, hydrophobic, electrostatic, hydrogen bonding and Vander Waal interactions. When nanoparticles are administered they may get trapped into the mucus through those interactions. This may be desired when the nanoparticles have landed in preferred target. However, off target deposition of nanoparticles may have undesirable effects to the normal functions of mucus and mucociliary clearance. Therefore, it is essential to understand the effects of drug delivery system (nanoparticles) on the mucus properties, rheology and mucociliary

clearance so that the drugs administered, themselves, do not alter rheology and affect the clearance mechanism.

1.1.4. Barrier Properties of Mucus

It can be known from characteristics of mucus that it may have multiple barrier properties. As a result, not all particles administered through mucus can penetrate it and reach their target. They face different barrier imposed by the mucus layer, and these barriers would depend not only on the properties of mucus but also on the characteristics of particle as well. For instance, the diffusion of hydrophobic drug particle through the mucus is limited due to overall hydrophilic nature of mucus and hydrophobicity of drug.[42]

The barrier properties of mucus can be understood on the basis of following:

- The interactive barrier:

It is already known that the mucus has capability to have interactions such as hydrophilic, hydrophobic, electrostatic, hydrogen bonding and Vander Waal interactions. It thus forms multiple low affinity interactions with substances present at the mucosal surfaces.[51] For instance, when hydrophobic nanoparticles such as PLGA land on mucus, there are multiple hydrophobic interactions between PLGA and the naked protein core of mucin. These hydrophobic nanoparticles when coated with hydrophilic molecules such as nucleic acid and chitosan, the hydrophobic interactions can be reduced, thus leading more improved transport through the mucus.[52]

- Dynamic Barrier

It is known that mucus is also continuously secreted and shed, therefore the drugs delivered through the mucosal surfaces, must penetrate the mucus layer before it is shed.[28] The balance between mucus secretion and degradation or shedding impacts the mucus thickness. It's lifetime ranges from minutes to hours. The fastest turnover response is seen in region with thinnest layer of mucus.[42] Due to this dynamic barrier, the drugs successful in adhering to mucosal surface may never reach the epithelium and the systemic circulation.

Mucociliary clearance is also an important phenomenon in maintaining the dynamic barrier. As mentioned before, in airway mucus, the underlying cilia beat in synchronized manner and remove the foreign particles trapped in the mucus.

- Steric Barrier:

The mucus is a complex mesh containing hydrophobic, hydrophilic interactions, hydrogen bonds, electrostatic interactions and disulphide linkages. These interactions lead to

heterogeneous pore size distribution. The mucin network can act as a size exclusion filter for large compounds. [51] For instance, in a research it was found that, nanosphere of size larger than 560nm could not penetrate the mucus layer in cystic fibrosis sputum. [53] In addition, the viscoelasticity of the mucus could also contribute to steric barrier properties of mucus. For instance, viscoelasticity of airway mucus is altered in case of asthma, where the mucin concentration is increased by seven times. [54] This increase in concentration leads to increased barriers when delivering the drugs through mucus.

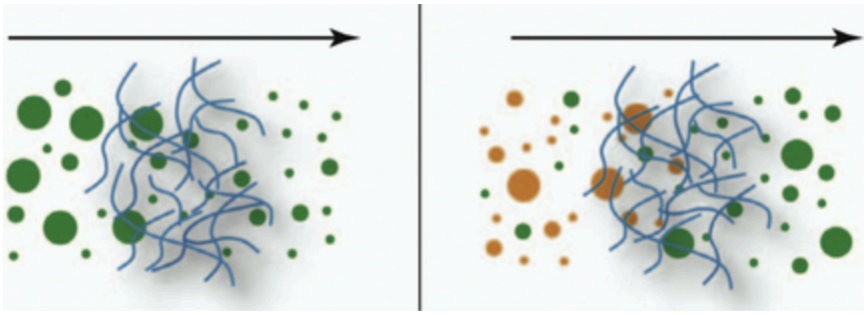

Figure 1-7 The steric barrier (left) prevents the particle diffusion based on size (only small particles pass through). The interactive barrier (right) allows particles with certain surface properties (green particles)[55]

Thus, it is very important to understand the mucus in terms of its barrier properties, rheology, composition and physiology. This helps to create a novel nanoparticle that can deliver effectively without getting blocked from mucus layer.[51]

1.1.5. Pig Gastric Mucus

Pig Gastric Mucus (PGM), is the mucus native to pig stomach. It is similar to the airway/lung mucus as it shares one of the major gene product, muc5ac with tracheobronchial mucus.[37] This mucus is chosen for this study, on the basis of its similar rheological behavior to that of lungs airway mucus. PGM also has a physiology similar to that of lung mucus. Thus, the fate and effects of experimental drug delivery system in PGM can be deduced to that of intact mucus of tracheobronchial region.

In this thesis, PGM mucus washed in 0.9% saline was used, thus making a modified PGM. The extracted PGM was washed, centrifuged and scrapped to remove any grit and food particles before the experiments. The protocol of this preparing modified PGM is presented in Appendix A.1. In comparison to commercial mucin, the modified PGM was more hydrated but

still contained materials in addition to glycoproteins that are responsible for change in rheological properties.[56]

Nevertheless, PGM could be considered one of the acceptable sources of mucus in terms of availability, easiness and amount. Other artificial mucus models cannot be compared to PGM without addition of non-mucus components.[57] And the addition of those component alter the mucus rheology by a large extent.

1.1.6. Nanoparticles

In the nano-systems, the active molecules are either dissolved, entrapped, encapsulated or chemically attached to nanoparticles. The characteristics, size and design of these nano-systems are of particular importance for drug delivery systems.[58] Generally, biodegradable nanoparticles made of synthetic hydrophobic amphiphilic polymers such as PLGA, PLA-PEG (poly lactic acid-poly ethylene glycol) are generally used.[59] Nevertheless, the nanoparticles could be polymers or proteins, lipid based molecules, magnetic materials and nucleic acid complexes.

The use of nanoparticle has tremendous influence and benefits when it comes to drug delivery. The major advantages include its size, surface characteristics, and release of active agents at particular site at pharmaceutically optimal dose and rate.[60] There are some disadvantages as well. For instance, the small size and comparatively large surface area could also lead to aggregation. Also, there are problems of poor bioavailability, instability in circulation and toxicity.[61] Therefore, variety of packing, combination techniques and surface modifications are employed for more effective drug delivery nanoparticles.[62]

In this thesis, polymer based, lipid based and nucleic acid complexes are used. All of the formulations have hydrophobic Poly(lactic-co-glycolic acid) (PLGA) core as shown in the figure below.

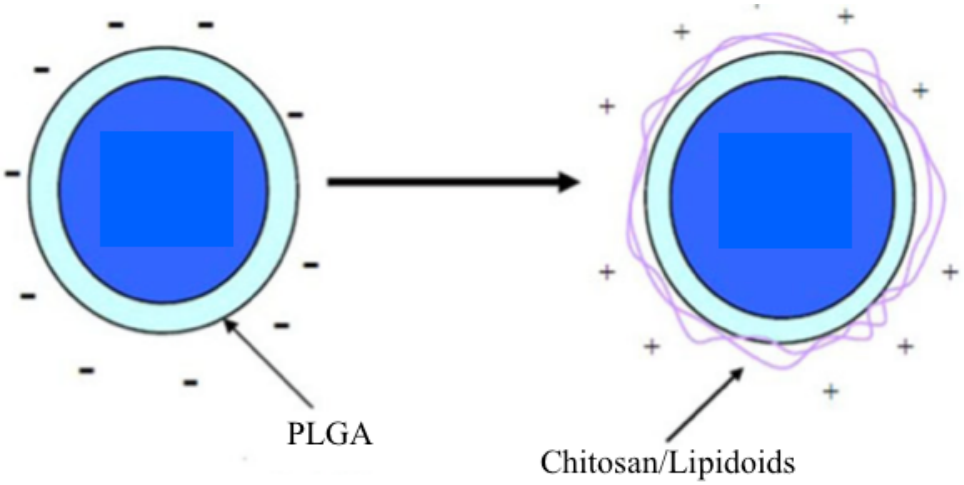

Figure 1-8 The surface coating of PLGA by Chitosan or Lipidoids. This coating leads to change in zeta potential of the nano particle with appreciable change in particle size. Modified from Wang et al.[63] siRNA loading occurs on the coated particle's surface.

As mentioned before, PLGA has limited applicability because of its hydrophobic nature, therefore they are coated by hydrophilic materials such as lipidoids and chitosan. These positively charge materials enhance the stability of the particle, increase the cellular and muco-adhesion and possibility of employing ligands to the surface, for targeting. In addition, these coatings help in loading of negatively charged nuclei acid such as siRNA, thus making nucleic acid complexes.

1.1.6.1. Poly(lactic-co-glycolic acid) PLGA:

PLGA (Poly(lactic-co-glycolic acid)) is a biodegradable polymer which has endogenous metabolites (lactic and glycolic acid) as its monomers. Therefore, PLGA can be easily removed through citric acid cycle once inside the body.[64] PLGA is used in different co-polymer compositions. In this particular study, PLGA 75:25 was used. The composition includes 75% lactic acid and 25% glycolic acid. Polylactide-co-glycolide (PLGA) is widely used as suitable matrix for drug delivery nanoparticles due to its ease of preparation, commercial availability at reasonable cost, versatility, biocompatibility, and hydrolytic degradation into absorbable and physiologically compatible products.[65] Moreover, the co-polymers results in low toxicity during the use of PLGA in drug delivery.[66] PLGA is, thus, approved by United States Food and Drug Administration (US FDA) as well as European Medicine Agency (EMA) for drug delivery use in human.

In mucus, the hydrophobic PLGA performs hydrophobic interactions with mucus.[67] These type of interactions occur between methyl group of PLGA and protein core of mucin. PLGA with higher content of lactic acid (75% in this case) are very less hydrophilic in nature.[68] This is because the PLA(Polylactic acid) has methyl side groups which are hydrophobic instead. In addition, PLGA can also interacts with the positive moieties present in the mucus such as positively charged amino acids.[69]

PLGA nanoparticle could be formed by adsorbing the drug on the surface of the particle or entrapping the drug inside the core of nano capsule.[70] In this thesis, the siRNA are desired to be delivered to lungs, but PLGA alone cannot bind to siRNA. This is because the hydrophilic and negatively charged siRNA do not interact with hydrophobic PLGA. Therefore, hydrophilic and positively charged materials such as chitosan and lipidoids are coated on the surface of PLGA as shown in the figure 1-8. This coating makes the loading of siRNA possible creating nucleic acid complexes. These surface modifications also have tremendous benefits from increasing biocompability to designed use in specific environments.[71] Nevertheless, it has been also reported that chitosan and lipidoids make the PLGA surface more chemically active.[63]

1.1.6.2. Chitosan

Chitosan is a linear polysaccharide composed of randomly distributed β-(1–4)-linked d-glucosamine and n-acetyl-d-glucosamine, which is positively charged at physiological pH.[72] Chitosan is conventionally obtained by de-acetylation of chitin.[73] Chitin which is a long chain polymer of N-acetylglucosamine, is found in cell walls of fungi, exoskeletons of crustaceans (eg: crabs, lobsters and shrimps) and insects, and internal shells of cephalopods (eg: squid and octopus).[74] The deacetylation of chitin results in protonated amine group in chitosan resulting in the polycationic property. The difference in deacetylation process results in chitosan with variable F_D (fraction of deacetylation).[75]

Furthermore, chitosan is capable interactions including hydrogen bonding (hydroxyl and amine group), hydrophobic interactions (acetyl group) and electrostatic interactions (protonated amine group).[76]

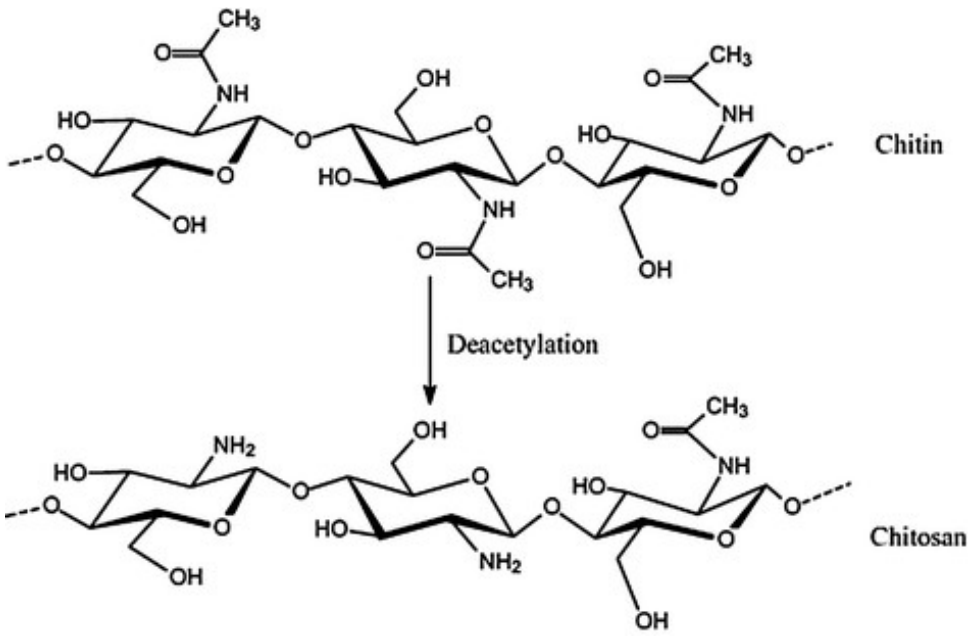

Figure 1-9 The above figure explains the mechanism of formation of chitosan from chitin through deacetylation. The deacetylation has occurred in sugar 1 and 2. Deacetylation produces chitosan of variable fraction of deacetylation (F_D) residues in the chain [77]

It has been reported that chitosan could be easily modified for a nano-system containing genetic material (siRNA), peptides and drugs.[78] Chitosan delivery system (in solution or powder) have high efficacy in delivering peptides and nucleotides through the mucus membranes. [79] Moreover, chitosan on the surface of PLGA nanoparticle act as a glue to hold loaded siRNA molecules. As mentioned before, chitosan also increases the stability of the particle, increase the cellular and muco-adhesion and possibility of employing ligands to the surface, for targeting.

After the particle lands on the mucus, there could be electrostatic interaction between positively charged chitosan and negatively charged mucin. This interaction occurs between mucin and protonated amine regions of chitosan[80]. There are also hydrogen bonds due to presence of amine and hydroxyl groups in chitosan. Also, the acetyl group in chitosan could have hydrophobic interactions with the mucin.[81] But, the chitosan used for this experiment is highly deacetylated (upto 90%), therefore hydrophobic interactions between chitosan and mucin are scarce.

1.1.6.3. Lipidoids

In addition to Chitosan-PLGA complexes, lipidoids are used as another approach to load siRNA onto the surface of nanoparticles. In the approach used in this thesis, new class of lipid like delivery molecules called lipidoids are used to make lipid-polymer hybrid nanoparticles

(LPNs) with polymers such as PLGA. Lipidoids are synthesized through the addition of alkyl-acrylates to amines.[82] Generally, these lipdoids are developed from modified chemical methods, that are designed to obtain a large and diverse library of lipidoids. [82] From this library, several further generations of lipidoids that can facilitate high levels of siRNA are created.

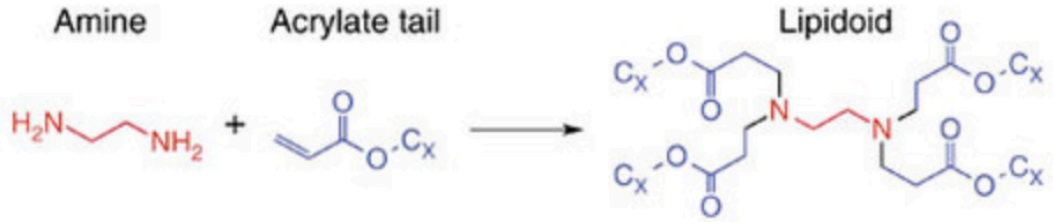

Figure 1-10 Formation of lipidoid by combination of amine and alkyl-acrylates.[83]

The lipid molecules mediate association within the nanoparticles in various ways[84]. The lipidoids are generally hydrophilic and cationic in nature. Therefore, there may be electrostatic interactions between the negatively charged carboxyl group in mucin and positively charged amine groups in the lipidoids.[82,84] Moreover, there could also be hydrophilic interactions between lipidoids and glycosylated region of mucin.

It has been reported that the efficiency of PLGA particle is very poor compared to lipid based carriers.[85] Therefore, lipid based cationic substances such as dioleoyltrimethylammoniumpropane (DOTAP) or lipidoids are combined with PLGA to obtain higher delivery efficiency for siRNA.[86] Thus, the lipid-polymer hybrid nano particles(LPNs) are created. These LPNs are created in different ratios with most desirable being weight/weightt lipid to PLGA ratio of 15:85. These formulations have resulted in high siRNA loading, sustained release, enhanced transfection efficiency and higher therapeutic efficiency.[87]

In this thesis, however, lipidoids are sandwiched between siRNA and PLGA cores. Lipidoids coating in PLGA makes the loading of siRNA possible. As with chitosan-PLGA formulations, hydrophilic and positively charged lipidoids are coated over the hydrophobic PLGA core. This coating interacts with hydrophilic and negatively charged siRNA and holds the nanoparticle together.

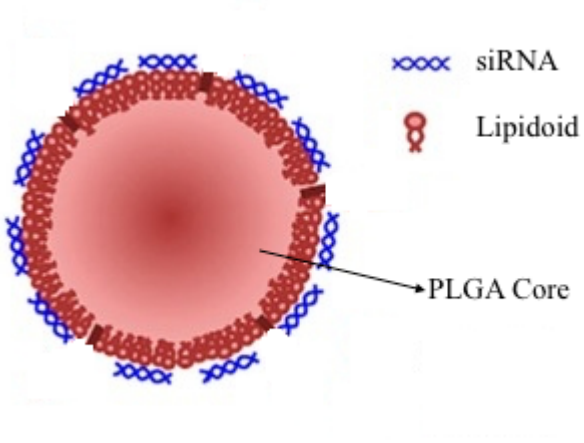

Figure 1-11 Architecture of PLGA nano particle coated with lipidoids and siRNA loading on the surface. Modified from Gandhi et al., 2014.[88]

1.1.6.4. Nanoparticles with siRNA

The use of siRNA in drug delivery is an appealing approach of drug delivery system. There is tremendous potential of siRNA as a drug. This is because of involvement of siRNA in RNA interference mechanism, gene therapy and anti -sense technology. [89]

However, cellular uptake of siRNA is very poor due to rapid degradation of naked siRNA by nuclease.[90] Even though viral vectors are frequently used, there are complications due to unnecessary inflammation and unwanted immunogenicity[91] Moreover, during drug delivery in airway and lungs, the nanoparticles are targeted to the underlying epithelium and the mucus layer acts as a barrier to siRNA. Therefore, there is need of efficient delivery systems. Thus, it is essential to have a nanoparticle formulation that can deliver the siRNA intact. The engineering and design of particle itself plays an important role in this regard. For instance, a particle with siRNA loaded on the surface could be used. However, use of only PLGA with siRNA is not desired because the delivery efficiency of PLGA nanoparticles for siRNA is very poor.[85] Therefore, PLGA core are coated with chitosan (or lipidoid) to efficiently load the siRNA. It has been reported that chitosan incorporated PLGA particles are also efficient for delivering smaller molecules such as antisense DNA and DNA itself.[92]

As seen in the figure 1-12, siRNA can also be involved in different types of interactions ranging from electrostatic to hydrophobic and hydrogen bonds.[93] The electrostatic interaction between chitosan coating (cationic) and siRNA (anionic) protects the siRNA from any degradation.[94] Thus, the use of chitosan or lipidoid to combine PLGA and siRNA is much desirable because of their positive charge, biodegradable nature and biocompatibility.[95]

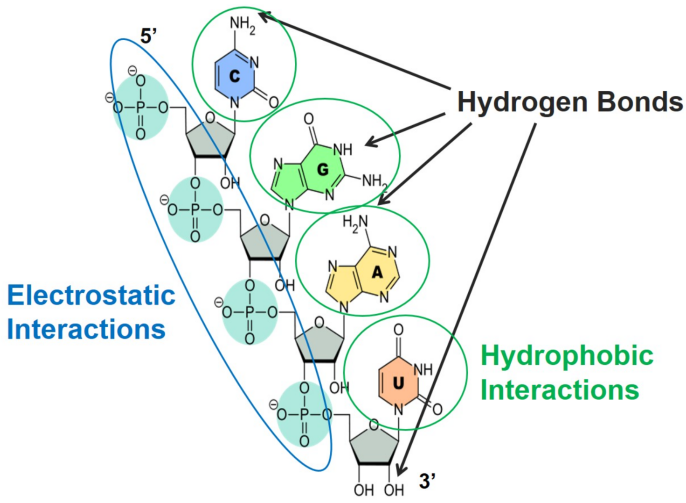

Figure 1-12 Structure of siRNA depicting the various kinds of interaction that siRNA is capable of[93]

1.2. Aim of thesis

The scope of thesis comes under COMPACT research focused to reduce delivery and targeting bottlenecks for developing novel innovative biopharmaceutical based medicines. In COMPACT, for drug delivery in lungs, all the nanoparticles have alveolar region as their delivery target.

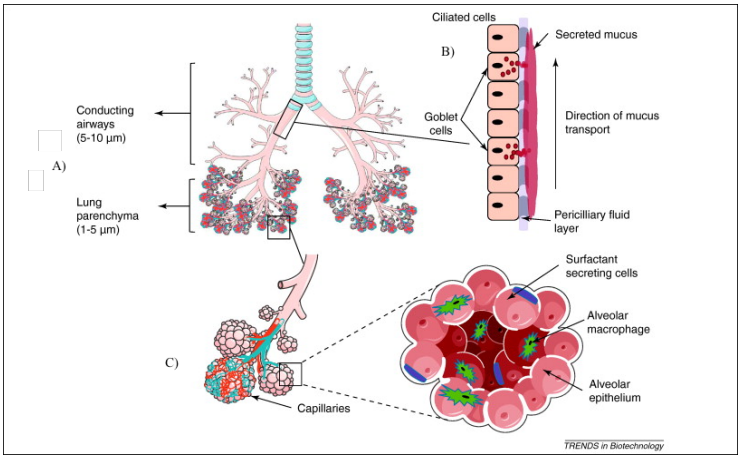

Figure 1-13 A) Depiction of different parts of the airway and alveoli. B) The presence of mucus and ciliated cells in airway (off target). C)The drug delivery target, alveolar epithelium and alveoli.[96]

The aerosol technology, at present, are not precise enough. Thus, during drug delivery, which is focused in the deep lungs (alveoli), some of the nanoparticles could get trapped in the airway (off target). Generally, the mucociliary clearance in the conducting airways is capable of removing particles and helping to keep the gas exchange surface of the alveoli clean. However, this clearance by cilia could depend upon the properties of the mucus layer above it.

And, the deposition of nanoparticles on the mucus layer could change the mucus properties, which may alter the dissipation of force through cilia. As a result of which, large number of nanoparticles may deposit in airway mucus after series of doses, without being cleared. Thus, it is desirable to understand if the trapped nanoparticles (in off targets) would not alter the normal mucus properties and its rheology. The mucus rheology may get altered by interactions of the trapped particles with mucin.

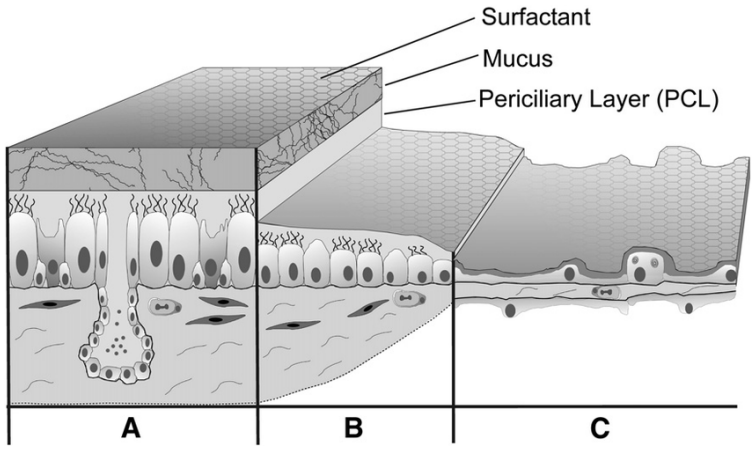

Figure 1-14 Layers of material in different parts of the lungs airway: A) Barrier due to presence of surfactant, mucus and periciliary layer in upper airways B) Decrease in thickness of the layer in region near deep lungs C) Presence of surfactant and epithelial layer in the alveoli[97]

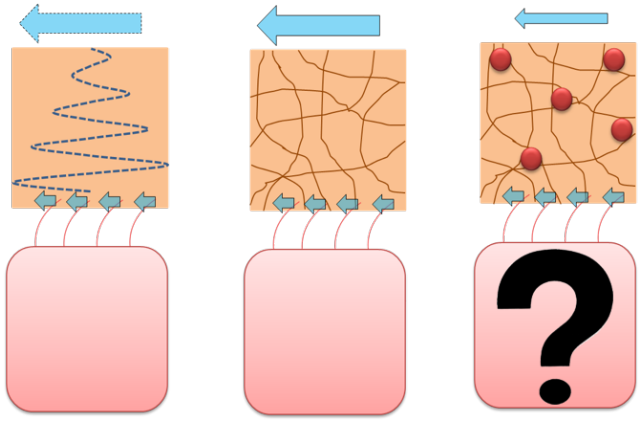

Figure 1-15 The fate of nanoparticle and mucus rheology after addition of nanoparticles[108]

Thus, the aim of this thesis to investigate the alteration in mucus rheological properties due to nanoparticles. Now to evaluate the alterations, the rheological properties of mucus are studied in presence of various drug delivery systems. The rheological properties of mucus vary as a function of shear stress, shear rate and time scale. We know that at macro-level, mucus is referred to as viscoelastic because of its flow (viscosity) and deformation properties (elasticity). Therefore, the rheological study of mucus focuses on its viscoelastic properties (viscous or loss

modulus and elastic or storage modulus and the phase angle) and stress-strain relationship of the mucus in presence of nanoparticles. Thus, in this thesis, these characteristics of mucus will be studied in a set of oscillatory experiments presented in methodology.

1.3. Technical Introduction

1.3.1. Rheology and Rheometer

All material flow when subjected to some stress over a period of time. In other words, under stress materials show some deformation. Rheology is a study to understand this phenomenon. In rheology, material is deformed and we measure how the material responds to the deformation. This deformation could be small or large which can be caused by compression or stretching or shear.[98]

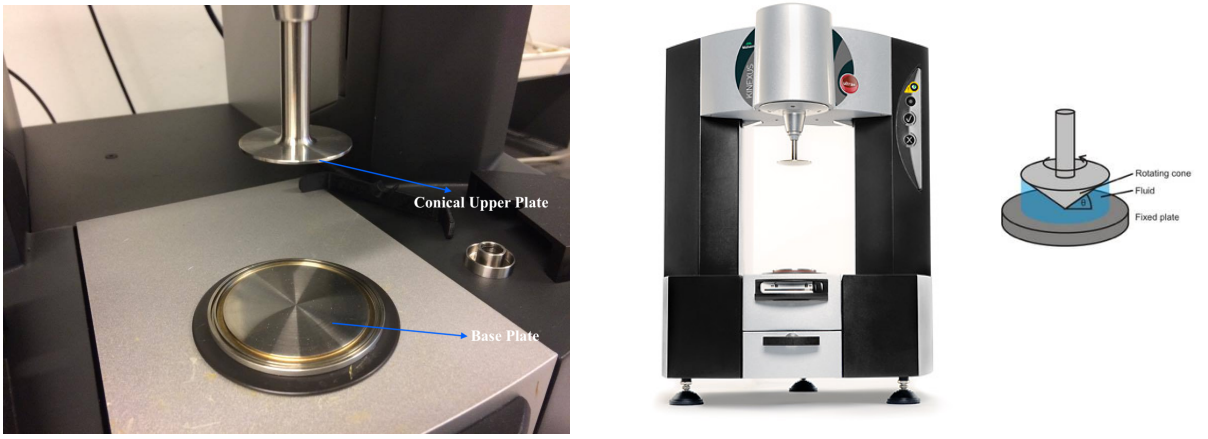

Figure 1-16 Kinexus Rheometer Ultra+[99] and Cone Plate[100] measuring system used in rheometer with θ as cone angle. It has rotating cone and a fixed plate. θ >4° are considered substandard. Represented as CP 25-1, where 25 is diameter of cone in mm and 1 is the cone angle.

A rheometer has a stationary plate (base) and a rotating plate (conical upper plate) as shown in the figure 1-16. When strain is applied to the sample by the rotating plate(cone), the sample dumps force on to the stationary plate, which is measured by the upper rotating plate. There are several types of rheometer that are used for analysis of the materials.[101] Cone/plate (CP) measuring systems (shown in figure 1-16) are one of the widely used system because of its uniform shear conditions in the entire conical gap. In absence of the cone (plate/plate arrangement), the shear rate is highest on the rim and zero at the center of the plate. As angle of inclination increases towards the rim, the shear decreases. This leads to uniform shear at the

center and rim or the plate. Also, in cone plate arrangement, only a small amount of sample is required for analysis.

The rheometer, however, can be stress controlled or strain controlled. A stress controlled rheometer applies a torque to either control the stress at a desired level or to drive the strain to a desired amount. In such instruments, the stress is the independent variable and is applied to the upper rotating plate. Also, the stress can be increased in a gradual, controlled way until the yield point is reached.[102] Moreover, in practice most stress controlled instruments use a feedback loop to maintain the strain constant.[103] However, in strain controlled instruments, the strain rate is independent variable. Thus, to observe the corresponding stress, yield point must be surpassed in such instruments.[102]

During rheological studies, the deformations can be created according to the purpose of study. For instance, viscosity measurement includes the continuous deformation of the sample. In this study, however, oscillatory deformation is used on the material (for instance in strain sweep).

1.3.2. Oscillatory Experiments

The oscillatory shear experiments are performed by subjecting the specimen to sinusoidal strain at an angular frequency and determining the response as steady sinusoidal stress.[104] From this type of experiment, elastic component (storage modulus G') and viscous (loss modulus G") can be determined along with phase angle(δ).

G' represents the stored deformation energy in the material while G" characterizes the deformation energy dissipated through internal friction when flowing. G' depicts the elastic properties of a material. Higher the value of G', the material is more solid like.[105] G" on the other hand depicts the viscous characteristics of the material. Therefore, higher the value of G". the material is more viscous. G' and G" are both measured in Pa.[105] And, the phase angle (δ) is the phase difference observed between the applied strain wave and resulting stress wave or vice versa. It is measured in degrees (°).[106]

The analysis in the study are based on G' and G" because the relative values of G' and G" in a frequency sweep help to understand over what frequency range (or time scale), is the material viscous or elastic dominant. Moreover, the phase angle, obtained from an oscillation test, can be used to understand the extent of viscous or elastic behavior of the viscoelastic material. In some cases, complex viscosity is used for analysis. But in the range where G'>G",

it is useless because at low frequencies, complex viscosity approaches infinity.[104] This means that material is more solid and would not flow.

For, viscoelastic solids, G'>G" is due to the strong interactions or links inside the materials. While, for viscoelastic liquids, G">G, where there are no such strong links or bonds but instead are uncrosslinked polymers with entanglements. tanδ describes the loss or damping factor(phase angle) which is the ratio of the two portions of viscoelastic behavior.[104]

$$\tan\delta = G''/G'$$

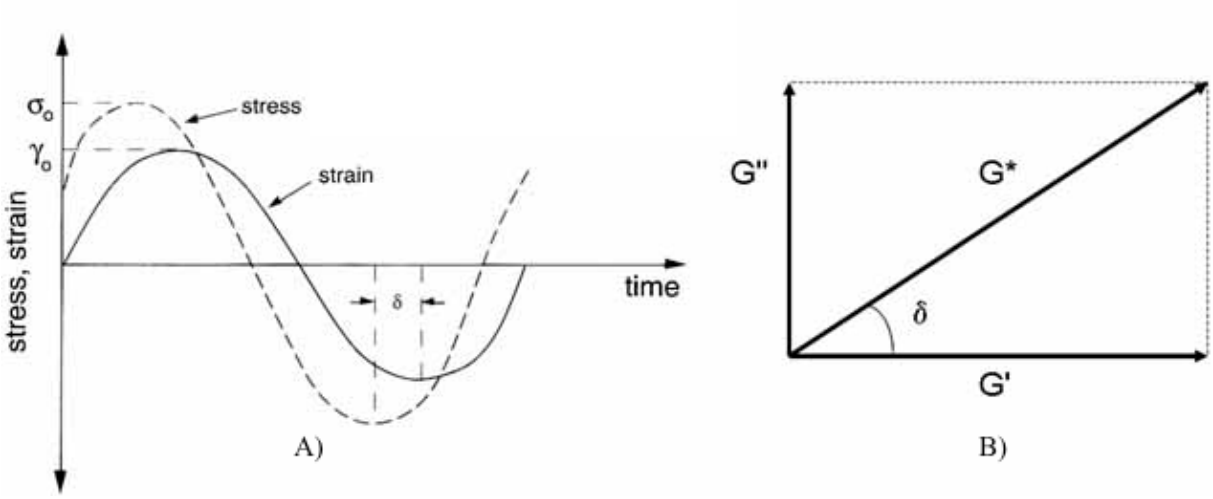

Figure 1-17 A) The difference in applied strain and stress response with the phase difference. B) Relation between phase angle (δ), elastic modulus (G') and viscous modulus (G")[107]

There are different series of measurements that can be employed to analyse the rheology of the material. In this study, mucus being the sample, a predefined series of measurements were done as shown in the methodology.[108]

In a normal oscillatory experiment, if a sinusoidal strain wave is applied to a perfectly elastic material, the strain and the resulting stress would share the same phase(0°). Similarly, for a perfectly viscous material, the phase difference would be exactly 90°. All the materials that are described as viscoelastic, have phase angle between 0 and 90°.[109]

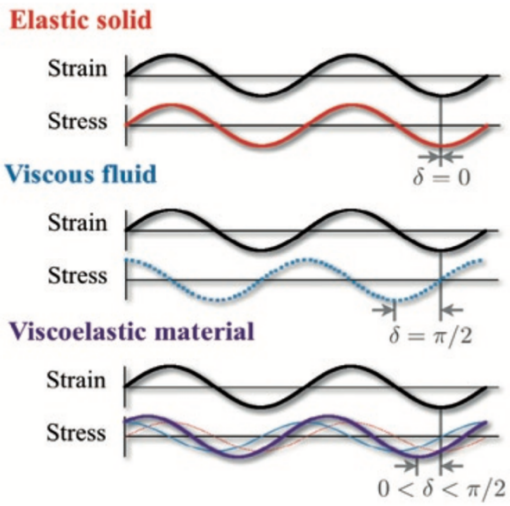

Figure 1-18 Stress response to oscillatory strain for elastic solid, viscous fluid and viscoelastic material [110]

In such experiments, oscillatory strain is applied to the material and then the resulting stress is measured or the shear stress could be applied, and the strain could be measured.[109]

In this study, the following sequence of steps are performed.

1. Single Frequency Oscillation
2. Frequency Sweep
3. Relaxation
4. Strain Sweep

The single frequency oscillation is performed to observe the time dependence of the characteristics of the material. It is important to know if the sample characteristics such as G', G" and phase angle change over time. This step done at a fixed frequency of 1Hz and at 1% strain (within LVR).

The frequency sweep on the other hand describes the frequency dependence of the material. It helps to gather information on the inner structure of the material along with its behavior.[104] The behavior observed in frequency sweep is due to time dependent entanglements, cross links and interactions in the material.[106] Frequency sweep help to actually determine if the material is a true gel or a concentrated solution or a dilute solution on the basis of relationship between G' and G". [111] For instance, a true gel would have moduli that is independent of the change in frequency, with G'>G" and display no entanglement effects.[106] Frequency sweeps are performed within the linear viscoelastic region (LVR) over a range of frequency, for instance from 0.01 to 10Hz. The oscillation frequency is actually the reciprocal of the time taken by rotating plate of rheometer to complete one sinusoidal oscillation. [111]

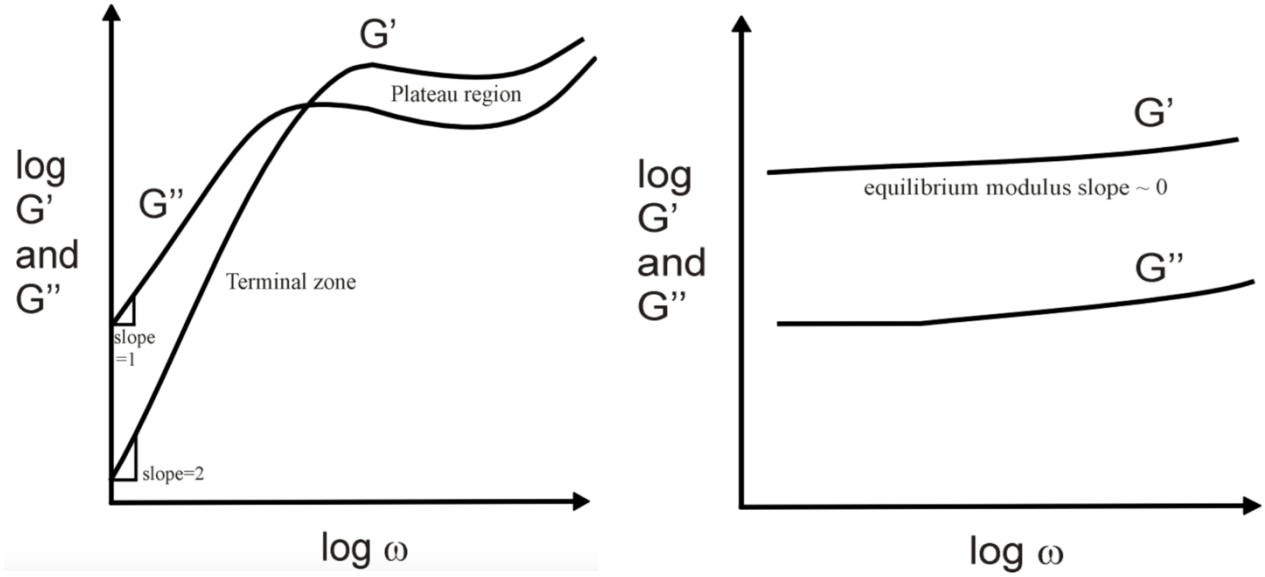

A) B)

Figure 1-19 The behavior of A) entangled network and B) gel system during the frequency sweep represented by logω [106]

After the frequency sweep, the materials are deformed with target strain of 5% and the relaxation pattern was observed. The materials are deformed, therefore, force/stress required to maintain the deformation at constant value is measured with time. The molecules of material move relative to one another. Thus, the stress required to hold material at constant deformation decays away with time.[112] In a normal stress relaxation of a viscoelastic material, the stress is function of the viscoelastic property of the material. The viscoelastic liquid if given enough time to reach equlibrium, will reach zero stress. While, a viscoelastic solid will reach a equilibrium stress at values greater than zero. Similarly, for a pure viscous liquid, the stress would become zero in no time, as the liquid would flow even at small deformation. And, closer the equlibrium stress is to the initial stress, the material is more elastic dominant.[111] In relaxation, the strain remains constant and the stress decreases, therefore, the moduli (G' and G") of viscoelastic material also decrease with increasing time. For viscoelastic liquids, if the testing is sufficiently long, complete stress relaxation can be observed. While viscoelastic solids do not relax completely, they approach an equilibrium stress asymptotically.

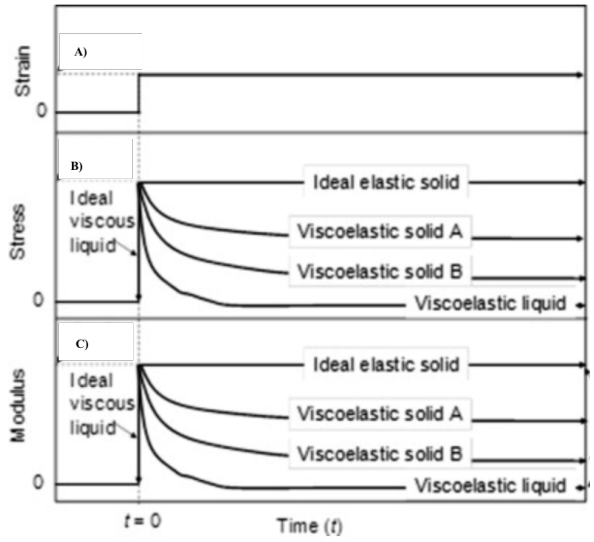

Figure 1-20 A) Application of mechanical strain which is held constant B) Force/stress required to maintain target strain for different materials C) Change in modulus for different materials when constant strain is applied [111]

Strain sweep on the other hand is performed under an oscillatory deformation to determine the upper limit of the non-destructive range. This range called the Linear Viscoelastic Range (LVR), is the region where the material properties such as G' and G" are independent to applied strain. The end point of LVR is known as the limit of linear viscoelastic region. However, after the upper limit of the range, the material starts to show dependence on the applied strain, that is the material starts to get deformed. For instance, in the figure 1-21, a non-linear strain dependence is observed after LVR.

Thus, this step is vital to determine the LVR region for the material. In strain sweep, the strain is increased gradually keeping the frequency constant.[104] For instance, 1Hz frequency is used for our experiments.

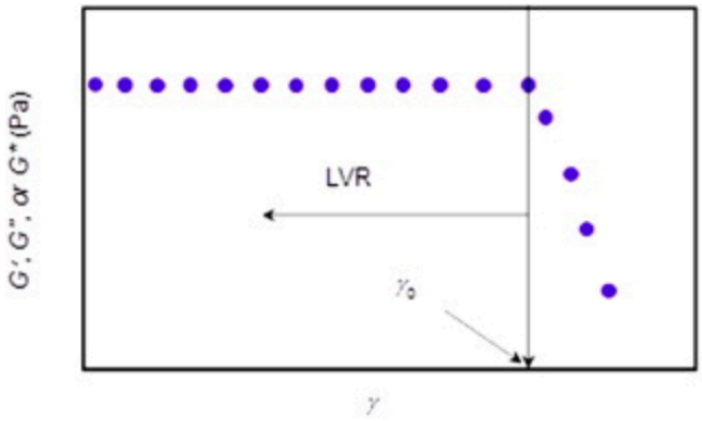

Figure 1-21 Behaviour of a material under a deformation range (strain sweep). The linear viscoelastic region (LVR) is also depicted with γ_0 as limit of LVR[111]

1.3.3. Zeta-potential and Z-Average Size

Zeta potential is a parameter used for characterizing the electrochemical equilibrium on the interfaces. Zeta potential depends upon the surface properties of the substance. It also gives an idea about aggregative stability of the substance.[113] For instance, the particle with high zeta potential repels other particle with greater electrostatic repulsion, making the whole system stable. However, as the zeta potential of the particle decreases, they are prone to aggregation. Thus, understanding zeta potential is vital to understand the stability of the system. In this study too, the zeta potential of the nanoparticle formulations are tested to confirm their stability at different pH conditions. For the measurement of zeta potential, Zetasizer Nano ZS was used.

Zetasizer Nano ZS uses Dynamic Light Scattering Method (DLS). The basic principle behind this method is the use of light scattering. It is also effective in size characterization. DLS is used for its quantitative results. For statistical uncertainty of 1% requires measurement of over 10000 characteristic decay times of the correlation function is required.[114] This would lead to difficulty in measurement thus, the particles of small size are often underestimated.[115] Furthermore, in DLS, the primary signal may contain the scattering from the solution (due to biological matter or the nanoparticles suspended in). Therefore, there other parameters that influence the measurement are sedimentation, temperature and concentration. Thus, it is highly advised the sample should be stable during measurement. [115]

DLS measures the fluctuation in intensity of light due to Brownian motion of the particles leading to constructive and destructive interferences.[116] From observations of motion, diffusion coefficient in the solution and fluctuations of scattered lights, hydrodynamic size of the particles is achievable.[117]

The Stoke-Einstein equation describes this phenomenon: [117]

$$D = \frac{kT}{3\pi\eta d}$$

where d is the hydrodynamic diameter; k is the Boltzmann constant; T is absolute temperature; η is the viscosity of the solution.

It is known from Stoke-Einstein Equation that Brownian motion is related to the size of the particles. Thus, large particles move slowly and smaller particles move quickly. This means that the intensity of the speckle pattern in case of large particle will fluctuate slowly while the intensity for small particles will fluctuate quickly. As a result, a correlation can be developed between the particle size and movement or motion of the particle. After this correlation, this information is used to obtain the size distribution.[118] The decay rates for a number of size classes

are used to produce a size distribution which could be displayed in terms of intensity, number and volume.

A number of inferences related to quality of data can be made from the correlation graph. As mentioned before, the size of the particles relates to the time when decay starts. This means that the decay would be faster in case of smaller particles and slower for larger particles. Also, the gradient of the decay curve relates to the polydispersity of the sample. In addition, the intercept indicates the signal to noise ratio where values less than 0.1 are considered poor data.[117]

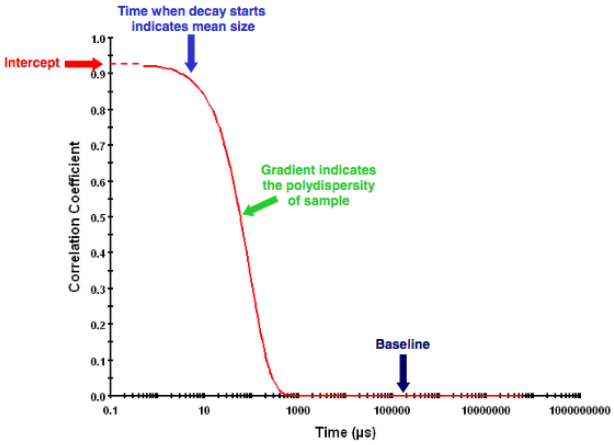

Figure 1-22 Typical Correlation graph from Zetasiser with arrows indicating different parts of the graph [119]

2. MATERIALS & METHODOLOGY

2.1. Materials

2.1.1. Pig Gastric Mucus (PGM)

The mucus used in this study was obtained from pig stomach. It was washed extensively in 0.9% saline to get rid of all non-essential materials, using the protocol presented in Appendix A.1. The mucus was stored at -40ºC at all times except before the use in rheological experiments. The modified PGM with nanoparticle formulations were kept at 4^0C overnight for rheological experiments conducted next day.

2.1.2. Saline

0.9% saline solution was prepared by dissolving Sodium Chloride (NaCl) in MiliQ water. This solution was used to wash the pig gastric mucus, thus forming modified PGM. The use of term PGM in this study actually means modified PGM, which has been washed in 0.9% saline.

2.1.3. Nanoparticles

Different formulations of nanoparticles were used for the experiments. Primarily, two sets of nanoparticles were obtained:

- The PLGA, Chitosan coated PLGA and siRNA were obtained from Helmholtz Institut für Pharmazeutische Forschung Saarland (HIPS), Germany with predetermined particle size, zeta potential and concentration (2mg/ml) in solution form. The nanoparticle formulations were:

Table 2-1 Z-average size, PDI, zeta potential and other details of nanoparticle formulations from HIPS.

Formulations	Z-Average (nm)	PDI	Zeta Potential (mV)	Remarks
PLGA	116-1±1.7	0.066±0.011	-23.3±0.007	Resomer (RG 752H 75:25)
Chitosan coated PLGA	120±2.6	0.133±0.02	28.2±0.2	Chitosan (Protosan UP CL 113)
siRNA	--	--	--	siRNA to np wt/wt ratio=1:50

- The nanoparticles obtained from Copenhagen University, Denmark with predetermined particle size, zeta-potential were in dry pellet form. The nanoparticle formulations were PLGA cores, Lipidoid coated PLGA and siRNA loaded Lipidoid coated PLGA.

Table 2-2 Z-average size, PDI, zeta potential and other details of nanoparticle formulations from CU

Formulations	Z-average (nm)	PDI	Zeta potential (mV)	Remarks
Blank PLGA NPs	185.6 ± 2.4	0.107 ± 0.006	-30.4 ± 2.3	Commercially available
Unloaded L_5 LPNs	196.3 ± 4.2	0.123 ± 0.017	+23.6 ± 1.8	Prepared at 15% (w/w) lipidoid content
siRNA-L_5 LPNs	243.8 ± 10.7	0.240 ± 0.054	+5.4 ± 0.4	siRNA equivalent to 40 μg

The important details following the nanoparticles from HIPS and CU have been presented in Appendix B.2.

2.2. Methodology

2.2.1. Load data analysis

The objective behind this analysis was to check if there is any pattern between the behavior of sample during loading and later oscillatory experiments.

After the sample had been loaded in the rheometer, the gap between upper and lower is recalibrated with the material on the lower plate. Thus, with the lowering of upper plate, the gap decreases and force applied to the material increases. The normal force starts to increase rapidly once the upper plate touches the material, and then reaches a maximum. After that the material starts to adapt to the force applied, therefore, the force applied by the material decreases. Finally, at the end of the measurement, the gap is at minimum.

Therefore, the contact gap, time for rise, end gap and maximum normal force were measured. The contact gap is the gap when the upper plate just touches the material. Therefore, it gives the height or thickness of the sample loaded on the lower plate of rheometer. The time of rise is the time taken to reach the maximum force applied to the sample. The end gap indicates the new height or thickness of material at the end of the measurement.

2.2.2. Rheological Measurements of Mucus control

The Pig Gastric Mucus (PGM) obtained was first washed properly and then, processed according to the protocol in Appendix A.1. This was done to remove food particles, grit and other undesired substances from the mucus. The washing was done in 0.9% saline. After

washing, aliquots of 1.5gm were prepared and stored in -40ºC. Thus, a modified PGM was used for the study.

Before rheological analysis, the stored mucus aliquots (1.5mg) were to be thawed and prepared by adding 200μl of 0.9% saline (to create controls) and stored at cold temperature (4ºC) overnight.

However, during preparation of mucus control, accidently 200μl saline was added to all of the PGM aliquots. Thus, later, when, 200μl of nanoparticle formulation would have been added to the PGM, the total volume added to PGM aliquot(1.5gm) would be 400μl. Therefore, it was necessary to check if addition of 400μl of solution in total would change the mucus rheology. Thus, following two control samples were compared with each other.

1. PGM (with 200μl 0.9% Saline)
2. PGM (with 400μl 0.9% Saline)

The subsequent rheological analysis was done 3 times in following sequence at 25ºC for each sample (1.5gm modified PGM). Each run consumed about 0.3gm of the modified PGM from the 1.5gm aliquot. CP 40-1 cone plate arrangement was used in Malvern Kinexus Rheometer for rheological analysis.

1. Isothermal temperature: 25ºC, 10 minutes
2. **Single Frequency Oscillation**: 1Hz, 1% Strain, 100 samples, Interval: 5secs
3. Isothermal temperature: 25ºC, 10 minutes
4. **Frequency Sweep:** 0.01Hz to 10 Hz, 1% Strain, 10 samples per decade, logarithmic sampling
5. Isothermal temperature: 25ºC, 10 minutes
6. **Relaxation:** Target Strain: 5%, rise time: 0.001secs, 10 samples per decade, maximum time: 30 minutes
7. Isothermal temperature: 25ºC, 10 minutes
8. **Strain Sweep:** 1Hz, 0.01-100% Strain, 10 samples per decade, logarithmic sampling

The detailed procedure of aliquot preparation and rheological analysis is shown in Appendix A.2.

2.2.3. Rheological Measurement of Mucus with nanoparticle formulations

As mentioned before, the Pig Gastric Mucus (PGM) obtained was first washed properly in normal saline and stored in -40ºC. Before rheological analysis, mucus aliquots (1.5mg with

200μl 0.9% saline) were prepared by adding 200μl nanoparticle formulation and stored at cold temperature (4ºC) overnight.

The nanoparticles from HIPS were all in solution form. Therefore, 200μl of formulations (for PLGA and Chitosan-PLGA) were simply pipetted out and loaded to PGM aliquot. However, it can be seen in table 2-1 that nanoparticle formulations from HIPS came without addition of siRNA. Thus, to create formulations siRNA loaded Chitosan coated PLGA, siRNA loading was done before whole nanoparticle formulation was added to the PGM aliquot. For this, to achieve 1:50 wt/wt ratio of siRNA:nanoparticle, 1.1μl of siRNA was added to 200μl Chitosan-PLGA formulation. The nanoparticle mix was mixed using a vortex and allowed to rest for 10 minutes and then, added to PGM, which was stored at 4^0C overnight before rheological analysis.

However, siRNA-L5-PLGA nanoparticles from CU came with preloaded siRNA formulations. Since, the formulations were in dry pellet form, they were dissolved in MiliQ water. 200μl nanoparticle formulation was then loaded to PGM and stored at 4^0C overnight before rheological analysis. Nevertheless, the particles from CU and HIPS both contained 8μg of siRNA in the siRNA loaded formulations.

Different combinations of nanoparticles were used in this experiment resulting in following test samples presented in Appendix B.1. For instance, for particles from HIPS, siRNA loaded nanoparticle contained 200μl of nanoparticle and 1.1 μl of siRNA. Moreover, other relevant details of nanoparticles from CU and HIPS can also be found in Appendix B.2

The subsequent rheological analysis (next day) was done 3 times in same sequence mentioned in section 2.2.1. CP 40-1 cone plate arrangement was used in Malvern Kinexus Rheometer. The detailed explanation of the steps of oscillatory experiments is provided in previous section.

2.2.4. Zetasizer Measurements

In this particular experiment, Zetasizer nano ZS (632.8nm) was utilized, that employed backscatter detection through the patented technology called Non Invasive Back Scatter (NIBS) operating at 175º angle. The pictorial methodology of measurement is given in Appendix E.1.Also, the procedure of performing the size and zeta potential measurements are given in Appendix A.4.

For size measurements, disposable cuvettes, with operating volume of 400μl, were used to load the samples inside the zetasizer. First, the comparison of aggregates mucin and modified pig mucus was done on the basis of size distribution. The experimental samples were prepared

at different concentrations: 1mg/ml, 0.5mg/ml, 0.25mg/ml, 0.125mg/ml and 0.0625mg/ml for mucin. However, the mucus sample were first diluted to be for the same concentrations as of mucin. But, when dry weight of mucus was measured, it was found that the presumed 1mg/ml of PGM solution actually was 9.8mg/ml. Thus, the subsequent concentrations were 4.9mg/ml, 2.45mg/ml, 1.225mg/ml and 0.6125mg/ml. These concentrations were obtained by serial dilution with MiliQ water.

Before rheological measurements, the nanoparticle formulations from HIPS (PLGA and Chitosan PLGA) were also analysed in zetasizer for their zeta potential in different buffers:

(i) 50mM Acetate Buffer (pH 5)

(ii) 50mM HEPES Buffer (pH 6.5)

(iii) 50mM Tris Buffer (pH 8)

(iv) MiliQ water

The siRNA loaded Chitosan-PLGA formulations from HIPS were not tested for zeta potential measurements because of low volume of siRNA available. The siRNA formulation could have been tested after high dilution of the formulation. But, the data of such measurements would have been too ambiguous. Nevertheless, Chitosan PLGA and PLGA nanoparticle solutions were diluted to (½)x concentration in series to reach 1mg/ml final concentration (stock concentration was 2mg/ml), in each of the above mentioned buffers and then zeta potential was analyzed. Folded capillary cells were used to load the samples inside the zetasizer with operating volume of more than 1ml. It was found during the experiments that letting the samples to rest in the cuvette caused sedimentation and altered the results. Therefore, the measurements were taken as soon as the samples were loaded.

The same nanoparticles from HIPS were also analysed for size measurements using the zetasizer. Additionally, the Chitosan PLGA siRNA nanoparticle formulation was tested for size measurement because this experiment required less volume (400μl for size measurements) of the test sample than zeta potential measurements (more than 1ml). Disposable cuvettes were used for size measurement experiments.

3. RESULTS AND DISCUSSION

3.1. Evaluation of Mucus Controls

As mentioned before, during preparation of mucus control sample, 200μl saline was added, mistakenly, to all of the PGM aliquots (each measuring 1.5gm) instead of just one. Later, when, 200μl of nanoparticle formulation would be added to the PGM, the total volume added would have been 400μl. So, it was necessary to check if addition of 400μl of solution in total would change the mucus rheology.

For this evaluation, two PGM control samples were created: first with 200μl saline solution and another with 400μl of saline solution. These two samples were tested independently in the rheometer. Since, the study is focused on effects on rheological properties, the comparison of two control samples was done based on the differences in their rheological properties. In addition, phase angle is considered to be more dependable for comparison as it is a measure of extent of viscous and elastic behavior of material. Finally, the comparison was done on the basis of percentage difference and student's t test.

3.1.1. Rheological Analysis of modified PGM with 200µl and 400µl of 0.9% Saline

Here, two different controls were tested independently by adding 200μl and 400μl of 0.9% saline to 1.5gm modified Pig Gastric Mucus. Each of controls went through the same experimental sequence. Three different runs were performed for each sample. And, the values used to plot all the graph below are mean derived from the three different runs. The timescale used to plot the graph are action time of the measurements.

3.1.1.1. Sample Load Data

The load data of both PGM with 200µl san 400µl saline were compared. This comparison was based on the gap after the material has been loaded and the normal force applied by the material once the upper plate starts squeezing the material.

For visual comparison, graphs from Run 1 of PGM with 200µl and 400µl saline are presented. The load data of rest of the runs can be found in Appendix D.1.

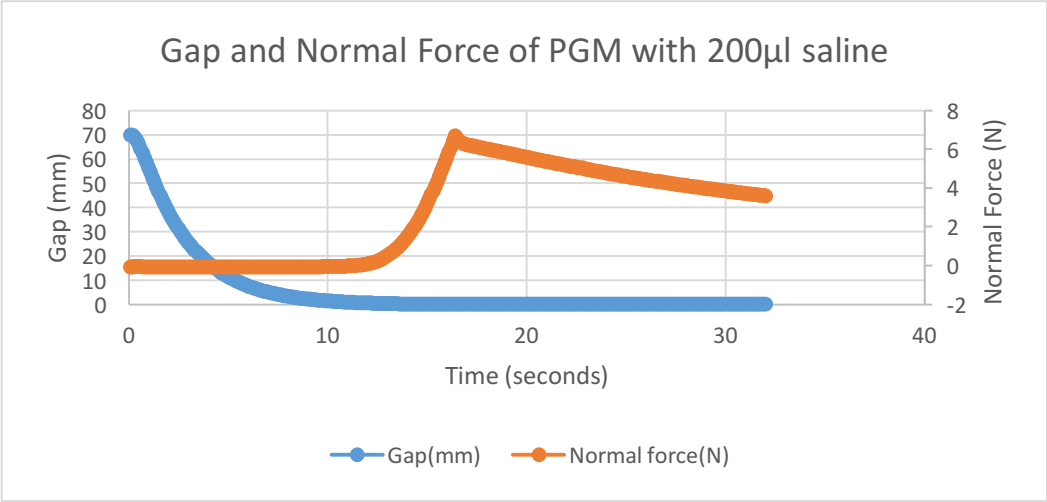

Graph 3-1 The change in gap and normal force over time for Run 1 of PGM with 200µl saline. The blue curve representing gap (mm) is plotted in primary Y axis, while orange curve representing normal force (N) is plotted in secondary Y axis, over time (seconds) in X axis

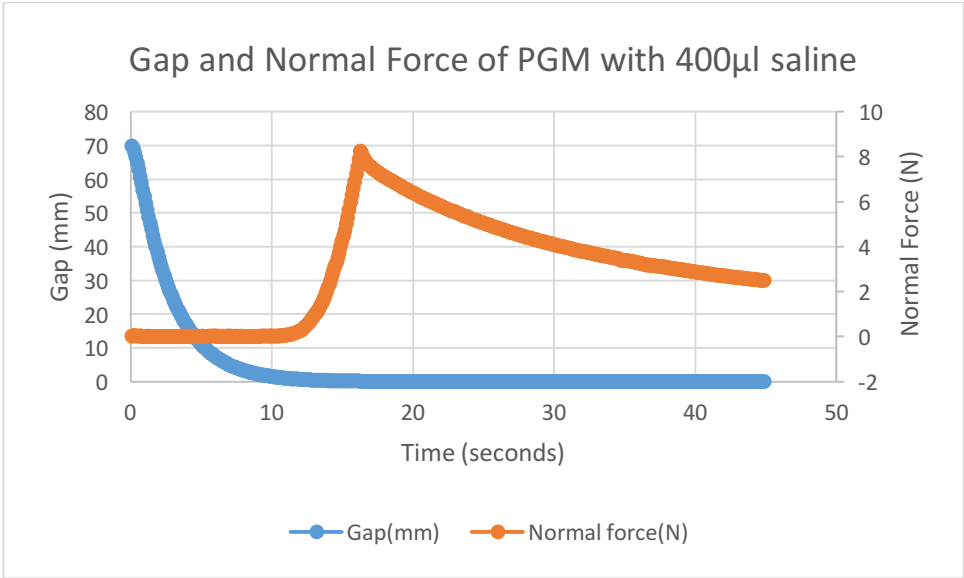

Graph 3-2 The change in gap and normal force over time for Run 1 of PGM with 400μl saline. The blue curve representing gap (mm) is plotted in primary Y axis, while orange curve representing normal force (N) is plotted in secondary Y axis over time (seconds) in X axis

It can be seen from the graphs that the curves of loading of the control samples does not have dramatic differences from each other. However, maximum normal force and rise time to reach that force, seems to be different from each other.

Nevertheless, the contact gap, time for rise, end gap and maximum normal force of all the runs of PGM with 200μl saline and 400μl saline are compared in the table below.

Table 3-1 Comparison of mucus controls in terms of contact gap, time for rise, end gap and maximum normal force. All the three runs performed for each sample have been presented.

Sample	Run	Contact Gap (mm)	Time for rise (s)	End Gap (mm)	Maximum Normal force (N)
PGM with 200μl saline	1	0.838	5.1	0.026	6.7
	2	2.25	7.4	0.026	6.3
	3	2.35	7.5	0.026	5.9
PGM with 400μl saline	1	1.68	6.7	0.026	8.2
	2	2.8	8	0.026	9.07
	3	2.25	7.4	0.026	7.9

From Table 3-1, it can be seen that the contact gap is variable for three different runs of the same material. For instance, for PGM with 200μl saline, the contact gaps are 0.83, 2.25 and 2.35mm. The contact gap represents the height or depth of the sample load. The variable contact gap could be because of the way the sample was loaded on the base plate. Moreover, the PGM used was not completely homogenized and thus, the mucus itself could have been highly variable due to presence of aggregates. A statistical correlation coefficient of 0.99 was found between contact gap and time of rise for both PGM with 200μl and 400μl saline. It was obvious that for a sample with small contact gap (depth or height of the loaded sample), the instrument takes less time to reach the maximum force.

Nevertheless, it was observed that more normal force was applied by PGM with 400μl saline than PGM with 200μl saline. The maximum normal forces can be compared in the graph below:

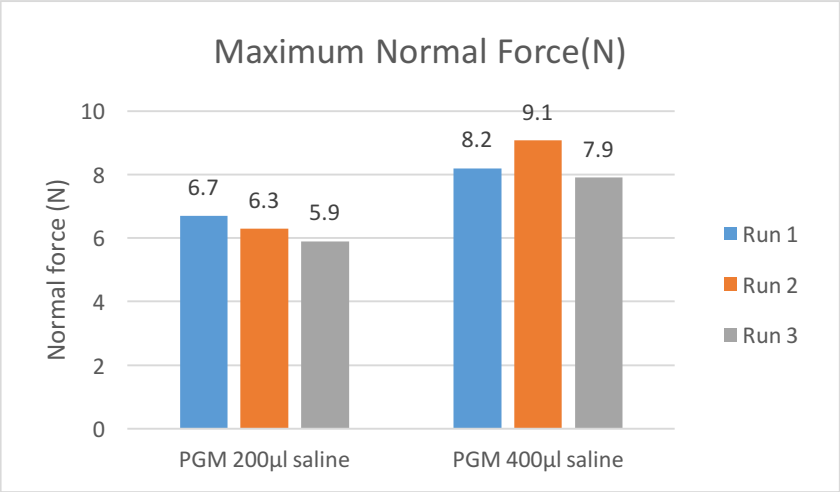

Table 3-2 Comparison of Maximum Normal Force of PGM with 200µl saline and PGM with 400µl saline for all the three runs. The values above the bar represent the normal force in each run for each sample in Newton

Here, it can be seen that the PGM with 400μl saline had greater maximum normal force in all the three runs than PGM with 200μl saline. This increase might or might not be related to the viscoelasticity and normal force of the material during frequency sweep. For instance, the material with highest normal force during loading could have high or low G' during frequency sweep. Therefore, these normal forces during loading were compared to G' and normal force in frequency sweep for all the runs, as discussed in section 3.1.1.3.

Except for the difference in the maximum normal force, no other conclusive differences were seen between PGM with 200μl and 400μl saline.

3.1.1.2. Single Frequency Oscillation

This is an essential step to see if the PGM controls' moduli and phase angle are in apparent equilibrium. This step was performed for around 9 minutes at single frequency of 1Hz and at 1% strain which within the linear viscoelasticity region (LVR).

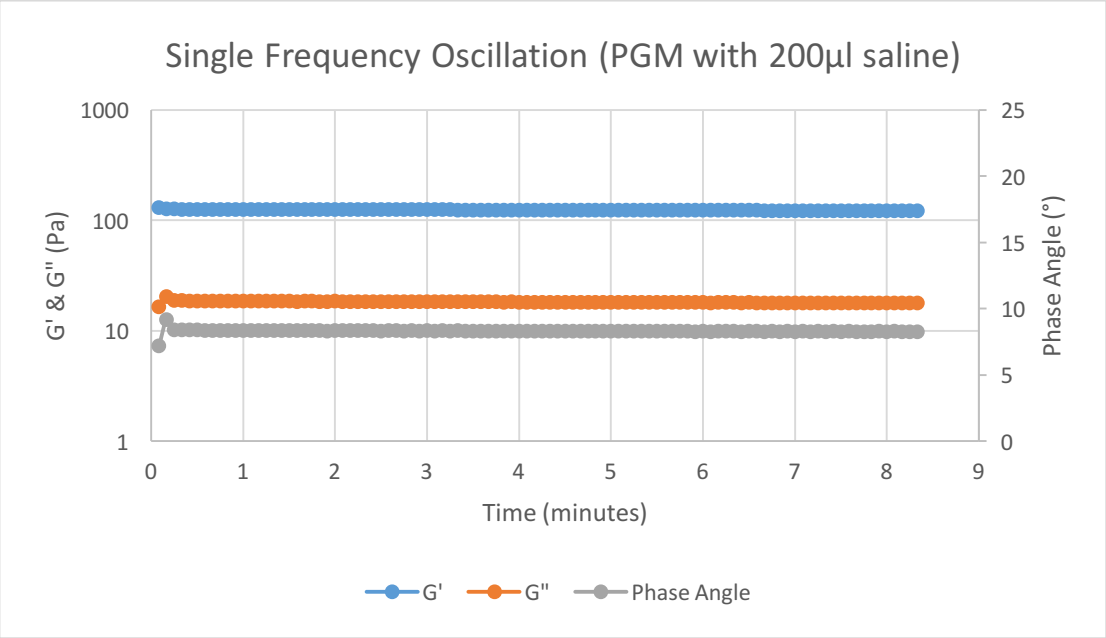

Graph 3-3 Single Frequency Oscillation of PGM with 200µl of 0.9% Saline, showing apparent equilibrium of G' and G" over tested time period. The moduli axis is in log scale while phase angle is plotted in secondary x axis.

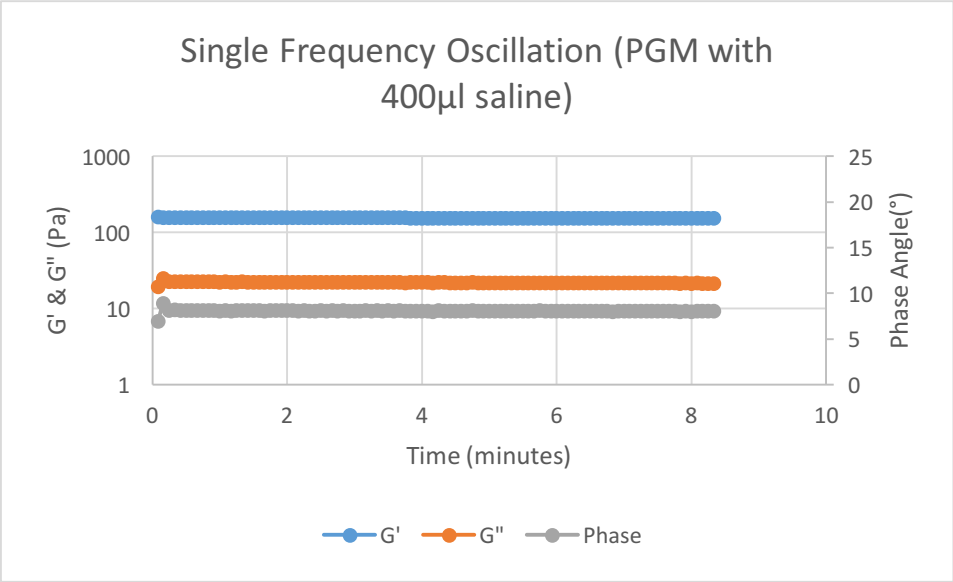

Graph 3-4 Single Frequency Oscillation of PGM with 400µl of 0.9% Saline, showing apparent equilibrium of G' and G" over tested time period. The moduli axis is in log scale while phase angle is plotted in secondary x axis.

It can be observed from the graphs that for both the samples: PGM with 200μl saline and 400μl saline, the moduli as well as phase angle are in equilibrium and do not change over time.

For instance, from graph 3-3, the difference in elastic modulus (G') at 3 and 8 minutes, for PGM with 200μl saline is just 1.9%, as seen in table 3-3. Similarly, the difference in phase angle is 1.2%. Thus, it can be said that the moduli and phase angle were in apparent equilibrium over the tested time period.

Table 3-3 Comparison of G' of PGM with 200µl saline at 3 minutes and 8 minutes. The comparison is done by percentage difference.

Time(minutes)	G' (Pa)	Percentage Difference
3	125.5	1.9%
8	123.1	

Similarly, from graph 3-4, the difference in G' for PGM with 400μl saline at 3 and 8 minutes is 2.1% as seen in table 3-4.

Table 3-4 Comparison of G' of PGM with 400µl saline at 3 minutes and 8 minutes. The comparison is done by percentage difference.

Time(minutes)	G' (Pa)	Percentage Difference
3	155.5	2.1%
8	152.23.	

And, for phase angle, at the same time period, the percentage difference is 0.9%. Thus, the moduli and phase angle were in apparent equilibrium for PGM with 400μl of saline as well.

Therefore, it can be said that the moduli and phase angle did not change for both of the controls over time and were in apparent equilibrium. Also, it can be seen that the elastic component (G') of shear modulus is higher than the viscous component (G"). This implies that the sample behaves as viscoelastic solid. However, more could be concluded about this property during later analytical steps.

3.1.1.3. Frequency Sweep

This step was done at a frequency range from 0.01 to 10Hz at 1% Strain. As mentioned earlier, 1% strain was known to be within the LVR. Both of the samples, PGM with 200μl and 400μl 0.9% saline were subjected to frequency sweep from 0.1Hz to 10Hz.

In the graphs, the values below 0.1 are omitted because of low signal to noise ratio.

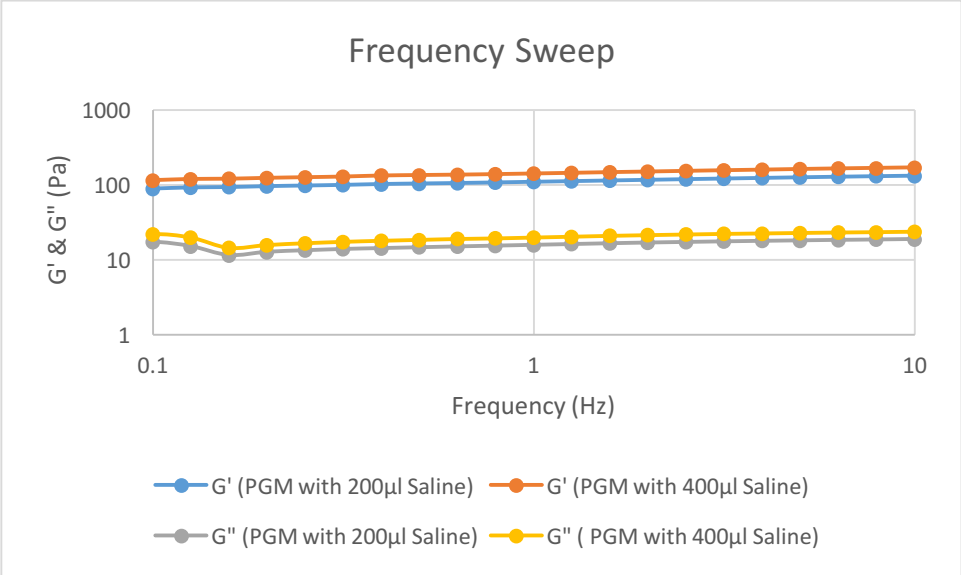

Graph 3-5 Elastic Modulus (G') and Viscous modulus (G") of PGM with 200µl and 400µl saline, over the frequency sweep from 0.1Hz to 10Hz. Both of the axes are in log scale.

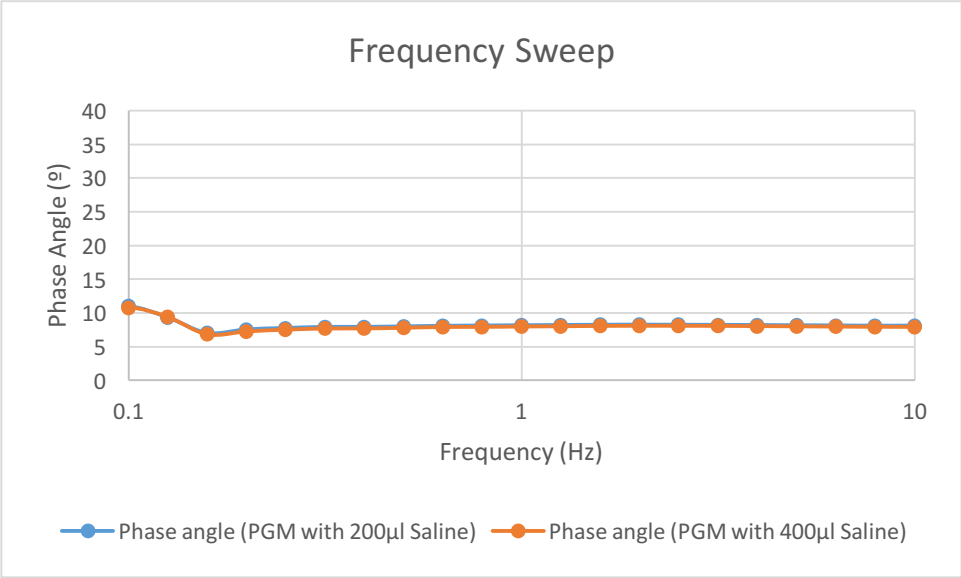

Graph 3-6 Change in phase angles of PGM with 200µl and 400µl saline, over the frequency sweep from 0.1Hz to 10Hz. The frequency axis (x-axis) is in log scale.

It can be seen from graphs 3-5 and 3-6 that both of the samples showed similar reaction to the applied frequency range. It can clearly be seen that there is increase in moduli and phase angle as the frequency is increased from 0.1 to 10Hz. This indicates that the samples are frequency dependent.

More specifically, from graph 3-5, at larger frequencies (shorter time scale), the PGM is more elastic. However, at smaller frequencies (longer time scale), the elasticity of the material decreases. This indicates the presence of timescale dependent interactions that are higher at shorter timescale and decreases at longer timescale. From graph 3-6, it can be seen that the phase angle is high at longer time scale (lower frequency) which then decreases. This depicts the more viscous nature of the material, that is mucus, flows when given enough time. However, this is not relevant because mucus turnover clears the mucus well before such timescale could be reached.[42]

From the graph 3-5, for both PGM with 200μl and 400μl saline, G'>G" with no signs of crossover. Thus, the both controls show characteristic of a gel system with phase angles of 8.17º (PGM with 200μl saline) and 7.98º (PGM with 400μl saline). Now, the samples, PGM with 200μl and 400μl saline were compared at 1Hz frequency. The results are presented in the table below:

Table 3-5 Comparison of G' and phase angle (at 1Hz) of PGM with 200µl saline and PGM with 400µl saline. The comparison is done by percentage difference.

Sample	G'	Difference	Phase Angle	Difference
PGM with 200μl Saline	110.30 Pa	22%	8.17	2.3%
PGM with 400μl Saline	141.96 Pa		7.98	

From the table 3-5, at 1Hz frequency, a difference of 22% is seen between the G' of the control samples. Similarly, at 1Hz frequency, the difference in phase angle is 2.32%. Since the difference in phase angle is very low, it can be concluded that the two samples do not show drastic differences in their viscoelastic properties.

Nevertheless, the statistical comparison of G' between the samples concluded that PGM with 200μl saline and 400μl saline were significantly different at 95% confidence level. Similarly, difference in phase angles was also significant. However, the error of mean of phase angles utilized in the student's t test were very low. For instance, phase angles of PGM with 400μl saline and 200μl saline were 7.98±0.02° and 8.10±0.009°. The distribution, on which the t-test is based on, was obtained from averages and error made up of just 3 runs performed for each sample. Thus, it could be debated that the two controls did not substantially differ from each other.

It was also interesting to observe, if the material had changed in terms of stress response to deformation during the time scale, after addition of extra 200μl saline. Thus, the stress values of this experiment are compared at the same frequency sweep from 0.1Hz to 10 Hz.

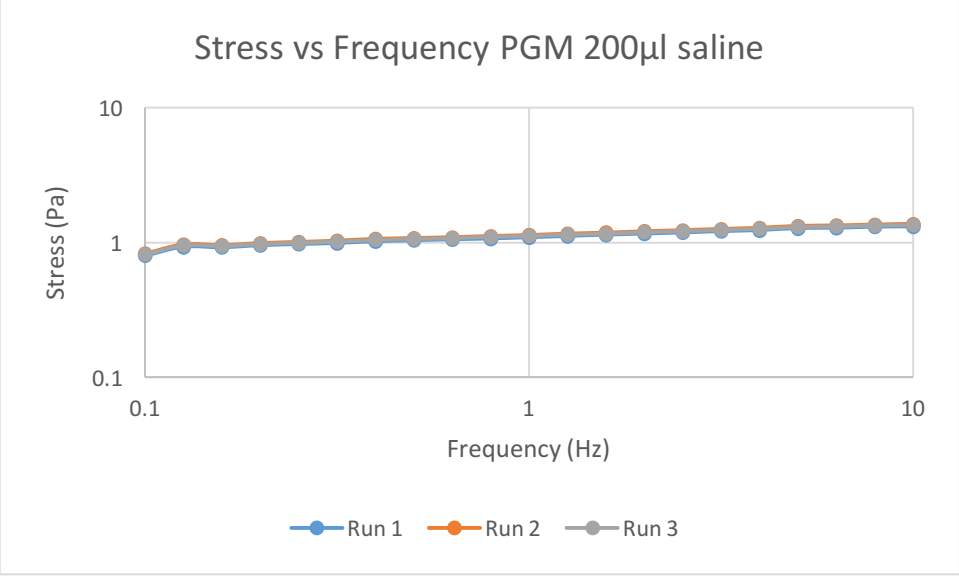

Graph 3-7 Stress developed in PGM with 200µl saline at 1% strain, during the frequency sweep from 0.1Hz to 10Hz.Both of the axes are in log scale.

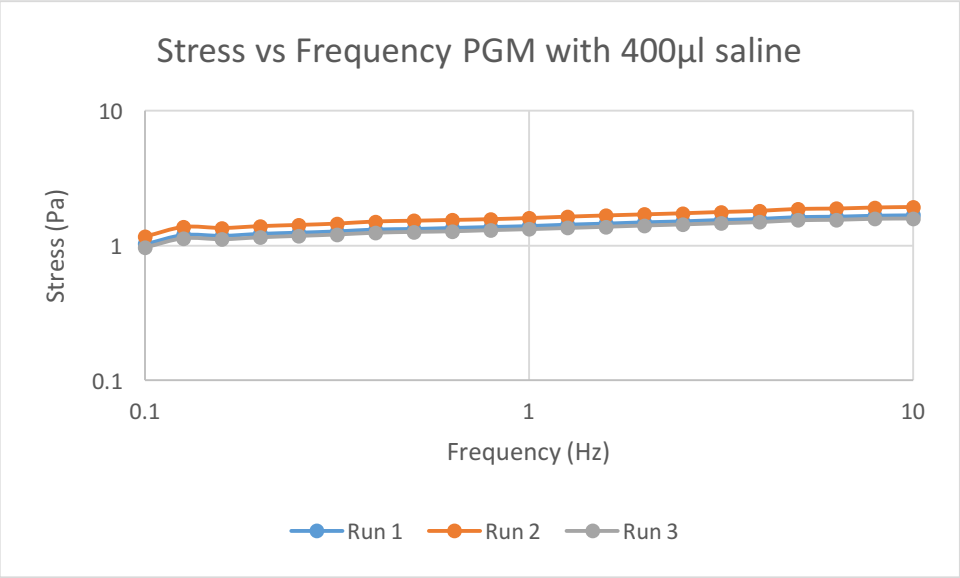

Graph 3-8 Stress developed in PGM with 400µl saline at 1% strain, during the frequency sweep from 0.1Hz to 10Hz.Both of the axes are in log scale.

From Graph 3-7 and 3-8, it can be seen that at deformation of 1%, the stress developed increases with increase in frequency from 0.1Hz to 1Hz for both PGM with 200μl and 400μl saline. The stress at 1Hz for PGM with 200μl saline and 400μl saline was 1.11±0.01Pa and 1.43+0.66 Pa respectively. It can be seen that PGM with 400μl saline develops slightly higher stress response than the PGM with 200μl saline. For better evaluation, a statistical comparison was done for stress values at 1Hz.

It was found that the stress at 1Hz for the two controls are significantly different at 95% confidence level. However, here as well, the error of the mean used in the t test were very small, probably leading to such difference. The distribution, on which the t-test is based on, is obtained from averages and error made up of just 3 runs performed for each sample. Thus, it could still be argued that the two controls did not differ from each other substantially.

As mentioned before, there could or could not be a pattern between the behavior of the material during loading and frequency sweep. Therefore, the maximum normal force of the material, G' and Normal force at the end (10Hz, short timescale) of frequency sweep are compared. The results are presented below:

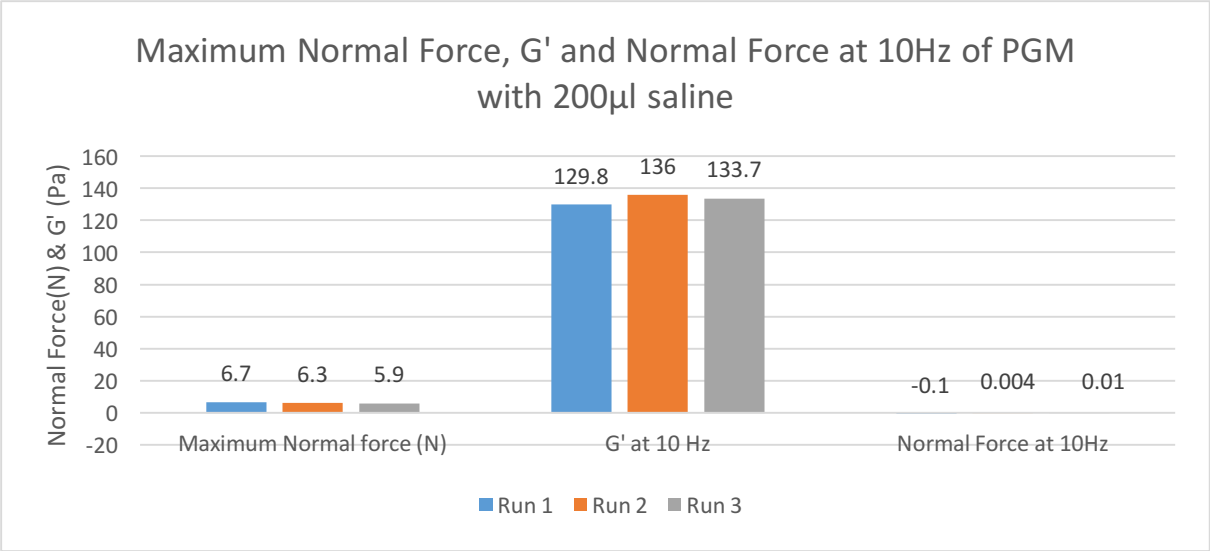

Graph 3-9 Comparison of Maximum Normal Force, G' and Normal Force at 10Hz for PGM with 200µl saline.

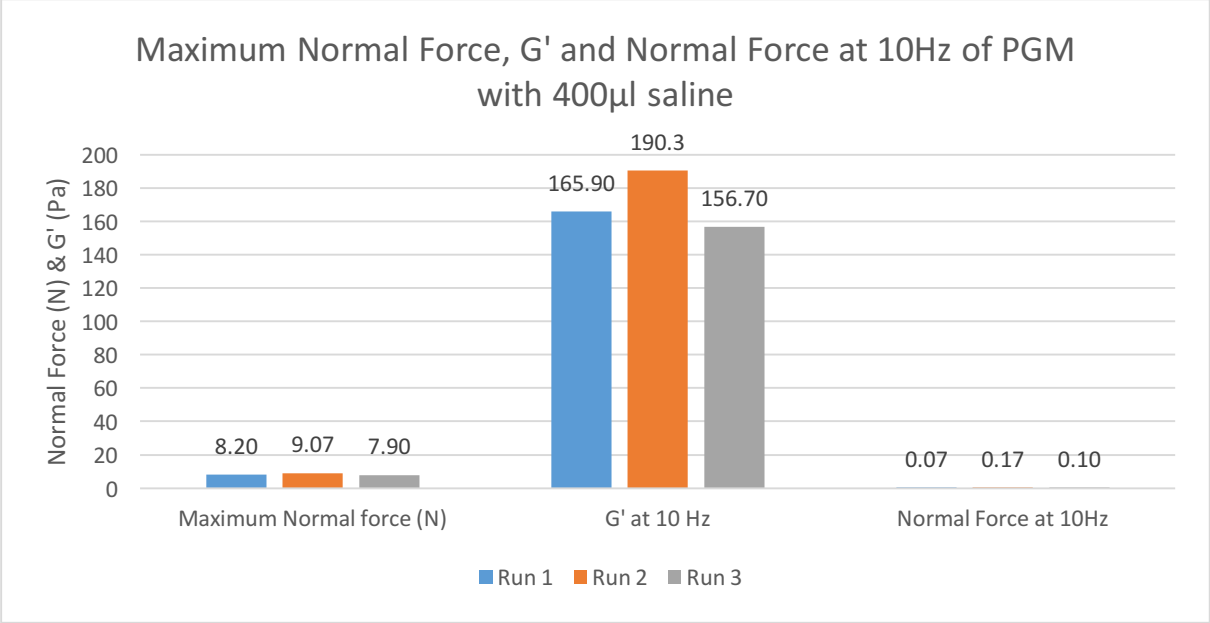

Graph 3-10 Comparison of Maximum Normal Force, G' and Normal Force at 10Hz for PGM with 400µl saline.

In graph 3-10, test sample in Run 2 for PGM with 400μl had highest maximum normal force (9.07 N), highest G' (190.3 Pa) and highest normal force (0.17 N) at the end (at 10Hz) of frequency sweep. However, sample in run 1 had second highest maximum normal force (8.2 N) during loading and second highest G' (165.9 Pa) but smallest normal force at 10Hz (0.07 N).

Similarly, the relations between these evaluated characteristics were random in PGM with 200μl as shown in graph 3-9. For instance, in run 1, the sample had maximum normal force (6.7 N), smallest G' (129.8 Pa) and smallest normal force (-0.1 N) at 10Hz.Therefore, it can be argued that the high normal force during sample loading might not be related to the timescale dependent interactions of the material.

3.1.1.4. Relaxation

In this step, the samples were deformed to the target strain of 5%. Force/stress required to maintain the deformation at constant value was measured with time. In relaxation, the molecules of material move relative to one another. And, the stress required to hold material at constant deformation, decays away with time.[111]

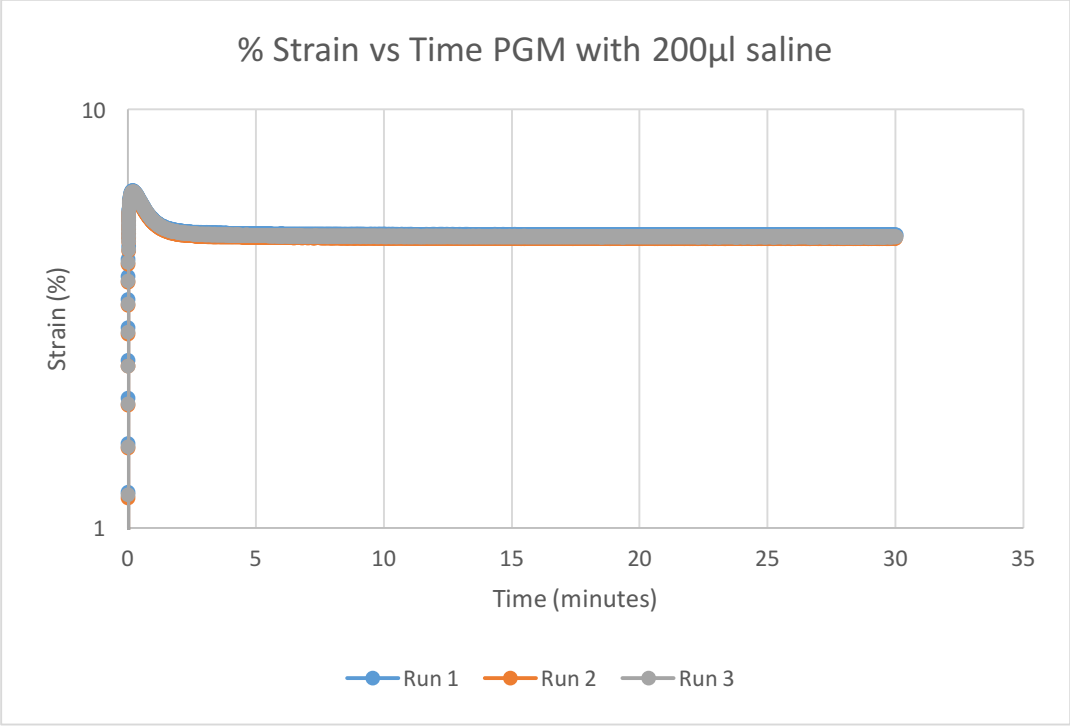

Graph 3-11 Strain or deformation applied to PGM with 200µl saline. The sample was subjected to constant deformation of 5%.

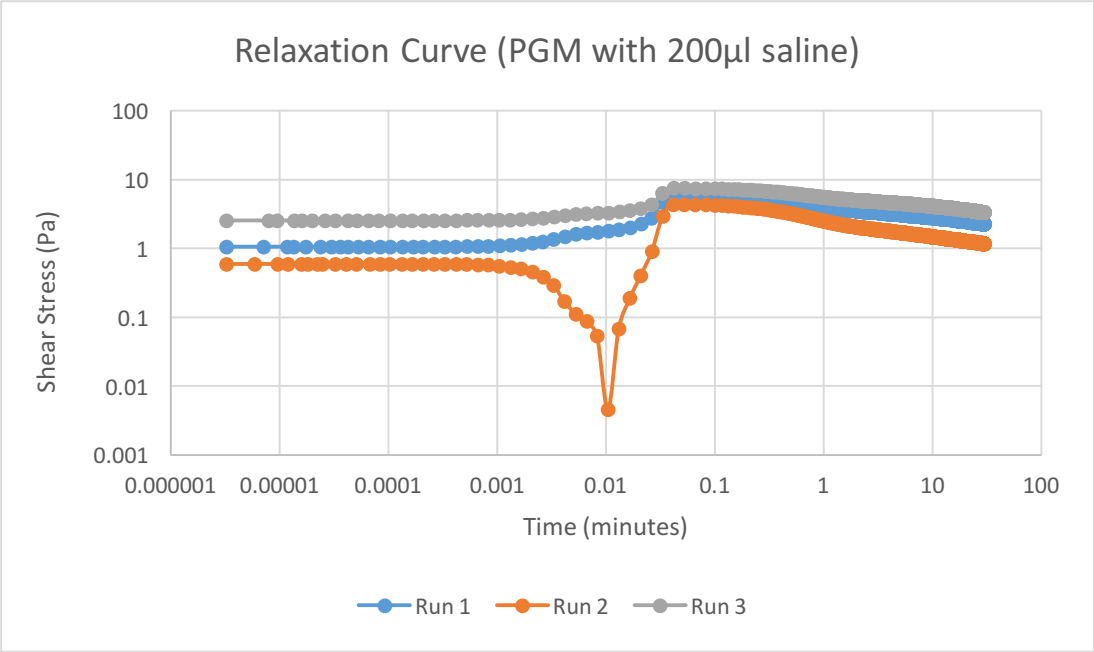

Graph 3-12 Response of PGM with 200µl saline during stress relaxation at constant deformation of 5%. The Y axis (Stress, Pa) is in log scale. A slip can be observed in Run 2 at 0.01minutes.

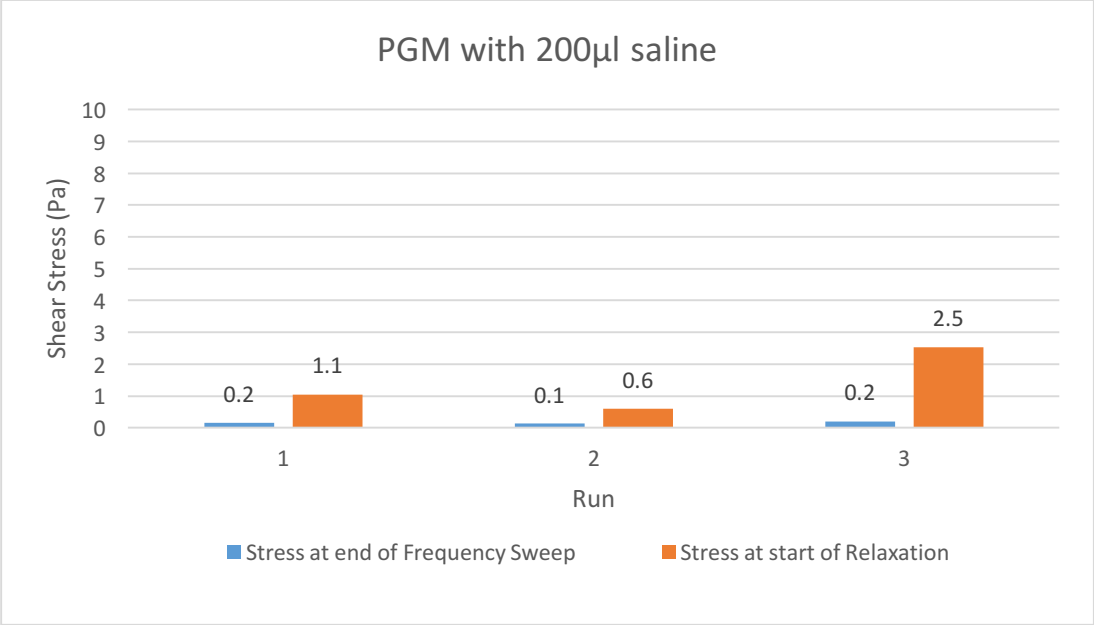

Graph 3-13 Comparison of shear stress values at the end of frequency sweep (at 10Hz) and the start of relaxation for PGM with 200µl saline

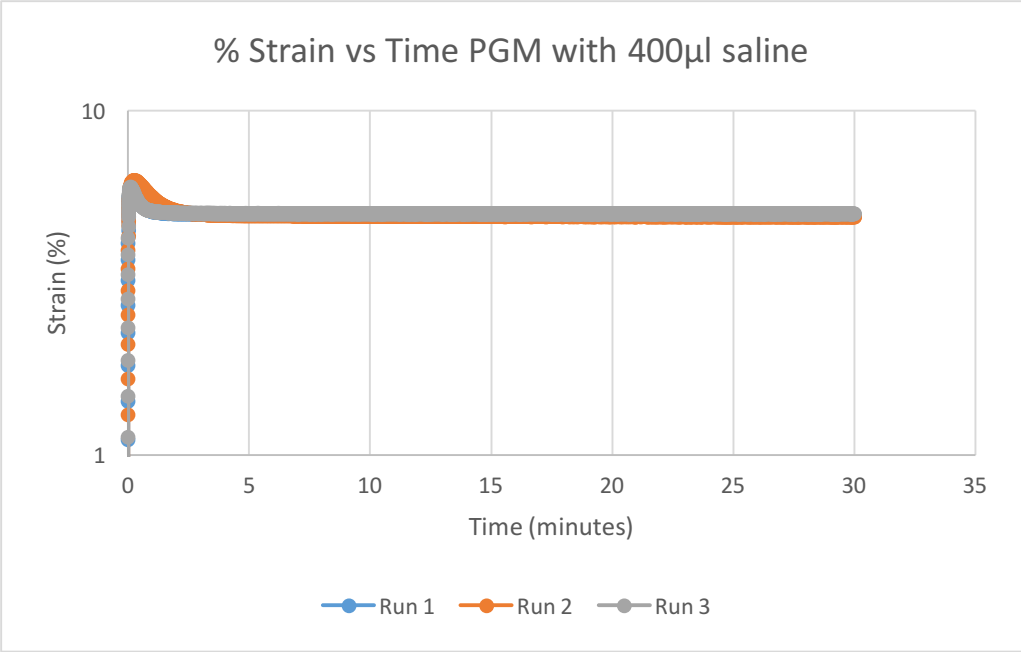

Graph 3-14 Strain or deformation applied to PGM with 400µl saline. The material was subjected to constant deformation of 5%.

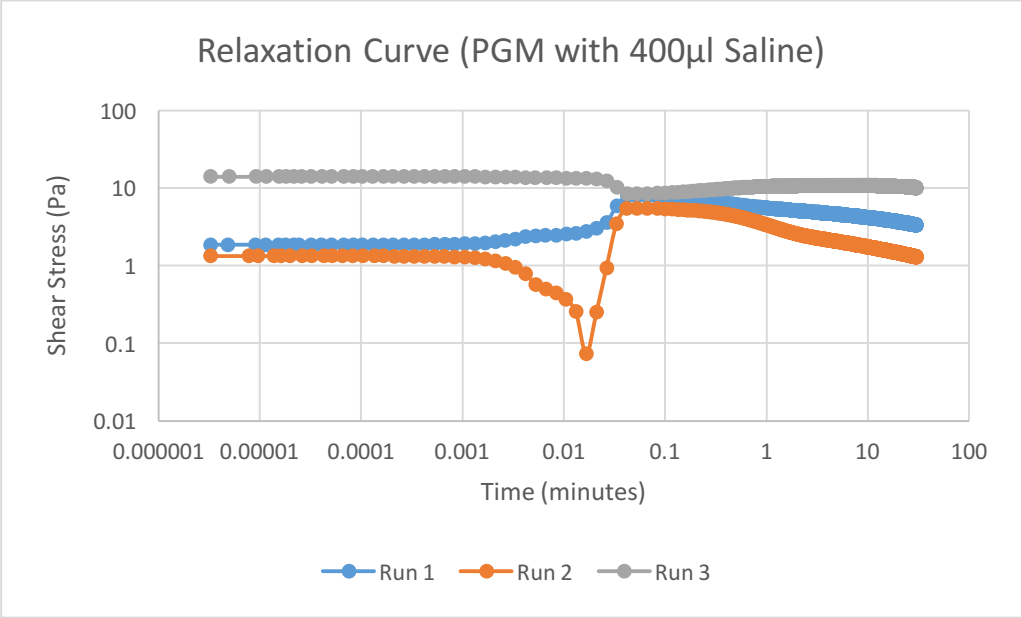

Graph 3-15 Response of PGM with 400µl saline during stress relaxation at constant deformation of 5%. The Y axis (Stress, Pa) is in log scale.

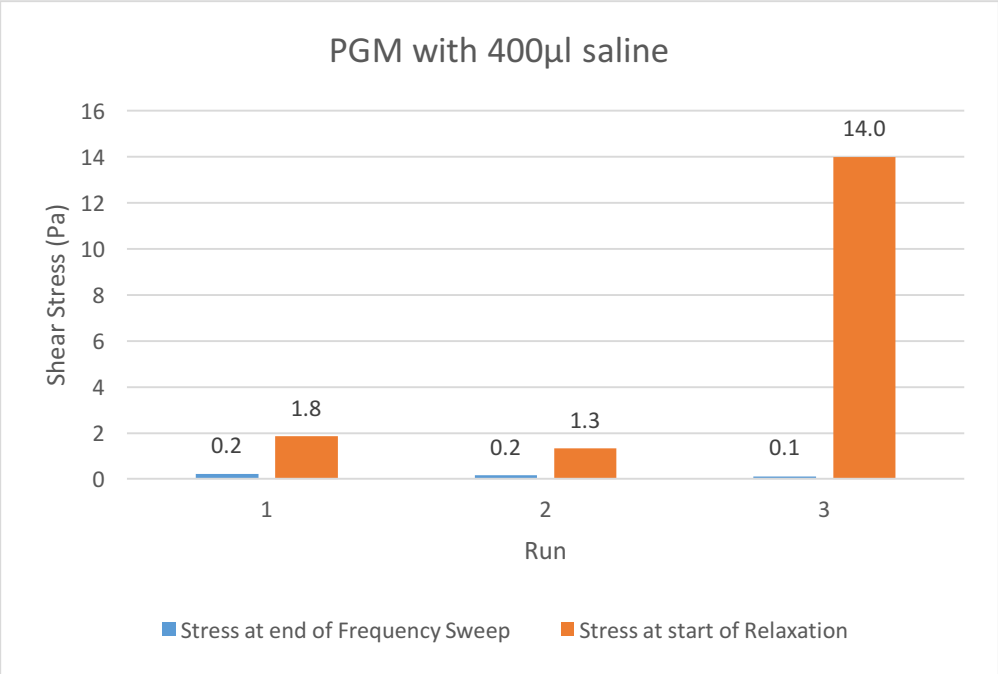

Graph 3-16 Comparison of shear stress values at the end of frequency sweep (at 10Hz) and the start of relaxation.

From graph 3-11 and 3-14, it was observed that a sudden strain was applied to the control samples (PGM with 200μl and 400μl saline). The strain then increases and remains constant throughout the measurement. However, the instrument used is an stress controlled rheometer. Thus, maintaing a constant deformation accurately could be difficult.[102]

In graph 3-12, for PGM with 200μl saline, three runs represented by three different curves showed di-fferent pattern of relaxation, with the decay pattern not being linear. The case was same for PGM with 400μl saline as shown in graph 3-15. The three runs had different pattern of relaxation though they were same material. This may relate to the variability and dynamic nature of the mucus. For instance, in graph 3-12, for run 1 of PGM with 200μl saline, the stress does not increase from 0 Pa, instead starts from 1.1 Pa, increases upto 5.8 Pa and then relaxes without reaching the equilibrium. This was quite different from normal expected relaxation pattern as shown in figure 1-20, where the relaxtion occurs gradually until a equlibrium stress is obtained.

Moreover, the stress developed at the end (at 10Hz) of frequency sweep was compared to the stress developed at the start of relaxtion, as shown in graph 3-13 for PGM with 200μl saline. The stress values were different for all the three runs. This could be because the samples were subjected to sudden deformation in just 1milisecond (rise time), thus not giving enough

time to appropriately develop a stress. Also, the stress controlled rheometer may not have been able to accurately control the strain throughout the measurement.

Similarly from graph 3-15, for run 1 of PGM with 400μl saline, the stress develops from 1.8Pa reaches to 7.8 Pa and then relaxes. When compared to the stress developed at the end (at 10Hz) of frequency sweep, the stress values at the start of relaxtion were different for all the three runs, as shown in graph 3-16.

Due to the type of plate arrangement of the rheometer, slip was also observed while applying the deformation. This can be seen in graph 3-12 for Run 2 of PGM with 200μl saline at 0.01 minutes, where the stress suddenly decreased. Similarly, in graph 3-15, for Run 2 of PGM with 400μl saline, a slip was obseved at 0.016 minutes.The slipping of material could be avoided by the use of cerated plates but would require higher amount of material, thus, not applicable for PGM.[101]

Considering the variability of the results, not much conclusive arguments could be developed from the relaxation pattern of the mucus controls.

3.1.1.5. Strain Sweep

This step was important to understand the structure of the material as well as for determining the linear viscoelastic region (LVR) for the material. A strain value within the LVR could be used in frequency sweep to deform the material. It was logical to perform this step at the end because in finding the LVR we could have damaged the material. As a result, the other important steps could not be carried out with a destroyed material, had this step was performed at the start.

This step was performed at 1Hz frequency and deformation range of 0.01-100% at 25ºC. Though the strain applied to the sample in this step was higher than that of relaxation step, the nature of strain was different. In strain sweep, oscillatory strain was applied to the material not mechanical deformation (as in relaxation step). In the graphs below, the values below 0.01% are omitted from the graph because of low signal to noise ratio.

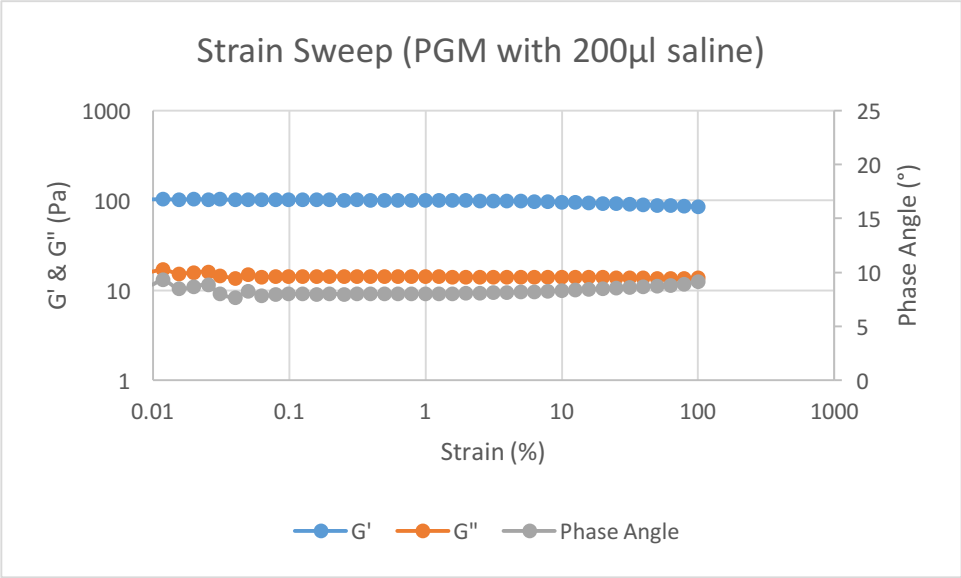

Graph 3-17 The change in elastic modulus (G'), viscous modulus (G") and phase angle of PGM with 200µl saline, over the deformation range of 0.01 to 100%. The primary Y axis and X axis are in log scale, while the phase angle in plotted in secondary Y axis

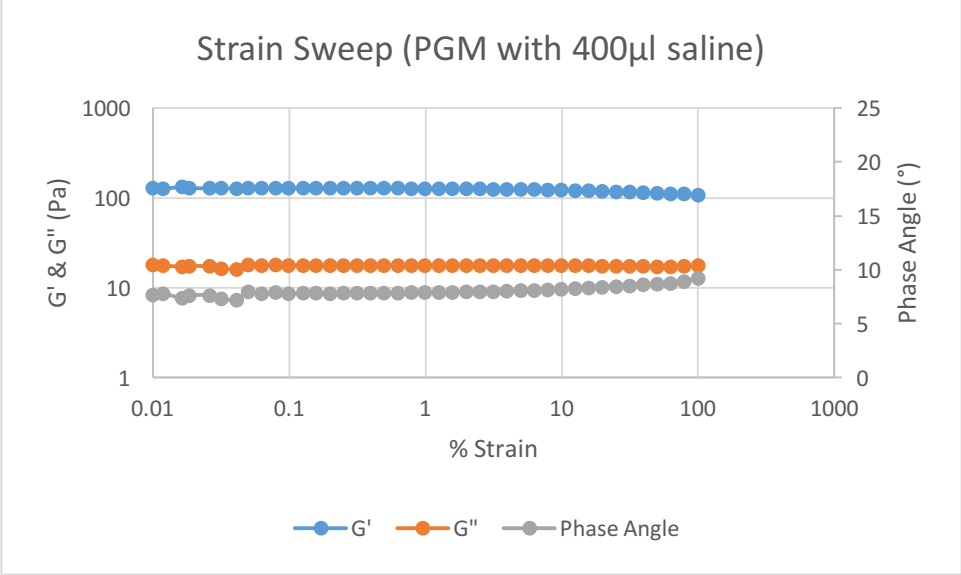

Graph 3-18 The change in elastic modulus (G'), viscous modulus (G") and phase angle of PGM with 400µl saline, over the deformation range of 0.01 to 100%. The primary Y axis and X axis are in log scale, while the phase angle is plotted in secondary Y axis.

From the graph 3-17 and 3-18, both the samples, PGM with 200μl and 400μl saline, have showed similar behavior under the deformation range. For better comparison between the controls, student's t test was done.

Here, the phase angle of PGM with 200μl saline and 400μl saline at 1.25% were 8.04 ± 0.005^0 and 7.92 ± 0.01^0. At 1.25% strain, the G' for PGM with 200μl saline and PGM with 400μl saline were significantly different based on t-test under 95% confidence level. Similarly, at 1.25% strain, phase angles of PGM with 200μl saline and 400μl saline were also significantly

different. However, it can be seen that the phase angles were quite close to each other and the error of mean used in the t-test were very small. Additionally, the distribution, on which the t-test was based on, was obtained from averages and error made up of just 3 runs performed for each sample. Thus, it could still be debated that the two controls did not differ from each other, substantially. Thus, it can be argued based on small difference in phase angle, that addition of extra 200μl volume does not seem to change the response of material substantially under the oscillatory strain.

Moreover, it can be seen, from the graphs 3-17 and 3-18, that both controls are independent to deformation until 1% strain and there is no significant change in moduli and phase angle until then. However, there is gradual increase in phase angle and viscous modulus after the material is subjected to strain higher than 1.25%. this means that the material was getting weaker or gel strength of PGM was decreasing. Thus, it can be said that the linear viscoelasticity region (LVR) for PGM was up to 1.25% where G', G" and phase angle were stable. And, 1.25% was the limit of linear viscoelasticity region. This proved that the frequency sweep and single frequency oscillation were performed within LVR, that is at 1 % strain.

Also, both of the controls showed that PGM is a viscoelastic solid since G'>G" over the deformation range (up to 100%). However, at higher deformation range, G' and G" could have a crossover where material could have been more liquid like. Thus, more specific conclusions on the structure and behavior could have been made once the material was subjected to higher deformation.

3.1.1.6. Summary

During loading it was observed that adding of additional 200μl increased the normal force of the material. Since, adding of 200μl saline had also changed the viscoelasticity of material to some extent, a comparison was desired, to check if behavior of material during loading had a pattern in relation to the way it behaved in the oscillatory experiments. Thus, when load data were compared to data from oscillatory experiments for each of the run, for each sample, no any pattern was found between maximum normal force during loading, G' and normal force at 10 Hz of frequency sweep, as discussed in section 3.1.1.1. Thus, it could be argued that there was no fix pattern between the tested characteristics.

From all the oscillatory tests, it was found that mucus showed solid dominant viscoelastic behavior. And, the addition of extra 200μl volume did change the mucus moduli. Dilution, generally, decreases the elastic behavior (elastic modulus) of the sample or the viscoelastic behavior.[120] However, this was not the case here. PGM with 400μl saline was more

elastic and viscous than PGM with 200μl saline. This adds to the argument that mucus itself is a very variable material in terms of its viscoelasticity.

Nevertheless, the phase angle was similar between the controls, PGM with 200μl saline and 400μl saline in all the tests. And such minor change in rheology is acceptable considering the variability of mucus. Therefore, it was harmless to add extra 200μl volume (nanoparticle formulations) to 1.5gm PGM with already 200μl saline. Therefore, for further comparisons, PGM with 400μl was, thus, used as a control.

3.1.2. Comparison of Pig Gastric Mucus and Mucin

In this experiment, the size of aggregates in modified PGM was measured and compared to that of Sigma™ Mucin. This experiment was performed to compare our mucus sample (Pig Gastric) with commercially available mucus model (Sigma Mucin) in terms of size. This would give a general idea about mucus aggregates and its dispersity.

In addition to this, zeta potential of mucus was also measured at different concentrations. It was observed that the zeta potential of mucus was highly variable ranging from negative to positive values. This indicated the highly variable nature of mucus itself. The zeta potential of mucus at different concentrations are presented in Appendix C.1.

Only few selected graphs that would be enough to understand the difference in mucin and pig gastric mucus are presented below. Graphs from all of the other concentrations are presented in Appendix C.3.

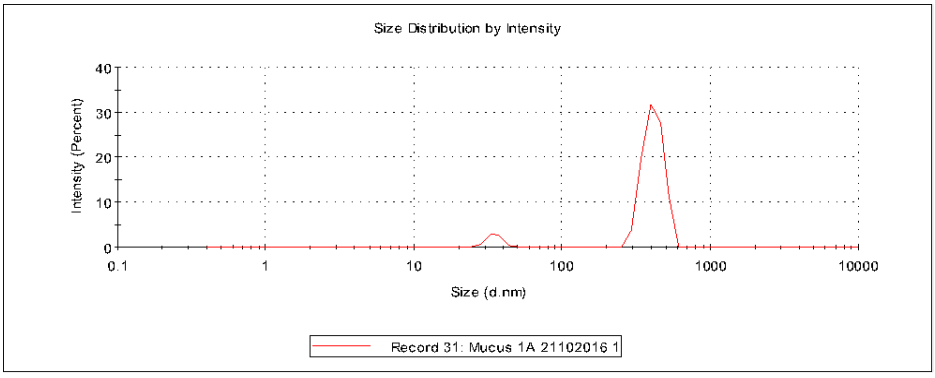

Graph 3-19 The size distribution by intensity of Mucus at concentration of 9.8mg/ml

The data sets from size distribution of mucus were found to be very random and part inconclusive. But it was observed that with increasing dilution, the data sets became less random. This could be, in theory, because of particulate matters in diluted sample posed less interference compared to the concentrated sample. Also, the second and third subsequent run in each data sets had higher size than the first one. This could be because the sample was not stable and aggregation had occurred over time. Temperature and time could be one of the factors

behind it. Thus, longer the sample remained in cuvette before the test started, there was more chance of aggregation of mucus material.

It was observed from the graph 3-19, for mucus concentration at 9.8mg/ml, that there are two different peaks giving bimodal distribution with peak averages at 415.2nm and 34.82nm. This type of distribution could be due to the particulate matters present in the mucus solution such as food particles, clumps and aggregates. Contrastingly, there were no any peaks seen in case of mucus at 1.225mg/ml concentration (not shown here, but shown in Appendix C.3). This could have been because sedimentation had already taken place before measurement and all the samples were at the bottom of the cuvette with no mucus suspended in the solution.

When Sigma Mucin was subjected to same experimental setup, the data were less random.

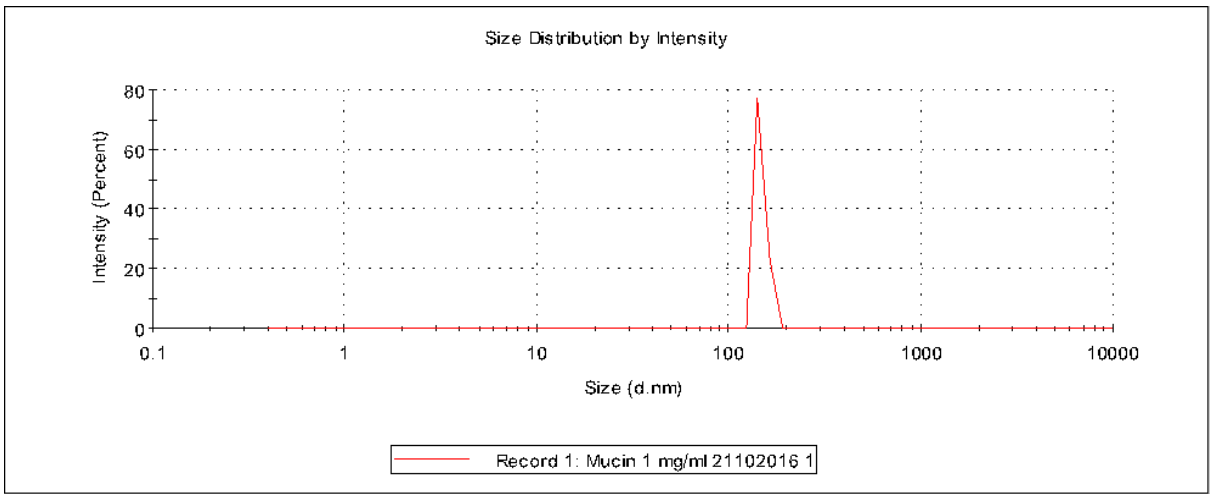

Graph 3-20 The size distribution by intensity of Sigma Mucin at concentration of 1mg/ml

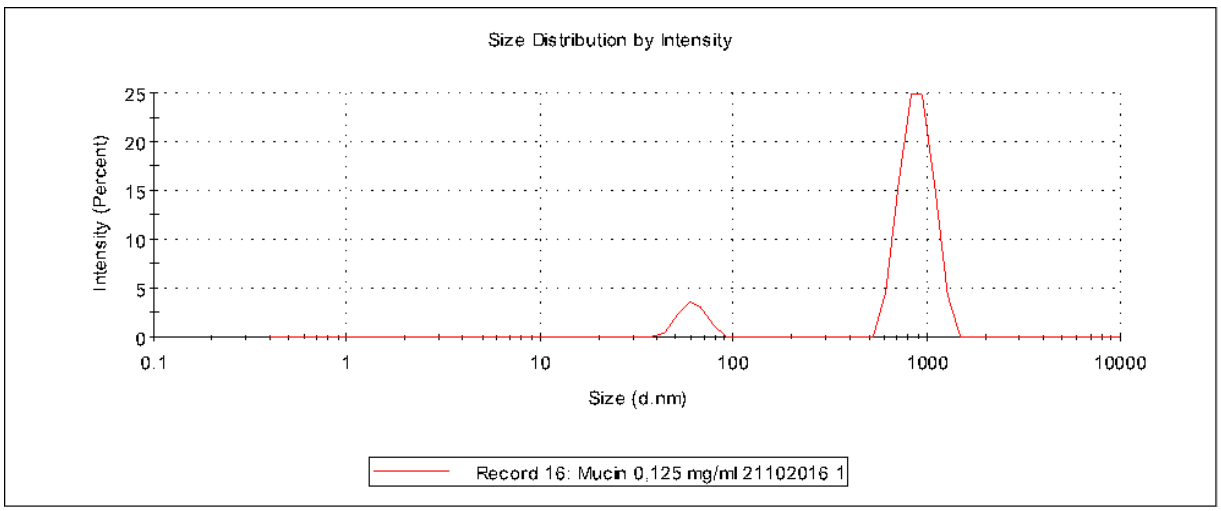

Graph 3-21 The size distribution by intensity of Sigma Mucin at concentration of 0.125mg/ml

It was observed from the size distribution graph of Sigma Mucin, that almost all the mucin samples had only one peak except mucin at 0.125mg/ml concentration (shown in the graph 3-21). The peak for Mucin at 1mg/ml was at 146nm, as shown in the figure above. Nevertheless, from the graphs it could be argued that the mucin samples were less random in comparison to PGM.

From the randomness of both mucus and mucin, it could be argued that the sample were too concentrated (causing multiple scattering) for the instrument to measure, as shown by the quality of the report. In addition, both of the samples had high polydispersity (>1), thus the average values presented by the instruments were random and meaningless. Also the attenuation factor used for the sample was always low at 0.09 (in average). This also implied that the samples were far too concentrated and polydispersed for measurement.[118]

The next parameter that clarifies the sample state and quality of obtained data more, is the Correlation data. This correlation function is supposed to be related to size of the particle. For instance, slower rate of decay is expected for large particle size.[115]

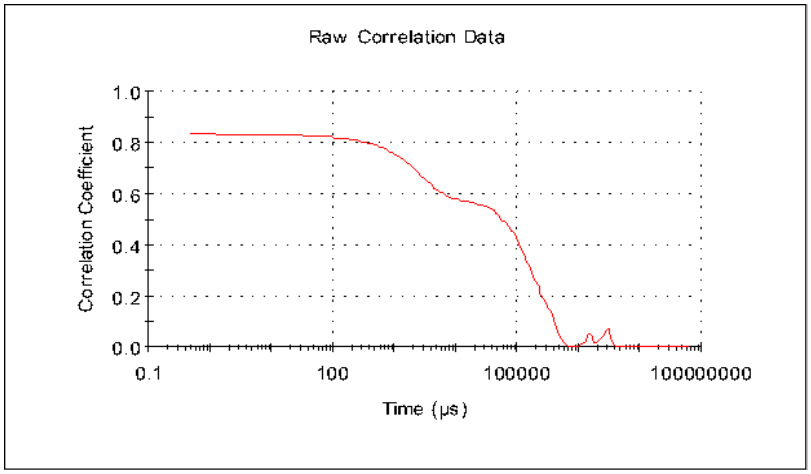

Graph 3-22 The correlation data of Sigma Mucin at concentration of 1 mg/ml

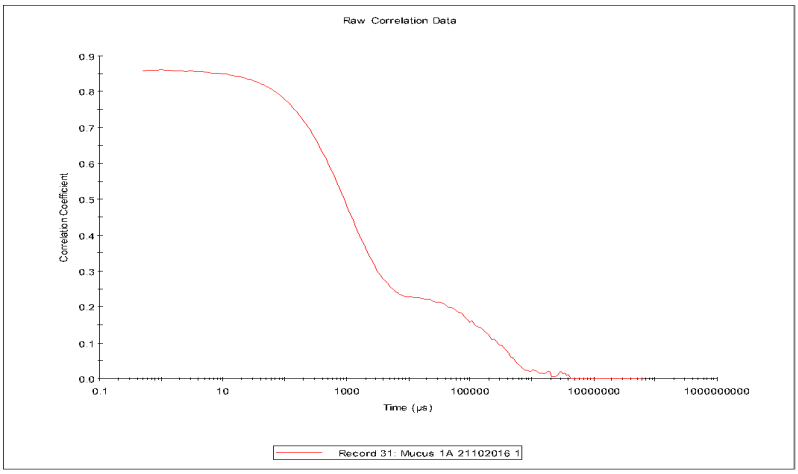

Graph 3-23 The correlation data of Mucus at concentration of 9.8 mg/ml

In both of the graphs, the speckle pattern moves very slowly almost resembling a plateau region which is characteristic for large particles. This is because large particles move slowly and take time to decay than the smaller particles.[121] In both of the samples, the intercept is between 0.8 to 0.9 indicating high signal to noise ratio. So, we can say that, at least, there was no interference from the solvent itself.

But still, these graphs are very inconclusive because of multiple decay patterns that change over time. Also, the at various concentrations of the samples, the data were quite random and sometimes un-relatable to each other. This could be, again, due to the high polydispersity of the samples leading to random output in correlation. Moreover, the zetasizer uses algorithms that extract the decay rates for a number of size classes to produce a size distribution.[118] Thus, it was clear from the correlation graph that the size distribution produced, would be inconclusive.

3.2. Evaluation of Mucus Rheology in presence of various nanoparticle formulations

The Pig Gastric Mucus(1.5gm) with already 200μl saline was added with 200μl of various nanoparticle formulations, as mentioned in methodology in section 2.2.

It was found that comparison of PGM with 200μl and 400μl saline that, addition of extra volume of 200μl would change the mucus rheology. However, comparison on the basis of phase angle showed that the change is not substantial.

Therefore, the mucus control presented in the graphs below is PGM with 400μl of 0.9% saline. Now, the PGM with nanoparticle was subjected to same sequence to test as to PGM control and comparison was done among them to see if addition of nanoparticles would change mucus rheology.

Two different sets of nanoparticles were tested. One set was from University of Copenhagen (CU) with PLGA core, Lipidoid coated PLGA core and siRNA loaded Lipidoid coated PLGA cores. The other set was from HIPS, Germany with PLGA core, Chitosan coated PLGA core, siRNA loaded Chitosan coated PLGA cores and siRNA alone. Three different runs were performed for each of the sample and mean values from them were used to plot the graphs presented below. And, the timescale used to plot the graph are action time of the measurements.

3.2.1. Pig Gastric Mucus with PLGA, Chitosan PLGA and siRNA loaded Chitosan PLGA

The nanoparticles from HIPs were used in 3 different formulations. (see figure 1-8)

- PLGA core (PLGA 1),
- chitosan coated PLGA core(Chitosan-PLGA)
- siRNA loaded chitosan coated PLGA core (Chitosan-PLGA siRNA).

PGM with siRNA alone was also tested. However, the rheological data from oscillatory experiments of PGM with siRNA alone has not been presented here. And, the data from frequency sweep of PGM with siRNA alone has been used in comparison of various nanoparticles in section 3.2.3. The rheological test for PGM with siRNA was done to understand the effect of addition of siRNA in nanoparticle formulation.

The comparisons are done by percentage difference and student's t test.

Also, phase angle is considered to be more dependable to comparison as it is a measure of extent of viscous and elastic behavior of material.

3.2.1.1. Sample Load Data

As mentioned before, the objective behind this analysis was to check if there was any pattern between the behavior of sample during loading and later oscillatory experiments.

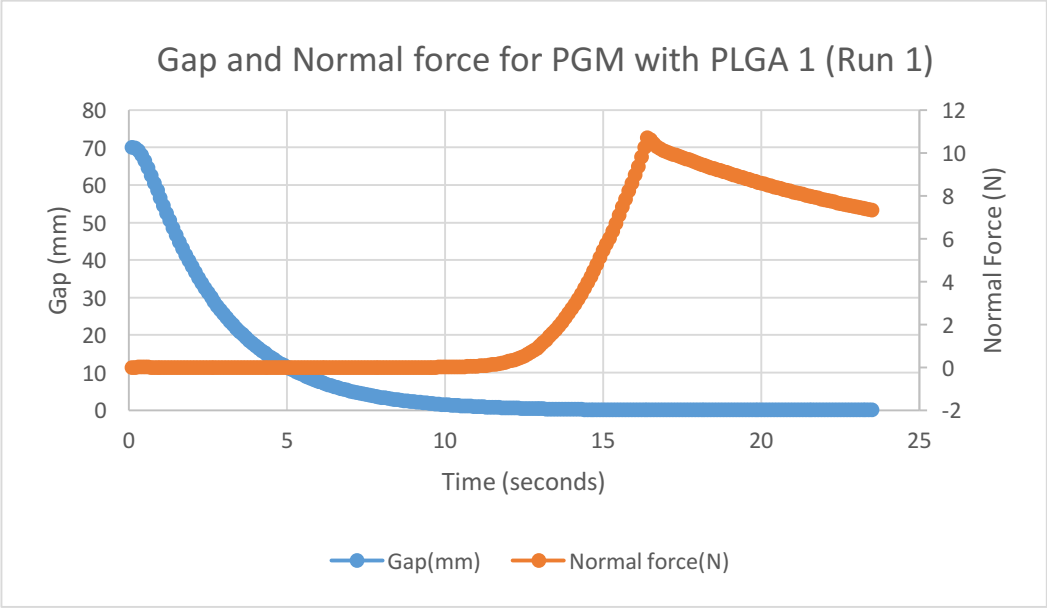

Graph 3-24 The change in gap and normal force over action time for Run 1 of PGM with PLGA 1. The blue curve representing gap (mm) is plotted in primary Y axis, while orange curve representing normal force (N) is plotted in secondary Y axis over time (sec) in X axis.

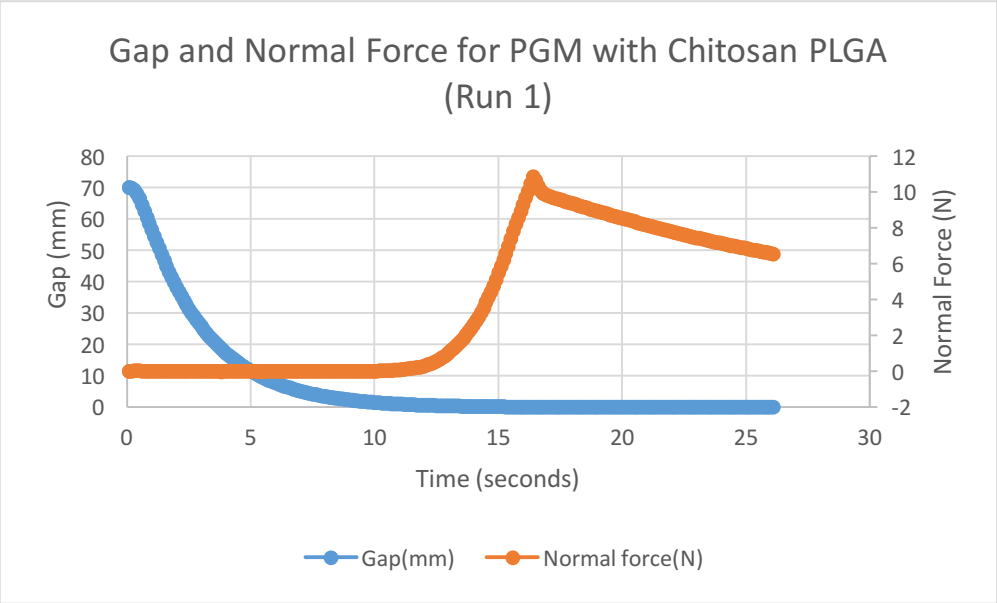

Graph 3-25 The change in gap and normal force over action time for Run 1 of PGM with Chitosan PLGA. The blue curve representing gap (mm) is plotted in primary Y axis, while orange curve representing normal force (N) is plotted in secondary Y axis over time (sec) in X axis.

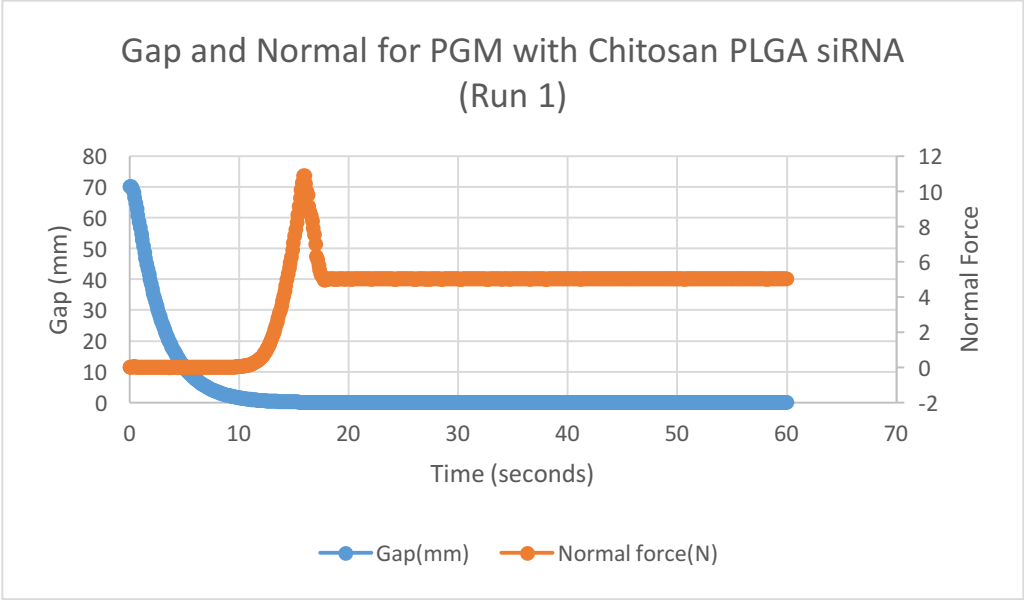

Graph 3-26 The change in gap and normal force over action time for Run 1 of PGM with Chitosan-PLGA siRNA. The blue curve representing gap (mm) is plotted in primary Y axis, while orange curve representing normal force (N) is plotted in secondary Y axis over time (sec) in X axis.

It is seen from the graphs that the loading data of the PGM with nanoparticles do not have dramatic difference from each other. However, maximum normal force and rise time seem to be different from each other. The graphical representation of load data of all the other runs are presented in Appendix D.1. Nevertheless, the contact gap, time for rise, end gap and

maximum normal force of all the runs of PGM with nanoparticles have been compared in the table below:

Table 3-6 Comparison of PGM with nanoparticles in terms of contact gap, time for rise, end gap and maximum normal force. All the three runs performed for each sample have been presented.

Sample (PGM with)	Run	Contact Gap (mm)	Time for rise (s)	End Gap (mm)	Maximum Normal force (N)
PLGA 1	1	1.61	6.7	0.026	10.6
	2	2.44	7.61	0.026	9.7
	3	2.4489	9.3	0.026	8.3
Chitosan PLGA	1	1.8	6.9	0.026	10.85
	2	2.25	7.3	0.0285	10.99
	3	2.7733	7.9	0.026	10.28
Chitosan PLGA siRNA	1	1.9075	6.5	0.0427	10.87
	2	2.2534	7	0.0474	10.96
	3	2.5596	7.6	0.026	10.99

From table 3-6, it can be seen that the contact gap is variable for three different runs of the same sample. For instance, for PGM with PLGA 1, the contact gaps are 1.61, 2.44 and 2.44mm.

This could be because of way with which the sample was loaded on the base plate. Moreover, as mentioned before, the PGM used was not completely homogenized and thus, the mucus itself could have been highly variable due to presence of aggregates.

A statistical correlation coefficient of 0.77, 0.92 and 0.99 were found between contact gap and time of rise for PGM with PLGA 1, Chitosan PLGA and Chitosan PLGA siRNA respectively. It was obvious for a sample with small contact gap that the instrument took less time to reach the maximum force.

Nevertheless, it was observed that more normal forces applied to the PGM with nanoparticles were than PGM with 400μl saline (mucus control in section 3.1.1.1). The maximum normal forces of PGM with nanoparticles are compared in the graph below:

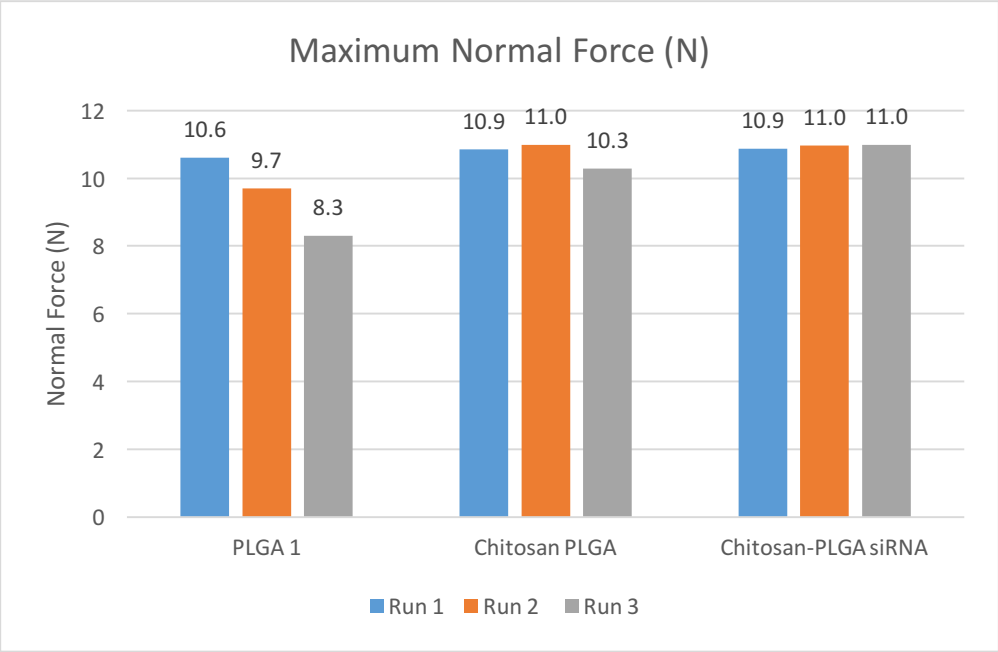

Graph 3-27 Comparison of Maximum Normal Force of PGM with nanoparticles for all the three runs

Here, the addition of nanoparticle formulation had increased the normal force of the PGM when compared to mucus control in section 3.1.1.1. However, it seems Chitosan-PLGA siRNA has the highest maximum normal force when compared to other nanoparticles. This increase might or might be related to the viscoelasticity and normal force of the sample during frequency sweep. For instance, the sample with highest normal force during loading could have high or low G' during frequency sweep. Therefore, these normal forces during loading were compared to G' and normal force in frequency sweep for all the runs, and are discussed in section 3.1.2.3.

Except for the difference in the maximum normal force, no other conclusive differences were observed between PGM with nanoparticles and control.

3.2.1.2. Single Frequency Oscillation

This was an important step to see if the moduli and phase angle, on which the analysis were based on, were in apparent equilibrium. This step was performed at frequency of 1Hz, 1% strain and at 25ºC for around 8 minutes, within the linear viscoelastic region (LVR).

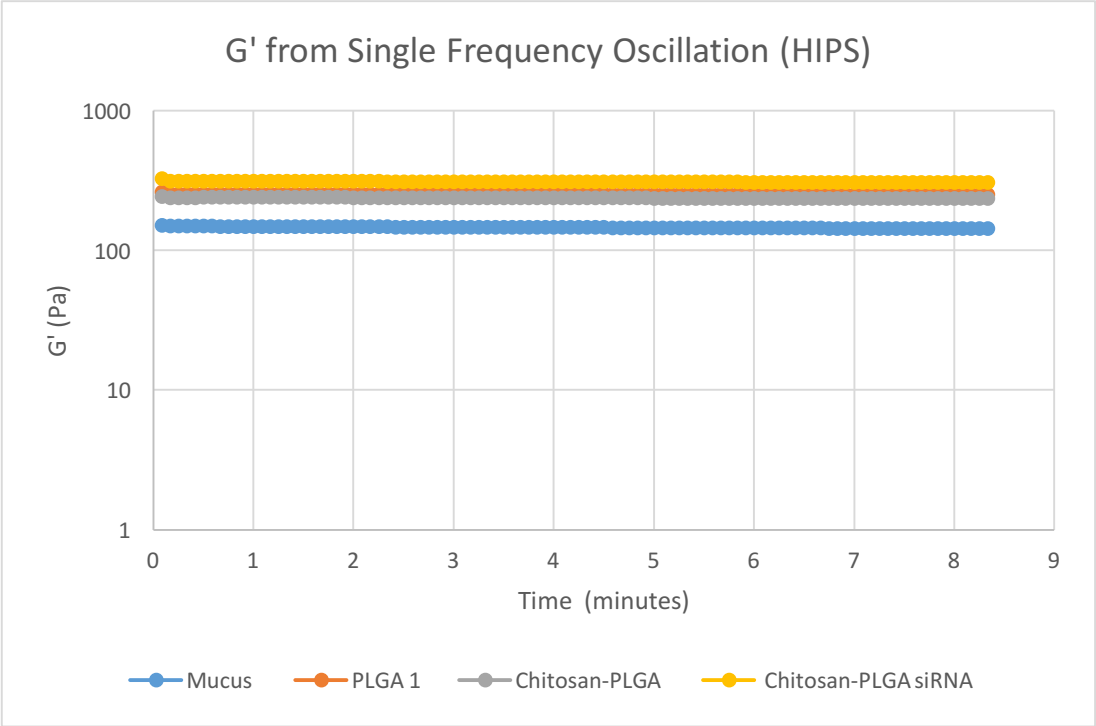

Graph 3-28 Elastic modulus (G') of PGM with nanoparticle formulations compared to mucus control (PGM with 400µl saline) depicted in different colors over a time period, at a single frequency of 1Hz throughout the measurement. The elastic moduli are plotted in a log scale

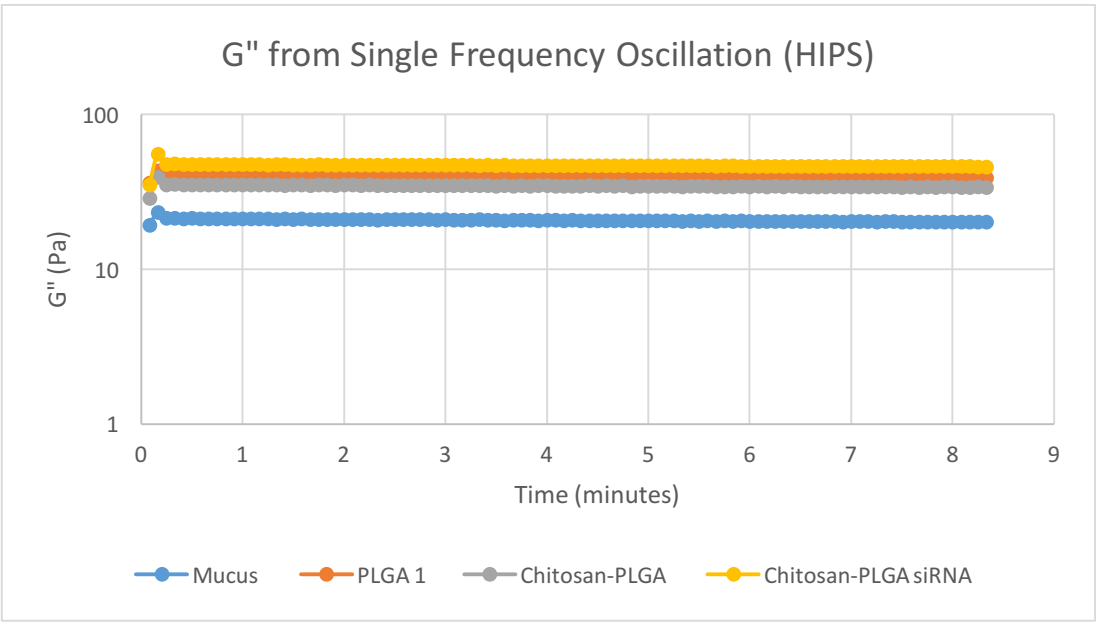

Graph 3-29 Viscous modulus (G") of PGM with nanoparticle formulations compared to mucus control (PGM with 400μl saline) depicted in different colors over a time period, at a single frequency of 1Hz throughout the measurement. The viscous moduli are plotted in a log scale.

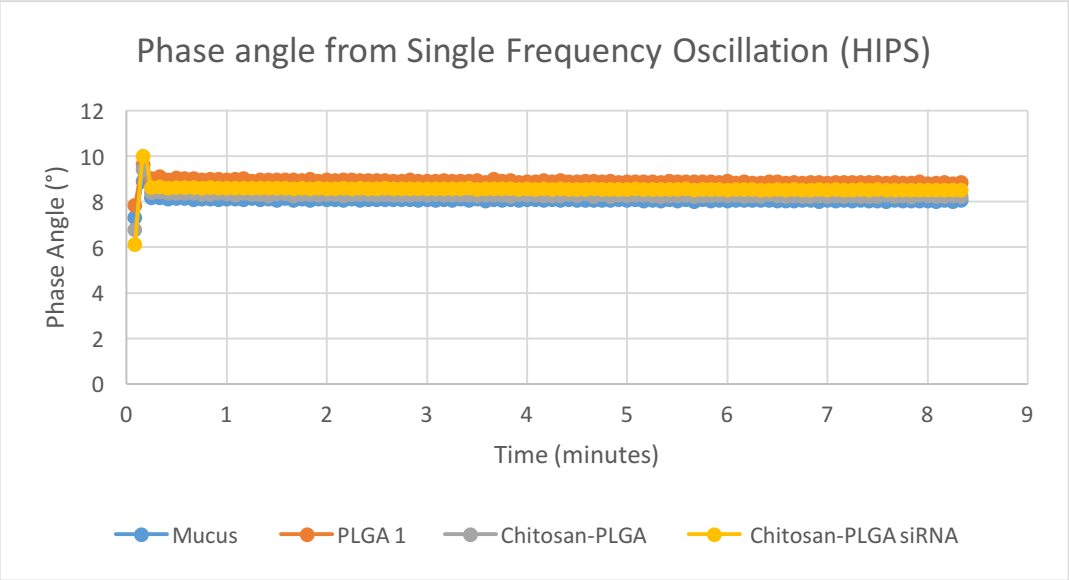

Graph 3-30 Phase angles of PGM with nanoparticle formulations compared to mucus control (PGM with 400µl saline) depicted in different colors over a time period, at a single frequency of 1Hz throughout the measurement.

It can be seen that the samples were in apparent equilibrium as the moduli and phase angle of the sample did not change over time throughout the experiment. This could be seen more clearly from the tables presented below for different nanoparticles.

Table 3-7 Comparison of G' for PGM with PLGA 1 at 3 minutes and 8 minutes to verify if the moduli had changed over time.

Time	G' (Pa)	Difference
3 minutes	253.3	1.3%
8 minutes	249.9	

It was seen that the difference of G' at 3 minutes and 8 minutes was just 1.3%. Similarly, the difference in phase angle at 3 minutes and 8 minutes was just 1.3%. These small differences showed that PGM with PLGA 1 was stable or in apparent equilibrium over the measured time period.

Table 3-8 Comparison of G' for PGM with Chitosan-PLGA at 3 minutes and 8 minutes to verify if the moduli had changed over time.

Time	G' (Pa)	Difference
3 minutes	238.3	1.5%
8 minutes	234.5	

It was seen that the difference of G' at 3 minutes and 8 minutes was just 1.5%. Similarly, the difference in phase angle at 3 minutes and 8 minutes was just 0.2%. These small differences showed that PGM with Chitosan-PLGA was stable or in apparent equilibrium over the measured time period.

Table 3-9 Comparison of G' for PGM with siRNA loaded Chitosan-PLGA 1 at 3 minutes and 8 minutes to verify if the moduli have changed over time

Time	G' (Pa)	Difference
3 minutes	310.7	1.4%
8 minutes	306.2	

It was seen that the difference of G' at 3 minutes and 8 minutes was just 1.4%. Similarly, the difference in phase angle at 3 minutes and 8 minutes was just 0.46%. These small differences showed that PGM with siRNA loaded Chitosan-PLGA was stable or in apparent equilibrium over the measured time period.

Now, from graphs 3-28 and 3-30, when compared to PGM control with 400μl of saline, the PGM with nanoparticle formulation had comparatively higher elastic moduli (G') while the phase angle remained almost the same for all the samples. Also, throughout the experiment time, G'>G", indicating that the material still behaves as viscoelastic solid after addition nanoparticles. Although, more on this can concluded from later steps of the oscillatory experiments.

3.2.1.3. Frequency Sweep

This step was done at the frequency range of 0.01Hz to 10 Hz. The experiment was performed at 25ºC and 1% strain, known to be within the LVR. The values below 0.1 in the graphs below are omitted because of low signal to noise ratio.

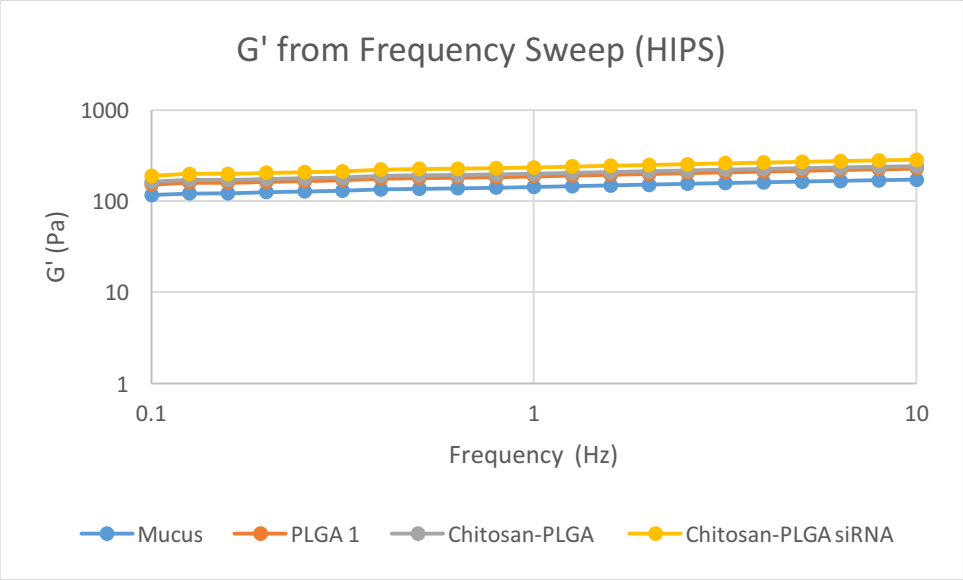

Graph 3-31 Elastic Modulus (G') of PGM with different nanoparticle formulations and mucus control (PLGA with 400µl saline) over the frequency range of 0.1 Hz to 10Hz, presented in different colors. Both of the axes are in log scale.

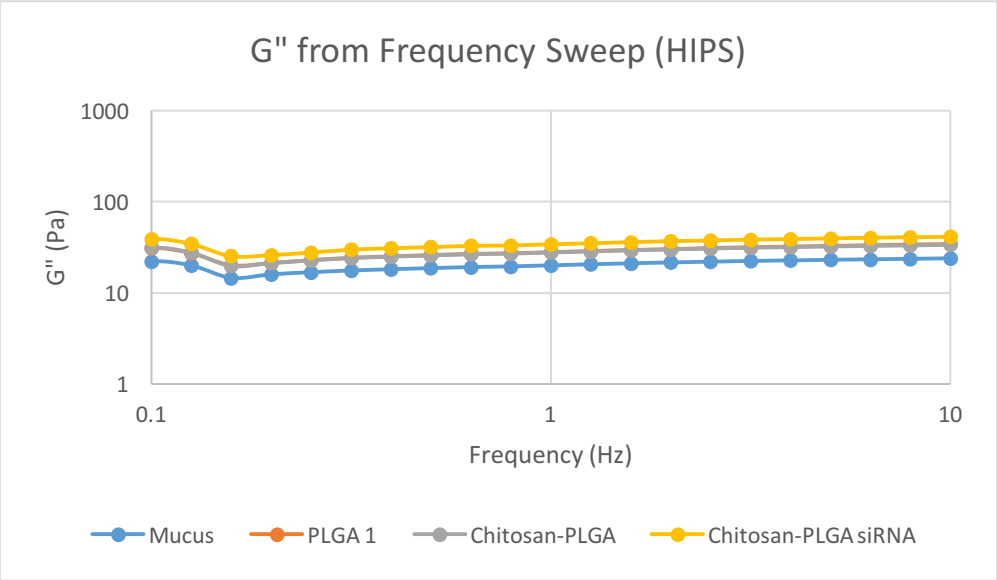

Graph 3-32 Viscous Modulus (G") of PGM with different nanoparticle formulations and mucus control (PLGA with 400µl saline) over the frequency range of 0.1 Hz to 10Hz, presented in different colors. Both of the axes are in log scale.

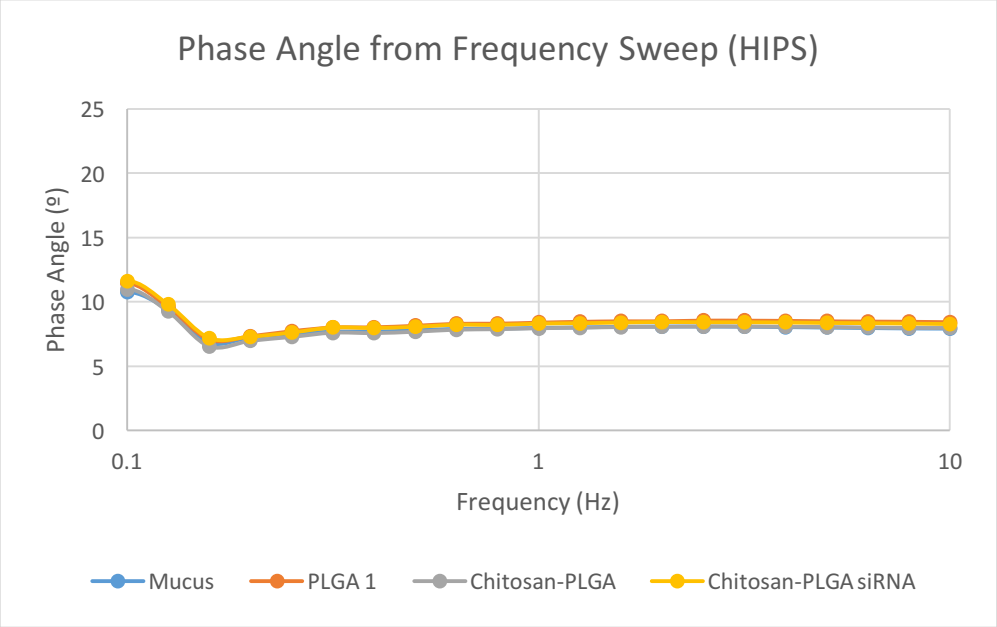

Graph 3-33 Phase angles of PGM with different nanoparticle formulations and mucus control (PLGA with 400µl saline) over the frequency range of 0.1 Hz to 10Hz, presented in different colors. The frequency range (x-axis) is plotted in log scale.

From the graphs, it can be observed that all of the samples showed similar reaction to the applied frequency range. It can clearly be seen that there is increase in moduli and phase angle as the frequency is increased from 0.1 to 10Hz. This indicates that the samples were

frequency dependent. From graph 3-31, at larger frequencies (shorter time scale), the material is more elastic. However, at smaller frequencies (longer time scale), the elasticity of the material decreases. This indicated the presence of timescale dependent interactions that were higher at shorter timescale and decreased at longer timescale. These interactions were slightly higher in PGM with nanoparticles than the mucus control. This could be observed from the higher G' of PGM with nanoparticles than mucus control.

From graph 3-33, the phase angle is high at longer time scale (lower frequency) which then decreases. This depicts the more viscous nature of the material, that is mucus flows when given enough time. However, this was not relevant because mucus turnover clears the mucus well before such timescale could be reached.[42]

From the graph 3-31 and 3-32, for PGM with nanoparticle formulations, G'>G" with no signs of crossover. Thus, PGM with nanoparticles was also solid dominant viscoelastic material. The samples show characteristic of a gel system with phase angles of 8.4° (PGM with PLGA 1) and 7.9° (PGM with Chitosan-PLGA) and 8.3^0 (PGM with Chitosan-PLGA siRNA) at 1Hz. However, the most prominent effect was shown by the addition of siRNA to the PGM among other nanoparticle formulations. A detail comparison of PGM with different nanoparticle formulations and mucus control at 1Hz and 10 Hz is presented in section 3.2.3.

It was also interesting to observe, if the material had changed in terms of stress response to deformation during the time scale. Thus, the stress values of this experiment are compared at the same frequency sweep from 0.1Hz to 10 Hz.

.

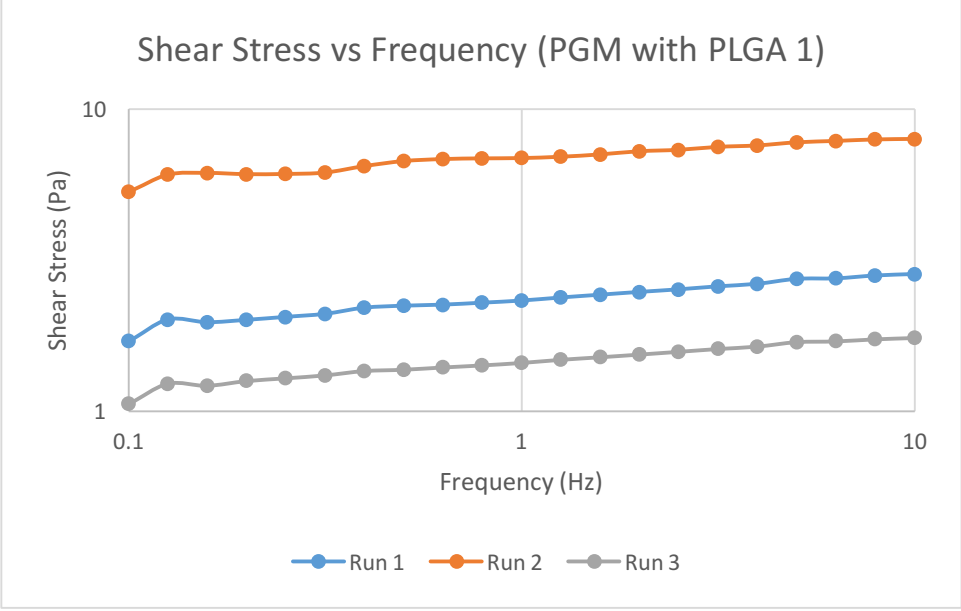

Graph 3-34 Stress developed in PGM with PLGA 1 saline at 1% strain, during the frequency sweep from 0.1Hz to 10Hz.Both of the axes are in log scale.

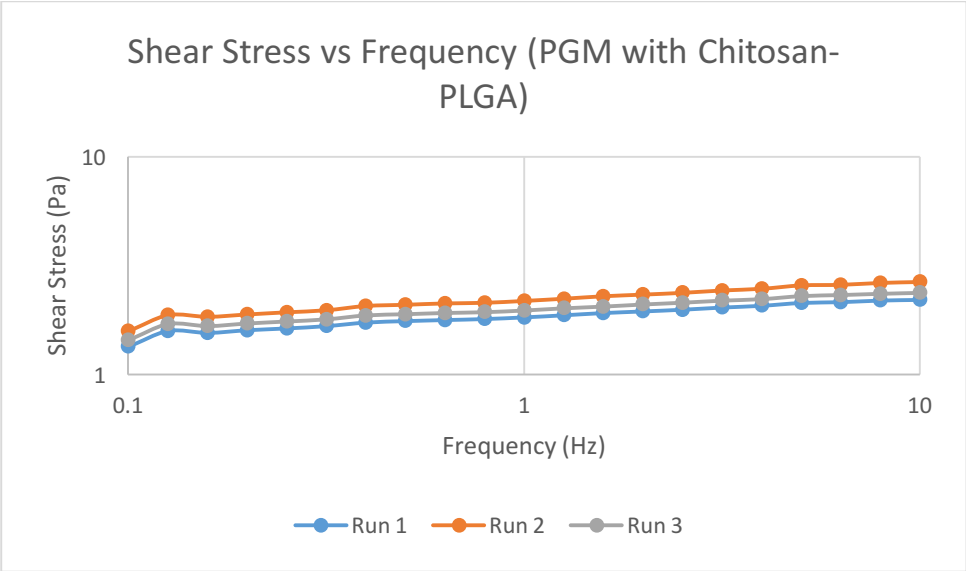

Graph 3-35 Stress developed in PGM with Chitosan-PLGA at 1% strain, during the frequency sweep from 0.1Hz to 10Hz.Both of the axes are in log scale.

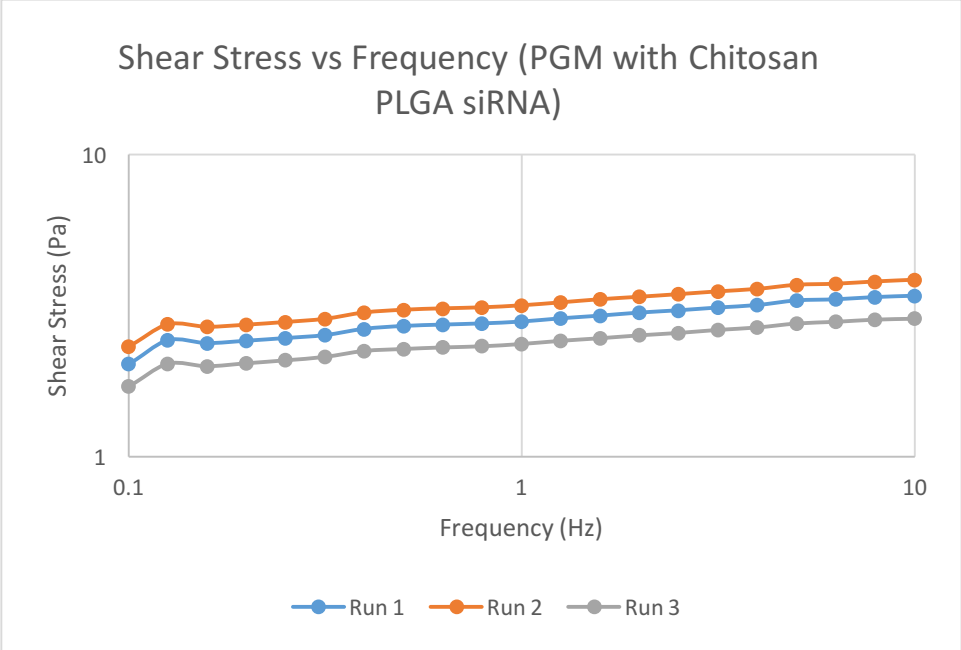

Graph 3-36 Stress developed in PGM with siRNA loaded Chitosan-PLGA at 1% strain, during the frequency sweep from 0.1Hz to 10Hz.Both of the axes are in log scale.

Table 3-10 Comparison of stress in mucus control and PGM with nanoparticle formulations at 1Hz Frequency. The comparison was based on student's t test at 95% confidence level. Each row represents each statistical comparison.

Test Sample 1	Shear Stress (Pa)	Test Sample 2	Shear Stress (Pa)	Confidence Level	Remarks
Mucus Control	1.43±0.06	PGM with PLGA 1	3.54±1.37	95%	No significant difference
Mucus Control	1.43±0.06	PGM with Chitosan PLGA	1.99±0.08	95%	Significant difference
Mucus Control	1.43±0.06	PGM with Chitosan PLGA siRNA	2.77±0.18	95%	Significant difference

During the statistical comparison of shear stress, it was found that shear developed in mucus control (PGM with 400μl saline) and PGM with PLGA 1 had no significant difference. However, as seen in table 3-10, the mean value of shear stress is double when compared to that of control. This was because the 3 runs of PLGA 1 were largely spread, as seen in graph 3-34. Similar differences between the 3 runs for a sample could have affected the statistical deductions during t-test.

Interestingly, when mucus control was compared to PGM with Chitosan PLGA and siRNA loaded Chitosan PLGA, the difference in stress developed was significant for each sample. As mentioned before, the distribution, on which the t-test was based on, was obtained from averages and error from just 3 runs performed for each sample. Moreover, the error of the mean used in t-test were very small leading to such significant difference at 95% confidence level. Thus, the result from t test could still be argued upon.

Moreover, even though the stress developed in the PGM with nanoparticle is higher than that of control with 400μl saline, the differences between the samples could be considered unsubstantial when compared to difference of stress between the controls (PGM with 200μl and 400μl saline in section 2.1.1.3).

Thus, based on stress developed in the material, it can be argued that the rheology of mucus would not change largely by addition of nanoparticles.

As mentioned before, there could have been a pattern between the behavior of the material during loading and frequency sweep. Therefore, the maximum normal force of the material, G' and Normal force at the end (10Hz, short timescale) of frequency sweep are compared. The results are presented below:

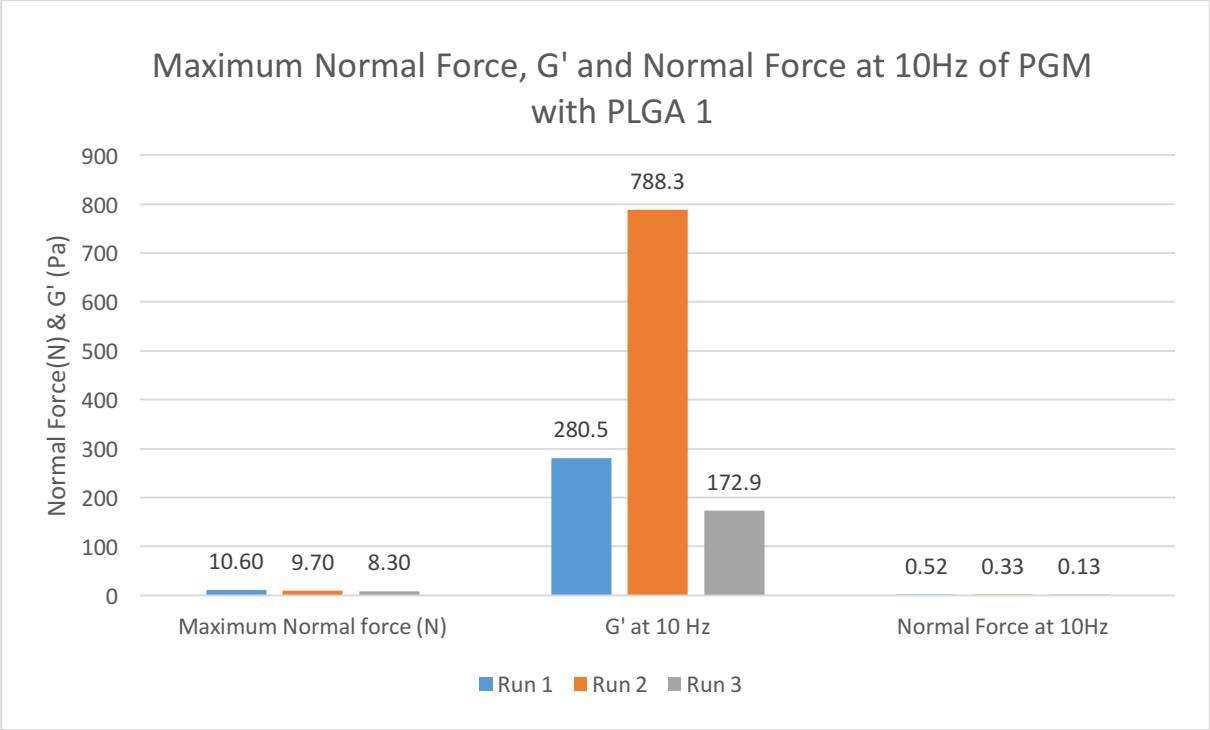

Graph 3-37 Comparison of Maximum Normal Force, G' and Normal Force at 10Hz for PGM with PLGA 1

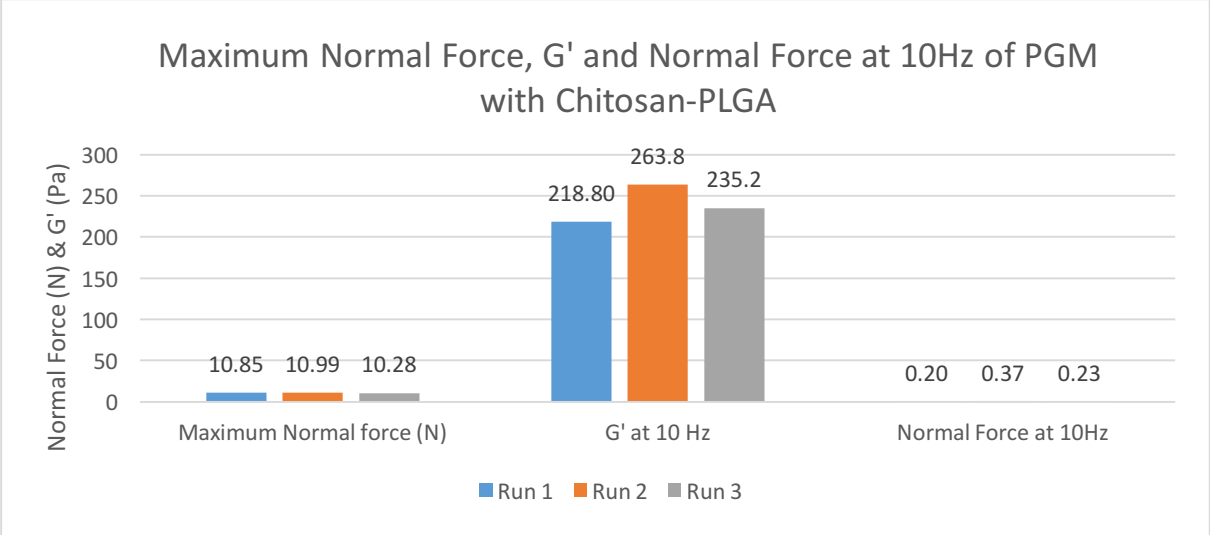

Graph 3-38 Comparison of Maximum Normal Force, G' and Normal Force at 10Hz for PGM with Chitosan PLGA

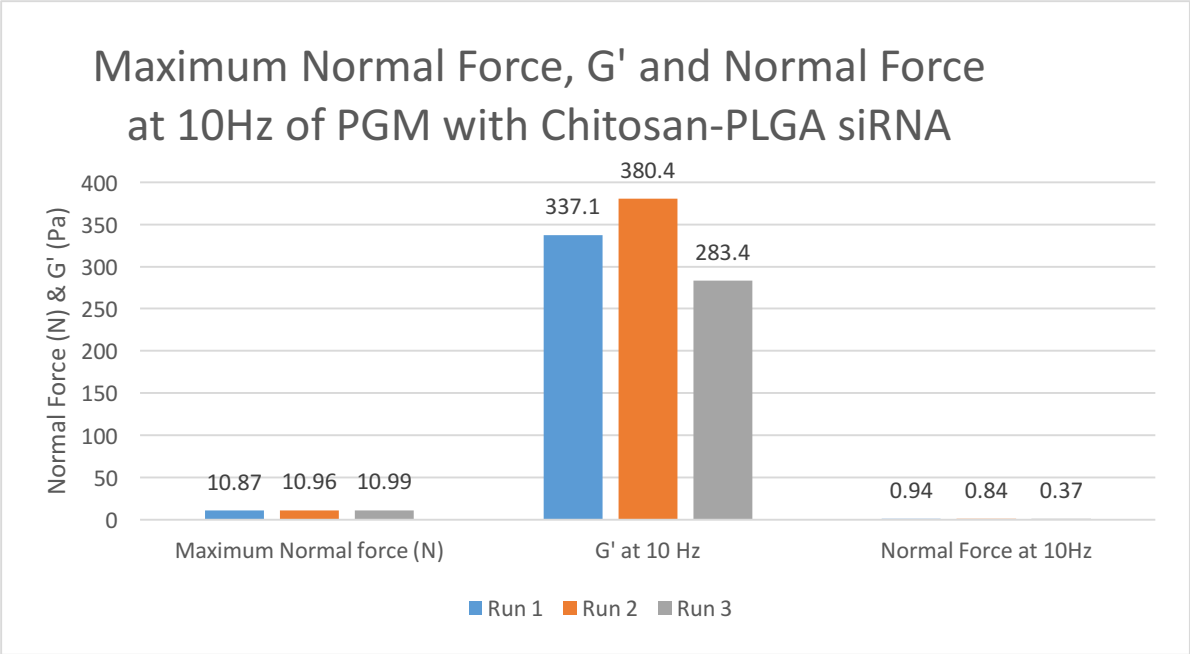

Graph 3-39 Comparison of Maximum Normal Force, G' and Normal Force at 10Hz for PGM with Chitosan-PLGA siRNA

Here in graph 3-37, for Run 1 of PLGA 1, the sample has the highest normal force (10.6 N) however, the G' at 10Hz was second highest (280.5 Pa) and normal force at 10Hz was highest (0.52 N) among the three runs. Similarly, run 2 had second highest normal force (9.7 N) during loading, but the G' was highest (788.3 Pa) at 10 Hz and normal force was second highest (0.3316) at 10Hz.

The pattern was random for PGM with Chitosan PLGA and PGM with Chitosan PLGA siRNA as well. Therefore, it can be argued that the high normal force during sample loading might not be related to the increase in G'.

3.2.1.4. Relaxation

The relaxation pattern of control PGM with 0.9% saline was already observed which concluded that mucus itself was highly variable and not one fixed relaxation pattern was observed, with slip in the material during the relaxation. Now, it was important to observe how the PGM with nanoparticles would behave under same conditions. For this step, target strain of 5% was applied for 30 minutes at 25ºC.

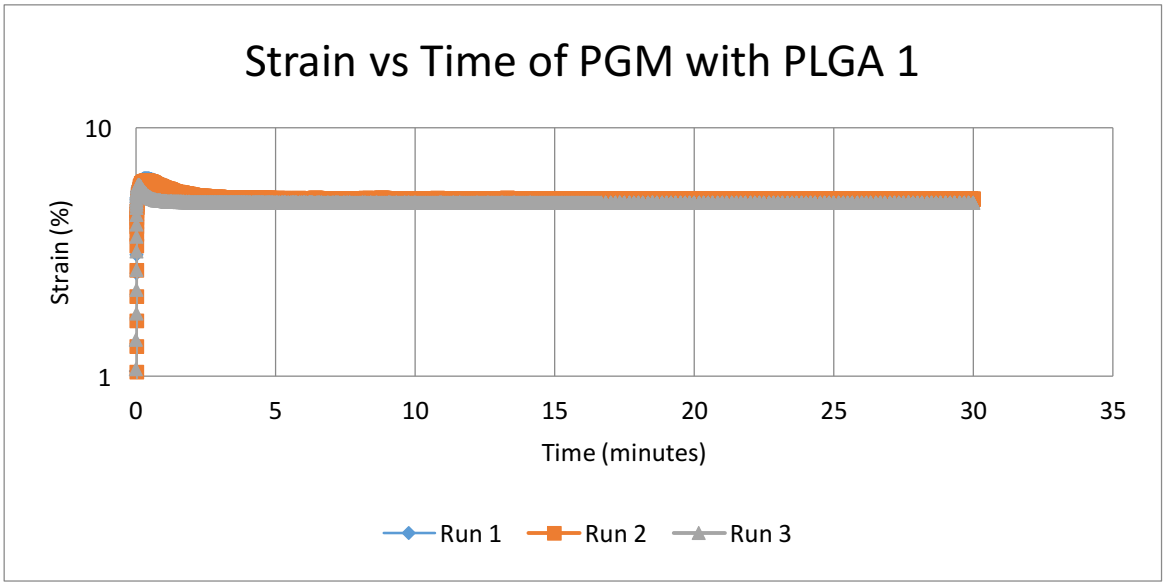

Graph 3-40 Strain or deformation applied to PGM with PLGA 1. The sample was subjected to constant deformation of 5% with rise time of 1 millisecond.

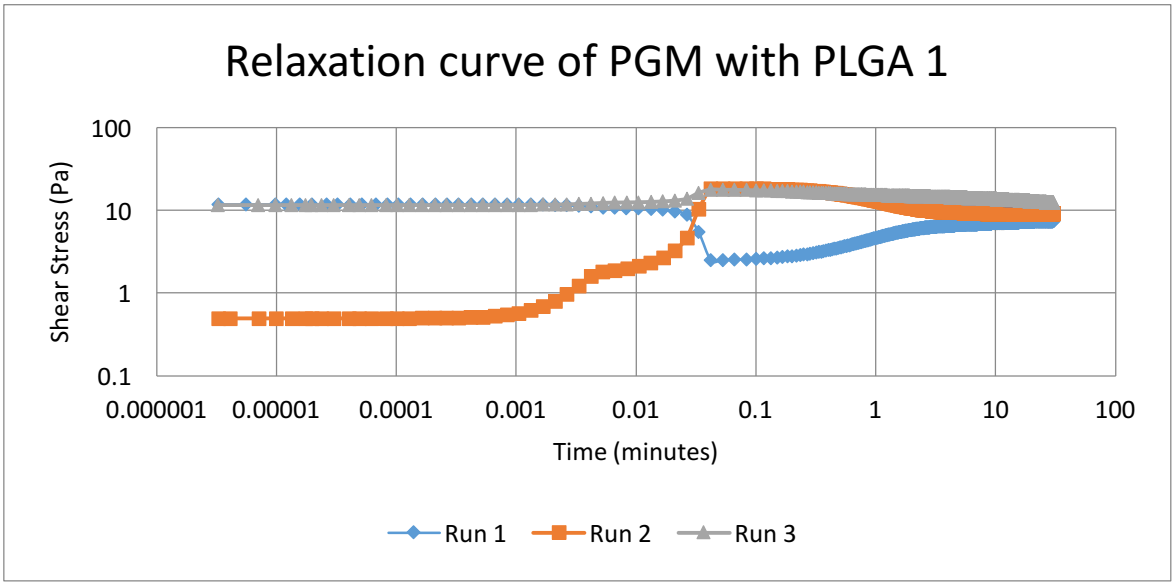

Graph 3-41 Response of PGM with PLGA 1 during stress relaxation at constant deformation of 5%. The Y axis (Stress, Pa) is in log scale.

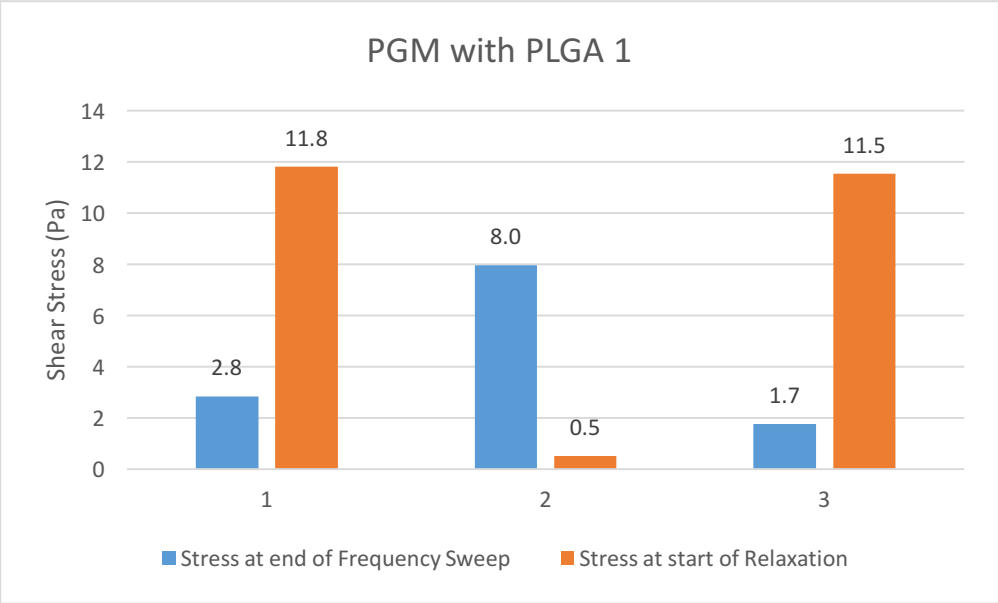

Graph 3-42 Comparison of shear stress values at the end of frequency sweep (at 10Hz) and the start of relaxation for PGM with PLGA 1.

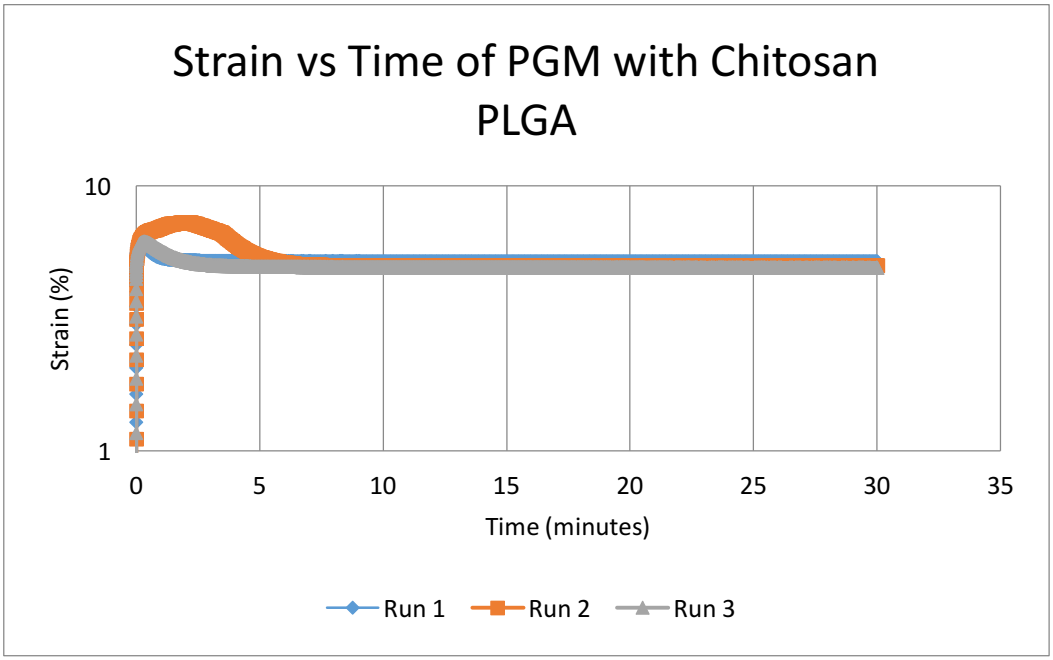

Graph 3-43 Strain or deformation applied to PGM with Chitosan PLGA. The sample was subjected to constant deformation of 5% with rise time of 1 millisecond.

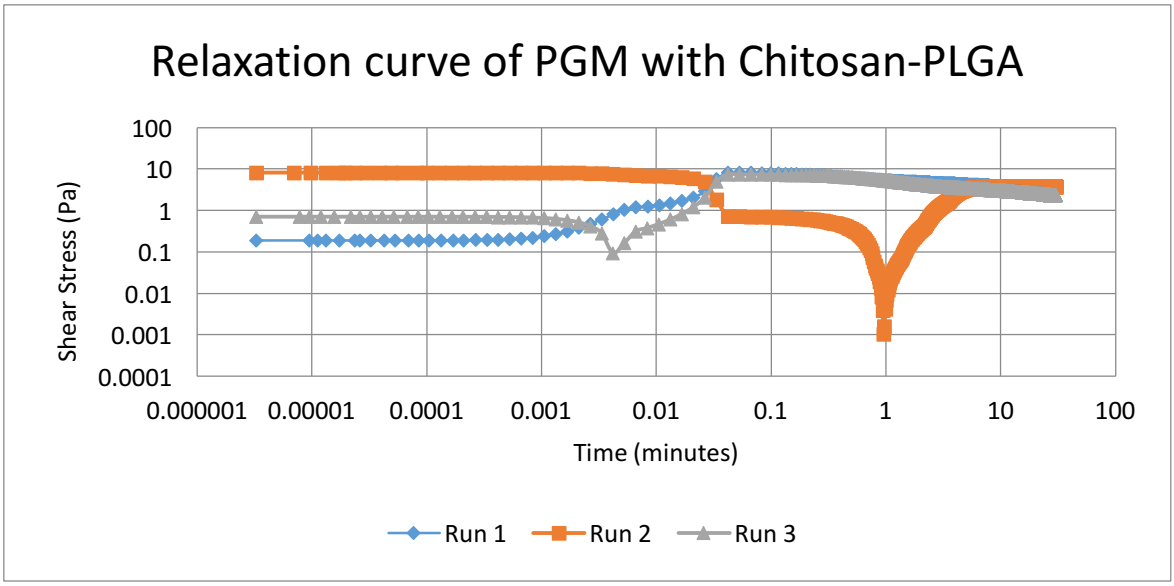

Graph 3-44 Response of PGM with Chitosan PLGA during stress relaxation at constant deformation of 5%. The Y axis (Stress, Pa) is in log scale

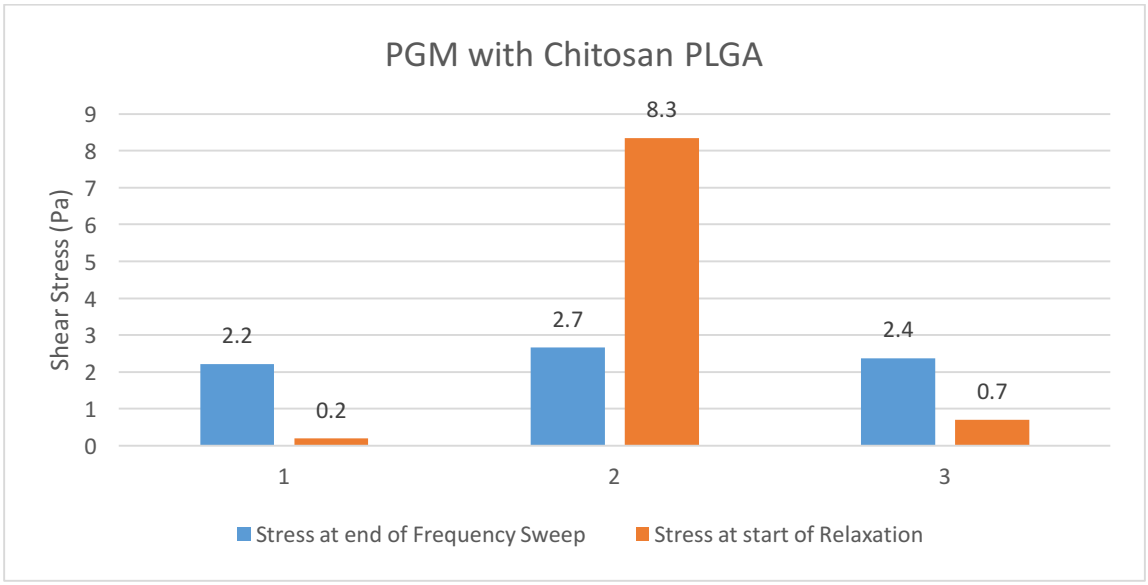

Graph 3-45 Comparison of shear stress values at the end of frequency sweep (at 10Hz) and the start of relaxation for PGM with Chitosan PLGA.

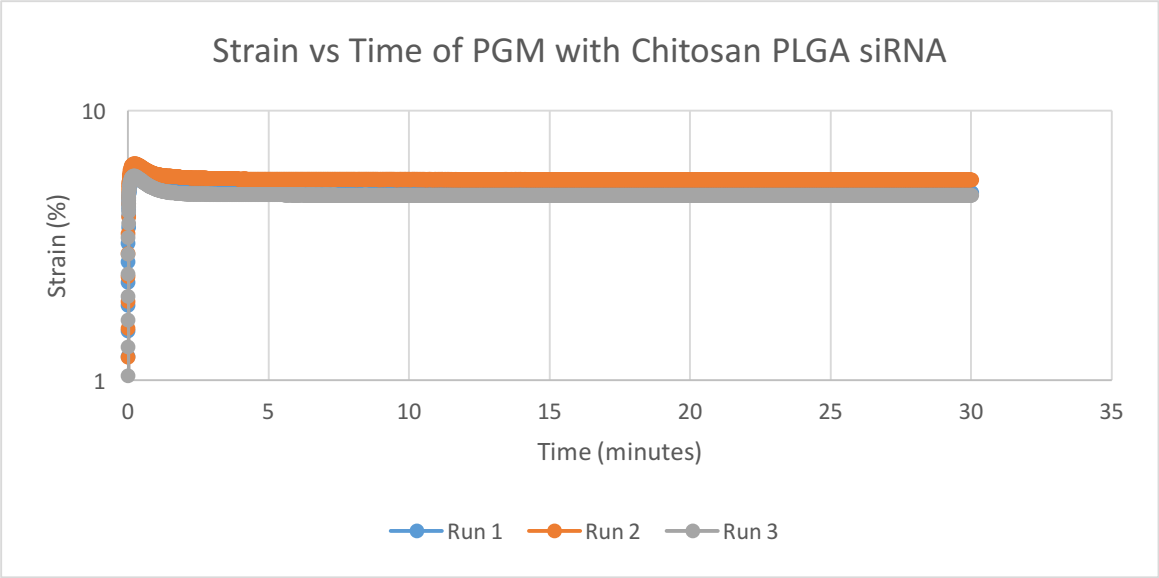

Graph 3-46 Strain or deformation applied to PGM with siRNA loaded Chitosan PLGA. The sample was subjected to constant deformation of 5% with rise time of 1 millisecond

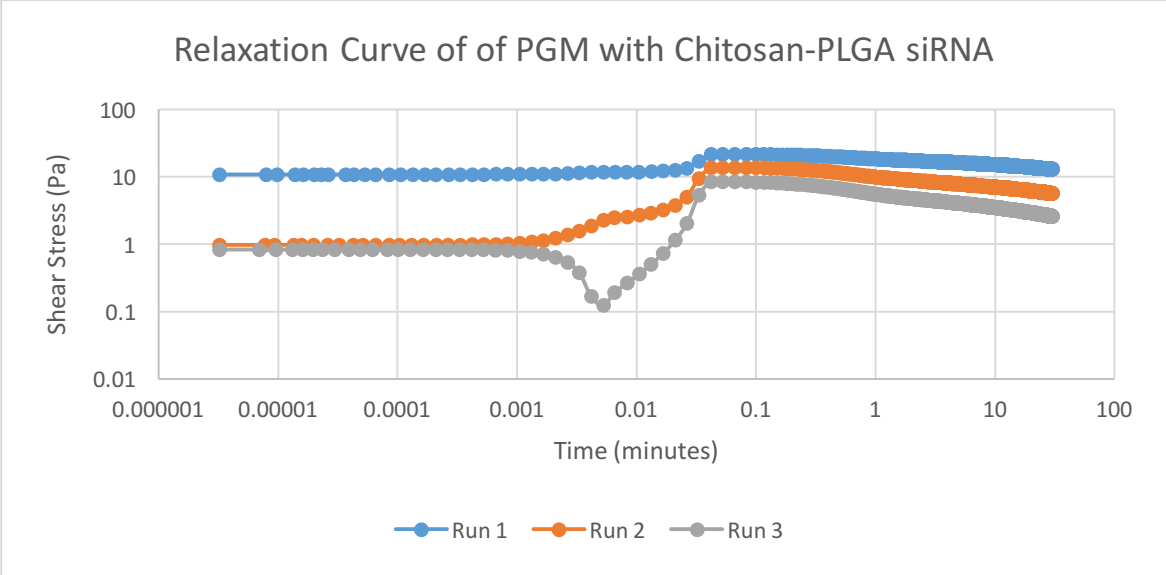

Graph 3-47 Response of PGM with siRNA loaded Chitosan PLGA during stress relaxation at constant deformation of 5%. The Y axis (Stress, Pa) is in log scale.

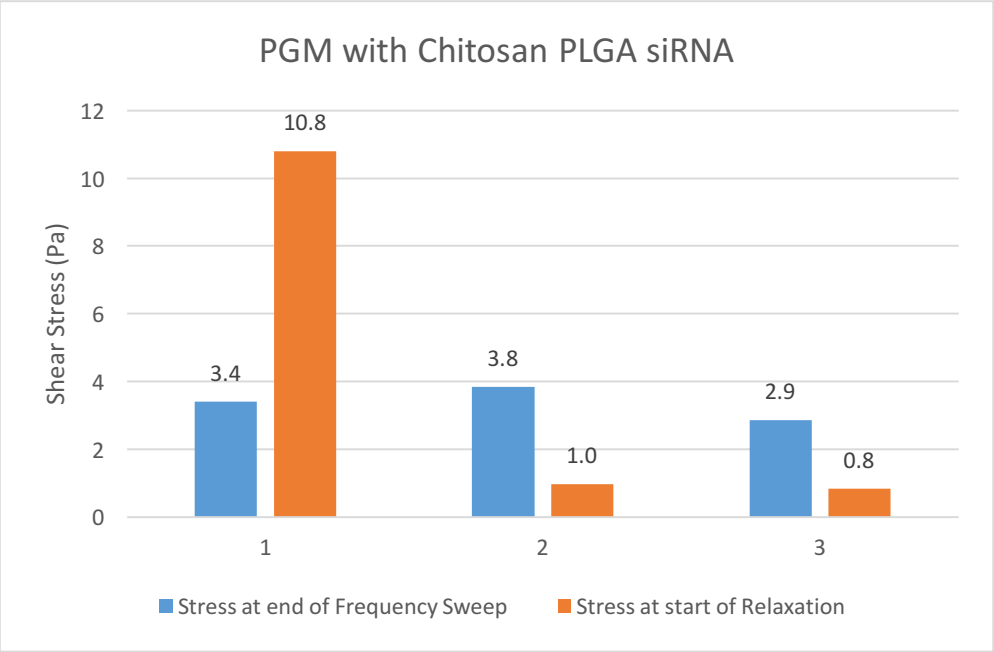

Graph 3-48 Comparison of shear stress values at the end of frequency sweep (at 10Hz) and the start of relaxation for PGM with siRNA loaded Chitosan PLGA.

From graph 40, 43 and 46, it was observed that a sudden strain was applied to the samples (PGM with PLGA, Chitosan PLGA and Chitosan-PLGA siRNA). The strain increases and remains constant throughout the measurement. However, as mentioned before, the instrument used was an stress controlled rheometer. Thus, maintaing a constant deformation accurately could be difficult.

In graph 41, for PGM with PLGA 1, three runs represented by three different curves showed different pattern of relaxation, with the decay pattern not being linear. The case was same for PGM with Chitosan-PLGA as shown in graph 44 and PGM with Chitosan-PLGA siRNA in graph 47. The three runs for each sample had different pattern of relaxation though they were same material. This may relate to the variability and dynamic nature of the mucus.

For instance, in graph 41, for run 2 of PGM with PLGA 1, the stress does not increase from 0 Pa, instead starts from 0.49 Pa, increases upto 18.29 Pa and then relaxes without reaching the equilibrium. This was quite different from normal expected relaxation pattern as shown in figure 1-20, where relaxtion occurs gradually until a equlibrium stress is obtained.Moreover, the stress developed at the end (at 10Hz) of frequency sweep was compared to the stress developed at the start of relaxtion, as shown in graph 42 for PGM with PLGA 1. The stress values were different for all the three runs. This could be because the material was subjected to sudden deformation in just 1millisecond (rise time), thus not giving enough time to

appropriately develop a stress. Also, the stress controlled rheometer may not have be able to accurately control the strain throughout the measurement.

Similarly for run 1 of PGM with Chitosan-PLGA shown in graph 44, the stress develops from 0.18Pa reaches to 8.17 Pa and then relaxes. And, when compared to the stress developed at the end (at 10Hz) of frequency sweep, the stress values at the start of relaxtion were different for all the three runs, as shown in graph 45.

Similarly for run 1 of PGM with siRNA loaded Chitosan-PLGA shown in graph 47, the stress develops from 10.8 Pa reaches to 21.62 Pa and then relaxes without an equilibrium. And, when compared to the stress developed at the end (at 10Hz) of frequency sweep, the stress values at the start of relaxtion were different for all the three runs, as shown in graph 48.

Due to the type of plate arrangement of the instrument, slip was also observed while applying the deformation. This can be seen in graph 44 for Run 2 of PGM with Chitosan PLGA at 1 minutes, where the stress had suddenly decreased. Similarly, in graph 47, for Run 3 of PGM with Chitosan-PLGA siRNA, a slip was obseved at 0.005 minutes (0.3 seconds).The slipping of material could be avoided by the use of cerated plates which would require higher amount of material, thus, not applicable for PGM. Considering the variability of the results, not much conclusive arguments could be developed from the relaxation pattern.

3.2.1.5. Strain Sweep:

These samples, PGM with nanoparticles, were subjected to deformation range of 0.01-100% at 25ºC and 1Hz Frequency. This step was important to understand the structure of the material as well as for determining the linear viscoelastic region (LVR) for the material. A strain value within the LVR could be used in frequency sweep to deform the material and understand its frequency dependence nature. As mentioned before, oscillatory strain was applied to the material in strain sweep.

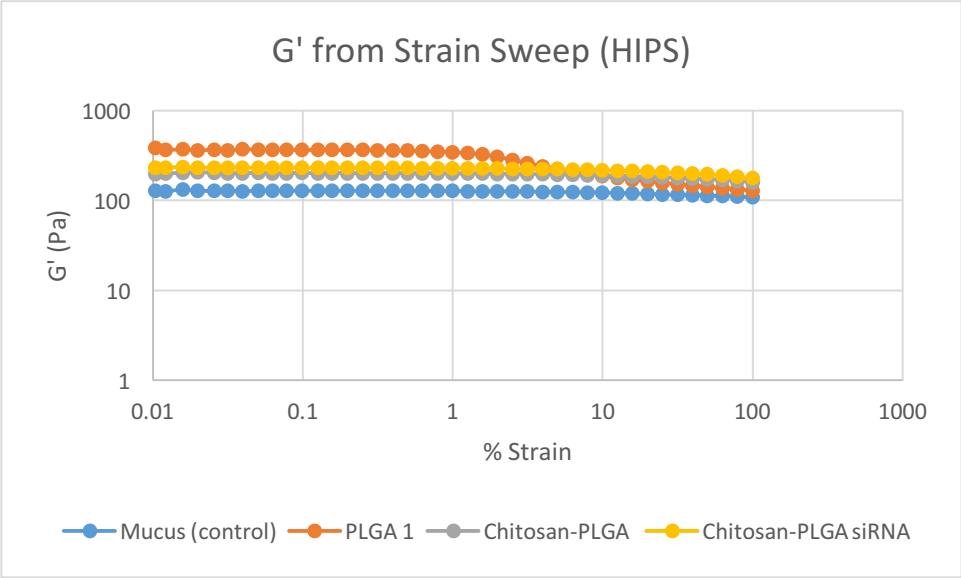

Graph 3-49 The change in elastic modulus (G') of PGM with different nanoparticles and mucus control, over the deformation range of 0.01 to 100%. The Y axis and X axis are in log scale.

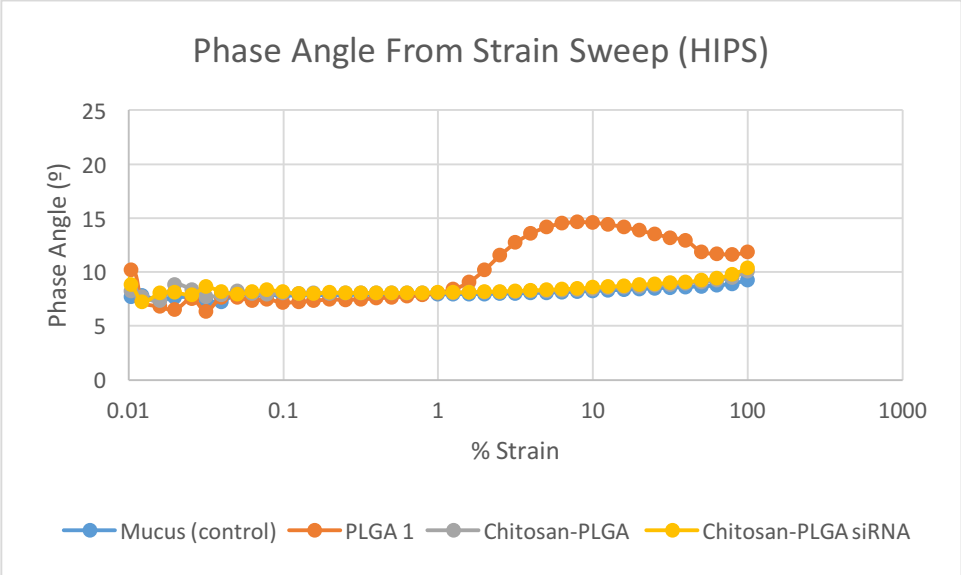

Graph 3-50 The change in phase angle of PGM with different nanoparticles and mucus control, over the deformation range of 0.01 to 100%. The X axis is in log scale, while the phase angle is plotted on Y axis.

From the graph 3-49 and 3-50, PGM with nanoparticle formulations, showed similar behavior under the deformation range except PGM with PLGA 1. For better comparison between the samples, student's t test was done.

Table 3-11 Comparison of G' in mucus control and PGM with nanoparticle formulations at 1Hz Frequency. The comparison was based on student's t test at 95% confidence level. Each row represents each statistical comparison.

Test Sample 1	G' (Pa)	Test Sample 2	G' (Pa)	Remarks
Mucus Control	127.43±6.24	PGM with PLGA 1	207.20±19.52	Significant Difference
Mucus Control	127.43±6.24	PGM with Chitosan-PLGA	178.96±9.09	Significant Difference
Mucus Control	127.43±6.24	PGM with Chitosan-PLGA siRNA	254.13±17.97	Significant Difference

The comparison on the basis of elastic modulus (G') showed significant difference between PGM with nanoparticles and mucus control. However, the distribution, on which the t-test was based on, was obtained from averages and error made up of just 3 runs performed for each sample.

For proper deductions, the difference between mucus control and nanoparticles can be compared to the difference between mucus controls themselves, which were deemed to of significant difference by the t-test, as well. Therefore, the results from t-test could still be argued upon. Similarly, comparison on the basis of phase angle was also done:

Table 3-12 Comparison of phase in mucus control and PGM with nanoparticle formulations at 1Hz Frequency. The comparison was based on student's t test at 95% confidence level. Each row represents each statistical comparison.

Test Sample 1	Phase Angle (^{0})	Test Sample 2	Phase Angle (^{0})	Remarks
Mucus Control	7.92±0.01	PGM with PLGA 1	8.00±0.06	No Significant Difference
Mucus Control	7.92±0.01	PGM with Chitosan-PLGA	7.94±0.06	No Significant Difference
Mucus Control	7.92±0.01	PGM with Chitosan-PLGA siRNA	8.39±0.31	No Significant Difference

It can be seen that the phase angles were quite close to each other and the error of mean used in the t-test were very small. Moreover, the comparison of phase angle showed the addition

of nanoparticles did not result in significant difference between control and PGM with nanoparticle formulations. Thus, it can be argued based on phase angle that addition of nanoparticles does not seem to change the response of material under the oscillatory strain.

It can be seen, from the graph, that sample is independent to deformation until 1% strain and there is no significant change in moduli and phase angle until then. However, the decrease in G' for PGM with PLGA 1 was more steep compared to other samples after the limit of LVR. And, there is gradual increase in phase angle and viscous modulus after the sample was subjected to strain higher than 1.25%. This meant that the material was getting weaker or gel strength of PGM was decreasing. Thus, it can be said that the linear viscoelasticity region (LVR) for PGM was up to 1.25% where G', G" and phase angle were stable. And, 1.25% was the limit of linear viscoelasticity region. This proved that the frequency sweep and single frequency oscillation were performed within LVR, that is at 1 % strain.

Also, all of the samples showed that PGM with nanoparticles was a viscoelastic solid since G'>G" over the deformation range (up to 100%). However, at even higher deformation range, G' and G" could have a crossover where material could have been more liquid like. Thus, more specific conclusions on the structure and behavior could be made once the material was subjected to higher deformation.

3.2.1.6. Summary:

During loading it was observed that adding of nanoparticles increased the normal force of the material. Since, adding of nanoparticles had also changed the viscoelasticity of material to some extent, a comparison was desired, to check if behavior of material during loading had any relation or pattern to the way it behaves in the oscillatory experiments. When load data were compared to data from oscillatory experiments for each of the run, for each sample, no any pattern could be found between maximum normal force during loading, G' and normal force at 10 Hz of frequency sweep. Thus, it could be argued that there was no fix pattern between the tested characteristics.

After the addition of nanoparticles, it was seen that mucus was still a viscoelastic solid with G'>G". However, the values of G', G" had increased while phase angle remained almost the same, when nanoparticles were added. The increase in moduli could be because of variety of interactions between the nanoparticles and the mucus. However, since the phase angle remained the same, which is an important indicator of rheology and viscoelasticity, it could be said that the mucus rheology did not change significantly.

Moreover, when the stress developed during the frequency sweep were compared, similar arguments could be developed stating that addition of nanoparticles did not change the

stress response of the material significantly, under 1% strain. Thus, significant alterations in mucus rheology were not observed after addition of nanoparticles.

3.2.2. Pig Gastric Mucus with PLGA, Lipidoid PLGA and siRNA loaded Lipidoid PLGA

The nanoparticles from HIPs were used in 3 different formulations. (see in figure 1-11)

- PLGA core (PLGA 2),
- Lipidoid coated PLGA core (Lipidoid-PLGA)
- siRNA loaded Lipidoid coated PLGA (Lipidoid- PLGA siRNA).

As mentioned earlier, the study was focused on effects on rheological properties, therefore, the comparison was done based on the differences in the rheological properties. And, the comparison was done on the basis of percentage difference and student's t test. Also, phase angle is considered to be more valuable to comparison as it is a measure of extent of viscous and elastic behavior of material.

As mentioned before, the values used in the graph are the average of the three runs performed for each of the samples.

3.2.2.1. Sample Load data

The objective behind this analysis was to check if there was any connection between the behavior of sample during loading and later oscillatory experiments.

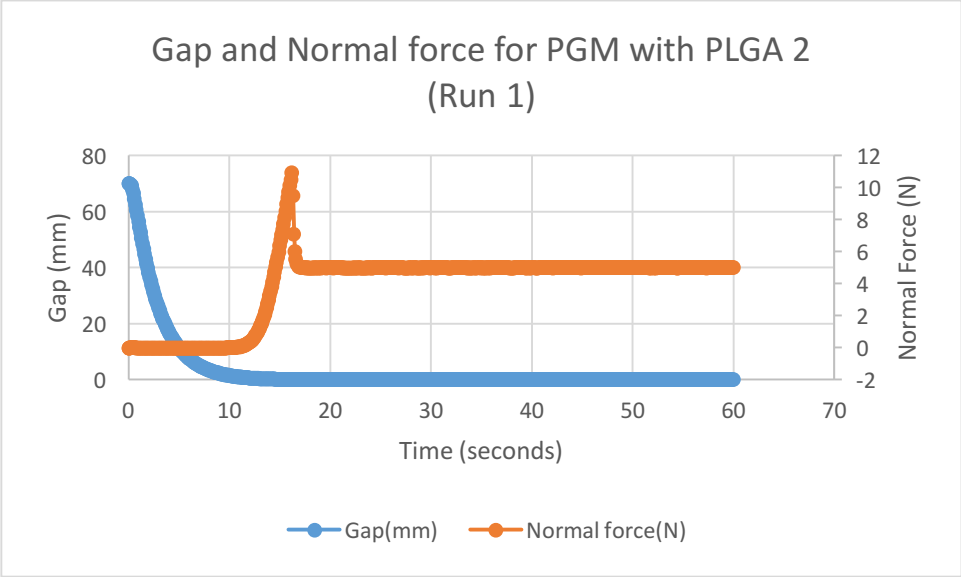

Graph 3-51 The change in gap and normal force over the experiment time for Run 1 of PGM with PLGA 2. The blue curve representing gap (mm) is plotted in primary Y axis, while orange curve representing normal force (N) is plotted in secondary Y axis, over time (sec) in X axis

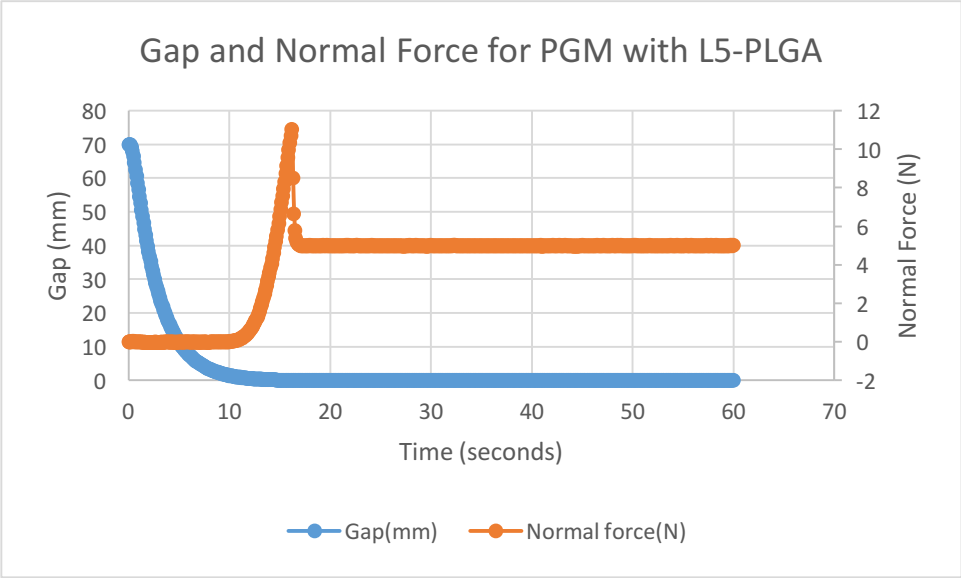

Graph 3-52 The change in gap and normal force over the experiment time for Run 1 of PGM with L5-PLGA. The blue curve representing gap (mm) is plotted in primary Y axis, while orange curve representing normal force (N) is plotted in secondary Y axis over time (sec), in x axis.

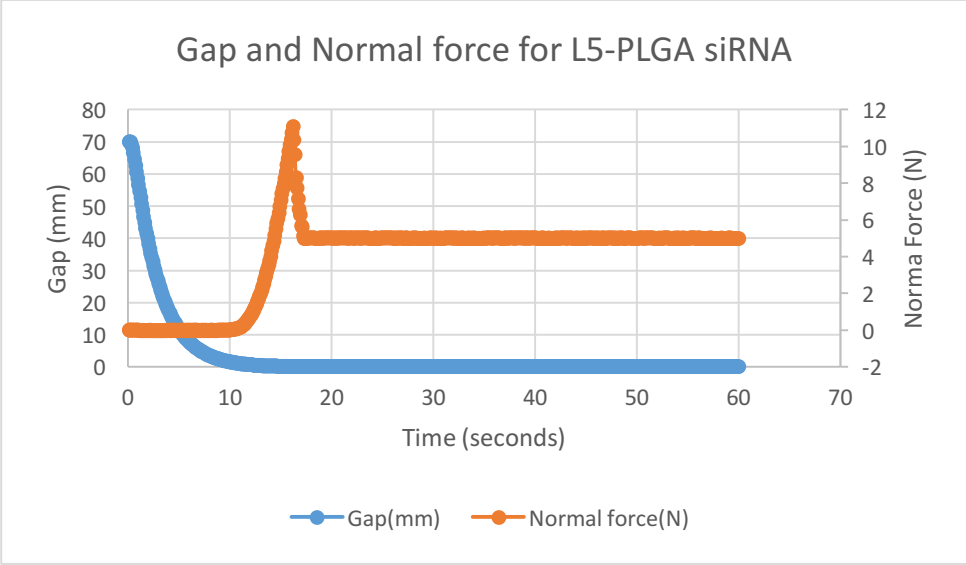

Graph 3-53 The change in gap and normal force over the experiment time for Run 1 of PGM with L5-PLGA siRNA. The blue curve representing gap (mm) is plotted in primary Y axis, while orange curve representing normal force (N) is plotted in secondary Y axis over time (sec), in X axis.

It can be seen from the graphs that the loading data of the PGM with nanoparticles does not have dramatic difference from each other. However, maximum normal force and rise time seem to be different from each other between the samples. The graphical representation of load data of all the other runs are presented in Appendix D.1. Nevertheless, the contact gap, time for rise, end gap and maximum normal force of all the runs of PGM with nanoparticles have been compared in the table below.

Table 3-13 Comparison of PGM with nanoparticles in terms of contact gap, time for rise, end gap and maximum normal force. All the three runs performed for each sample have been presented.

Sample (PGM with)	Run	Contact Gap (mm)	Time for rise (s)	End Gap (mm)	Maximum Normal force (N)
PLGA 2	1	1.30	5.90	0.03	10.92
	2	1.99	7.00	0.03	11.06
	3	1.90	7.00	0.03	9.86
L5-PLGA	1	1.83	6.71	0.03	11.02
	2	1.99	6.70	0.04	10.92
	3	2.45	6.72	0.07	10.95
siRNA L5-PLGA	1	1.36	6.00	0.03	11.06
	2	2.90	7.50	0.05	10.91
	3	2.25	7.10	0.04	10.95

From table 3-13, it can be seen that the contact gap is variable for three different runs of the same sample. For instance, for PGM with PLGA 2, the contact gaps are 1.30, 1.99 and 1.90mm. This could be because of the way with which the sample was loaded on the base plate. Moreover, the PGM used was not completely homogenized and thus, the mucus itself could be highly variable due to presence of aggregates.

Statistical correlation coefficients of 0.99, 0.71 and 0.98 were found between contact gap and time of rise, among runs of PGM with PLGA 2, L5-PLGA and siRNA L5-PLGA respectively. It was obvious that for a sample with small contact gap, the instrument took less time to reach the maximum force. However, the maximum force applied to the material does not seem to be related to this correlation.

Nevertheless, it was observed that more normal force was applied to the PGM with nanoparticles than PGM with 400μl saline (shown in section 3.1.1.1). The maximum normal forces of PGM with nanoparticles can be compared in the graph below.

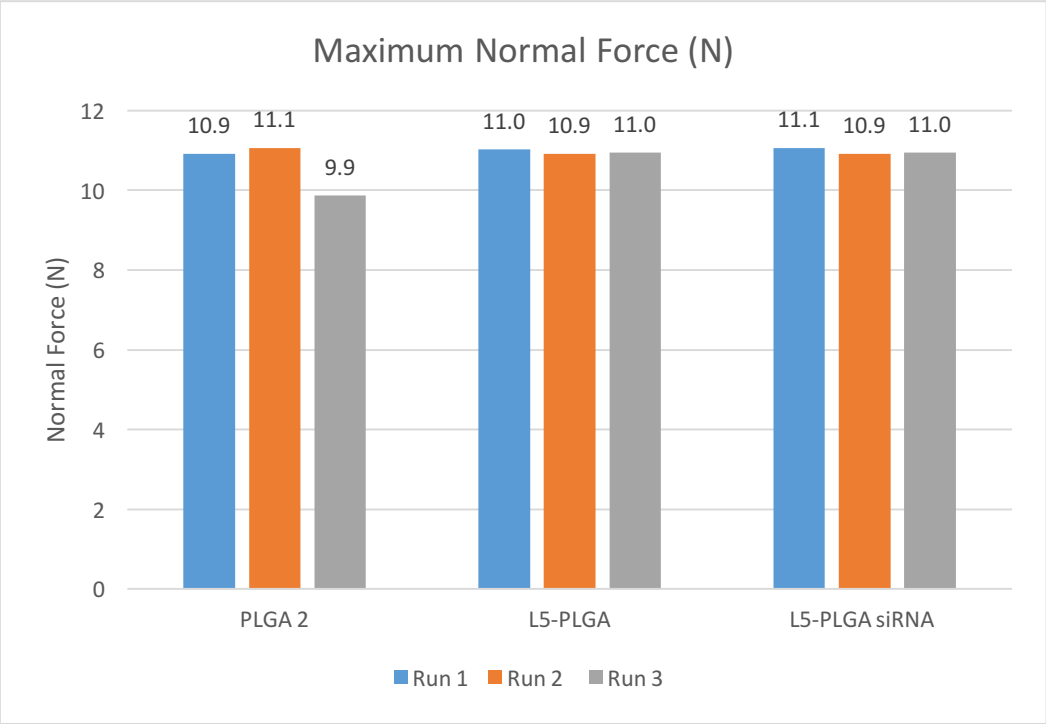

Graph 3-54 Comparison of Maximum Normal Force of PGM with nanoparticles for all the three runs

Here, the addition of nanoparticle formulation had increased the normal force of the PGM when compared to control presented in in section 3.1.1.1. However, it seemed all nanoparticles had similar and comparable maximum normal force.

The general increase over control, might or might not be related to the increase viscoelasticity and normal force of the material during frequency sweep. For instance, the sample with highest normal force during loading could have high or low G' during frequency sweep or have no relation at all. Therefore, these normal forces during loading were compared to G' and normal force in frequency sweep for all the runs and are discussed in section 3.2.2.3.

Except for the difference in the maximum normal force, no other conclusive differences were seen between PGM with nanoparticles and PGM control.

3.2.2.2. Single Frequency Oscillation

This was an important step to find out if the moduli and phase angle, on which the analysis are based on, were in apparent equilibrium. This step was performed at frequency of 1Hz, 1% strain and at 25ºC for around 8 minutes, within the linear viscoelastic region (LVR).

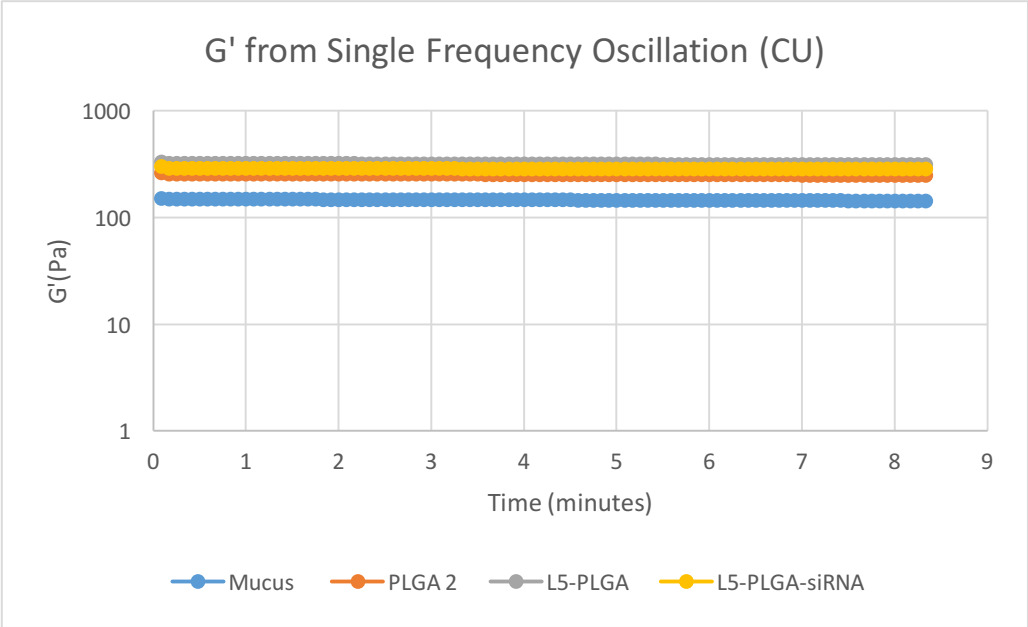

Graph 3-55 Elastic modulus (G') of different nanoparticle formulations compared to mucus control (PGM with 400μl saline) depicted in different colors over a time period, at a single frequency of 1Hz throughout the measurement. The elastic moduli are plotted in a log scale.

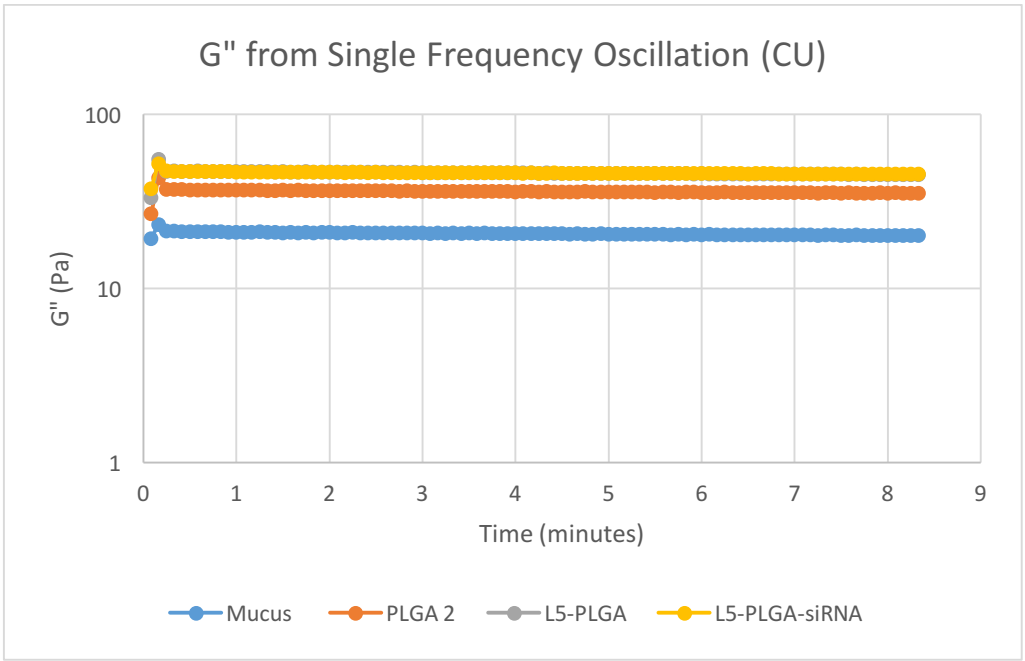

Graph 3-56 Viscous modulus (G") of different nanoparticle formulations compared to mucus control (PGM with 400µl saline) depicted in different colors over a time period, at a single frequency of 1Hz throughout the measurement. The viscous moduli are plotted in a log scale

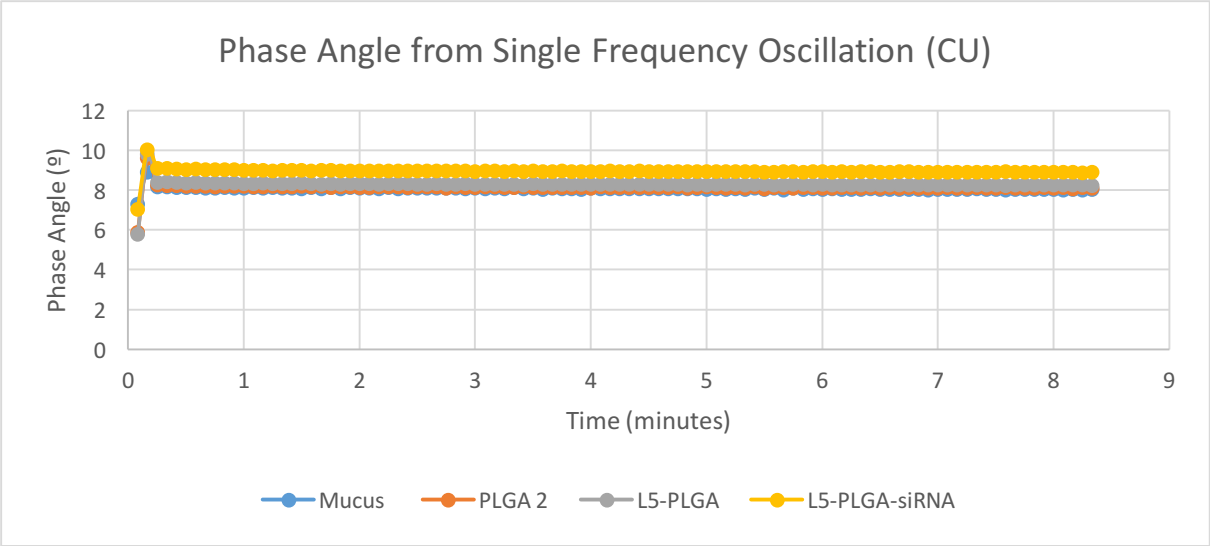

Graph 3-57 Phase angles of different nanoparticle formulations compared to mucus control (PGM with 400µl saline) depicted in different colors over a time period, at a single frequency of 1Hz throughout the measurement.

It can be seen from the graphs, that the all samples are in apparent equilibrium, as the moduli and phase angle of the sample do not change over time throughout the experiment. This could be seen more clearly from the table presented below:

Table 3-14 Comparison of G' for PGM with PLGA 2 at 3 minutes and 8 minutes to verify if the moduli had changed over time.

Time	G' (Pa)	Difference
3 minutes	253.67	1.9%
8 minutes	248.6	

It was seen that the difference of G' at 3 minutes and 8 minutes was just 1.9%. Similarly, the difference in phase angle at 3 minutes and 8 minutes was just 0.6%. These small differences showed that PGM with PLGA 2 was stable or in apparent equilibrium over the measured time period.

Table 3-15 Comparison of G' for PGM with L5-PLGA at 3 minutes and 8 minutes to verify if the moduli had changed over time.

Time	G' (Pa)	Difference
3 minutes	318.87	2.04%
8 minutes	312.36	

It was seen that the difference of G' at 3 minutes and 8 minutes was just 2.04%. Similarly, the difference in phase angle at 3 minutes and 8 minutes was just 0.4%. These small differences showed that PGM with L5-PLGA was stable or in apparent equilibrium over the measured time period.

Table 3-16 Comparison of G' for PGM with siRNA loaded L5-PLGA at 3 minutes and 8 minutes to verify if the moduli has changed over time.

Time	G' (Pa)	Difference
3 minutes	286.73	1.2%
8 minutes	283.07	

It was seen that the difference of G' at 3 minutes and 8 minutes was just 1.2%. Similarly, the difference in phase angle at 3 minutes and 8 minutes was just 0.5%. These small differences showed that PGM with siRNA loaded L5-PLGA was stable or in apparent equilibrium over the measured time period.

When compared to PGM control with 400μl of saline, the PGM with nanoparticle formulations had comparatively higher elastic moduli (G') while the phase angle remained almost the same for all the samples.

Also, throughout the experiment time, G'>G" indicating that the material was still as viscoelastic solid. Although, more on this can concluded from later steps of the oscillatory experiments.

3.2.2.3. Frequency Sweep

This step was done at the frequency range of 0.01Hz to 10 Hz. The experiment was performed at 25ºC and 1% strain, known to be within the LVR, thus would not destroy the material. The values below 0.1 are omitted from the graph because of low signal to noise ratio.

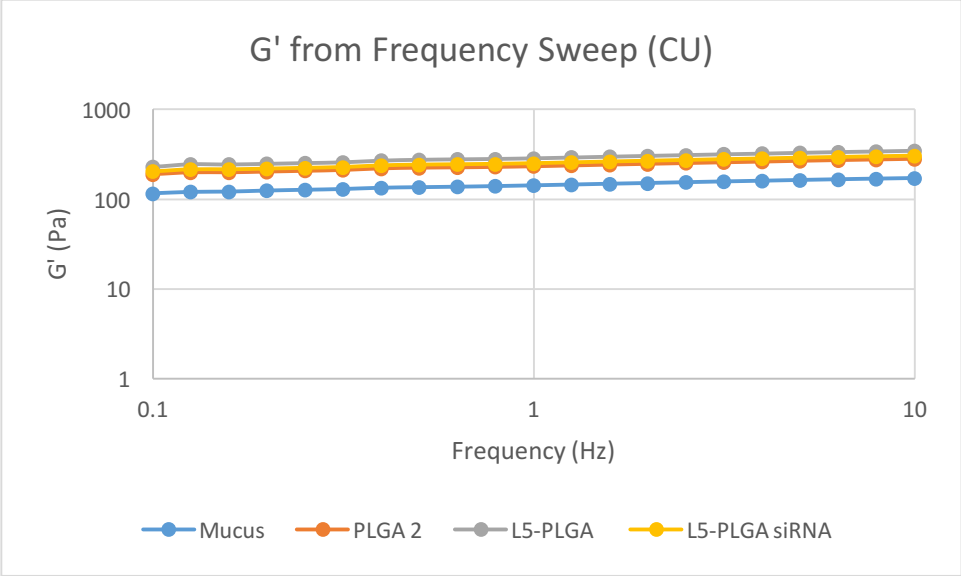

Graph 3-58 Elastic Modulus (G') of PGM with different nanoparticle formulations and mucus control (PLGA with 400µl saline) over the frequency range of 0.1 Hz to 10Hz, presented in different colors. Both of the axes are in log scale.

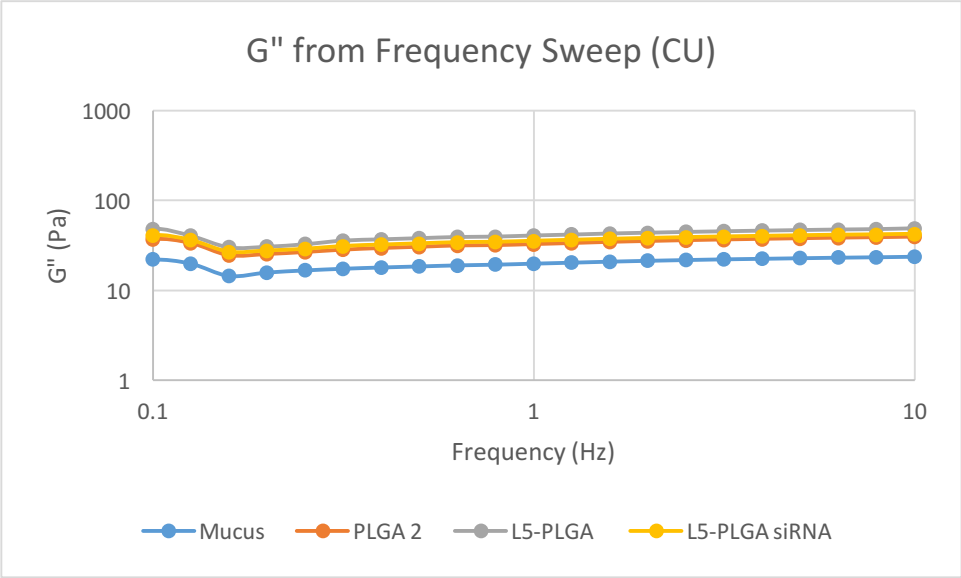

Graph 3-59 Viscous Modulus (G") of PGM with different nanoparticle formulations and mucus control (PLGA with 400µl saline) over the frequency range of 0.1 Hz to 10Hz, presented in different colors. Both of the axes are in log scale.

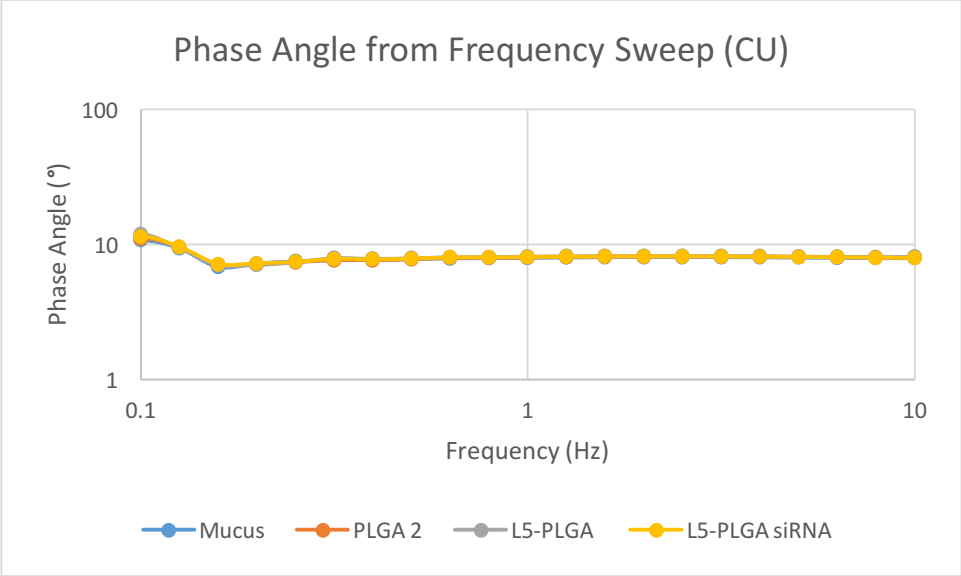

Graph 3-60 Phase angles of PGM with different nanoparticle formulations and mucus control (PLGA with 400µl saline) over the frequency range of 0.1 Hz to 10Hz, presented in different colors. The frequency range (x-axis) is plotted in log scale.

All of the samples showed similar reaction to the applied frequency range. It can clearly be seen that there was increase in moduli and phase angle as the frequency was increased from 0.1 to 10Hz.

This indicated that the interactions in materials were frequency (or timescale) dependent. From graph 3-58, at larger frequencies (shorter time scale), the material is more elastic. However, at smaller frequencies (longer time scale), the elasticity of the material

decreases. This indicated the presence of timescale dependent interactions that were higher at shorter timescale and decreased at longer timescale.

These interactions were slightly higher in PGM with nanoparticles than the mucus control. This could be observed from the higher G' of PGM with nanoparticles than mucus control.

From graph 3-60, the phase angle is high at longer time scale (lower frequency). which then decreases. This depicted the more viscous nature at longer timescale that is, mucus flows when given enough time. However, this was not relevant because mucus turnover clears the mucus well before such timescale could be reached.[42]

From the graph 3-58 and 3-59, for PGM with nanoparticle formulations, G'>G" with no signs of crossover. Thus, PGM with nanoparticles was also solid dominant viscoelastic material. The materials showed characteristic of a gel system with phase angles of 8.01° (PGM with PLGA 2) and 8.17° (PGM with L5-PLGA) and 8.07° (PGM with L5-PLGA siRNA) at 1Hz. However, the most prominent effect was shown by the addition of L5 coated PLGA cores to the PGM among other nanoparticle formulations. A detailed comparison of PGM with different nanoparticle formulations along with the analysis of another set of nanoparticles from HIPS and mucus control at 1Hz and 10 Hz is presented in section. 3.2.3.

It was also interesting to observe, if the sample had changed in terms of stress response to deformation during the time scale. Thus, the stress values of this experiment were compared at the same frequency sweep from 0.1Hz to 10 Hz.

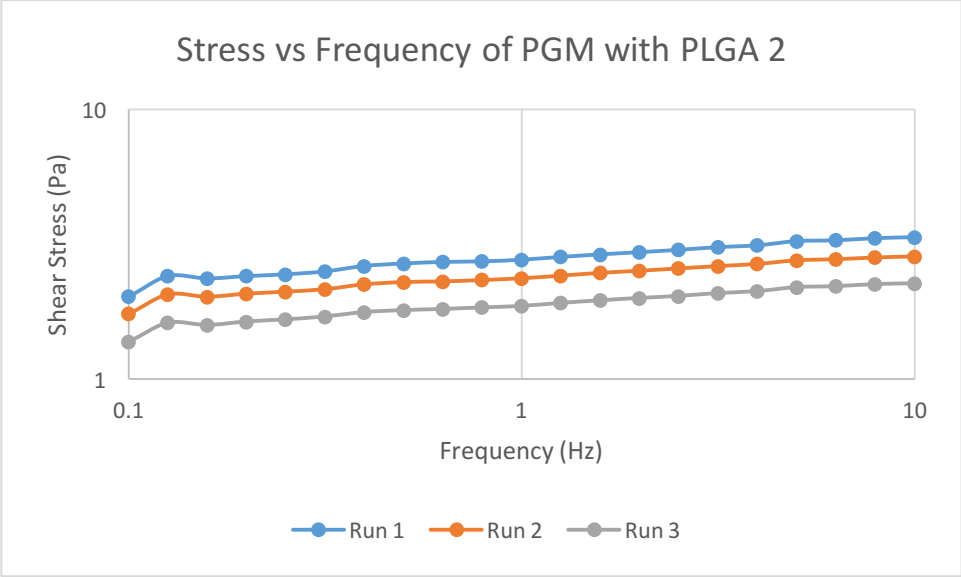

Graph 3-61 Stress developed in PGM with PLGA 2 saline at 1% strain, during the frequency sweep from 0.1Hz to 10Hz.Both of the axes are in log scale.

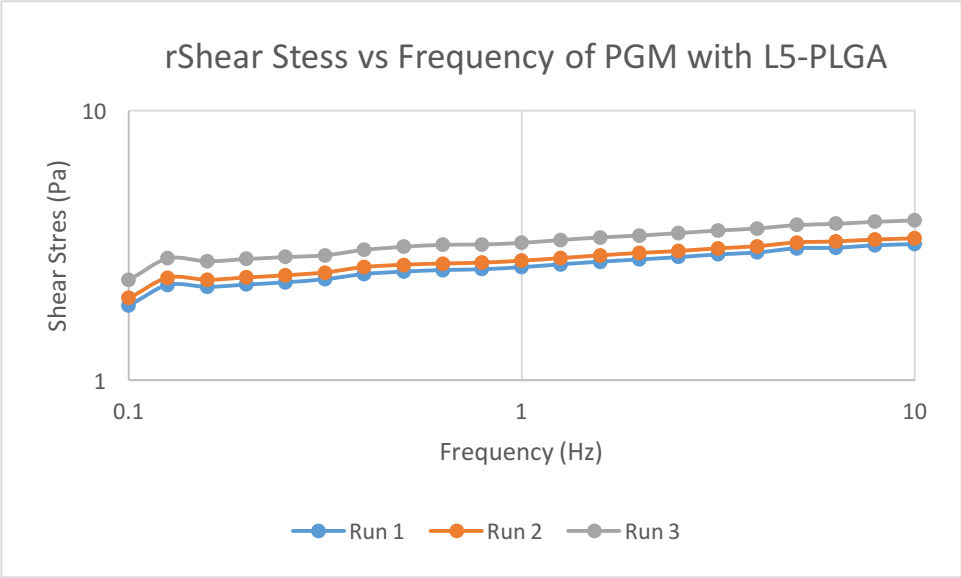

Graph 3-62 Stress developed in PGM with L5-PLGA at 1% strain, during the frequency sweep from 0.1Hz to 10Hz.Both of the axes are in log scale.

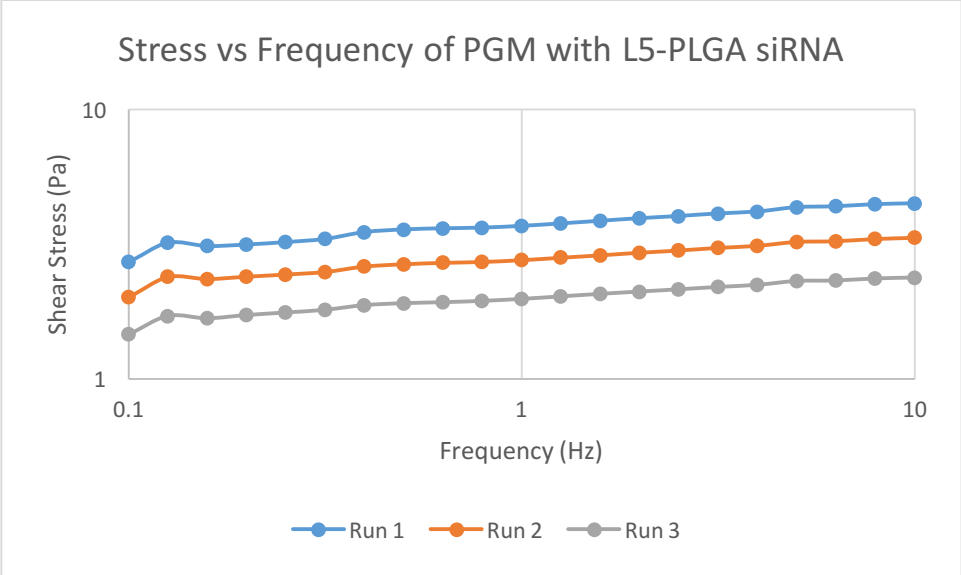

Graph 3-63 Stress developed in PGM with siRNA loaded L5-PLGA at 1% strain, during the frequency sweep from 0.1Hz to 10Hz.Both of the axes are in log scale.

Table 3-17 Comparison of stress in mucus control and PGM with nanoparticle formulations at 1Hz Frequency. The comparison was based on student's t test at 95% confidence level. Each row represents each statistical comparison.

Test Sample 1	Shear Stress (Pa)	Test Sample 2	Shear Stress (Pa)	Confidence Level	Remarks
Mucus Control	1.43±0.06	PGM with PLGA 2	2.36±0.21	95%	Significant difference
Mucus Control	1.43±0.06	PGM with L5 PLGA	2.88±0.14	95%	Significant difference
Mucus Control	1.43±0.06	PGM with L5 PLGA siRNA	2.81±0.40	95%	Significant difference

During the statistical comparison of shear stress, it was found that shear developed in mucus control (PGM with 400μl saline) and PGM with PLGA 2 had significant difference. However, this was not the case for PGM with PLGA 1(from HIPS), discussed in section 3.2.1.3. This could be due to differences in PLGA cores which are discussed in section 3.2.4.

Similarly, when mucus control was compared to PGM with L5 PLGA and siRNA loaded L5 PLGA, the difference in stress developed was significantly different. This could be because the 3 runs are largely spread, as seen in graph 3-62 and 3-63. Such differences between the 3 runs for each sample could affect the statistical deductions of t-test.

Interestingly, the stress developed in the PGM with nanoparticles was higher than that of control with 400μl saline. As mentioned before, the distribution, on which the t-test was based on, was obtained from averages and error from just 3 runs performed for each material. Moreover, the error of the mean used in t-test were very small leading to such significant difference at 95% confidence level. Thus, the result from t test could still be argued upon. Moreover, even though the stress developed in the PGM with nanoparticles is higher than that of control with 400μl saline, the differences between them can be considered unsubstantial when compared to difference of stress between the controls themselves (PGM with 200μl and 400μl saline), discussed in section 3.1.1.3.

Thus, based on stress developed in the material, it can be concluded that the rheology of mucus would not change substantially by addition of nanoparticles.

As mentioned before, there could have been a pattern between the behavior of the material during loading and frequency sweep. Therefore, the maximum normal force of the

material, G' and Normal force at the end (10Hz, short timescale) of frequency sweep are compared. The results are presented below:

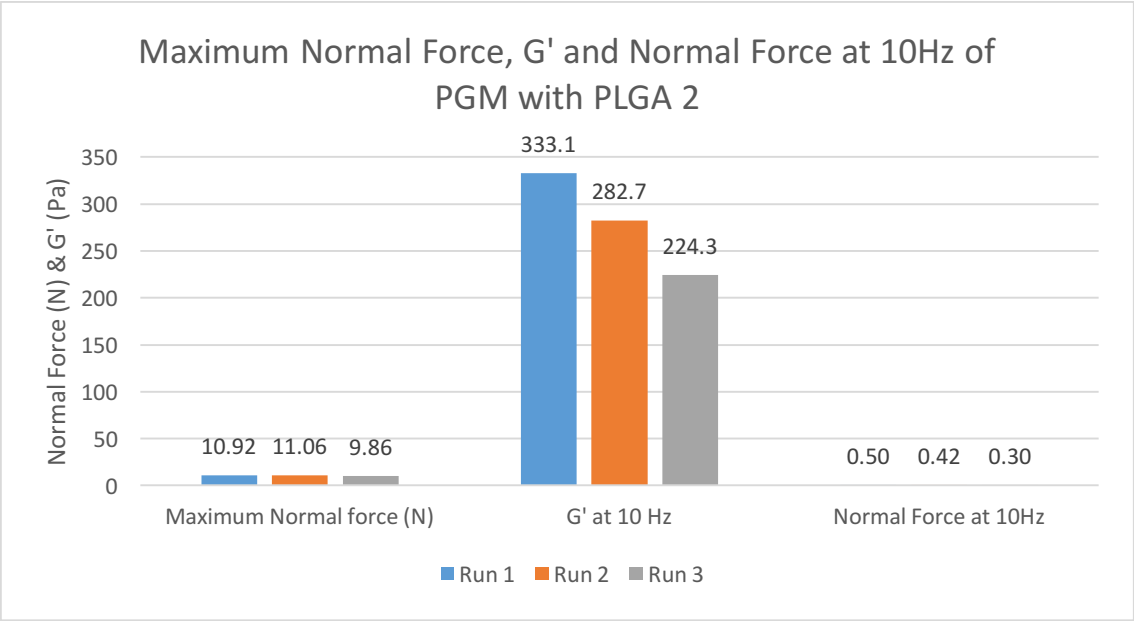

Graph 3-64 Comparison of Maximum Normal Force, G' and Normal Force at 10Hz for PGM with PLGA 2.

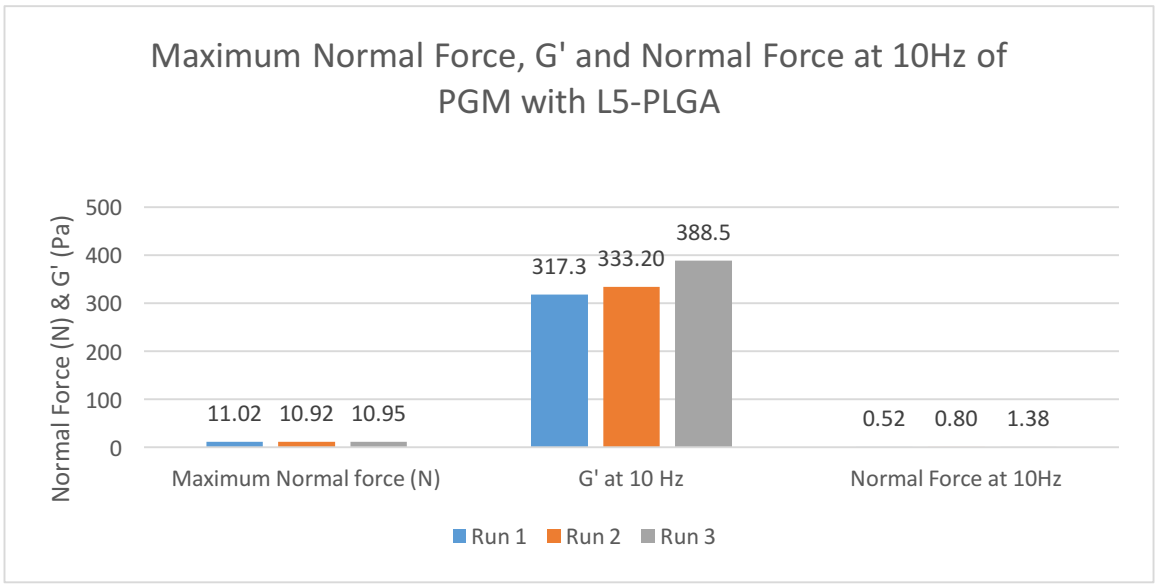

Graph 3-65 Comparison of Maximum Normal Force, G' and Normal Force at 10Hz for PGM with L5-PLGA.

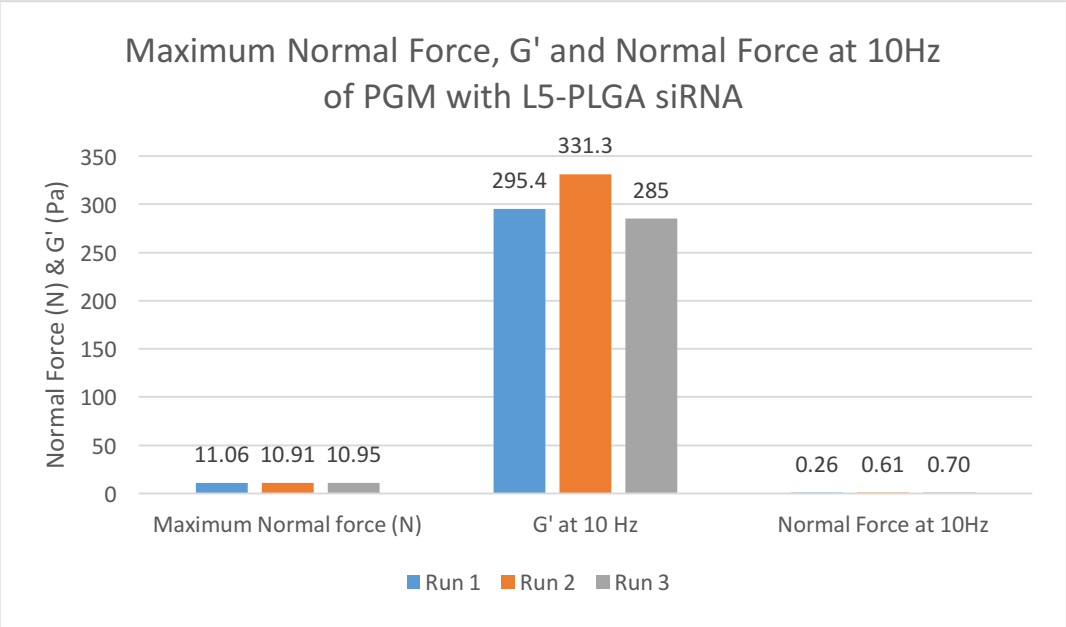

Graph 3-66 Comparison of Maximum Normal Force, G' and Normal Force at 10Hz for PGM with L5-PLGA siRNA

Here in graph 3-64, for Run 2 of PLGA 2, the sample had the highest normal force (11.6 N) however, the G' at 10Hz was second highest (282.5 Pa) and normal force at 10Hz was also second highest (0.41 N) among the three runs. Similarly, run 1 had second highest normal force (10.9 N) during loading, but the G' was highest (333.1 Pa) at 10 Hz and normal force was highest (0.49) at 10Hz.

The relation was random for L5 PLGA and L5-PLGA siRNA as well. Moreover, the pattern found for PGM with CU nanoparticles could not be related to PGM with HIPS nanoparticles: PLGA 1, Chitosan PLGA and Chitosan PLGA siRNA, which are discussed in section 3.1.2.3.

Therefore, it can be argued that the high normal force during sample loading may not be related to increment in G' during frequency sweep.

3.2.2.4. Relaxation

The relaxation patterns of PGM with saline and HIPS nanoparticles were already observed which concluded that mucus itself was highly variable and not one fixed relaxation pattern was observed. Material slip was also observed during the relaxation of mucus control and PGM with nanoparticles from HIPS. Now, it was important to observe how the PGM with CU nanoparticles would behave under same conditions. For this step, target strain of 5% was used for 30 minutes at 25ºC.

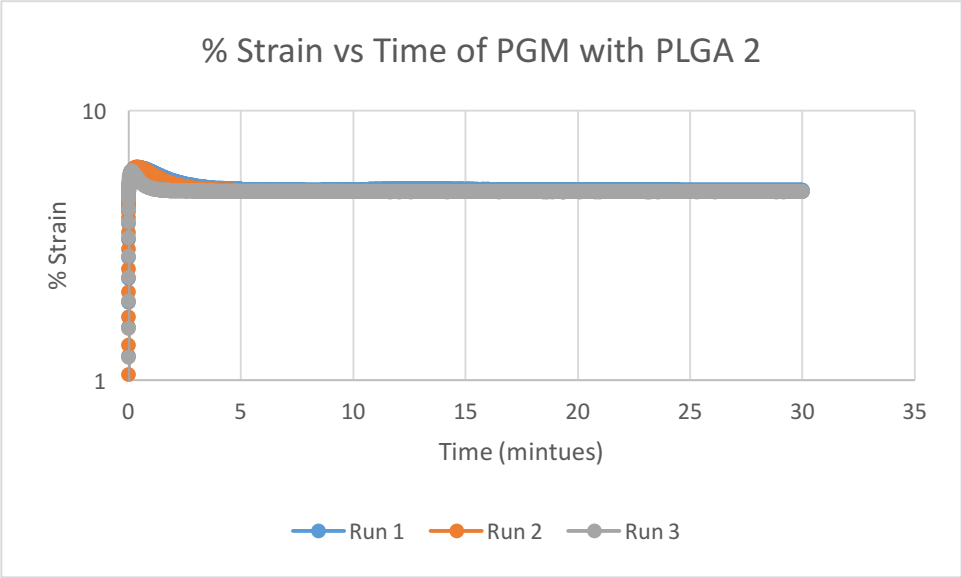

Graph 3-67 Strain or deformation applied to PGM with PLGA 2. The sample was subjected to constant deformation of 5% with rise time of 1 millisecond.

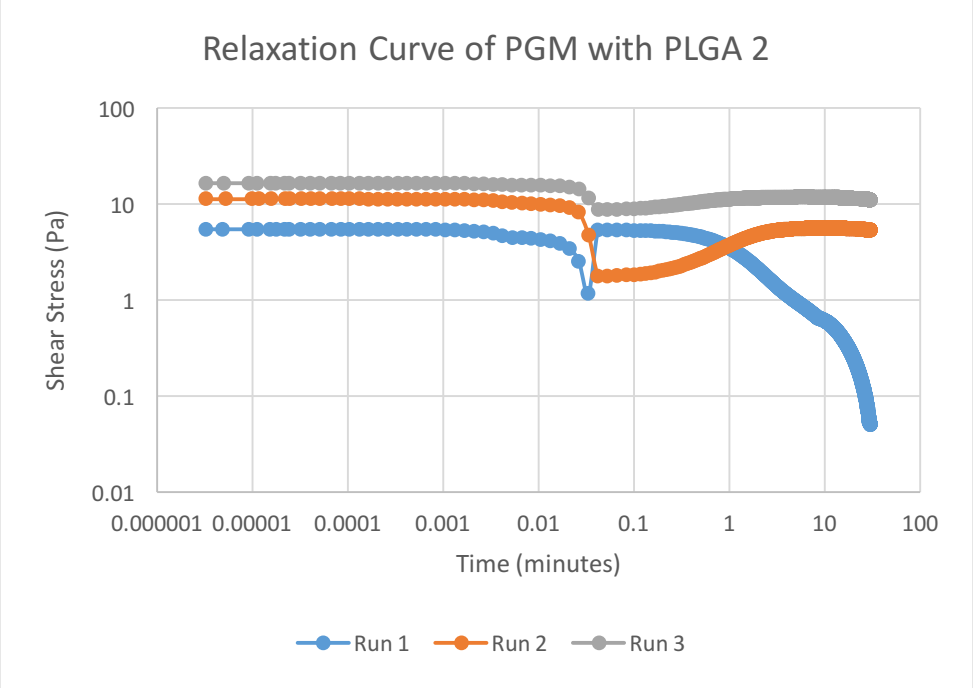

Graph 3-68 Response of PGM with PLGA 2 during stress relaxation at constant deformation of 5%. The Y axis (Stress, Pa) is in log scale.

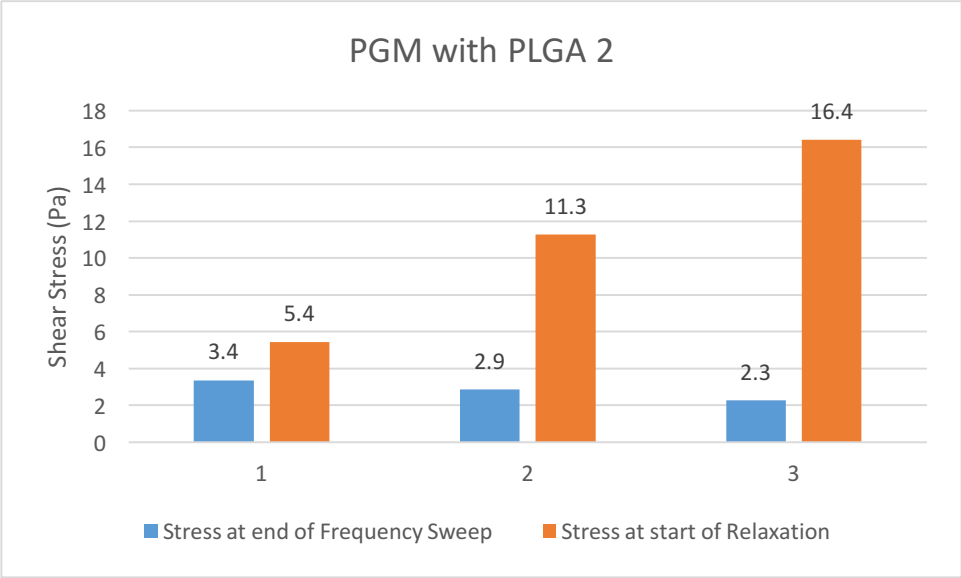

Graph 3-69 Comparison of shear stress values at the end of frequency sweep (at 10Hz) and the start of relaxation for PGM with PLGA 2.

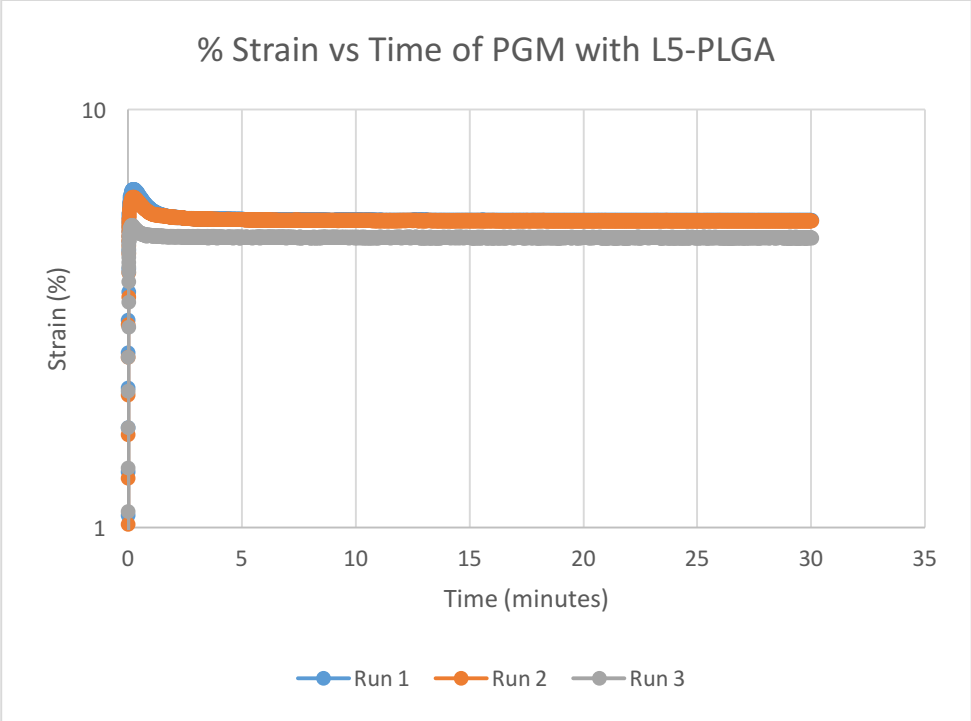

Graph 3-70 Strain or deformation applied to PGM with L5 PLGA. The sample was subjected to constant deformation of 5% with rise time of 1 millisecond.

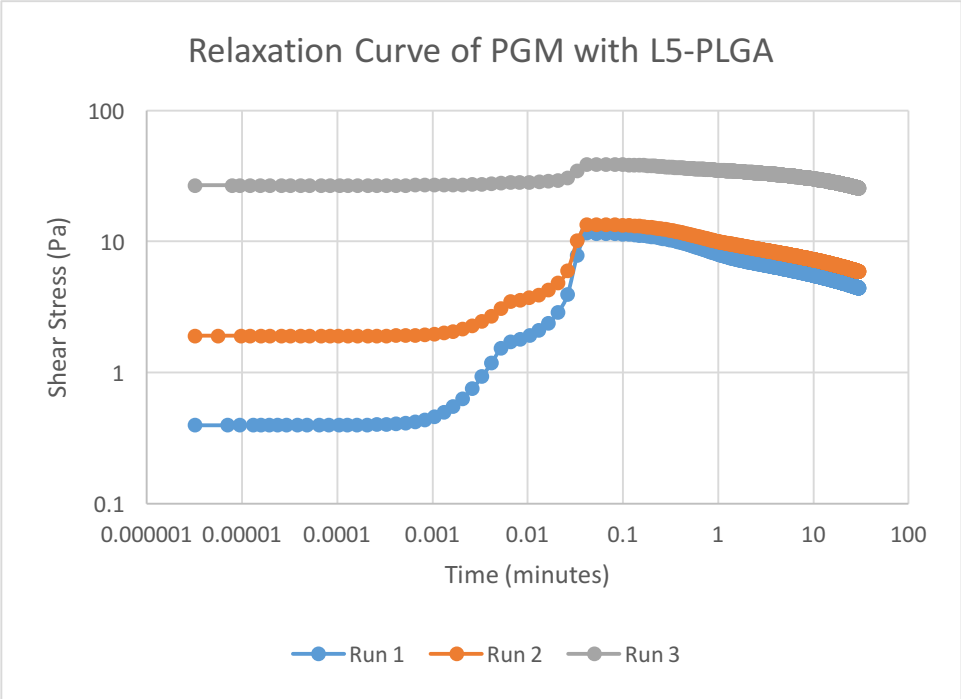

Graph 3-71 Response of PGM with L5 PLGA during stress relaxation at constant deformation of 5%. The Y axis (Shear Stress, Pa) is in log scale.

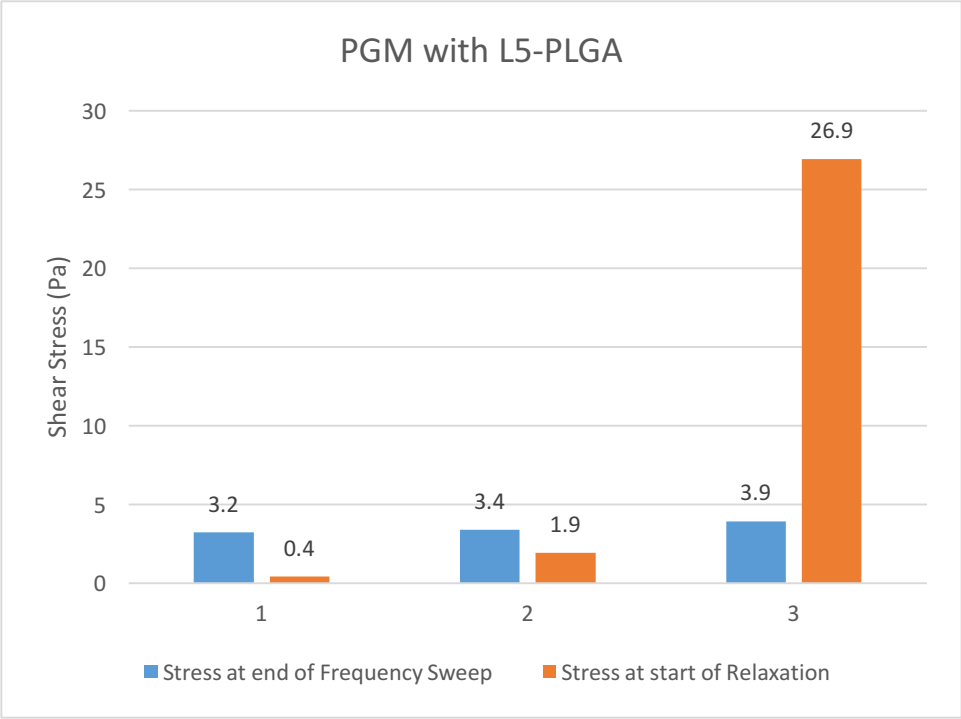

Graph 3-72 Comparison of shear stress values at the end of frequency sweep (at 10Hz) and the start of relaxation for PGM with L5 PLGA.

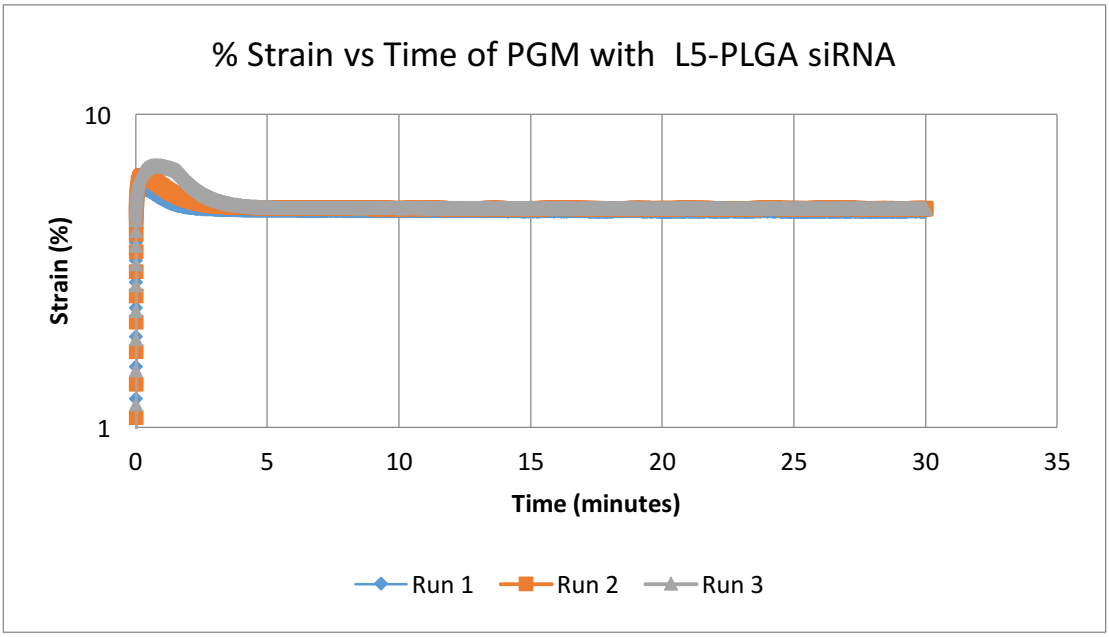

Graph 3-73 Strain or deformation applied to siRNA loaded PGM with L5 PLGA. The sample was subjected to constant deformation of 5% with rise time of 1 millisecond.

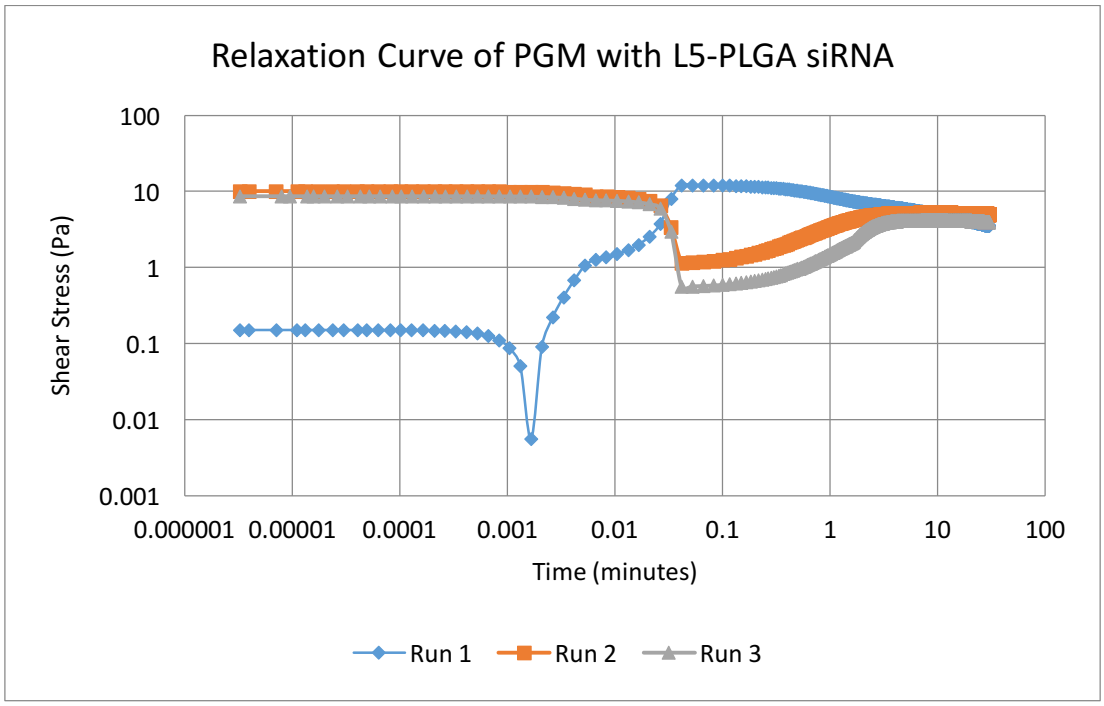

Graph 3-74 Response of PGM with siRNA loaded L5 PLGA during stress relaxation at constant deformation of 5%. The Y axis (Stress, Pa) is in log scale.

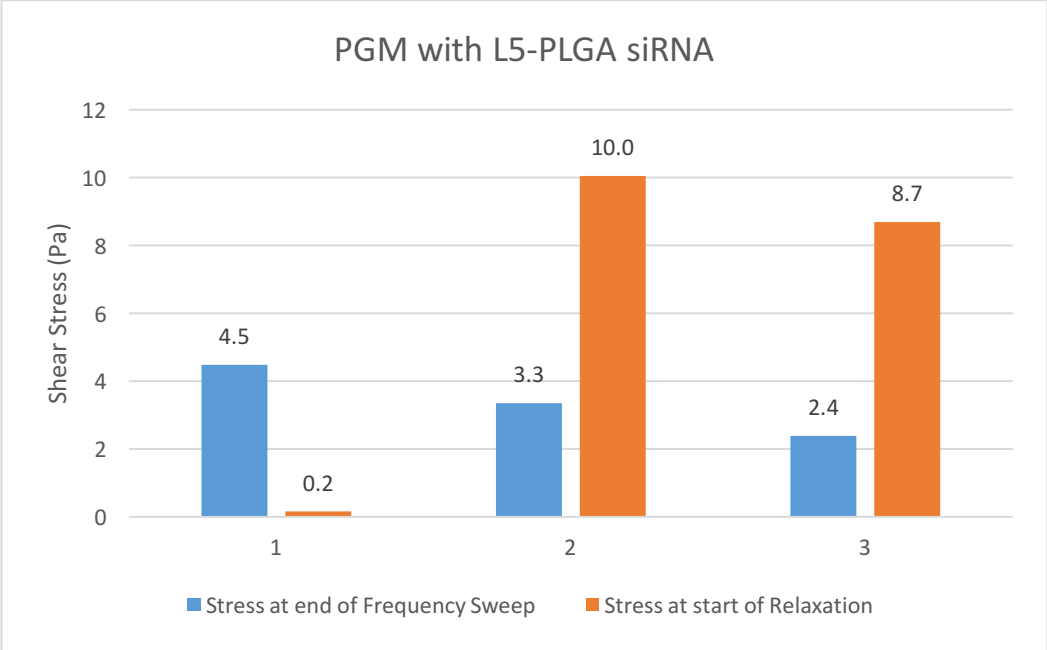

Graph 3-75 Comparison of shear stress values at the end of frequency sweep (at 10Hz) and the start of relaxation for PGM with siRNA loaded L5 PLGA.

From graph 3-67, 3-70 and 3-73, it was observed that a sudden strain was applied to the samples (PGM with PLGA, L5 PLGA and L5-PLGA siRNA). The strain increased and the remained constant throughout the measurement. However, the instrument used was an stress controlled rheometer. Thus, maintaing a constant deformation accurately could be difficult.

In graph 3-68, for PGM with PLGA 2, three runs represented by three different curves showed different pattern of relaxation, with the decay pattern not being linear. The case was same for PGM with L5 -PLGA as shown in graph 3-71 and PGM with L5-PLGA siRNA in graph 3-72. The three runs had different pattern of relaxation though they were same material. This may relate to the variability and dynamic nature of the mucus. For instance, in graph 3-68, for run 1 of PGM with PLGA 2, the stress does not increase from 0 Pa, instead starts from 5.4 Pa, decreases upto 1.16 Pa, again increases and then only relaxes without reaching the equilibrium. This was quite different from normal expected relaxation pattern as shown in figure 1-20, where relaxtion occurs gradually until a equlibrium stress is obtained. Moreover, the stress developed at the end (at 10Hz) of frequency sweep was compared to the stress developed at the start of relaxtion, as shown in graph 3-69 for PGM with PLGA 2. The stress values were different for all the three runs. This could be because the material was subjected to sudden deformation in just 1milisecond (rise time), thus not giving enough time to appropriately develop a stress. Also, the stress controlled rheometer may not have be able to accurately control the strain throughout the measurement.

Similarly for run 2 of PGM with L5-PLGA shown in graph 3-71, the stress develops from 1.9 Pa reaches to 13. 19 Pa and then relaxes. When compared to the stress developed at the end (at 10Hz) of frequency sweep, the stress values at the start of relaxtion were different for all the three runs, as shown in graph 3-72.

Similarly for run 1 of PGM with siRNA loaded L5-PLGA shown in graph 3-73, the stress develops from 0.15 Pa reaches to 12.06 Pa and then relaxes without an equilibrium. When compared to the stress developed at the end (at 10Hz) of frequency sweep, the stress values at the start of relaxtion were different for all the three runs, as shown in graph 3-74.

Due to the type of plate arrangement of the rheomter, slip was also observed while applying the deformation. This can be seen in graph 3-68 for Run 1 of PGM with PLGA 2 at 0.03 minutes, where the stress had suddenly decreased. Similar slips were observed at Run 2 at 0.04 minutes and at Run 3 at 0.04 minutes.

Similarly, in graph 3-73, on Run 2 of PGM with L5-PLGA siRNA, a slip was obseved at 0.04 minutes and on Run 3, a slip was observed at 0.04 minutes. A slip was obseved on Run 1 at 0.001 minutes as well for PGM with L5-PLGA siRNA. The slipping of material could be avoided by the use of cerated plates which would require higher amount of material, thus, not applicable for PGM.

Considering the variability of the results, not much conclusive arguments could be developed from the relaxation pattern.

3.2.2.5. Strain Sweep

These samples, PGM with nanoparticles, were subjected to deformation range of 0.01-100% at 25ºC and 1Hz Frequency. This step was important to understand the structure of the material as well as for determining the linear viscoelastic region (LVR) for the material. As mentioned before, oscillatory strain was applied to the material in strain sweep.

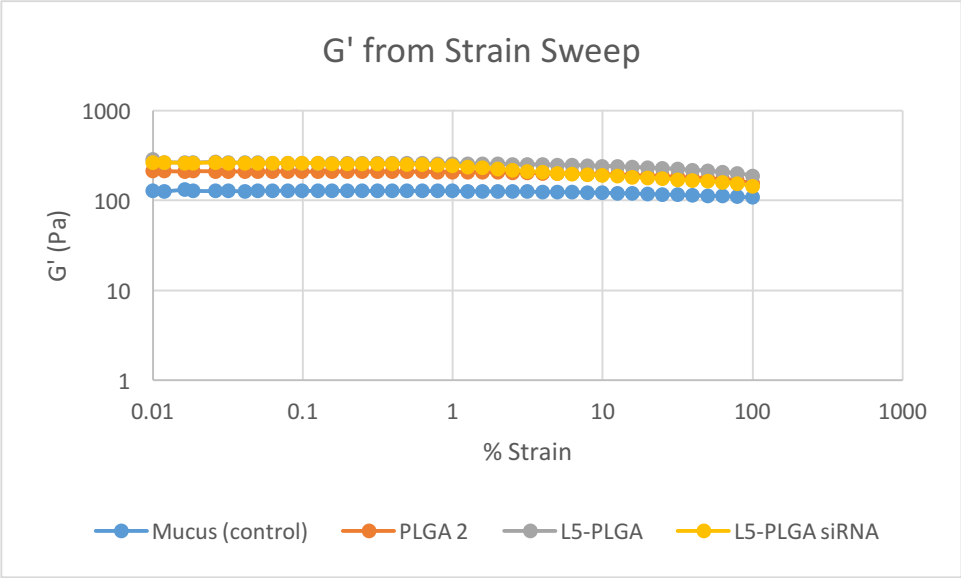

Graph 3-76 The change in elastic modulus (G') of PGM with different nanoparticles and mucus control, over the deformation range of 0.01 to 100%. The Y axis and X axis are in log scale.

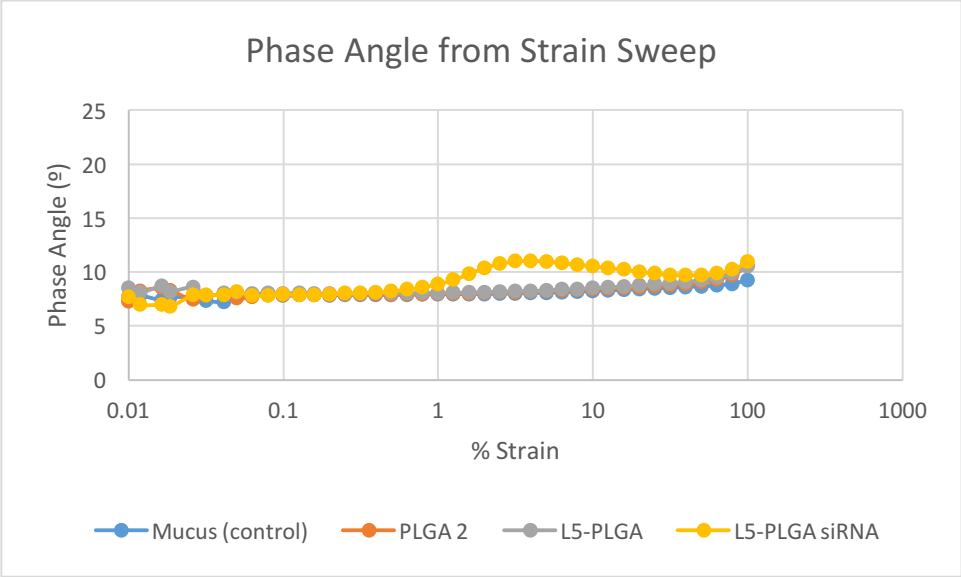

Graph 3-77 The change in phase angle of PGM with different nanoparticles and mucus control, over the deformation range of 0.01 to 100%. The X axis is in log scale, while the phase angle is plotted on Y axis.

From the graphs 3-76 and 3-77, PGM with nanoparticle formulations, showed similar behavior under the deformation range. For better comparison between the samples, student's t test was done and presented in the table below.

Table 3-18 Comparison of G' in mucus control and PGM with nanoparticle formulations at 1Hz Frequency. The comparison was based on student's t test at 95% confidence level. Each row represents each statistical comparison.

Test Sample 1	G' (Pa)	Test Sample 2	G' (Pa)	Remarks
Mucus Control	127.43±6.24	PGM with PLGA 2	207.20±19.52	Significant Difference
Mucus Control	127.43±6.24	PGM with L5-PLGA	256.90±12.36	Significant Difference
Mucus Control	127.43±6.24	PGM with L5-PLGA siRNA	237.33±38.03	Significant Difference

The comparison on the basis of elastic modulus (G') showed significant difference between PGM with nanoparticles and mucus control. However, the distribution, on which the t-test was based on, was obtained from averages and error made up of just 3 runs performed for each sample. For proper deductions, the difference between mucus control and nanoparticles can be compared to the difference between mucus controls themselves, which were deemed of significant difference by the t-test. Therefore, the results from t-test could still be argued upon.

In addition, comparison on the basis of phase angle was also done, which is presented in table below:

Table 3-19 Comparison of phase in mucus control and PGM with nanoparticle formulations at 1Hz Frequency. The comparison was based on student's t test at 95% confidence level. Each row represents each statistical comparison.

Test Sample 1	Phase Angle (^{0})	Test Sample 2	Phase Angle (^{0})	Remarks
Mucus Control	7.92±0.01	PGM with PLGA 2	8.00±0.06	No Significant Difference
Mucus Control	7.92±0.01	PGM with L5-PLGA	8.08±0.06	No Significant Difference
Mucus Control	7.92±0.01	PGM with L5-PLGA siRNA	9.27±0.79	No Significant Difference

It can be seen that the values were close to each other and the error of mean used in the t-test were very small. Moreover, the comparison of phase angle showed the addition of nanoparticles did not result in significant difference between control and PGM with

nanoparticle formulations. Thus, it can be argued based on phase angle that addition of nanoparticles did not change the response of sample under the oscillatory strain significantly.

It can be seen, from the graph, that material is independent to deformation until 1% strain and there is no significant change in moduli and phase angle until then. However, there is gradual increase in phase angle and viscous modulus after the material is subjected to strain higher than 1.25%. This means that the material was getting weaker or gel strength of PGM was decreasing.

Thus, it can be said that the linear viscoelasticity region (LVR) for PGM was up to 1.25% where G', G" and phase angle are stable. And, 1.25% was the limit of linear viscoelasticity region. Thus, the LVR of the material did not change after addition of nanoparticles when compared to mucus control in section 3.1.1.5 and other set of nanoparticles (HIPS) in section 3.1.2.5.

This proved that the frequency sweep and single frequency oscillation were performed within LVR, that is at 1 % strain.

Also, all of the samples showed that PGM is a viscoelastic solid since G'>G" over the deformation range (up to 100%). However, at higher deformation range, G' and G" could have a crossover where material could have been more liquid like. Thus, more specific conclusions on the structure and behavior could be made once the material was subjected to even higher deformation.

3.2.2.6. Summary

During loading it was observed that adding of nanoparticles increased the normal force of the material. Since, adding of nanoparticles had also changed the viscoelasticity of material to some extent, a comparison was desired, to check if behavior of material during loading had any pattern related to the way it behaved in the oscillatory experiments. When load data were compared to data from oscillatory experiments for each of the run, for each sample, no any pattern could be found between maximum normal force during loading, G' and normal force at 10 Hz of frequency sweep. Thus, it could be argued that there was no fix pattern between the tested characteristics.

After the addition of nanoparticles, it was seen that mucus was still a viscoelastic solid with G'>G". However, the values of G', G" had increased while phase angle remained the same, when nanoparticles were added. This could be because of variety of interactions between the nanoparticles and the mucus. However, since the phase angle remained the same, which is

an important indicator of rheology and viscoelasticity, it could be said that the mucus rheology did not change significantly.

Moreover, when the stress developed during the frequency sweep were compared, similar arguments could be developed stating that addition of nanoparticles did not change the stress response of the material significantly, under 1% strain.

Thus, significant alterations in mucus rheology were not observed after addition of nanoparticles.

3.2.3. Comparison of PGM with different nanoparticle formulations

For better comparison of the PGM with different nanoparticle formulations, the moduli and phase angles of the samples were selected at 1Hz and 10Hz and normalized on PGM control with 400μl of 0.9% saline.

Here, the PGM with 200μl saline is also compared to the control PGM with 400μl saline. This relative difference in G' and phase angle due to the addition of just 200μl saline was thought to help understand the differences after addition of 200μl nanoparticle formulations.

Here, all PGM with nanoparticles have comparatively higher G' values than the mucus controls. The moduli for PGM with lipidoid L5-PLGA nanoparticles (201.21%) are highest followed by PGM with siRNA loaded chitosan coated PLGA nanoparticles (193.34%).

For particles from HIPS, at 1Hz (graph 3-78), the moduli are 131.16% for PLGA 1 and 139.29% for Chitosan coated PLGA and 193.34% for siRNA loaded nanoparticles compared to 100% for PGM control. For particles from CU, at 1Hz (graph 3-78), when compared to mucus (100%), the elastic modulus (G') increases to 163.17% for PGM with PLGA 2, 201.21% for lipidoid coated PLGA particles and 176.48% for PGM with siRNA loaded nanoparticles.

A statistical comparison was done between the G' of PGM with nanoparticles from HIPS and mucus control at 1Hz, to observe if the difference among them is significant or not. Therefore, students' t test at 95% confidence level was performed. The results are presented in the table below:

Table 3-20 Statistical comparison (at 95% confidence level) of G' of PGM with different nanoparticles (HIPS) and control at 1Hz. The comments in the table indicate the type of statistical difference between the samples.

Sample (PGM with)	400μl saline	PLGA 1	Chitosan PLGA	Chitosan PLGA siRNA
400μl saline	--	Not significant	Significant	Significant
PLGA 1	Not significant	--	Not significant	Significant
Chitosan PLGA	Significant	Not significant	--	Significant
Chitosan PLGA siRNA	Significant	Significant	Significant	--

From the table 3-20, it can be seen that, statistically, addition of only PLGA 1 did not have significant difference with mucus control (PGM with 400μl saline) in terms of G' at 1Hz. While, addition of Chitosan-PLGA and Chitosan-PLGA siRNA had significant difference. However, this was not the case when phase angles were compared, where the addition of any type of nanoparticles did not have significant difference when compared to mucus control. Moreover, it was observed that PGM with PLGA 1 and PGM with Chitosan PLGA were not significantly different.

However, PGM with siRNA loaded nanoparticles was significantly different from other two nanoparticles (Chitosan-PLGA and PLGA) but not from PGM with siRNA alone (not present in table). Therefore, it could be argued that loading of siRNA could have most profound effect on PGM among the tested nanoparticle formulations. Contrastingly, during comparison of phase angle, all the nanoparticles did not have significant difference among each other.

Similar statistical tests were performed at 95% confidence level for the other set of nanoparticles(CU). The results have been presented below:

Table 3-21 Statistical comparison (at 95% confidence level) of G' of PGM with different nanoparticles (CU) and control at 1Hz. The comments in the table indicate the type of statistical difference between the samples

Sample (PGM with)	400μl saline	PLGA 2	L5-PLGA	L5-PLGA siRNA
400μl saline	--	Significant	Significant	Significant
PLGA 2	Significant	--	Not significant	Not significant
L5-PLGA	Significant	Not significant	--	Not significant
L5-PLGA siRNA	Significant	Not significant	Not significant	--

Here from table 3-21, it can be seen that addition of any type of nanoparticles have caused significant difference when compared to mucus control (PGM with 400μl saline) in terms of G' at 1Hz. However, when phase angles were observed, no any significant differences were found. Similarly, the differences in G' amongst the PGM with nanoparticles were insignificant. The case was same when phase angles were compared amongst the PGM with nanoparticles.

Interestingly, when G' of PGM with Chitosan-PLGA siRNA were compared to G' of PGM with L5-PLGA siRNA at 1Hz, no significant difference was found. This also added to the fact that addition of siRNA had more profound effect when loaded to nanoparticles in any form. And, this observation was related to the fact that 8μg of siRNA was present in both type of formulations.

The G" values were also higher for PGM with nanoparticles compared to mucus control. (shown in Appendix D.2) Thus, the elastic as well as viscous moduli of PGM increased when nanoparticles were present, with G'>G" throughout the frequency range. This meant that PGM with nanoparticles were viscoelastic solid, and more elastic and viscous than mucus control. But when the phase angle, was observed, the addition of nanoparticles had not caused any significant changes.

However, it is also important to understand the differences in the two control samples. PGM used in this study was a modified pig gastric mucus which has been washed in 0.9% saline. But, when extra 200μl saline was added to a control already with 200μl saline, the G' and phase angle increased. 200μl is a small amount of saline compared to the amount used in washing (350ml). This gives an idea about the variability of the system itself. Thus, when difference among the controls (22% from graph 3-78 and 3-79) is compared to that between the nanoparticles and control (PGM with 400μl), the changes are not that dramatic.

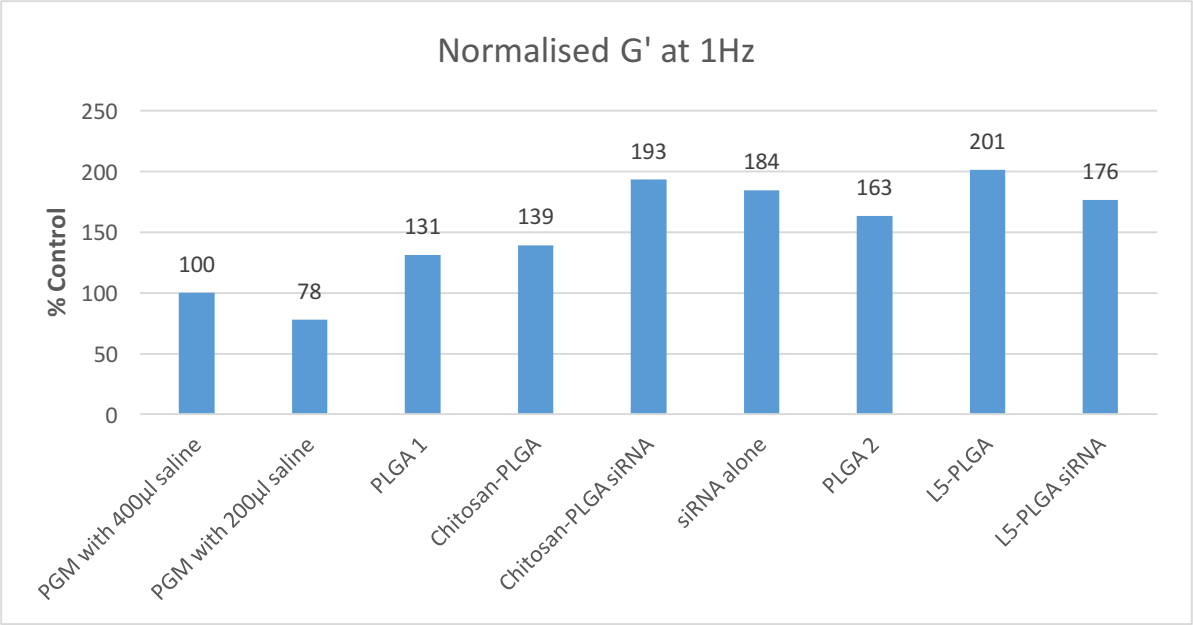

Graph 3-78 Comparison of G' at 1Hz for mucus control and all the nanoparticle formulations. The values above the bar represent the percent G' normalized to mucus control PGM with 400µl saline. The values above the bar are normalized G' of the PGM.

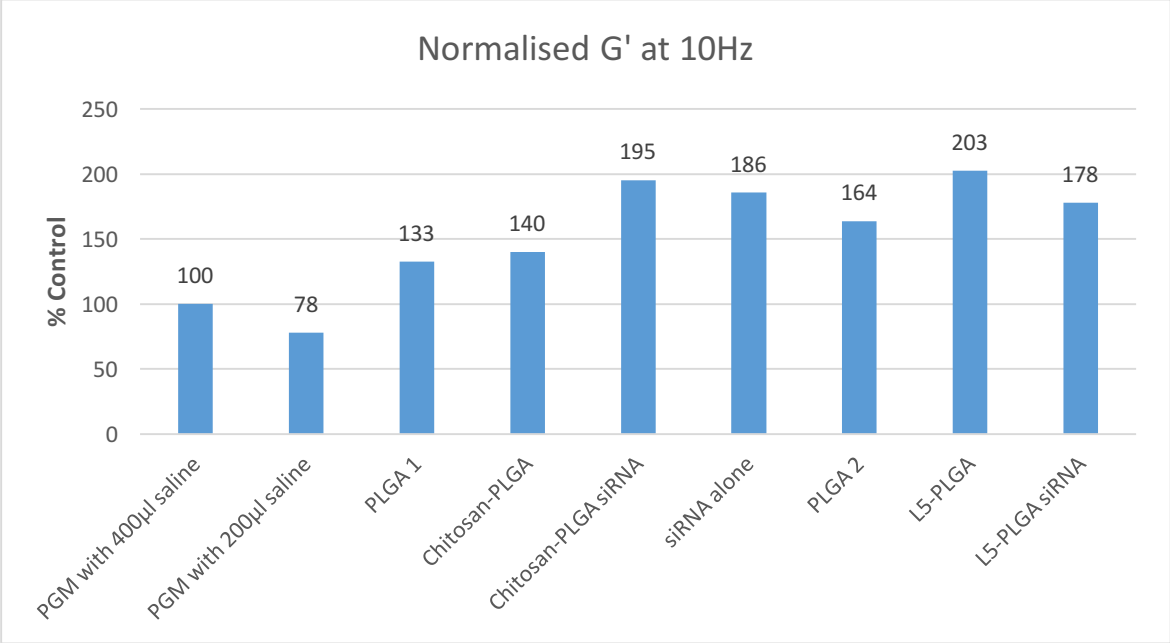

Graph 3-79 Comparison of G' at 10Hz for mucus control and all the nanoparticle formulations. The values above the bar represent the percent G' normalized to mucus control PGM with 400µl saline. The values above the bar are normalized G' of the PGM.

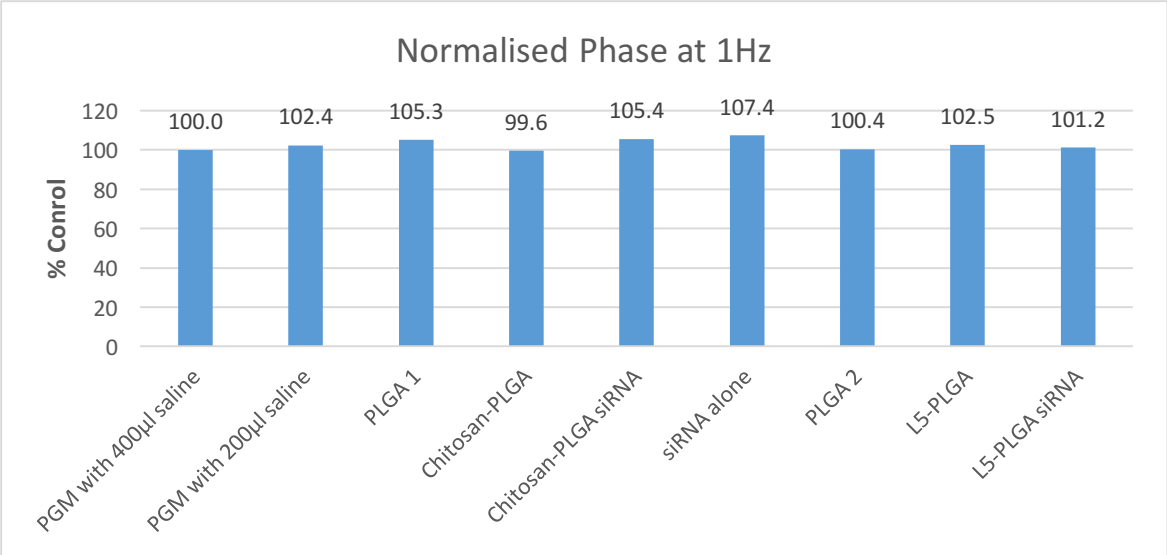

Graph 3-80 Comparison of Phase angles at 1Hz for mucus control and all the nanoparticle formulations. The values above the bar represent the percent phase normalized to mucus control PGM with 400µl saline. The values above the bar are normalized phase angle of the PGM.

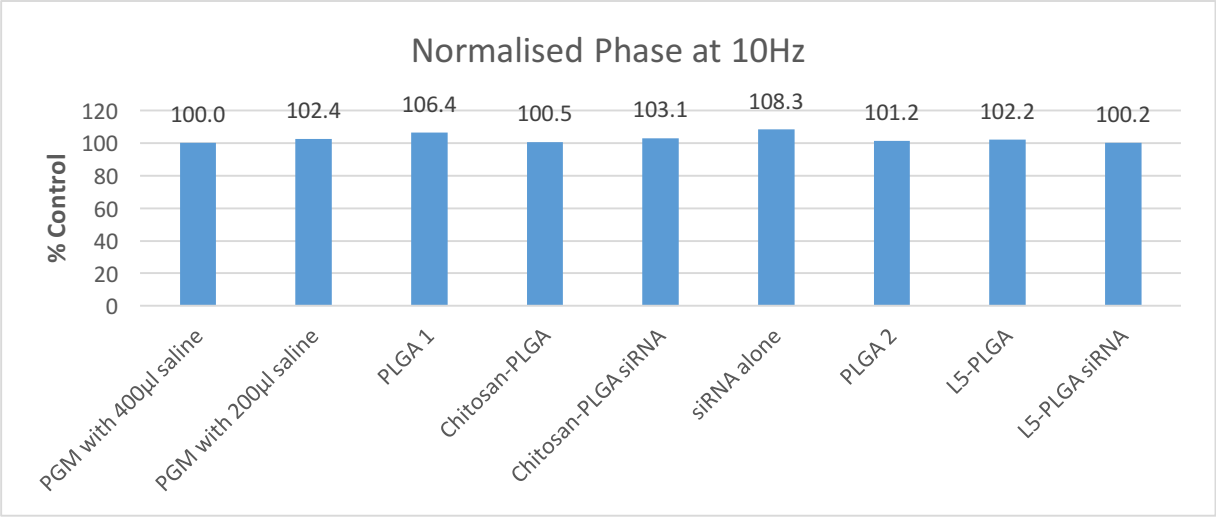

Graph 3-81 Comparison of Phase angles at 10Hz for mucus control and all the nan particle formulations. The values above the bar represent the percent phase normalized to mucus control PGM with 400µl saline. The values above the bar are normalized phase angle of the PGM.

Nevertheless, the reason behind the increment in moduli could be due to variety of interactions between the nanoparticles and mucin.

As seen in the graphs, the siRNA loaded Chitosan coated nanoparticle had more profound effect than siRNA loaded lipidoid coated nanoparticles. This could be because of different extent of interactions of Chitosan and lipidoid coatings as well as the size of particles with lipidoid coated particles (196.3 ± 4.2nm) being comparatively larger than chitosan coated particles (120±2.6nm).

Nevertheless, as mentioned before, the moduli are greater for PGM with siRNA (in any form: loaded on other particles or alone) because siRNA is capable of forming hydrophilic interactions with the mucus. This is because siRNA itself is hydrophilic in nature and so are the glycosylated regions in mucin. It has been reported that there are also few hydrophobic interactions between siRNA and mucin.[93] The nitrogen bases in the nuclei acid are responsible for those kind of interactions with protein cores of mucin. The siRNA loaded nanoparticles could also be supported by the electrostatic interactions between coated chitosan (or lipidoids) and mucin. The presence of electrostatic interactions could be postulated from the results of zeta potential measurements (graph 3-82) where, the chitosan coated PLGA cores had negative zeta potential.

PLGAs on the other hand could interact to mucin through hydrophobic interactions. These type of interactions occurs between methyl group of PLGA and protein core of mucin. It was also found in other research that PLGA with higher content of lactic acid (75% in this case) are very less hydrophilic in nature.[122]

In case of chitosan coated nanoparticles, there could be electrostatic interaction between mucin and protonated amine regions of chitosan[123]. Chitosan is capable of forming hydrogen bonds due to presence of amine and hydroxyl groups. Also, the acetyl group in chitosan could have hydrophobic interactions with the mucin.[124] But, the chitosan used for this experiment is highly deacetylated (upto 90%), therefore hydrophobic interactions between chitosan and mucin are scarce.

The lipidoids are also hydrophilic and cationic in nature. There could be electrostatic interactions between the negatively charged carboxyl group in mucin and positively charged amine groups in the lipidoids.[82,84] Hydrophilic interactions between lipidoids and glycosylated region of mucin could also happen.

However, the extent of interactions cannot be related to the changes in viscoelasticity and rheology, because the strength and nature of these interactions have not been measured and studied in this thesis. These changes in viscoelasticity and rheology could also be different when higher doses of nanoparticle formulations are delivered to lungs, leading to increase in off target depositions.

Nevertheless, there does not seem to be significant differences in rheological properties of PGM and PGM with nanoparticles. This observation suggests that when nanoparticles land in healthy airway mucus (off target), the viscoelastic properties and mucus rheology would not change significantly.

This could also be related to situation where mucociliary clearance remains unaffected. But more conclusive arguments can be produced for MCC when the force required to dissipate the materials out of the mucus is evaluated in presence of nanoparticles. This force would also depend where the nanoparticle lands on the airway mucus (on surface of mucus or within the mucus layer), which is not known for our system.

3.2.4. Comparison of two different PLGA cores

It was observed from previous graphs, that addition of PLGA 1 and PLGA 2 to PGM showed different extent of changes to mucus.

The differences in these PLGA cores could be because of number of particles, size and zeta potential. The number of particles in PLGA 1 as well as PLGA 2 have not been measured. PLGA 1 would later go on to be coated with chitosan and loaded with siRNA to form one set of nanoparticles, from HIPS. While, PLGA 2 would be coated with lipidoids and loaded with siRNA to form second set of nanoparticles, from CU.

In the table below, the basic differences between the two PLGA cores are summarized:

Table 3-22 Comparison of Size, Zeta potential and PDI of PLGA cores as provided by the source CU and HIPS.

Nanoparticle	Size(nm)	Zeta-potential (mV)	PDI
PLGA 1	116-1±1.7	-23.3±0.007	0.066±0.011
PLGA 2	185.6±2.4	-30.4 ± 2.3	0.107 ± 0.006

It can be seen that the PLGA 1 is smaller in size with lower negative charge, thus lower intensity of electrostatic interaction with mucus. This could also mean that the interactions of PLGA 2 with mucus could be higher than PLGA 1. This effect can be seen in the graphs 3-78 to 3-81, where the effect of PLGA 1 addition on G' of PGM is 131.6% while effect of PLGA 2 is 163.17% at 1Hz frequency. However, during statistical comparison of G' at 1Hz, there was no significant difference between PGM with PLGA 1 and PGM with PLGA 2. This could be because after all they may have same composition.

3.2.5. Evaluation of zeta potential and size of nanoparticle formulations

It is important to understand the state of stability of the nanoparticles before rheological measurements were done. Thus, this step was done to check the just the nanoparticle formulations for its particle size and zeta potential. The zeta potential and size both were measured by Zeta Sizer Nano from Malvern Instruments. The stability of nanoparticles was

checked by verifying their size and zeta potential at different pH. However, the size and zeta potential of the nanoparticle formulations in MiliQ water was already provided by CU and HIPS. (shown in Appendix B.2).

3.2.5.1. Measurement and evaluation of zeta potential of PLGA 1 and Chitosan-PLGA in different pH

This step was performed to see if the nanoparticle formulations showed any irregularities in terms of stability, when subjected to different pH values. The different pH was obtained by the use of different buffers: acetate, HEPES and Tris. The nanoparticles PLGA 1 and Chitosan-PLGA were diluted (½)x (in series) in MiliQ water, acetate buffer (pH 5.0), HEPES (pH 6.5) and Tris Buffer (pH 8.0). The final solutions were then analysed for zeta potential. The nanoparticle formulation with loaded siRNA was not analysed in this experiment because of small volume of siRNA available and large sample volume requirement for zeta potential measurement.

The chart below summarizes the 3 different runs to observe the zeta potential.

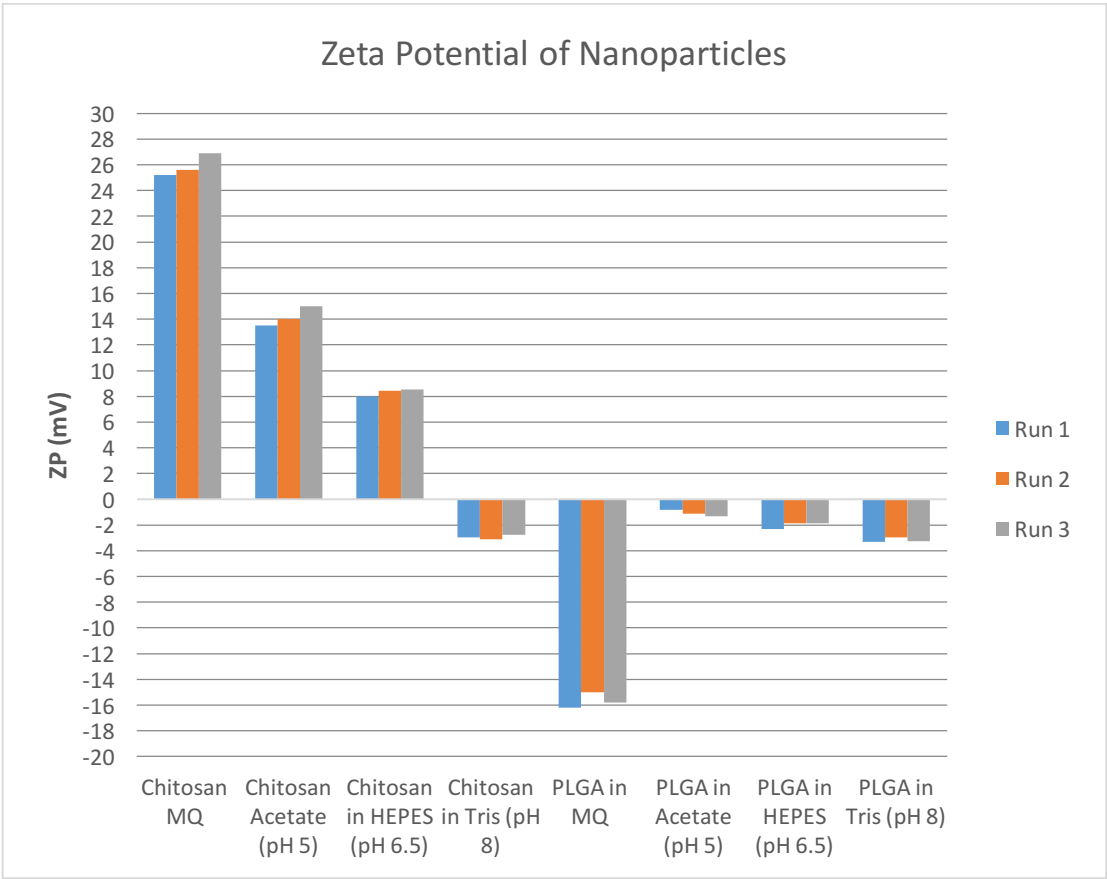

Graph 3-82 The chart above shows zeta potential of diluted Chitosan-PLGA and PLGA in different buffers as acetate(pH 5), HEPES (pH 6.5), Tris (pH 8). Different colors represent different runs for each sample.

Chitosan-PLGA formulation in MiliQ water (concentration of 1mg/ml) had zeta potential around +25.9mV compared to 28±0.2 mV in data provided by HIPS. In HEPES buffer with pH 6.5 (which is around the pka value of Chitosan of 6.5), the average zeta potential was around +9mV which could be due to dilution of the nanoparticle. In acetate with pH 5, which is less than the pka of chitosan, chitosan-PLGA would get protonated increasing the already positive charge. This, thus, justified higher zeta potential in acetate (+14) than in HEPES (+9). Contrastingly, in Tris which has pH higher than pka of chitosan, there is deprotonation and some chitosan detaches from PLGA as result of which chitosan loses its positive charge resulting in negative zeta potential of -3mV.

In case of PLGA, when diluted in MiliQ water, the mean zeta potential is -15.6 mV which is around the value provided by HIPS i.e., -23±0.007 mV. The pka of PLGA is 3.5 so all the buffers have pH greater than the pka value of PLGA. Therefore, with eventual increase in pH there was eventual increase in deprotonation resulting in more negative charge. These observations could also be because the nanoparticle was not stable and was losing charge. However, quality report of the nanoparticles did not suggest the presence of such instability. Nevertheless, dilution resulted in low negative charge of -1mV in acetate (pH 5.0), relatively higher negative charge of -2mV in HEPES (pH 6.5) and highest in Tris (pH 8.0).

Nevertheless, this suggests that the nanoparticles formulations of PLGA 1 and Chitosan-PLGA are stable at different pH. This stability information would prove be very beneficial when these nanoparticles are administered.

3.2.5.2. Measurement and Evaluation of Particle size of nanoparticle formulations: PLGA 1 and Chitosan coated PLGA and siRNA loaded nanoparticles in different pH

The different nanoparticle formulations were checked for the irregularities in particle size when subjected to different pH. For this experiment, only nanoparticles from HIPS were analysed as they were already present in liquid form. Here too, the samples were diluted (1/2)x, in series, in acetate buffer (pH 5), HEPES (pH 6.5) and Tris (pH 8), as done for zeta potential.

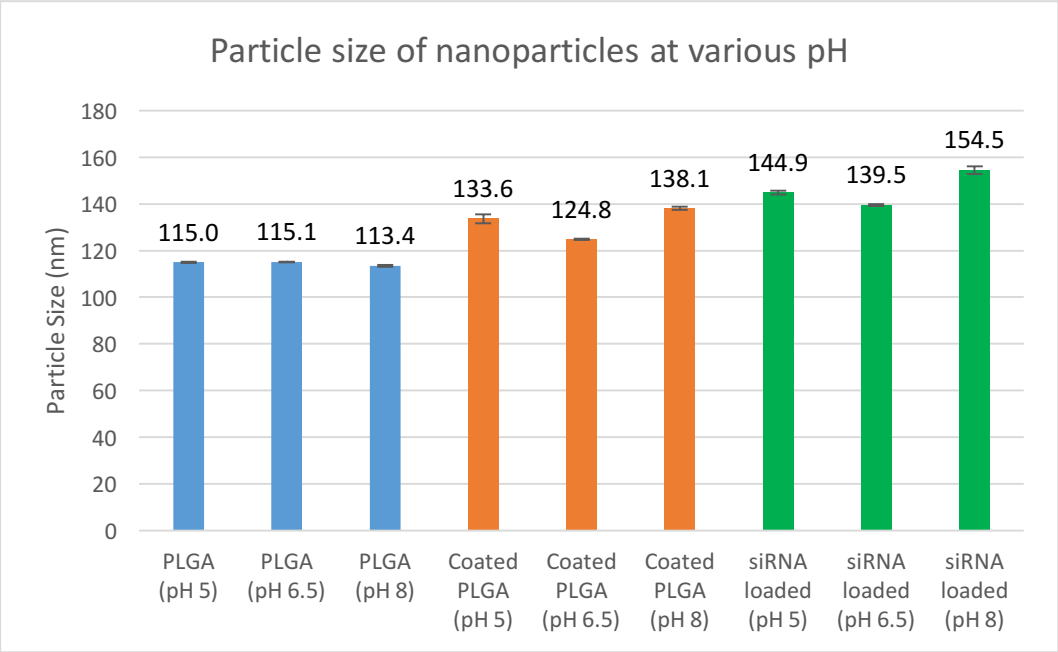

Graph 3-83 Particle size of PLGA, Chitosan coated PLGA and siRNA loaded Chitosan PLGA at different pH. The different colors represent different nanoparticles.

As seen on the graph 3-83, the particle sizes for each nanoparticle in different pH do not differ with each other. However, the size of particles with siRNA loaded to them was slightly larger when compared to PLGA 1 and Chitosan coated nanoparticles. This was an expected result as siRNA loading was done on the surface of chitosan coated PLGA cores. However, the difference was not large. Most possibly the interaction between positively charged chitosan and negatively charged siRNA over negatively charged PLGA core kept the loading stable.

3.2.5.3. Summary

Thus, it was observed that the particle size was stable and not much bothered by the change in pH of the solution it was in. Also, the change in zeta potential of nanoparticle formulations at different pH was seen, however their overall nature of charge did not change.

No any dramatic changes were seen in both of the experiment that would have suggested that the nanoparticle formulation were unstable by themselves. These results were also supported by the additional information obtained from the nanoparticle providers presented in Appendix B.2.2.

4. GENERAL DISCUSSION

The objective of comparing the control samples PGM with 200μl saline and 400μl saline was to observe if the addition of extra 200μl would change the rheology of mucus. Normally, the dilution of material decreases the elastic modulus of the viscoelastic material.[120] Contrastingly, the elastic modulus of the material increased with the addition of 200μl saline while the phase remained almost the same. This suggested that the mucus itself was highly variable. Moreover, the PGM used in this study was washed extensively in saline, thus addition of 200μl saline should not have made much difference to the material. But as stated earlier, the viscoelastic property of PGM with 400μl saline was different from that of PGM with 200μl saline. This too adds to the argument that mucus was itself highly variable in its viscoelastic properties. This was supported by results from zetasizer experiments where it was found that mucus was a polydisperse material with variable aggregates as discussed in section 3.1.2. Nevertheless, comparison of phase angle during frequency sweep (section 3.1.1.3) suggested that the change in rheological properties was not drastic. Moreover, similar results were obtained when the shear stress values between the controls were compared in section 3.1.1.3. It was found that the slightly higher shear stress was developed in PGM with 400μl when compared to that of PGM with 200μl. However, the difference or increment was not substantial enough to change the rheology to a great extent.

The nanoparticles used in the study were stable formulations. This was observed when the formulations were subjected to various pH solutions, and size and zeta potential were measured. The results of these measurements are presented in section 3.2.5. It is worth mentioning that the number of nanoparticles in the formulations were not known in this study. However, 8μg of siRNA have been used in both, siRNA loaded Chitosan-PLGA and siRNA loaded L5-PLGA particles. Therefore, when statistical comparison at 95% confidence level was done between PGM with these two nanoparticles, no any significant difference was observed in G' at 1Hz.

During the rheology tests of PGM, it was found that the samples were stable during sample loading as discussed in sections 3.1.1.1 (mucus control), 3.2.1.1 and 3.2.2.1 (mucus with nanoparticle formulations). Moreover, the first step in the oscillatory experiment was dedicated in finding if the material was indeed in apparent equilibrium at a single frequency of 1Hz, at 1% strain for a period of time. All of the PGM samples were indeed in apparent equilibrium. Most of the comparisons were done during frequency sweep step, where timescale dependent interactions within the material were observed.

During frequency sweep it was found that, with the addition of nanoparticle formulations, the elastic and viscous modulus increased, however, the phase angles remained almost the same when compared to mucus control as discussed in section 3.2.3. It was observed that at larger frequencies (shorter time scale), the sample was more elastic. However, at smaller frequencies (longer time scale), the elasticity of the material decreased. This indicated the presence of timescale dependent interactions that are higher at shorter timescale, which decreases at longer timescale. These interactions are slightly higher in PGM with nanoparticles than the mucus control. This could be observed from the higher G' of PGM with nanoparticles than mucus control in graph 3-78 and 3-79. The phase angle was also high at longer time scale (lower frequency). This depicted the more viscous nature of the material, that is mucus flows when given enough time. However, this was not relevant because mucus turnover clears the mucus well before such timescale is reached.[42]

As mentioned earlier, addition of 200μl saline to a system already washed and processed in saline changed the moduli of the material. Therefore, it was expected that the addition of nanoparticles, which may be capable of interacting with mucus, would change the moduli of the material. Nanoparticles could interact to mucin through variety of interactions such as electrostatic, hydrophilic, hydrophobic and hydrogens bonds depending upon the surface characteristics of the particles. For instance, the PLGA particles could perform hydrophobic interactions with mucin.[67] The PLGA particles in our study too, could take part in hydrophobic interactions with mucin, thus increasing the moduli of the material. However, the extent of interactions has not been measured and also the position of nanoparticles in the mucus layer (on surface or within the layer after mucopenetration). Nevertheless, a different research showed that even the topically applied nanoparticles are capable of interaction with the mucus particles through association based on the surface characteristics of the particles.[125]

Along with PLGA, the positively charged chitosan (protonated amine) and lipidoids (positively charged amine) coated PLGA nanoparticles could interact to mucin but, the interactions would be electrostatic. This was supported by the fact that chitosan coated nanoparticles used in this study had negative zeta potential (graph 3-82). According to a research, the positively charged particles increase the mucin aggregation acting as a crosslinker.[126] And, the mucin aggregation could increase the elastic property (G') of the material. The increase in elastic modulus can be observed in our study as well (Section 3.2.3). The siRNA coated nanoparticles (negatively charged) had more profound effect on viscoelastic properties of the mucus when compared to other nanoparticles. However, it was found in a different research that negatively charged particles rather enhance the mucus dispersion because

of repulsion between negatively charged surface of the nanoparticles and mucin.[126] This difference was seen because those studies were done specifically for carboxyl containing particles which are not present in siRNA. The negative charge in siRNA is rather due to phosphate groups in the backbone of siRNA.[193] In addition to electrostatic interactions, siRNA is capable of hydrophobic interactions and hydrogen bonding with mucin. These interactions could have led to increase in moduli of mucus too. However, the interactions have not been measured, therefore, they could not be quantified. As mentioned before, the number of nanoparticles used in the formulations was also not known. Thus, the extent of change in viscoelastic property of PGM could not be quantitatively related to type of nanoparticles added. For instance, L5-PLGA had more profound effect (201% compared to normalized control at 1Hz) on elastic modulus(G') than Chitosan PLGA (131% at 1Hz). This could not be only because of interactions between L5-PLGA and mucin, but due to presence of higher number of L5-PLGA particles in the formulations than Chitosan PLGA.

During the frequency sweep, change in shear stress developed in the material after addition of nanoparticles was observed. It was found that the shear stress developed in the material (at 1% strain) does change after addition of nanoparticles. As mentioned before, the change in shear stress was observed even in addition of extra 200μl saline and for these studies, a mucus model: modified PGM was used.

During the oscillatory experiment, the relaxation step under constant deformation of 5%, showed some random relaxation pattern of the material. This could have been mostly due to instantaneous rise time of 1 millisecond used to reach the target deformation of 5%. Moreover, a strain controlled experiment was being performed in a stress controlled instrument. The strain sweep showed that during oscillatory deformation from 0.01% to 100%, there was no significant difference between PGM control and PGM with nanoparticles. This was based on the comparison of phase angles at limit of linear viscoelasticity region (1.25%). Furthermore, addition of nanoparticles did not alter the limit of LVR. This supported the argument that addition of nanoparticles did not have significant effect on viscoelastic property over a range of oscillatory deformation. However, it must be realized that strain sweep, where LVR is discovered, is done at the end of the oscillatory experiment because the oscillatory strain in strain sweep could damage the material.

The change in moduli, which is related to rheology, could be related to the change in mucociliary clearance. In normal condition, there is dissipation of force from the top of cilia to epithelial region resulting in clearance of particles.[127] The change in mucus viscoelastic property may alter this dissipation of force. However, inside the body, the homeostasis of mucociliary

clearance may be able to handle the changes in mucus caused by nanoparticle landing.[128,129]Moreover, a feedback loop is developed in the MCC system to handle the changes in shear stress developed in the mucus layer. However, these controlled systems may get affected when dose and lifetime of drug administration is increased. In such conditions, the mucociliary clearance may not be able to handle the changes in mucus by itself and normal MCC could get altered. Nonetheless, for a single dose used for this study, it was argued that the change in moduli and stress was not significant enough to alter the viscoelastic property of the mucus.

5. CONCLUSION

The aim of this study was to observe the effect of nanoparticle formulations on the viscoelastic properties of airway mucus (off target effects), relating to mucus rheology.

From the comparison of mucus controls, PGM with 200μl and 400μl saline, it was found that even the addition of just 200μl saline to a system, which was previously washed extensively in saline, did change the moduli of mucus. This supported the argument that mucus itself is variable material with aggregates. Nevertheless, addition of nanoparticles to PGM changed the moduli of viscoelasticity. However, the changes were not substantial enough to change the rheology of the material. This argument was based on the comparison of phase angles (at different steps of oscillatory experiments), stress developed in the material (which remained substantially unchanged) and the observation that even addition of 200μl 0.9% saline could change the viscoelasticity.

The increment in moduli could be due to the interactions between nanoparticles and mucin. Interactions such as hydrophobic, hydrophilic, electrostatic and hydrogen bonding could occur between the nanoparticles and mucin, based on the surface properties of nanoparticles. However, the extent and strength of interactions have not been measured and the number of nanoparticles in the formulations were not known. Therefore, it is difficult to quantify and compare the strength of interactions based just on the type of nanoparticles (surface properties).

It was found that in some instances, the mucus properties showed some difference when the runs were compared to each other. Therefore, when, loading data was compared to oscillatory experiments. However, no any fixed pattern was found which could relate the maximum normal force during loading, elastic modulus (G') and normal force at 10Hz. Nevertheless, it was found that the normal force of material had increased after addition of nanoparticles to the PGM when compared to mucus control.

During administration of nanoparticles into the lungs, the aerosol technology is not accurate enough to deliver all the nanoparticles into the target, alveoli. Normally, some of the nanoparticles land on the airway mucus, thus termed off target. With the observations and arguments developed in this study, it was postulated that those off target nanoparticles do not create substantial changes in viscoelastic properties and rheology of the mucus. And, the observed alteration in mucus may be handled by homeostasis and feedback loop of the mucociliary clearance inside the body and may not cause any problems at all. However, in this thesis, only a single dose of nanoparticle formulations has been studied. Therefore, the observations could change when multiple doses are administered into the lungs. And, the study of effects on mucociliary clearance would also require the information about position of

nanoparticles in the mucus layer (on the surface or within the mucus layer) and measurement of force required to clear the nanoparticles from of airway mucus.

6. FUTURE WORK

As mentioned before several times, the number of particles in the formulation used was not known. Moreover, the study on type, extent or strength of interactions between mucin and nanoparticles was not part of this thesis. However, with these information, the effect of different nanoparticle formulations on viscoelastic property of mucus could be quantitatively compared.

In addition, the position of nanoparticles formulation in the airway mucus after delivery was not known. The particle could be on the surface of the mucus or could penetrate the mucus and be within the mucus layer. The effect on rheology and mucociliary clearance could be different in such different situations. This is because the dissipation of force would be different when nanoparticles are distributed throughout the mucus depth compared to being on the surface. Thus, particle tracking of nanoparticles by Multiple Particle Tracking (MPT) could be done to track the position of nanoparticles.

Moreover, only a single dose of nanoparticle formulations was studied. The observations found in this study could change significantly when multiple doses are administered to the lungs, leading to additional off target deposition in airway mucus. For relating the change in viscoelasticity and rheology to mucociliary clearance, the change in dissipation of force before and after addition of nanoparticles could be studied. This would help to understand the extent of change in MCC due to off target deposition of nanoparticles in airway.

Moreover, the strain controlled step such as relaxation, where constant deformation of 5% is maintained, are better performed in strain controlled instruments rather than stress controlled instruments or alternatively an additional creep measurement could be done in stress controlled instruments.

REFERENCES

[1] Doctors Net. Pros and Cons of different route of drug administration. Accessed 6 April 2017. Retrieved from: https://www.doctors.net.uk/_datastore/ecme/mod1227/Drug_dosage_Table1.pdf

[2] Rasool Hassan, B. A. (2012). Overview of Drug Delivery System. Pharmacuetica Analytical Acta, 3(10).

[3] Ravichandiran et al. (2011). Drug delivery to the lungs. International Journal of Pharmaceutical Sciences Review and Research,10(2).

[4] EMT National Training. (2008). EMT Basic Airway Module 2.1. Retrieved From: http://www.emt-national-training.com/ceu-emt/airway-ceu.php.

[5] Patil, J.S and Sarasija, S. (2012). Pulmonary drug delivery strategies: A concise, systematic review. Lung India, 29(1).

[6] O'Callaghan, C. (1994). Targeting drug delivery into lungs by inhalation. Mediators of Inflammation, 3, S31-33.

[7] Kumov, A. and Minko, T. (2015). Nanotechnology approaches for inhalation treatment of lung diseases. Journal of Controlled Release, 219(10).

[8] Patton, J.S., Byron, P.R. (2007) Inhaling medicines: Delivering drugs to the body through the lungs. Nature Reviews Drug Discovery, 6(1).

[9] Chan, H. K. (2003). Inhalation drug delivery devices and emerging technologies. Expert Opin Ther Patents, 13, 1333–43.

[10] Henry RR, Mudaliar SR, Howland WC. (2003). 3rd Inhaled insulin using the AERx insulin Diabetes management system in healthy and asthmatic subjects. Diabet Care,26,764–69.

[11] Patton, et al. (2010). The particle has landed—Characterizing the fate of inhaled pharmaceuticals. Journal of Aerosol mediated Pulmonary Drug delivery, 23, S71–S87.

[12] Škalko-Basnet, N. (2014). Biologics: the role of delivery systems in improved therapy. Biologics: Targets & Therapy, 8, 107-114.

[13] Minko et al. (2008). Multifunctional Pharmaceutical Nanocarriers, Springer Science & Business Media, 309–335.

[14] Garbuzenko et al. (2014). Inhalation treatment of lung cancer: the influence of composition, size and shape of nanocarriers on their lung accumulation and retention. Cancer Biol. Med., 11, 44–55.

[15] Pridgen et al. (2008) Factors Affecting the Clearance and Biodistribution of Polymeric Nanoparticles. Mol Pharm, 5, 505–515.

[16] Pridgen et al.(2015) Polymeric Nanoparticle Drug Delivery Technologies for Oral Delivery Applications. Expert Opinion on drug delivery. 12(9). 1459-1473

[17] R. Savla and T. Minko. (2013). Nanotechnology approaches for inhalation treatment of fibrosis. J. Drug Target., 21,914–925.

[18] Beck-Broichsitter et al. (2013). Controlled pulmonary drug and gene delivery using polymeric nano-carriers. Journal of Controlled Release, 161, 214–224.

[19] Shahnaz et al. (2014). Development and in vitro evaluation of slippery nanoparticles for enhanced diffusion through native mucus. Nanomedicine, 9, 387-396.

[20] Patton J.S.(1996). Mechanisms of macromolecular absorption by the lungs. *Advanced Drug Delivery Review,* 19,3–36.
[21] Patton et al. (2004) The Lungs as a Portal of Entry for Systemic Drug Delivery. Proceedings of American Thoracic Society, 1.
[22]Masood A.R and Thomas S.H.L. (1964). Systemic absorption of nebulized morphine compared with oral morphine in healthy subjects. *Br Journal of Clinical Pharmacology,*41, 250–252.
[23] BBC NEWS. (2006) Inhaled insulin given UK launch. Accessed 6 April 2017.
[24] Carroll, John. (2014). Sanofi fills some big shoes in $925M Afrezza pact with MannKind. Fierce Biotech. Accessed 6 April 2017.
[25] Bansil, R. and Turner, B.S. (2006), Mucin Structure, aggregation, physiological functions and biomedical applications, Current Opinion in Colloid and Interface Science, 11.
[26] Allen A. (1981). Structure and function of gastrointestinal mucus. In: Johnson L, editor. Physiology of the gastroenterology tract, 1st edition. New York, NY' Raven Press, 617 – 39.
[27] Neutra, M and Forstner, J. (1987). Gastrointestinal mucus: synthesis, secretion, and function. In: Johnson L, editor. Physiology of the gastrointestinal tract, 2nd edition. New York, NY' Raven Press.
[28] Cone, Richard A. (2009) Barrier Properties of Mucus. Advanced Drug Delivery Reviews, 61, 75-85.
[29] Moniaux et al. (2000). Alternative splicing generates a family of putative secreted and membrane-associated MUC4 mucins. *Eur J Biochem,* 267, 4536– 4544.
[30] Bell et al. (2003) N-linked oligosaccharides play a role in disulphide-dependent dimerization of intestinal mucin Muc2. Biochem J 2003, 373(3),893–900.
[31] Kornfeld, R. and Kornfeld, S. (1976) Comparative aspects of glycoprotein structure. Annual Review of Biochemistry, 45, 217-237.
[32]Cone, R. A. (2005). Chapter 4: Jiri et al. Mucosal Immunology (Third Edition). Burlington Academic Press
[33] Shogren et al. (1989). Role of glycosylation on the conformation and chain dimensions of O-linked glycoproteins: light-scattering studies of ovine submaxillary mucin. Biochemistry., 28, 5525–5536.
[34] Carraway et al. (2002). Muc4/sialomucin complex, the intramembrane ErbB2 ligand, in cancer and epithelia: to protect and to survive. *Prog Nucleic Acid Res Mol Biol,*71, 149–185.
[35] Evans *et al*. (2004). Mucin is produced by clara cells in the proximal airways of antigen-challenged mice. *Am J Respir Cell Mol Biol,* 31,382–394.
[36] Escande et al. (2001) Human mucin gene MUC5AC: organization of its 5 -region and central repetitive region. *Biochem J,* 358,763–772.
[37] Sheehan et al. (2004). Identification of molecular intermediates in the assembly pathway of the MUC5AC mucin. *J Biol Chem,* 279,15698–15705.
[38] Williams et al.(2006). Airway Mucus: From production to secretion.Americal Journal of Respiratory cell and Molecular Biology, 34.
[39] Smart, J.D. (2005) The basics and underlying mechanisms of mucoadhesion. Adv. Drug Deliv. Rev, 57, 1556–1568.

[40] Das et al. (2011) Mucoadhesive nanomedicines:Characterization and modulation of mucoadhesion at the nanoscale. Exp. Opin. Drug Deliv., 8, 1085–1104.
[41]Ahuja, A., Khar, R.K. and Ali, J. (1997) Mucoadhesive drug delivery systems. Drug Dev. Ind. Pharm., 23, 489– 515.
[42] Lei et al. (2009) Mucus Penetrating nanoparticles for drug and gene delivery to mucosal tissues. Advanced Drug Delivery Review, 61(2).
[43] Liu et al. (2015). Development of Mucus Penetrating Particles. 10(4).
[44] Munkolm, M. and Mortensen, J. (2014). Mucociliary clearance: pathophysiologicalaspectsScandinavian Society of Clinical Physiology and Nuclear Medicine, 34.
[45] Livraghi, A. and Randell S.H. (2007). Cystic fibrosis and other respiratory diseases of impaired mucus clearance. Toxicol Pathol, 35, 116–129.
[46] Evans et al. (2010). Inducible innate resistance of lung epithelium to infection. Annu Rev Physiol,72, 413– 435.
[47] Knowles M.R. and Boucher R.C. (2002). Mucus clearance as a primary innate defense mechanism for mammalian airways. J Clin Invest,109, 571–577.

[48] Brocheictasis Toolbox. Airway Clearance in Normal Lungs. Retrieved from: http://bronchiectasis.com.au/physiotherapy/principles-of-airway-clearance/airway-clearance-in-the-normal-lung Acessed 4 May 2017
[49] Wanner et al. (1996) Muco- ciliary clearance in the airways. Am J Respir Crit Care Med,154,1868–1902.
[50] Norton et al.(2011) Model of ciliary clearance and the role of mucus rheology. Physical Review, 83(1).

[51] Boegh, M. and Nielsen, H. M. (2015) Mucus as a Barrier to Drug Delivery – Understanding and Mimicking the Barrier Properties. Basic and Clinical Pharmacology and Toxicology. 116(3).
[52] Dawson et al. (2004). Transport of polymeric nanoparticle gene carriers in gastric mucus. Biotechnol Prog, 20, 851-857.
[53] Sanders. et al. (2000) Cystic fibrosis sputum: a barrier to the transport of nanospheres. Am J Respir Crit Care Med, 162, 1905-1911.
[54] Sheehan et al. (1995). Analysis of respiratory mucus glycoproteins in asthma: a detailed study from a patient who died in status asthmaticus. Am J Respir Cell Mol Biol, 13, 748-756.
[55] Lieleg O, Ribbeck K. (2011) Biological hydrogels as selective diffusion barriers. *Trends Cell Biol*, 21, 543–51.
[56] Caramella et al. (1999). A Rheological Approach. Bioadhesive Drug Delivery Systems. Marcel Dekker Inc, 98.
[57] Boegh et al. (2014). Property profiting of biosimilar mucus in a novel mucus containing invitro model for assessment of intestinal drug absorption. European Journal of Pharmaceutics and Biopharmaceutics, 87(2), 227-235

[58] Peppas et al. (2009) Molecular aspects of mucoadhesive carrier development for drug delivery and improved absorption. J. Biomater. Sci. Polym. Ed., 20, 1– 20.
[59] Bala, et al. (2004) PLGA nanoparticles in drug delivery: the state of the art. Crit. Rev. Ther. Drug Carrier Syst., 21, 387– 422.
[60] Bravo-Osuna et al. (2008). Specific Permeability Modulation of Intestinal Paracellular Pathway by Chitosan-Poly(isobutylcyanoacrylate) Core-Shell Nanoparticles. Eur J Pharm Biopharm, 69(2), 436
[61] Barratt G. (2003). Colloidal drug carriers: achievements and perspectives. Cell Mol Life Sci,60(1),21-37.
[62] Rawat et al. (2006). Nanocarriers: promising vehicle for bioactive drugs. Biol Pharm Bull , 29(9), 1790-1798.
[63] Wang et al. (2013). Chitosan Modfied PLGA nanoparticles with versatile surface for Improved Drug Delivery, AAPS PharmSciTech, 14(2).
[64] Panyam, J, and Labhasetwar, V. (2003) Biodegradable nanoparticles for drug and gene delivery to cells and tissue. Adv Drug Deliv Rev, 55, 329–47.
[65]Edlund et al. (2002) Degradable polymer microspheres for controlled drug delivery. *Advances in Polymer Science*.157.
[66] A. Kumari, S.K and Yadav, S.C. (2010). Yadav Biodegradable polymeric nanoparticles based drug delivery systems Colloids Surf. B Biointerfaces, 75, 1–18
[67] Sellers, et al. (2014) Poly(lactic-co-glycolic) acid microspheres encapsulated in Pluronic F-127 prolong hirudin delivery and improve functional recovery from a demyelination lesion Biomaterials, 35, 8895–8902
[68] Gentile et al. (2014) An Overview of Poly(lactic-*co*-glycolic) Acid (PLGA)-Based Biomaterials for Bone Tissue Engineering. International Journal of Molecular Sciences. 15(3).
[69] Sørensen, S.L. (2015) Penetrating Mucus Barrier, Norwegian University of Science and Technology.
[70] Danhier et al. (2012) PLGA based nanoparticles: An overview of biomedical applications. Journal of Controlled Release, 161(2).
[71] Hans, M.L., (2002) Lowman, A.M. Biodegradable nanoparticles for drug delivery and targeting. Curr. Opin. Solid State Material Science, 6.
[72] Haugstad, K.E., Håti, A.G., (2015) Direct Determination of Chitosan–Mucin Interactions Using a Single-Molecule Strategy: Comparison to Alginate–Mucin Interactions. Polymers, 7, 161-185.
[73] Alain, D and Monique, D. (2001) Chitosan, Polymeric Biomaterials, Revised and Expanded; CRC Press: Boca Raton, FL, USA.
[74] Tang et al. (2015). Chitin is endogenously produced in vertebrates. Current Biology. 25(7).
[75] Kumar et al. (2016) On the Electrical Properties of Chitosan: Influence of Degree of Deacetylation. Journal of Chitin and Chitosan Science, 4(1), 9-13/
[76] Sogias, I.A., Williams, A.C. and Khutoryanskiy, V.V. (2008) Why is chitosan mucoadhesive? Biomacromolecules, 9, 1837– 1842.
[77] Zuber et al. (2013) Advanced Structured Materials. Advances in Natural Polymers, Springer-Verlag.

[78] Nagpal, K., Singh, S.K. and Mishra, D.N. (2010) Chitosan nanoparticles: a promising system in novel drug delivery. Chem. Pharm. Bull., 58, 1423– 1430.
[79] Luppi, B., Bigucci, F., Cerchiara, T. and Zecchi, V. (2010) Chitosan-based hydrogels for nasal drug delivery: from inserts to nanoparticles. Expert Opin. Drug Deliv., 7, 811– 828.
[80] Haugstad et al. Direct Determination of Chitosan–Mucin Interactions Using a Single Molecule Strategy: Comparison to Alginate–Mucin Interactions, Polymers, 2015.
[81] Sogias, I.A., Williams, A.C. and Khutoryanskiy, V.V. (2008) Why is chitosan mucoadhesive? Biomacromolecules, 9, 1837– 1842.
[82] Akinc et al. (2008) A combinatorial library of lipid-like materials for delivery of RNAi therapeutics. Nature Biotechnology, 26 (5).
[83] Whitehead et al. (2014) Degradable lipid nanoparticles with predictable *in vivo* siRNA delivery activity. Nature Communications. 5.
[84] Colombo et al. (2015) Mechanistic profiling of the siRNA delivery dynamics of lipid–polymer hybrid nanoparticles. Journal of Controlled Release, 201.
[85] Cartiera et al. (2009). The uptake and intracellular fate of PLGA nanoparticles in epithelial cells, Biomaterials 30 2790–2798.
[86] Tahara, et al. (2008). Establishing chitosan coated PLGA nanosphere platform loaded with wide variety of nucleic acid by complexation with cationic compound for gene delivery, Int. J. Pharm. 354 , 210–216.
[87] Jensen, et al. (2012). Design of an inhalable dry powder formulation of DOTAP-modified PLGA nanoparticles loaded with siRNA, J. Control. Release, 157, 141–148.
[88] Gandhi et al. (2014) Nanocarrier mediated Delivery of siRNA/miRNA in Combination with Chemotherapeutic Agents for Cancer Therapy: Current Progress and Advances. Journal of Controlled Release.
[89] Davidson et al. (2011). Current prospects for RNA interference-based therapies. Nat. Rev. Genet. 12, 329–340.
[90] Suri et al. (2007) Nanotechnology-based drug delivery systems. J Occup Med Toxicol. 2:16.
[91] Smith AE. (1995) Viral vectors in gene therapy. Annu Rev Microbiol, 49, 807–838.
[92] Taetz et al.(2009). The influence of chitosan content in cationic chitosan/PLGA nanoparticles on the delivery efficiency of antisense 2′-O-methyl- RNA directed against telomerase in lung cancer cells. Eur J Pharm Biopharm, 72, 358–69.
[93] Giraud et al. (2016). Interaction between single strands of siRNA and different chemical groups. Frontiers Bioeng. Biotechnol. Conference Abstract: 10th World Biomaterials Congress
[94] Howard, et al. (2009). Chitosan/siRNA nanoparticle-mediated TNF-alpha knockdown in peritoneal macrophages for anti-inflammatory treatment in a murine arthritis model. Mol. Ther. 17, 162– 168.
[95] Aiba, S.(1989). Studies on chitosan: 2. Solution stability and reactivity of partially N-acetylated chitosan derivatives in aqueous media. Int J Biol Macromol, 11, 249–52.
[96] Sou et al. (2011). New development in dry powder pulmonary vaccine delivery. Trends in Biotechnology, 29(4).

[97] Kirch et al. (2012). Computational fluid dynamics of nanoparticle disposition in the airways: Mucus interactions and mucociliary clearance. Computing and Visualisation in Science, 14(7).
[98] Merzger, T.(2011). The Rheology handbook, Vincentz Network.
[99] Malvern Instruments Ltd. Kinexus Ultra+. Accessed from http://www.malvern.com/en/products/product-range/kinexus-range/kinexus-ultra-plus/default.aspx
[100] TUM Molecular and Cellular Biophysics. Polymers Under Flow. Accessed from: http://bio.ph.tum.de/home/e27-prof-dr-bausch/research-areas/complex-microfluids-andbiomaterials/polymers-under-flow.html
[101] Ibarz et al.(2009) Newtonian and Non-Newtonian Flow, Food Engineering-Vol. II, EOLSS, United Kingdom.
[102] Peyronel, M.F. and Maragoni, A. G. (2017) Controlled Stress Rheometry. AOCS Lipid Library.
[103] Aho et al. (2015). Rheology as a tool for evaluation of melt processability of innovative dosage form. International Journal of Pharmaceutics. 494.
[104] Merzger, Thomas.(2014). Applied Rheology, Anton Paar.
[105] Smisrød et al. (2008). Biopolymer Chemistry, Tapir Academic Press.
[106] Picout, D.R., Ross-Murphy, S.B. (2003). Rheology of biopolymer solutions and gels. Scientific World Journal, 24(3), 105-21.
[107] Detiger et al. (2013). Biomechanical and rheological characterization of mild intervertebral disc degeneration in a large animal model. Journal of Orthopaedic Research. 31(5).
[108] Nordgård, C. N., Dextran nano/microgel induced alterations in mucus rheology, COMPACT/NTNU.

[109] Murphy, SB. (1994). Rheological Methods, Physical Techniques of the Study of Food Biopolymers, Chapman & Hall
[110] Wyss et al. (2007). Oscillatory Rheology-Measuring the viscoelastic behavior of soft materials. G.I.T Laboratory Journal. 3(4)
[111] Zhong, Q., Daubert C. R., (2013) Food Rheology. In: Kutz, M. Handbook of Farm, Dairy and Food Machinery Engineering. Second Edition. San Diego: Academic Press.
[112] Vincent, J.(2012). Structural Biomaterials, Princeton University Press,3rd Edition

[113] Verwey, E.J.W. and Overbeek, J.Th.G. (1948). Theory of the Stability of Lyophobic Colloids, Elsevier
[114] Dai, Y.(2008). Introduction of Dynamic Light Scattering, SHPYRKO Research Group, 2008.
[115] Nickel et al. (2014). Dynamic light-scattering measurement comparability of nanomaterial suspensions, Nanopart Res, 16: 2260
[116]Schimitz, K.(2012) Introduction to Dynamic Light Scattering by Macromolecules, Academic Press Inc.,
[117] Kaszuba et al.(2008).Measuring sub nanometre sizes using dynamic light scattering. J Nanopart Res, 10, 823–829.

[118] Malvern Instruments Ltd. Zetasizer Nano User Manual, Malvern, UK, 2013
[119] Shaw, R. Dynamic Light Scattering Training, Malvern, UK, 2014.
[120] Rubin et al. (1992). Respiratory mucus from asymptomatic smokers is better hydrated and more easily cleared by mucociliary action. Am Rev Respir Dis, 145, 545–547.
[121] [Shaw, R.(2014). Dynamic Light Scattering Training, Malvern, UK.
[122] Gentile et al. (2014). An Overview of Poly(lactic-*co*-glycolic) Acid (PLGA)-Based Biomaterials for Bone Tissue Engineering. International Journal of Molecular Sciences. 15(3).
[123] Haugstad et al. (2015) Direct Determination of Chitosan–Mucin Interactions Using a Single Molecule Strategy: Comparison to Alginate–Mucin Interactions, Polymers.
[124] Sogias et al. (2008) Why is chitosan mucoadhesive? Biomacromolecules, 9, 1837– 1842.
[125] McGill et al. (2010). Disruption of the mucus barrier by topically applied exogenous particles, Mol Pharm. 7(6).
[126] Chen et al. (2010) Functionalised Positive nano particle reduce mucus swelling and dispersion. PLOS One.
[127] Norton et al. (2011). Model of ciliary clearance and the role of mucus rheology. Physical Review,83(1).
[128] Haq et al.(2016). Airway surface liquid homeostasis in cystic fibrosis: pathophysiology and therapeutic targets. BMJ Journals, 71(3).
[129] Ukai et al.(1984). Effect of infection and SO2 exposure on nasal and paranasal mucociliary clearance in intact chickens. European Archives of Oto-Rhino-Laryngology. 239(1)

LIST OF APPENDICES

APPENDIX A: PROTOCOLS

A.1. Mucus Washing Protocol and Aliquot Preparations:

The steps include:

1. Thawed mucus was added to 5X volume of normal saline (0.9%NaCl) and stirred vigorously with magnetic stirrer for 1-2 hours.
2. The suspension was filled into centrifuge tubes.
3. The centrifugation was performed at 9000rpm at 10ºC for 2 hours.
4. The supernatant was discarded and grit was removed from the base of pellet.
5. The pellet was re-suspended in normal saline but in half of the volume used in Step 1.
6. Step 3 was performed again.
7. If the pellet was without any grit and looked as homogenous gel, the samples were weighed in 1.5gm aliquots and stored at -40ºC. If the samples still had grit and was not homogenous, the process was continued from Step 5 onwards.

A.2. Rheological Analysis:

The 1.5gm aliquot sample was added with 200μl of nanoparticle (or saline for control) mix The mix was kept at 4ºC overnight. This sample was used as the analyte for rheometer next day. The amount of sample used in rheometer was 0.29ml (0.29gm) for each run. Total of 3 runs were performed for each sample.

The cone plate arrangement of rheometer was covered and applied with oil and water on the grooves to prevent dryness of the sample. The over-run of the sample was also checked before the starting the sequence. CP 1/40 cone plate arrangement was used in Malvern Kinexus Rheometer Ultra+ with base plate PLS61 S2579 SS in a passive solvent trap method.

The instrument first runs sequence of sample loading. This includes the setting gap before sample loading, loading of sample into the base plate of the rheometer and trimming the gap after sample has been loaded. Only after sample loading sequence is complete, the oscillatory experiments start.

The sequence run for oscillatory experiment is as follows:

1. Isothermal temperature: 25ºC, 10 minutes
2. **Single Frequency Oscillation**: 1Hz, 1% Strain, 100 samples, Interval: 5secs
3. Isothermal temperature: 25ºC, 10 minutes
4. **Frequency Sweep:** 0.01Hz to 10 Hz, 1% Strain, 10 samples per decade, logarithmic sampling
5. Isothermal temperature: 25ºC, 10 minutes
6. **Relaxation:** Target Strain: 5%, rise time: 0.001secs, 10 samples per decade, maximum time: 30 minutes
7. Isothermal temperature: 25ºC, 10 minutes
8. **Strain Sweep:** 1Hz, 0.01-100% Strain, 10 samples per decade, logarithmic sampling

A.3. Drying

After the washing was done, the concentration of mucus solution, later used in zetasizer experiments, was checked by drying. This 5ml solution of mucus was taken. The mucus

solution before and after the filtration were dried and compared to see how much material is lost.
The protocol for drying was:

1. Empty beakers were dried in an oven at 105^0C.
2. The beakers are allowed to cool in a dessicator for 10 minutes.
3. 5ml mucus solution was poured into the empty beaker and kept in the oven overnight at 105^0C.
4. After that, the beaker with mucus was again weighed.
5. The dry amount of mucus was obtained by subtracting the weight before and after loading mucus.

A.4. Zetasizer Experiments

The zetasizer experiment included the measurement of size and zeta potential. Different types of cuvettes were used for these experiments. Size measurement used disposable cuvettes while zeta potential measurement used folded capillary zeta cell. During zetasizer experiments, the cuvettes were inserted inside the instruments as soon as the sample was loaded. This was done because, it was found during the experiments that letting the samples to rest in the cuvette caused sedimentation and altered the results.

Size Measurements:

1. The nanoparticle formulation is diluted in different pH buffers used.
    a. The mucus and mucin however were diluted in series to reach the concentrations of :1mg/ml, 0.5 mg/ml, 0.25 mg/ml, 0.125 mg/ml and 0.0625 mg/ml for mucin and 9.8 mg/ml, 4.9mg/ml, 2.45mg/ml, 1.225mg/ml and 0.6125mg/ml for mucus.
2. The dilution is done to reach the operating volume of 400μl, which is required by the instrument for size measurements.
3. The cuvette is loaded into the instruments and measurement is taken.

Zeta potential Measurements:

1. The nanoparticle formulation was diluted twice in series to obtain a volume enough to fill the capillary cell.
2. The mix was poured into the cell using a syringe from one side in inverted position until the level of solution reaches the base of the capillary.
3. Then the cell is again brought to upright position and rest of the mix was poured. This was done to avoid any bubbles in the measurement capillary.
4. The cuvette was loaded in the instrument and measurement was taken.

APPENDIX B: NANOPARTICLE FORMULATIONS

B.1. Nano particle formulations including the volume used in the experiments

Table B.1.1. Different nanoparticle formulations used in the experiment with volume of the formulations

S.N.	Source	Sample	Nanoparticle	siRNA	Remarks
1	HIPS	PGM (1.5gm)	PLGA (200μl)	--	
2	HIPS	PGM (1.5gm)	PLGA-Chitosan (200μl)	--	
3	HIPS	PGM (1.5gm)	PLGA-Chitosan (200μl)	8μg (1.1μl)	siRNA and nps mix was added at once
4	HIPS	PGM (1.5gm)	--	8μg (1.1μl)	200μl of MiliQ water was added
5	CU	PGM (1.5gm)	PLGA (200μl)	--	Dry pellet containing PLGA was dissolved and 200μl was added to mucus
6	CU	PGM (1.5gm)	PLGA-L5 (200μl)	--	Dry pellet containing PLGA-L5 was dissolved and 200μl was added to mucus
7	CU	PGM (1.5gm)	PLGA-L5 (200μl)	8μg	Dry pellet containing PLGA-L5-siRNA was dissolved and 200μl was added to mucus

B.2. Nanoparticle Information from the sources

B.2.1. Nano particles from CU:

Material(s), solvent, label:

Lipid: Lipidoid 5 Polymer: PLGA 50:50, molecular weight: 20 kD Stabilizer: Polyvinyl alcohol Cryoprotectant: Trehalose

siRNA: TNF-alpha siRNA, Mol wt: 17958

Total drug content: -

Encapsulated drug: ~100%

Details:

- The formulations are non-immunogenic at tested concentrations (tested up till 2 μg/ml equivalent formulation).
- Each vial of loaded L5-PLGA contains siRNA equivalent to 40 μg and trehalose 50 mg
- The L5-PLGA and PLGA formulations do not contain any siRNA but dilution pattern equivalent to siRNA loaded L5-PLGA can be followed to have equivalent particle burden.
- The formulations contain PLGA (commercially available biodegradable polymer), Lipidoid 5 (a synthetic cationic lipid prepared in-house), TNF-alpha siRNA (synthesized by GSK), polyvinyl alcohol (commercially available surfactant stabilizer), and Trehalose (routine lab chemical).
- These ingredients are supposed to be safe if general Good Laboratory Practices are followed.

B.2.2 Nano particles from HIPS:

35 x 2mg/ml in total 70mg of Chitosan-PLGA Nanoparticles and 30x 2mg/ml in total 60mg of PLGA Nanoparticles + siRNA luc

Storage and re-suspension

Do not freeze particle suspension

Sample characteristics

Chitosan-PLGA Nanoparticles:

Size:	(120 ± 2.6) nm
PDI:	0.133 ± 0.02
Zeta potential:	(28.2 ± 0.2) mV
Concentration:	2mg/ml

PLGA Nanoparticles:

Size:	(116-1 ± 1.7) nm
PDI:	0.066 ± 0.011
Zeta potential:	-23.3 ± 0.007
Concentration:	2mg/ml

APPENDIX C: ZETASIZER DATA

C.1. Size measurements of Mucus and Mucin at different concentrations and Zeta potential measurements of Mucus

Table C.1.1: The Z average value of Mucus at different concentrations with three runs for each sample. Different peak means obtained for each of sample have also been presented.

Sample Name	Z-Ave d.nm	Derived Count Rate kcps	PdI	Pk 1 Mean Int d.nm	Pk 2 Mean Int d.nm	Pk 3 Mean Int d.nm	Pk 1 Area Int Percent	Pk 2 Area Int Percent	Pk 3 Area Int Percent	Scattering Angle °
Mucus 9.8 mg/ml 1	806.3	5982.9	0.621	415.2	34.82	0	94	6	0	173
Mucus 9.8 mg/ml 2	695.2	5327.7	0.541	431.3	41.38	0	93.3	6.7	0	173
Mucus 9.8 mg/ml 3	652.3	5387.7	0.598	499.3	62.88	0	89.6	10.4	0	173
Mucus 4.9mg/ml 1	841.9	5221.4	0.628	376.2	0	0	100	0	0	173
Mucus 4.9mg/ml 2	742.8	3934	0.569	388.7	0	0	100	0	0	173
Mucus 4.9mg/ml 3	814.5	4421	0.617	383.4	26.69	0	94.6	5.4	0	173
Mucus 2.45mg/ml 1	1604	12849	0.985	174.3	0	0	100	0	0	173
Mucus 2.45mg/ml 2	1299	11782.9	0.946	195.4	0	0	100	0	0	173
Mucus 2.45mg/ml 3	1504	12694.8	0.926	186.2	0	0	100	0	0	173
Mucus 1.225mg/ml 1	4.39E+04	17477.4	0.586	0	0	0	0	0	0	173
Mucus 1.225mg/ml 2	5.41E+04	20489.4	0.308	0	0	0	0	0	0	173
Mucus 1.225mg/ml 3	4.06E+04	17811.1	0.387	0	0	0	0	0	0	173
Mucus 0.6125mg/ml 1	533.7	486.2	0.57	600.4	84.51	0	85.7	14.3	0	173
Mucus 0.6125mg/ml 2	499.8	455.4	0.496	489.1	100.1	0	85.7	14.3	0	173
Mucus 0.6125mg/ml 3	513.2	503	0.542	589	92.02	0	86.6	13.4	0	173

Table C.1.2: The Z average value of Mucin at different concentrations with three runs for each sample. Different peak means obtained for each of sample have also been presented.

Sample Name	Z-Ave d.nm	Derived Count Rate kcps	PdI	Pk 1 Mean Int d.nm	Pk 2 Mean Int d.nm	Pk 3 Mean Int d.nm	Pk 1 Area Int Percent	Pk 2 Area Int Percent	Pk 3 Area Int Percent	Scattering Angle °
Mucin 1 mg/ml 1	4083	17216.8	1	146.9	0	0	100	0	0	173
Mucin 1 mg/ml 2	3057	15394.4	1	390.5	0	0	100	0	0	173
Mucin 1 mg/ml 3	2578	14008.7	0.886	549.5	0	0	100	0	0	173
Mucin 0,5 mg/ml 1	2553	10788.1	0.981	385	0	0	100	0	0	173
Mucin 0,5 mg/ml 2	2322	9639.9	0.74	754.3	0	0	100	0	0	173
Mucin 0,5 mg/ml 3	2582	8846	0.709	1008	0	0	100	0	0	173
Mucin 0,25 mg/ml 1	1616	5547.5	0.852	413.7	0	0	100	0	0	173
Mucin 0,25 mg/ml 2	1572	6485.1	0.609	627	0	0	100	0	0	173
Mucin 0,25 mg/ml 3	2043	7125.4	0.776	609.5	0	0	100	0	0	173
Mucin 0,125 mg/ml 1	1458	1915.3	0.753	900.8	61.56	0	89.5	10.5	0	173
Mucin 0,125 mg/ml 2	1442	1991.1	0.793	950.6	82.9	0	87	13	0	173
Mucin 0,125 mg/ml 3	1869	3080.1	0.813	1183	69.78	0	91.5	8.5	0	173
Mucin 0,0625 mg/ml 1	3141	4947.2	0.35	762.6	0	0	100	0	0	173
Mucin 0,0625 mg/ml 2	2537	4014.3	0.76	542.2	0	0	100	0	0	173
Mucin 0,0625 mg/ml 3	2163	3164.3	0.974	324.3	0	0	100	0	0	173

Table C.1.3: The zeta potential of mucus at different concentration with three runs of each sample

Sample Name	ZP mV	Mob μmcm/Vs	Cond mS/cm	Attenuation Factor
Mucus 9.8mg/ml 1	-9.2	-0.721	15.6	0.00362
Mucus 9.8mg/ml 2	-11.7	-0.9153	16.5	0.00362
Mucus 9.8mg/ml 3	-11.1	-0.8703	17.1	0.00362
Mucus 4.9mg/ml 1	-9.49	-0.7436	16.2	0.044
Mucus 4.9mg/ml 2	-10.2	-0.8024	16.9	0.044
Mucus 4.9mg/ml 3	-11.3	-0.8828	17.4	0.044
Mucus 2.45mg/ml 1	-1.25	-0.09778	16.2	0.0126
Mucus 2.45mg/ml 2	0.673	0.05273	18.9	0.0126
Mucus 2.45mg/ml 3	1.29	0.1015	19.6	0.0126
Mucus 1.225mg/ml 1	-12	-0.9379	16.1	0.111
Mucus 1.225mg/ml 2	-11.2	-0.877	16.8	0.111
Mucus 1.225mg/ml 3	-12.4	-0.9717	17.3	0.111
Mucus 0.6125mg/ml 1	-10.4	-0.8174	16.1	0.281
Mucus 0.6125mg/ml 2	-10.7	-0.8399	16.9	0.281
Mucus 0.6125mg/ml 3	-12.8	-1.001	17.4	0.281

C.2. Zeta potential of Nanoparticles

Table C.2.1. Zeta potential of Chitosan coated PLGA nanoparticles (represented by Chitosan) and PLGA nanoparticles in different pH buffers: MiliQ water, acetate (pH 5), HEPES (pH 6.5) and Tris (pH 8). The zeta potential (mV) for each of the runs have been presented.

Sample Name	Zeta Potential (mV)		
	Run 1	Run 2	Run 3
Chitosan MQ	25.2	25.6	26.9
Chitosan Acetate (pH 5)	13.5	14	15
Chitosan in HEPES (pH 6.5)	7.99	8.45	8.55
Chitosan in Tris (pH 8)	-2.95	-3.09	-2.76
PLGA in MQ	-16.2	-15	-15.8
PLGA in Acetate (pH 5)	-0.814	-1.1	-1.3
PLGA in HEPES (pH 6.5)	-2.3	-1.89	-1.88
PLGA in Tris (pH 8)	-3.32	-2.98	-3.27

C.3. Size distribution of Mucin and Mucus at different concentration

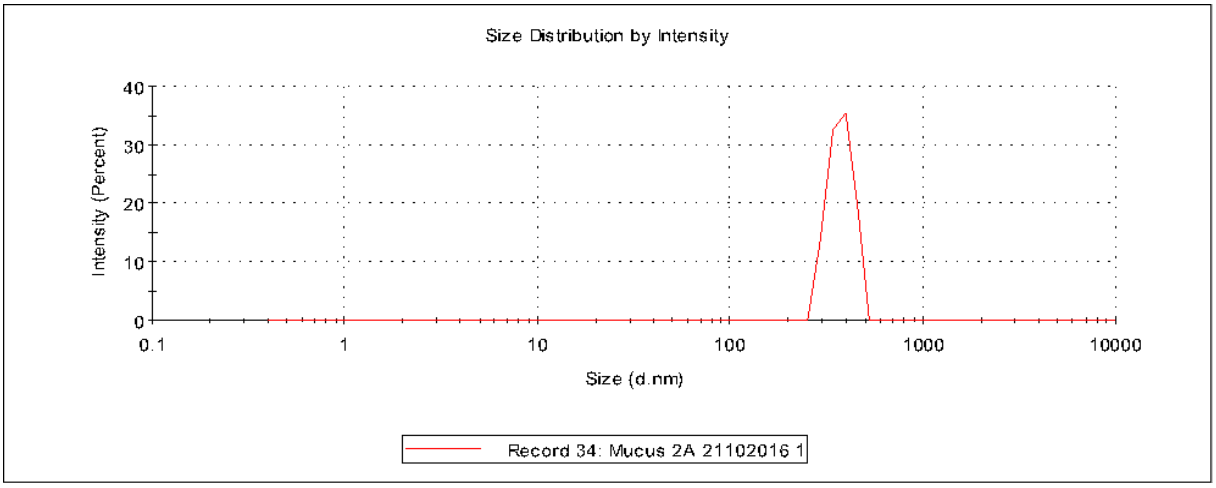

Figure C.3.1: The size distribution of Mucus by intensity at concentration of 4.9mg/ml

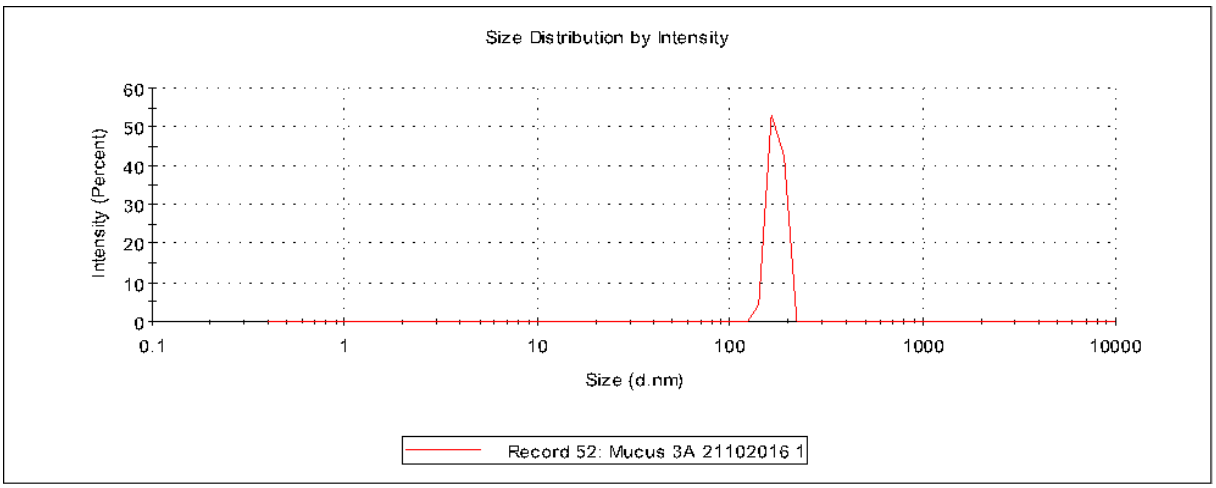

Figure C.3.2: The size distribution of Mucus by intensity at concentration of 2.45mg/m

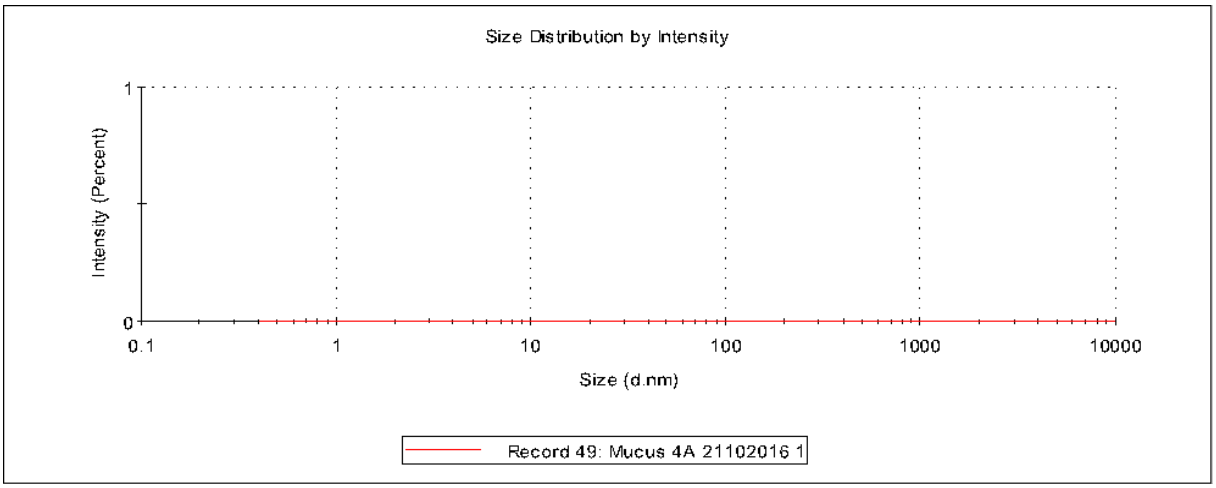

Figure C.3.3: The size distribution of Mucus by intensity at concentration of 1.225mg/ml

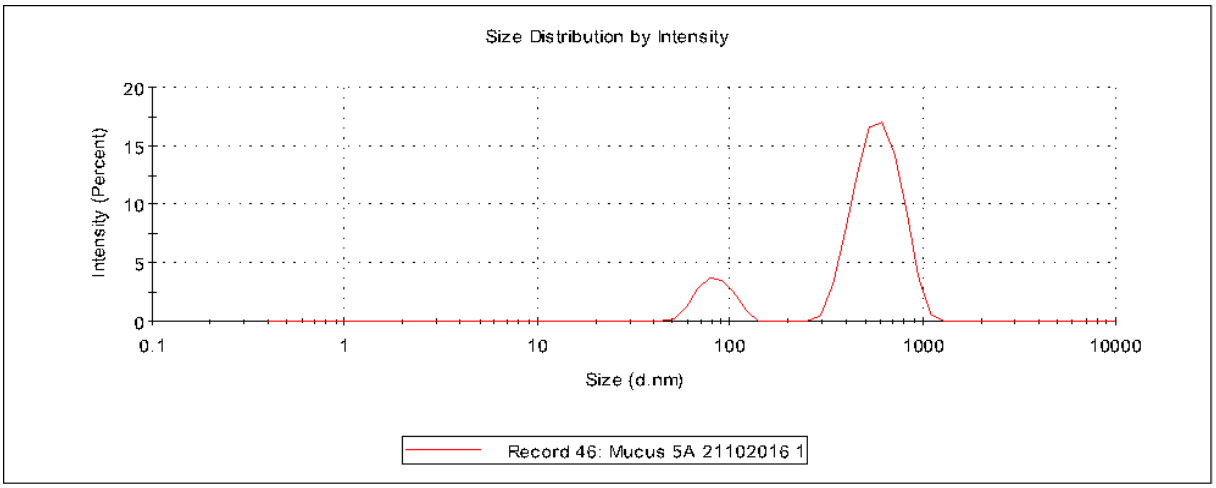

Figure C.3.4: The size distribution of Mucus by intensity at concentration of 0.6125mg/ml

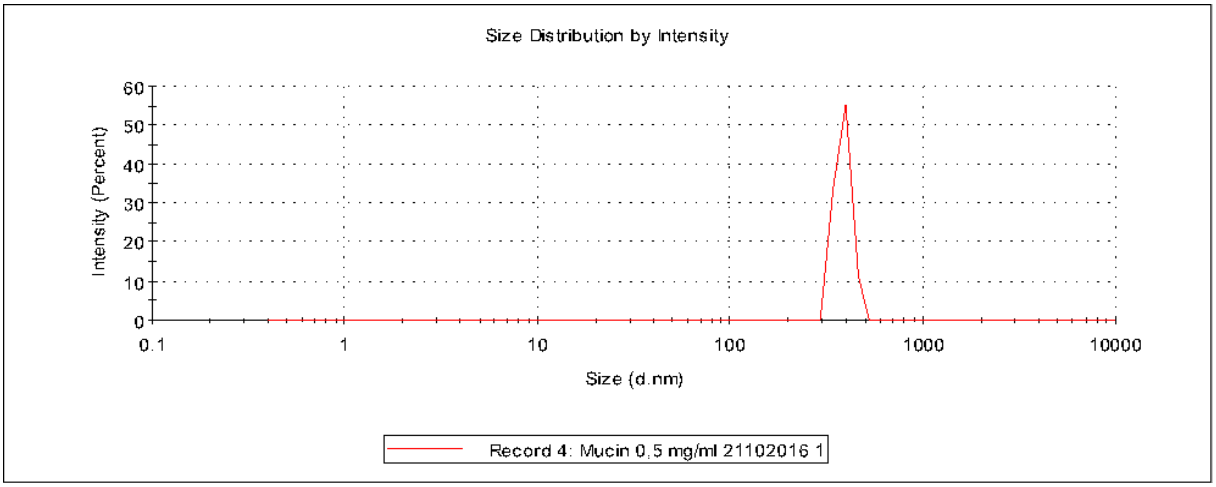

Figure C.3.5: The size distribution of Mucin by intensity at concentration of 0.5mg/ml

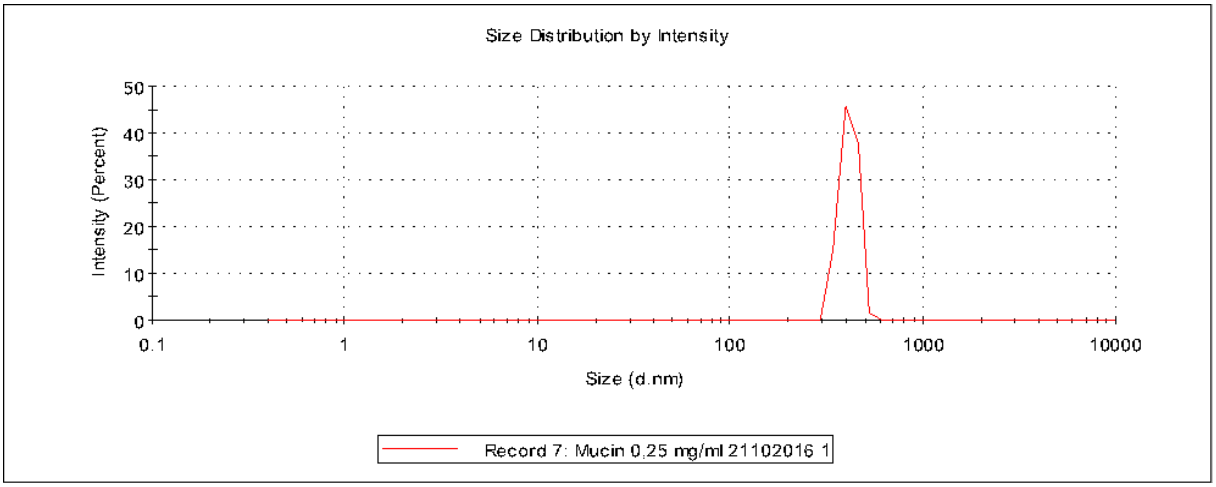

Figure C.3.6: The size distribution of Mucin by intensity at concentration of 0.25mg/ml

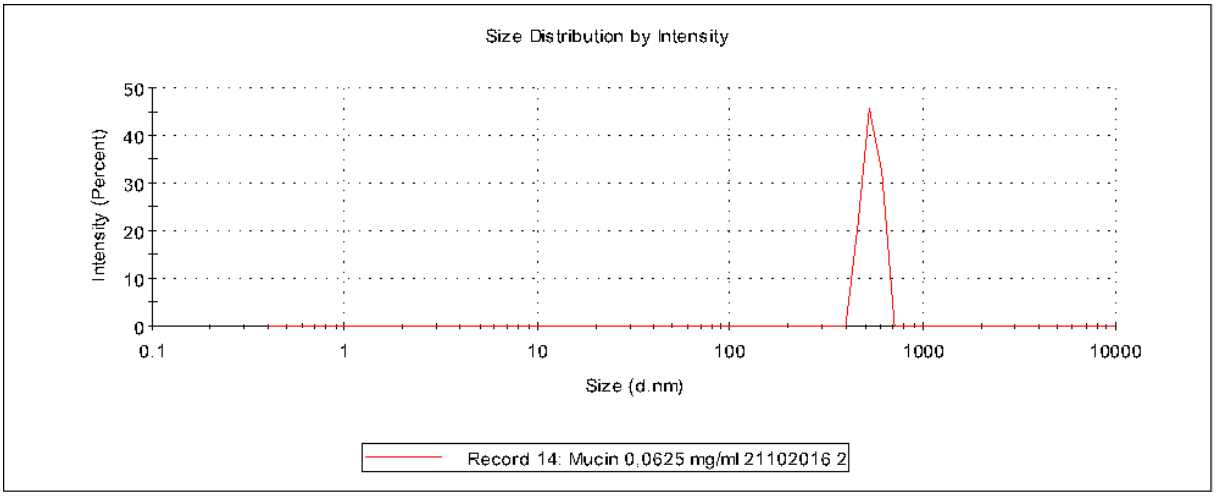

Figure C.3.7: The size distribution of Mucin by intensity at concentration of 0.0625mg/l

APPENDIX D: RHEOLOGICAL DATA

D.1. Load data of PGM control and PGM with nanoparticles

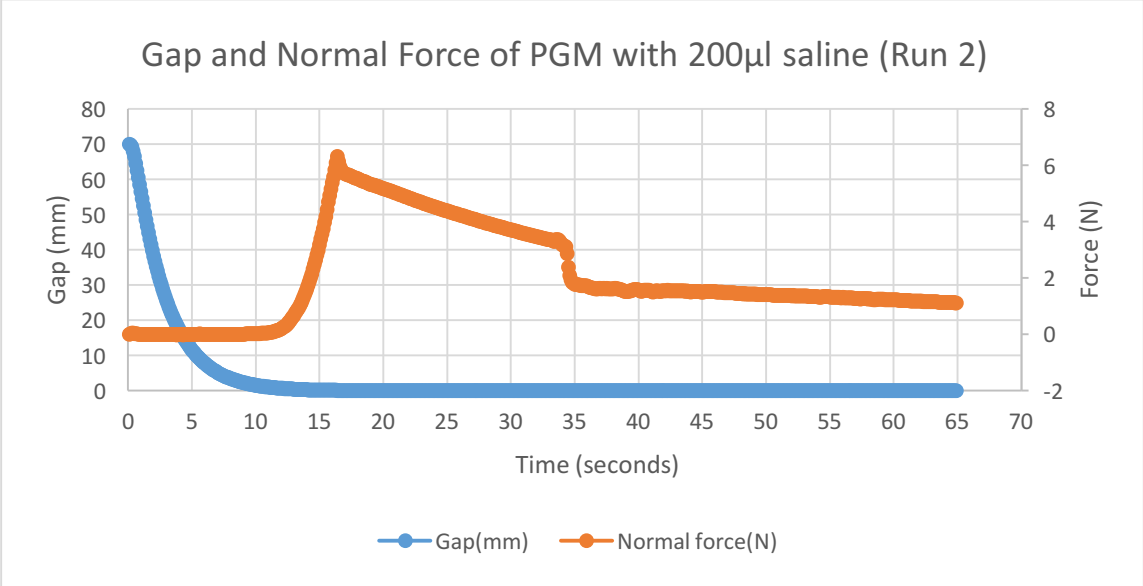

Figure D.1.1: The change in gap and normal force over the experiment time for Run 2 of PGM with 200μl saline. The blue curve representing gap (mm) is plotted in primary Y axis, while orange curve representing normal force (N) is plotted in secondary Y axis over time (seconds) in X axis

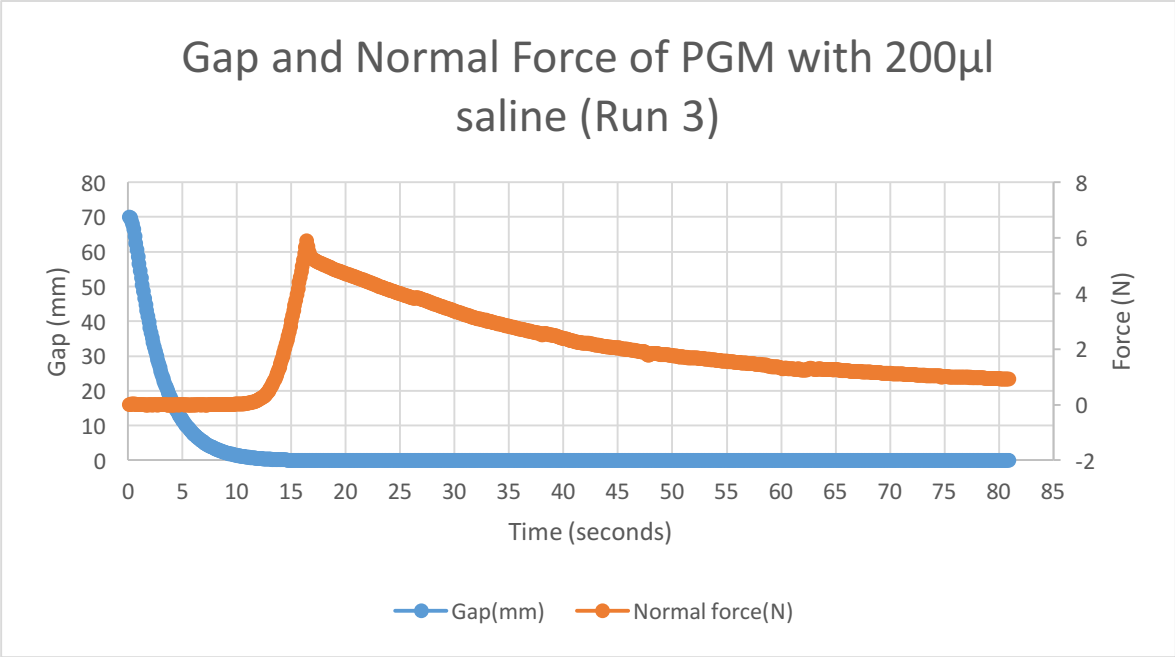

Figure D.1.2: The change in gap and normal force over the experiment time for Run 3 of PGM with 200μl saline. The blue curve representing gap (mm) is plotted in primary Y axis, while orange curve representing normal force (N) is plotted in secondary Y axis over time (seconds) in X axis

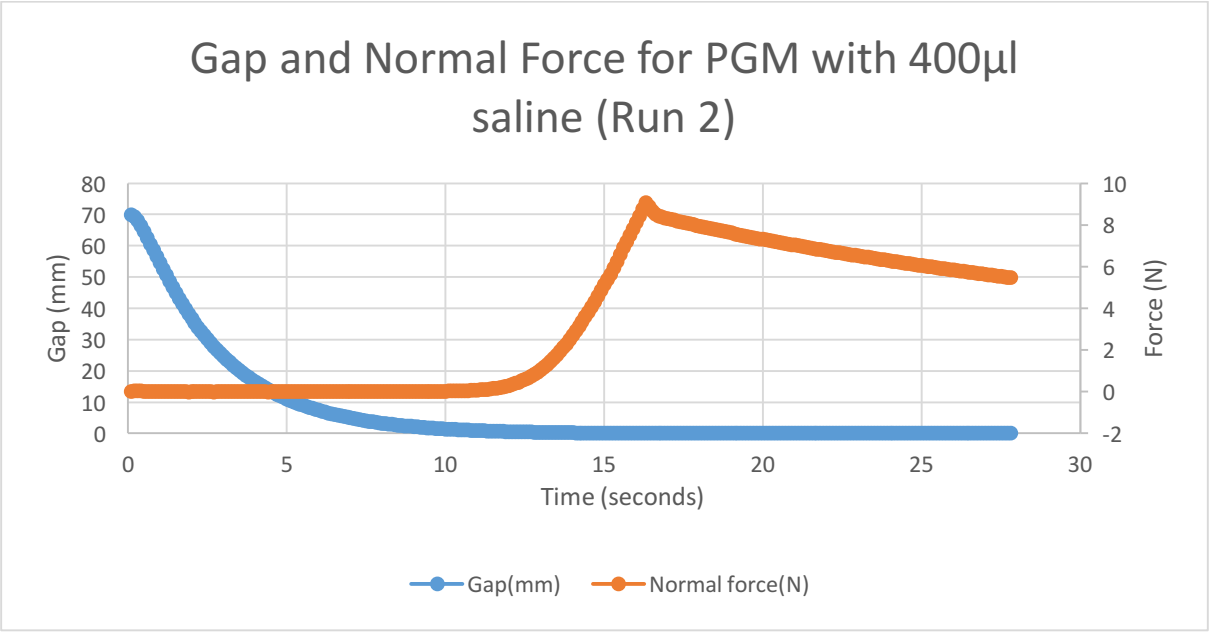

Figure D.1.3: The change in gap and normal force over the experiment time for Run 2 of PGM with 400μl saline. The blue curve representing gap (mm) is plotted in primary Y axis, while orange curve representing normal force (N) is plotted in secondary Y axis over time (seconds) in X axis

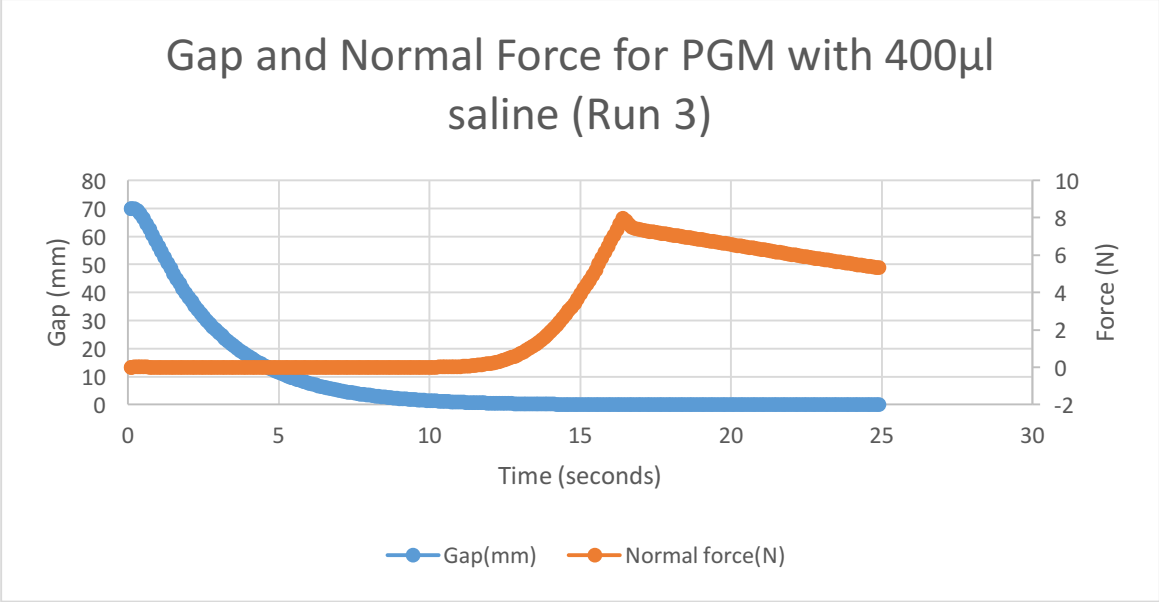

Figure D.1.4: The change in gap and normal force over the experiment time for Run 3 of PGM with 400μl saline. The blue curve representing gap (mm) is plotted in primary Y axis, while orange curve representing normal force (N) is plotted in secondary Y axis over time (seconds) in X axis

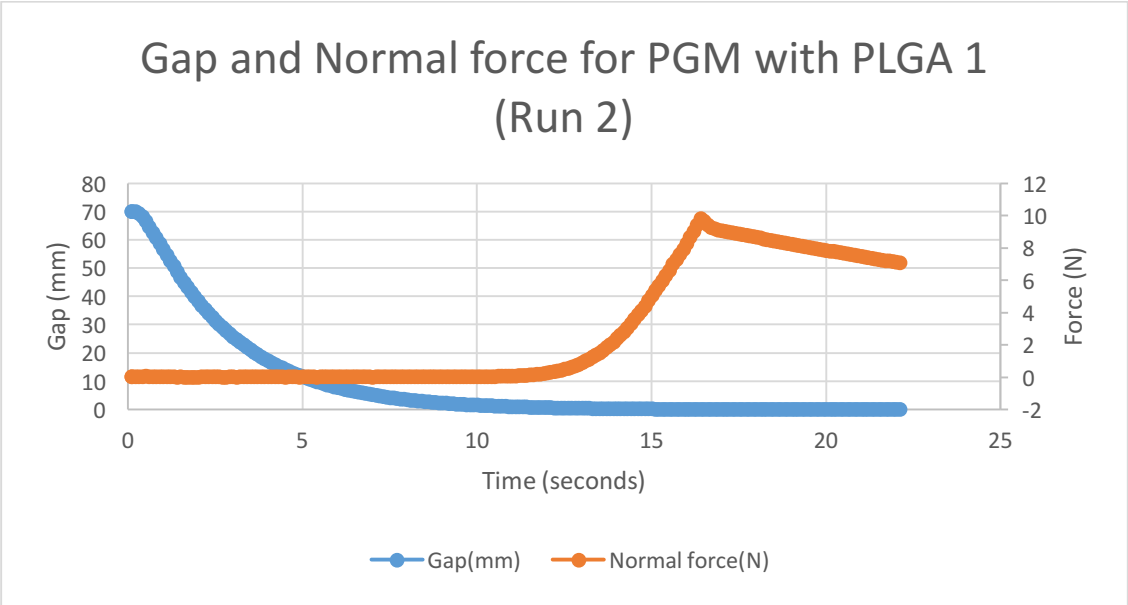

Figure D.1.5: The change in gap and normal force over the experiment time for Run 2 of PGM with PLGA 1. The blue curve representing gap (mm) is plotted in primary Y axis, while orange curve representing normal force (N) is plotted in secondary Y axis over time (seconds) in X axis

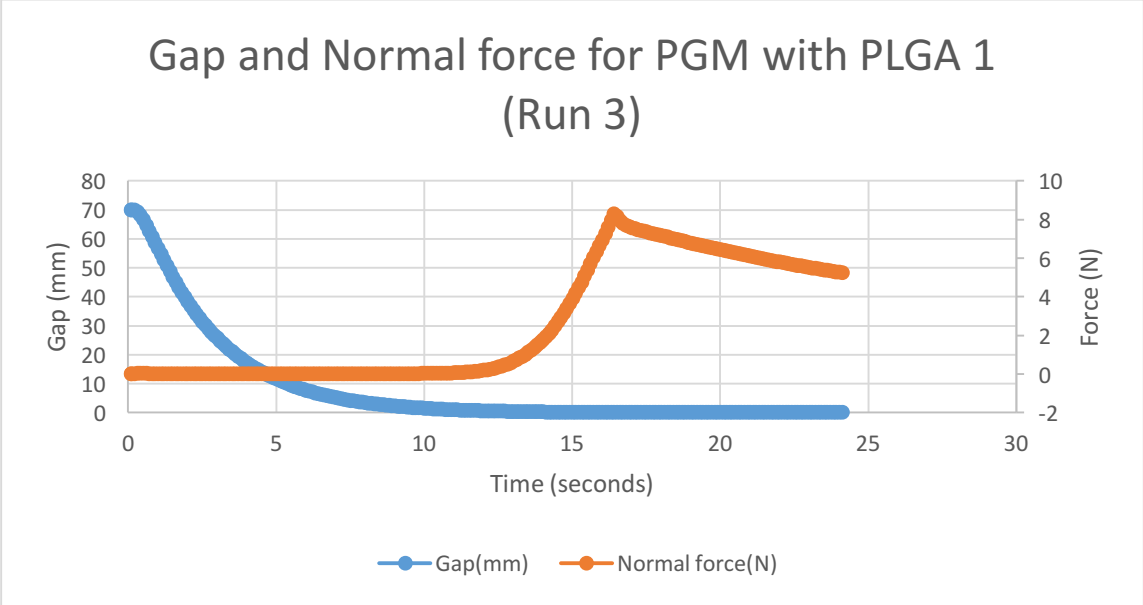

Figure D.1.6: The change in gap and normal force over the experiment time for Run 3 of PGM with PLGA 1. The blue curve representing gap (mm) is plotted in primary Y axis, while orange curve representing normal force (N) is plotted in secondary Y axis over time (seconds) in X axis

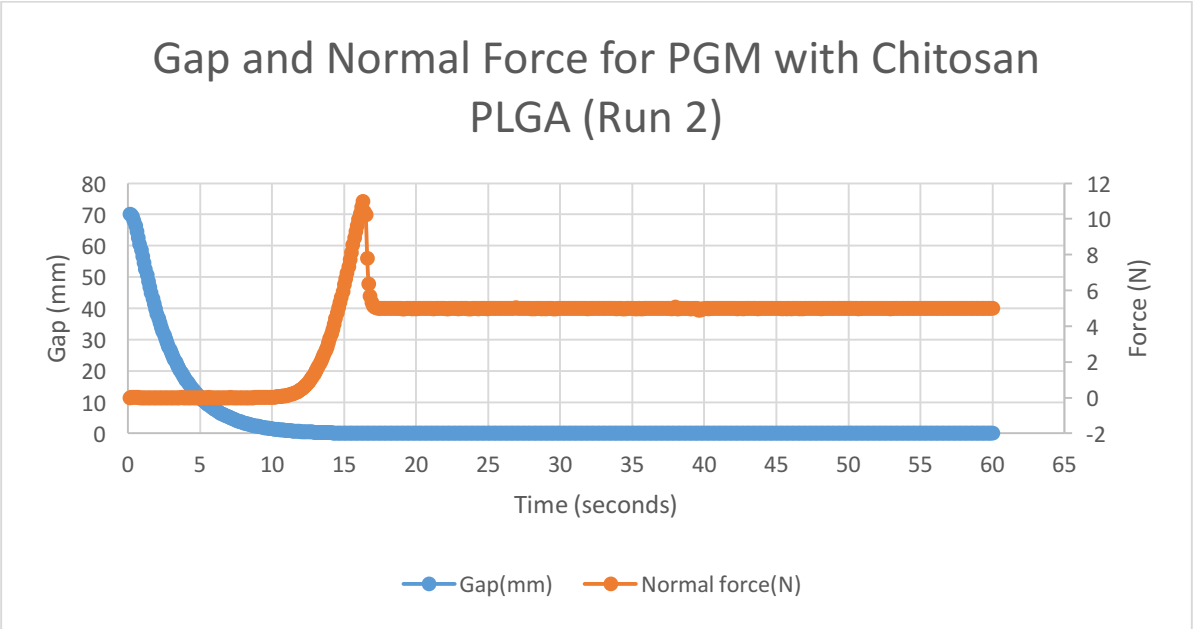

Figure D.1.7: The change in gap and normal force over the experiment time for Run 2 of PGM with Chitosan PLGA. The blue curve representing gap (mm) is plotted in primary Y axis, while orange curve representing normal force (N) is plotted in secondary Y axis over time (seconds) in X axis

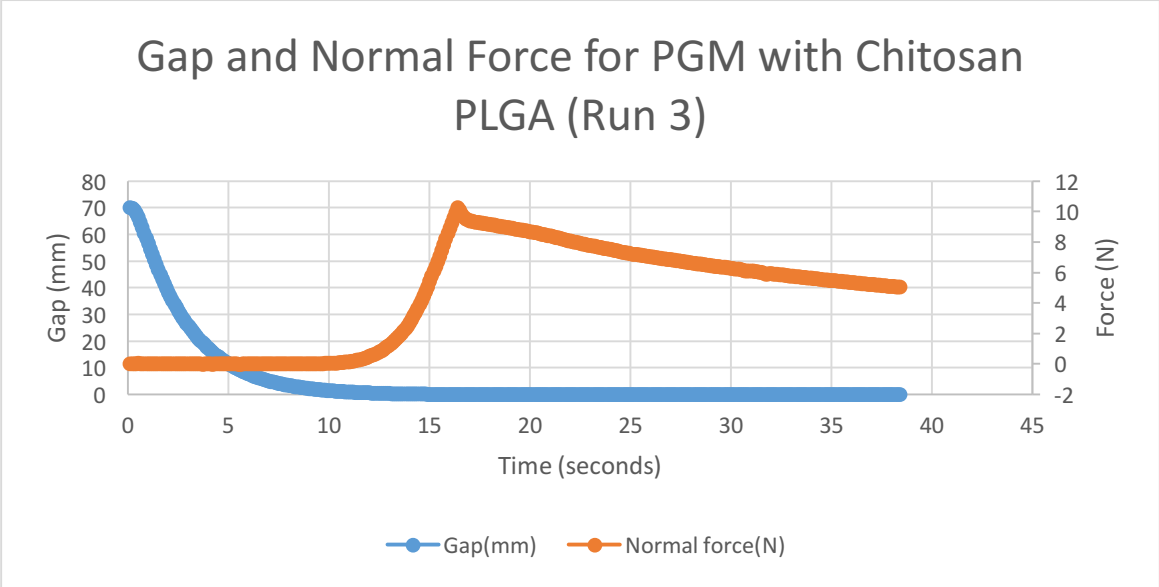

Figure D.1.8: The change in gap and normal force over the experiment time for Run 3 of PGM with Chitosan PLGA. The blue curve representing gap (mm) is plotted in primary Y axis, while orange curve representing normal force (N) is plotted in secondary Y axis over time (seconds) in X axis

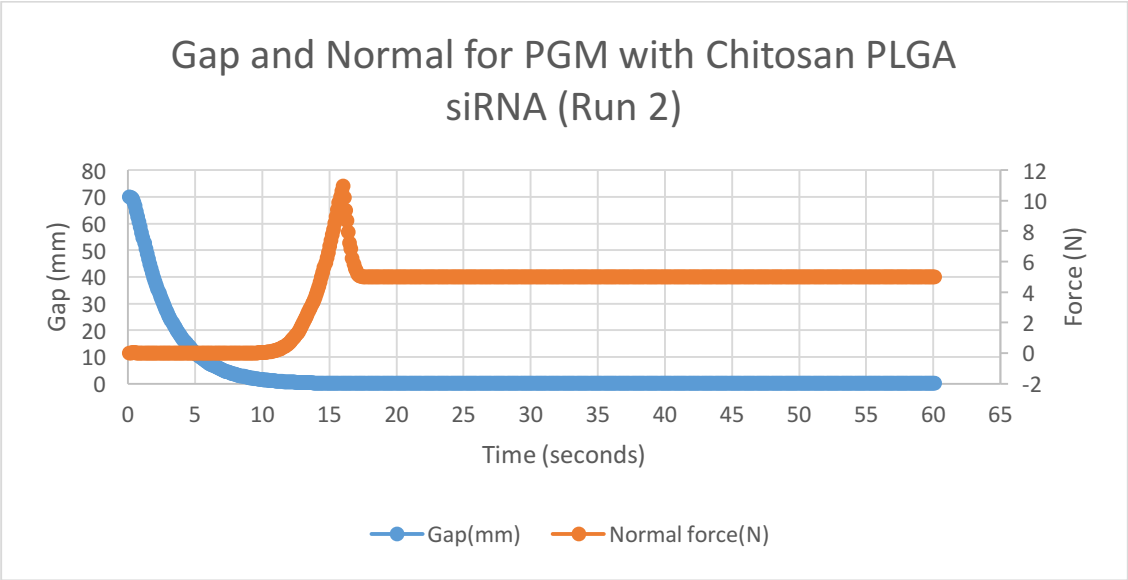

Figure D.1.9: The change in gap and normal force over the experiment time for Run 2 of PGM with Chitosan PLGA siRNA. The blue curve representing gap (mm) is plotted in primary Y axis, while orange curve representing normal force (N) is plotted in secondary Y axis over time (seconds) in X axis

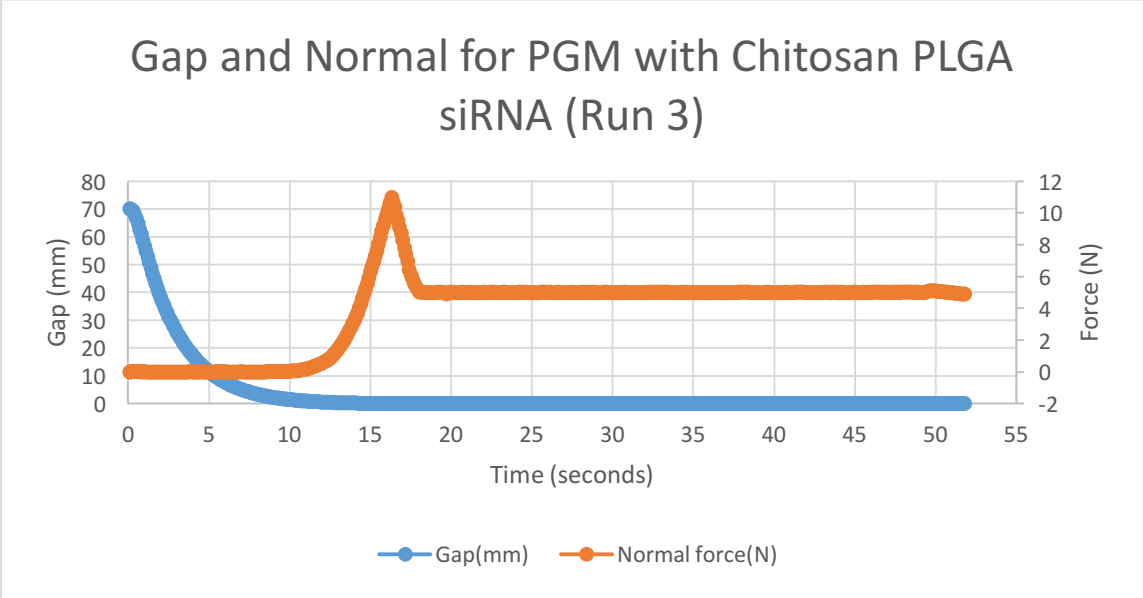

Figure D.1.10: The change in gap and normal force over the experiment time for Run 3 of PGM with Chitosan PLGA siRNA. The blue curve representing gap (mm) is plotted in primary Y axis, while orange curve representing normal force (N) is plotted in secondary Y axis over time (seconds) in X axis

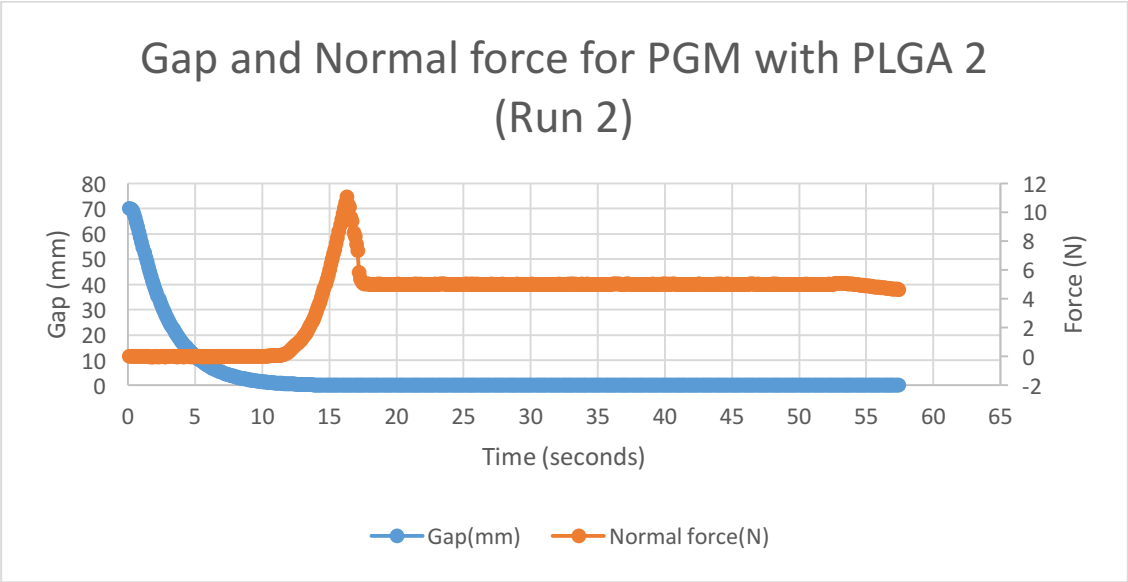

Figure D.1.11: The change in gap and normal force over the experiment time for Run 2 of PGM with PLGA 2. The blue curve representing gap (mm) is plotted in primary Y axis, while orange curve representing normal force (N) is plotted in secondary Y axis over time (seconds) in X axis

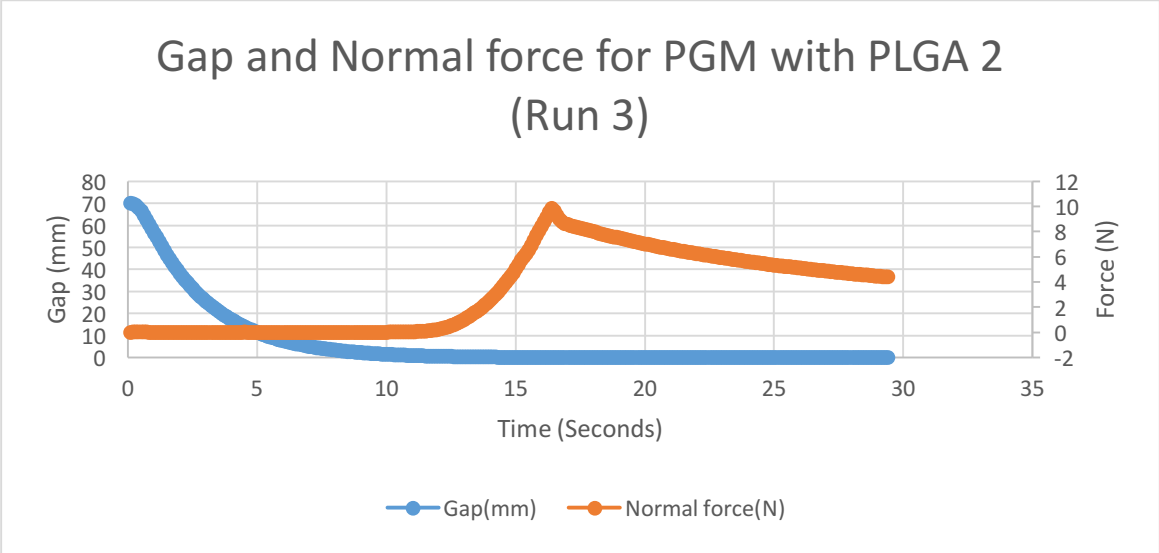

Figure D.1.12: The change in gap and normal force over the experiment time for Run 3 of PGM with PLGA 2. The blue curve representing gap (mm) is plotted in primary Y axis, while orange curve representing normal force (N) is plotted in secondary Y axis over time (seconds) in X axis

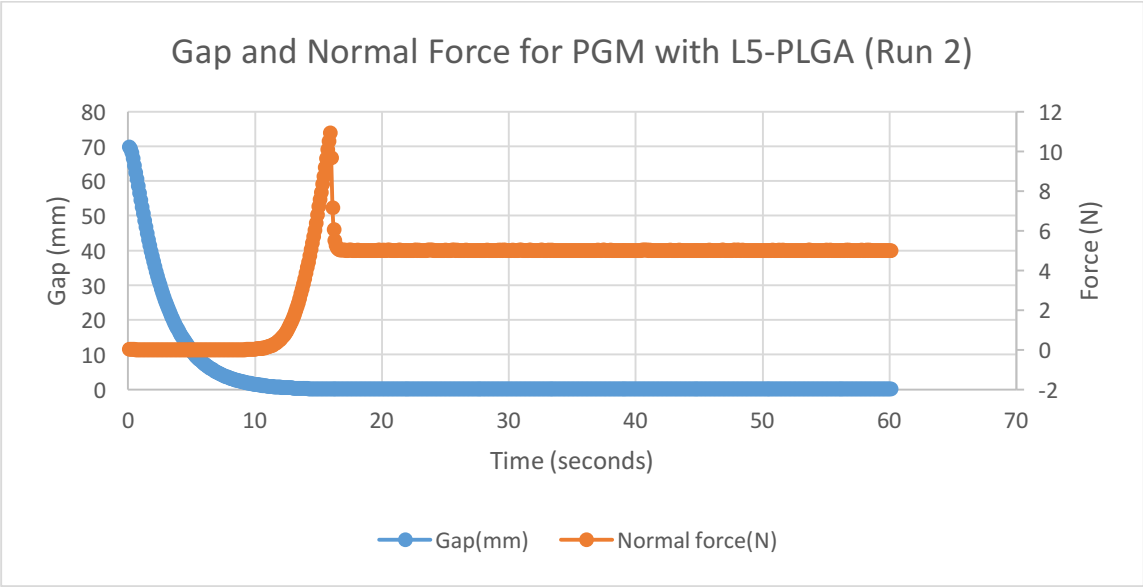

Figure D.1.13: The change in gap and normal force over the experiment time for Run 2 of PGM with L5-PLGA. The blue curve representing gap (mm) is plotted in primary Y axis, while orange curve representing normal force (N) is plotted in secondary Y axis over time (seconds) in X axis

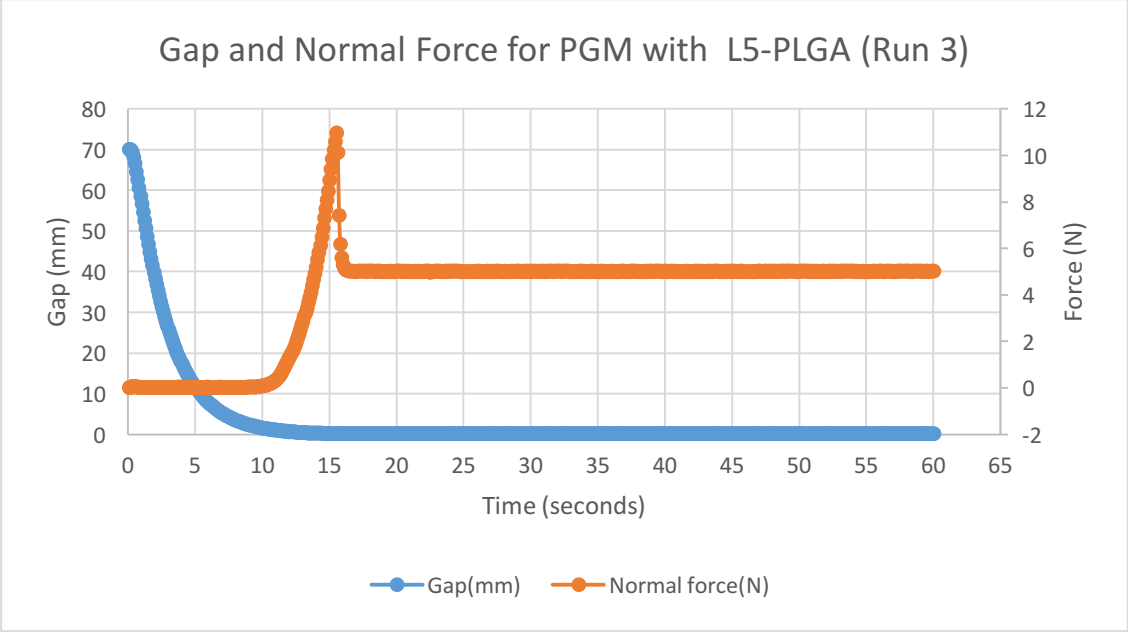

Figure D.1.14: The change in gap and normal force over the experiment time for Run 3 of PGM with L5-PLGA. The blue curve representing gap (mm) is plotted in primary Y axis, while orange curve representing normal force (N) is plotted in secondary Y axis over time (seconds) in X axis

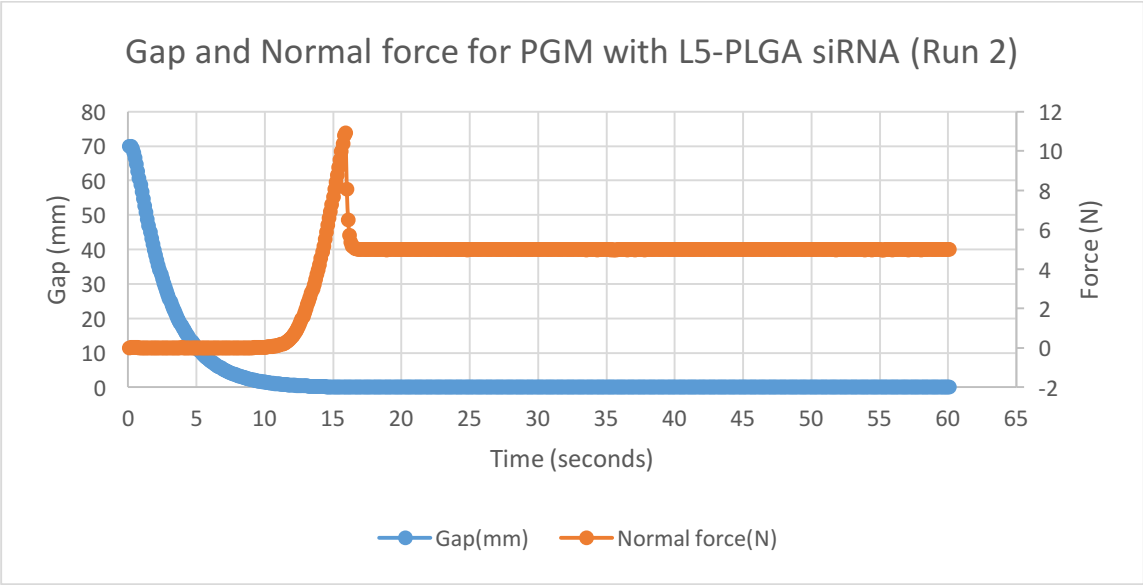

Figure D.1.15: The change in gap and normal force over the experiment time for Run 2 of PGM with L5-PLGA siRNA. The blue curve representing gap (mm) is plotted in primary Y axis, orange red curve representing normal force (N) is plotted in secondary Y axis over time (seconds) in X axis

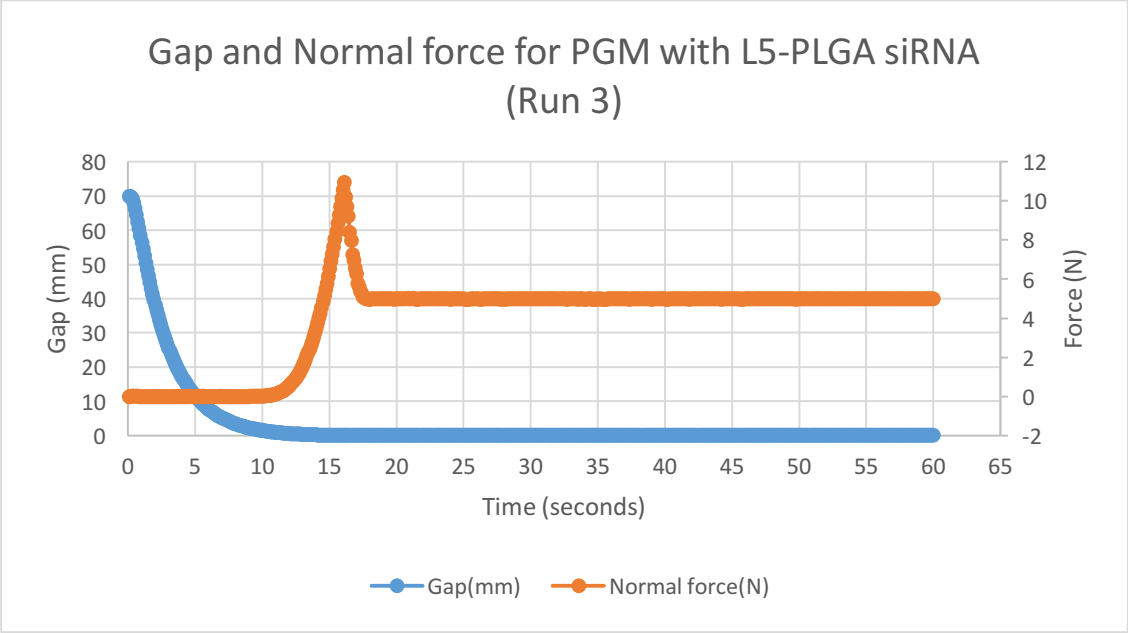

Figure D.1.16: The change in gap and normal force over the experiment time for Run 3 of PGM with L5-PLGA siRNA. The blue curve representing gap (mm) is plotted in primary Y axis, orange red curve representing normal force (N) is plotted in secondary Y axis over time (seconds) in X axis

D.2 Viscous Modulus (G”) of PGM with nanoparticles at 1Hz and 10Hz.

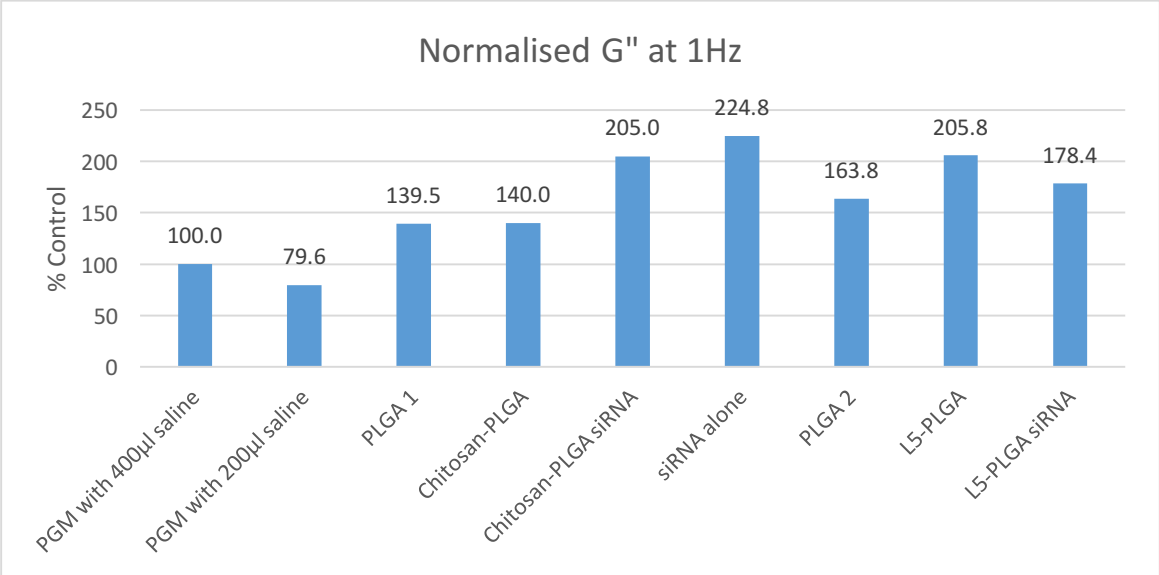

Figure D.2.1.: Comparison of Viscous Modulus (G”) at 1Hz for mucus control and all the nanoparticle formulations. The values above the bar represent the percent phase normalized to mucus control.

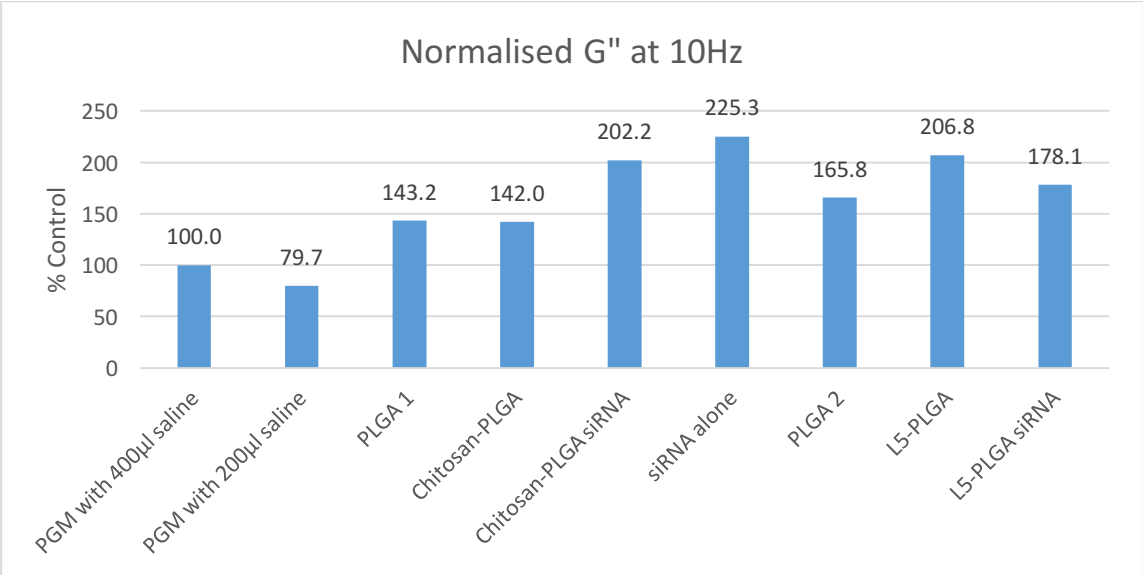

Figure D.2.2: Comparison of Viscous Modulus at 10Hz for mucus control and all the nano particle formulations. The values above the bar represent the percent phase normalized to mucus control.

D.3 Example of Rheological Data

D.3.1. Single Oscillation Frequency

Table D.3.1. Rheological data obtained from single frequency oscillation of PGM with PLGA 1 at 1Hz frequency, 25^{0}C and 1% strain.

Time (action)(s)	Frequency(Hz)	Shear modulus (elastic component)(Pa)	Shear modulus (viscous component)(Pa)	Phase angle(°)
5	1	262.6	36.09	7.83
10	1	254.4	43.23	9.64
15	1	254.4	40.33	9.01
20	1	254.2	40.72	9.1
25	1	254.5	40.14	8.96
30	1	254.4	40.48	9.04
35	1	254.5	40.34	9.01
40	1	254.6	40.41	9.02
45	1	254.7	40.13	8.95
50	1	254.7	40.24	8.98
55	1	254.6	40.34	9
60	1	254.8	40.16	8.96
65	1	254.7	40.23	8.98
70	1	254.5	40.44	9.03
75	1	254.6	39.92	8.91
80	1	254.5	40.08	8.95
85	1	254.4	40.16	8.97
90	1	254.5	40.16	8.97
95	1	254.3	40.08	8.96
100	1	254.3	40.16	8.97
105	1	254.2	39.97	8.94
110	1	254	40.22	9
115	1	254.1	39.82	8.91
120	1	253.9	40.07	8.97
125	1	253.9	39.92	8.93
130	1	253.8	40	8.96
135	1	253.8	40.02	8.96
140	1	253.7	39.89	8.93
145	1	253.7	39.89	8.93
150	1	253.7	39.89	8.94
155	1	253.6	39.85	8.93
160	1	253.5	39.79	8.92
165	1	253.5	39.78	8.92
170	1	253.4	39.92	8.95

175	1	253.4	39.78	8.92
180	1	253.3	39.77	8.92
185	1	253.2	39.72	8.91
190	1	253.2	39.83	8.94
195	1	253.1	39.72	8.92
200	1	253.1	39.65	8.9
205	1	253	39.63	8.9
210	1	252.9	39.8	8.94
215	1	253	39.41	8.85
220	1	252.8	39.95	8.98
225	1	252.8	39.64	8.91
230	1	252.7	39.74	8.94
235	1	252.7	39.4	8.86
240	1	252.6	39.52	8.89
245	1	252.6	39.49	8.89
250	1	252.4	39.68	8.93
255	1	252.4	39.39	8.87
260	1	252.3	39.65	8.93
265	1	252.3	39.43	8.88
270	1	252.3	39.4	8.88
275	1	252.1	39.49	8.9
280	1	252.1	39.47	8.9
285	1	252.1	39.4	8.88
290	1	252.1	39.51	8.91
295	1	252	39.28	8.86
300	1	251.9	39.39	8.89
305	1	251.9	39.37	8.88
310	1	251.8	39.33	8.88
315	1	251.7	39.38	8.89
320	1	251.7	39.21	8.85
325	1	251.6	39.42	8.9
330	1	251.6	39.26	8.87
335	1	251.5	39.28	8.88
340	1	251.5	39.28	8.88
345	1	251.4	39.28	8.88
350	1	251.3	39.33	8.89
355	1	251.3	39.1	8.84
360	1	251.2	39.36	8.91
365	1	251.2	38.95	8.81
370	1	251.1	39.24	8.88
375	1	251.1	39.03	8.83
380	1	251	39.01	8.83
385	1	251	39.16	8.87
390	1	250.9	39.22	8.89
395	1	250.8	38.98	8.83

400	1	250.7	39.08	8.86
405	1	250.8	38.97	8.83
410	1	250.6	39	8.84
415	1	250.6	38.96	8.84
420	1	250.6	38.91	8.83
425	1	250.5	39.07	8.86
430	1	250.5	38.97	8.84
435	1	250.4	39.02	8.86
440	1	250.3	39.04	8.86
445	1	250.3	38.95	8.85
450	1	250.2	38.99	8.86
455	1	250.2	38.83	8.82
460	1	250.1	38.95	8.85
465	1	250.1	38.81	8.82
470	1	250	38.81	8.83
475	1	249.8	39	8.87
480	1	249.9	38.68	8.8
485	1	249.7	38.78	8.83
490	1	249.8	38.87	8.85
495	1	249.7	38.67	8.8
500	1	249.7	38.88	8.85

D.3.2. Frequency Sweep

Table D.3.2. Rheological data obtained from frequency of PGM with PLGA 1 from 0.1Hz-10Hz frequency, 25^{0}C and 1% strain.

Frequency(Hz)	Shear modulus (elastic component)(Pa)	Shear modulus (viscous component)(Pa)	Phase angle(°)
0.01	148.5	30.56	11.63
0.01259	176.3	41.16	13.14
0.01585	196.4	18.71	5.44
0.01995	147.4	14.81	5.74
0.02512	200.9	30.81	8.72
0.03162	62.82	57.09	42.27
0.03981	192.5	41.75	12.24
0.05012	198.3	46.85	13.3
0.0631	184.4	28.85	8.89
0.07943	184	30.4	9.38
0.1	186.8	39.11	11.82
0.1259	195.9	34.82	10.08
0.1585	195.4	25.64	7.48
0.1995	199.4	26.68	7.62
0.2512	203.5	28.89	8.08
0.3162	208	30.52	8.35
0.3981	216.7	31.72	8.33

0.5012	220.4	32.83	8.47
0.631	222.4	33.89	8.66
0.7943	225	34.13	8.62
1	229.2	35.35	8.77
1.259	234	36.3	8.82
1.585	239.4	37.39	8.88
1.995	244.3	38.25	8.9
2.512	249.3	39.41	8.98
3.162	254.6	40.29	8.99
3.981	259.5	40.95	8.97
5.012	265.1	41.78	8.96
6.31	270.2	42.51	8.94
7.943	275.1	43.33	8.95
10	280.5	44	8.91

D.3.3. Relaxation

Table D.3.3. Part of Rheological data obtained from relaxation pattern of PGM with PLGA 1 from at 25^0C and constant deformation of 5% strain. The following data is only from 70 to 111 seconds. The whole data is too long to be shown here.

Time action (s)	Shear Stress (Pa)	Shear Strain (%)
70.98	4.933	5.76544
71.98	4.958	5.75319
72.98	4.984	5.74023
73.98	5.009	5.73161
74.98	5.033	5.7242
75.98	5.057	5.70665
76.98	5.081	5.69594
77.98	5.104	5.68888
78.98	5.127	5.68042
79.98	5.15	5.66782
80.98	5.172	5.66026
81.98	5.194	5.65205
82.98	5.216	5.64168
83.98	5.237	5.6307
84.98	5.258	5.62196
85.98	5.279	5.61785
86.98	5.3	5.60378
87.98	5.32	5.5931
88.98	5.34	5.59041
89.98	5.359	5.58059
90.98	5.378	5.57065
91.98	5.397	5.55813
92.98	5.416	5.55655

93.98	5.434	5.54529
94.98	5.452	5.53678
95.98	5.47	5.52856
96.98	5.488	5.52286
97.98	5.505	5.51233
98.98	5.522	5.50583
99.98	5.539	5.49948
101	5.555	5.48886
102	5.571	5.48525
103	5.587	5.47834
104	5.603	5.46792
105	5.619	5.46184
106	5.634	5.45828
107	5.649	5.44875
108	5.664	5.43852
109	5.678	5.43541
110	5.692	5.4282
111	5.706	5.4204

D.3.4. Strain Sweep

Table D.3.4. Rheological data obtained from strain sweep of PGM with PLGA 1 from 0.01%-100% at 25^{0}C.

Complex shear strain(%)	Shear modulus (elastic component)(Pa)	Shear modulus (viscous component)(Pa)	Phase angle(°)
3.35E-05	261.8	68.48	90
1.54E-04	28.8	8.96	-162.72
2.39E-04	135.4	52.45	-21.17
1.52E-03	262.8	13.27	-2.89
3.01E-03	205.1	18.24	5.08
3.68E-03	182.7	42.39	13.06
3.41E-03	234.8	62.3	14.86
4.47E-03	209.8	6.107	1.67
6.07E-03	232	31.45	7.72
7.89E-03	226.5	35.15	8.82
9.45E-03	238.8	37.32	8.88
0.012783	239.5	33.04	7.86
0.0153441	241.4	39.6	9.32
0.0200427	235.5	28.97	7.01
0.0260685	238.9	35.44	8.44
0.0319769	234.1	31.65	7.7
0.0403331	235.7	33.53	8.09
0.0500776	235.1	34.2	8.28
0.0648702	235	33.19	8.04

0.0796674	233.9	32.93	8.01
0.0990979	233.9	33.16	8.07
0.125166	232.5	32.64	7.99
0.158374	232.2	33.21	8.14
0.200346	231	33.12	8.16
0.25217	230.1	32.99	8.16
0.317371	229.3	33.36	8.28
0.398289	228.4	33.3	8.29
0.502891	226.6	33.25	8.35
0.631527	225	33.35	8.43
0.792801	223	33.28	8.49
0.997504	220.9	33.22	8.55
1.25571	218.7	33.18	8.63
1.5815	216.3	33.07	8.69
1.99334	213.6	32.92	8.76
2.50947	210.5	32.72	8.84
3.1653	206.7	32.38	8.9
3.98694	203.6	32.1	8.96
5.02203	200.3	31.79	9.02
6.32513	196.7	31.52	9.1
7.95374	193.4	31.25	9.18
10.0107	189.8	30.89	9.24
12.6004	186.1	30.56	9.32
15.8611	182.1	30.29	9.44
19.9643	177.8	30.21	9.64
25.1221	172.9	29.97	9.83
31.6452	167.9	29.83	10.07
39.8245	162.5	30.07	10.48
50.1593	157.4	30.28	10.89
63.118	152.9	30.03	11.11
79.5465	149	29.52	11.21
100.176	144	29.05	11.4

APPENDIX E: INSTRUMENTATION

E.1 Zetasizer

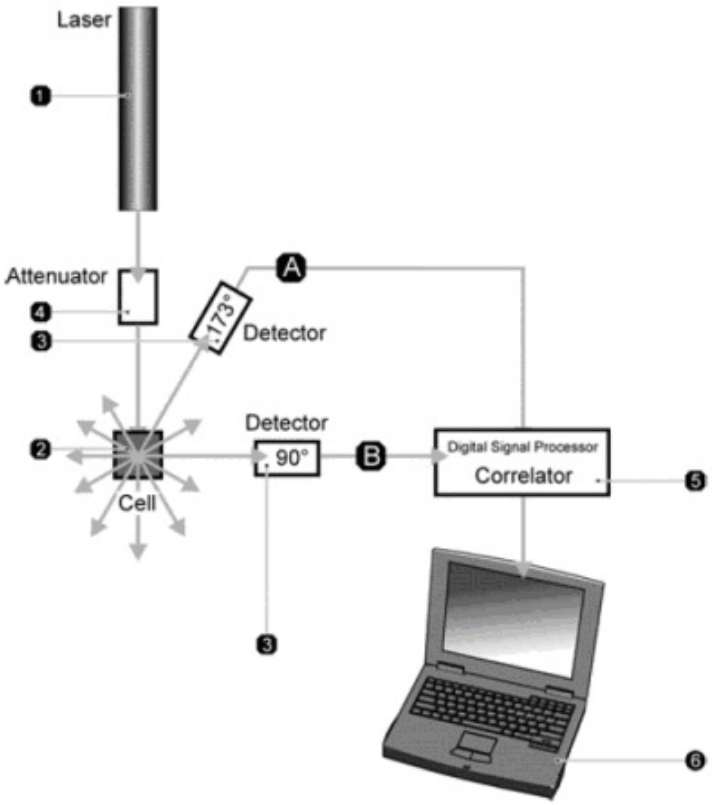

Figure E.1.1. The method of measurement using a zetasizer. 1) Laser-632.8nm; 2) Cuvette with Sample; 3) Detectors for observing the scattered light;
4) Attenuator to control the amount of laser;
5) Correlator to derive the correlation from signal given by detectors; 6) Computer to display the observation and for further analysis *Source: AZONano, 2013*.

E.2. Rheology

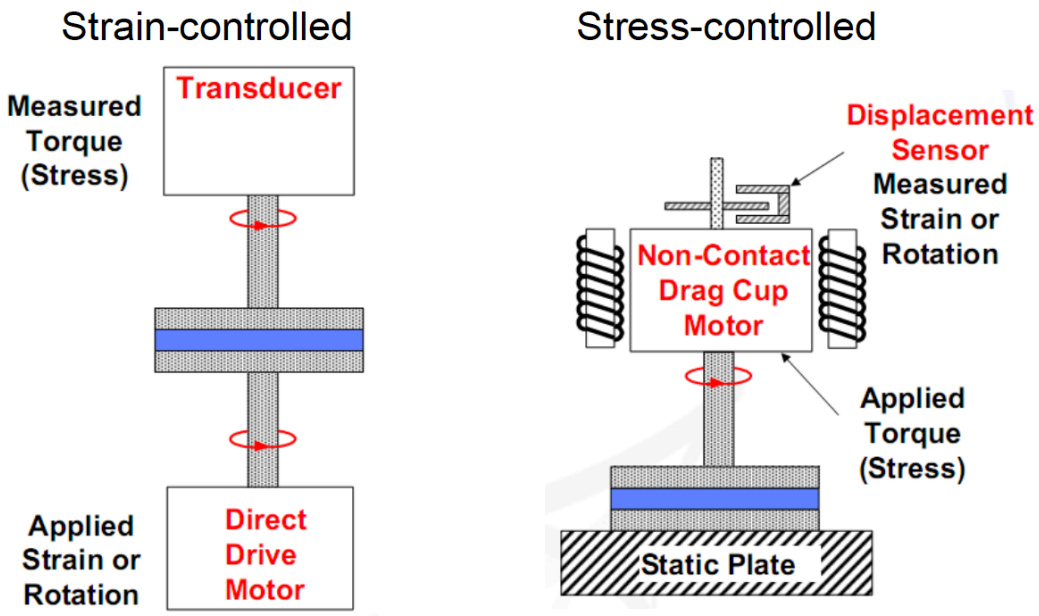

Figure E.2.1: Difference in Stress Controlled and Strain Controlled rheometer. *Source: Weitzlab group*.